SOLAR INTENSE MAGNETIC FIELDS

Andrew Robert Webb

A Thesis Submitted for the Degree of PhD
at the
University of St Andrews

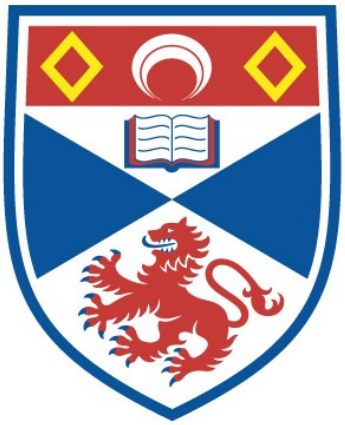

1980

SOLAR INTENSE MAGNETIC FIELDS

ANDREW ROBERT WEBB

THESIS SUBMITTED FOR THE DEGREE OF DOCTOR OF PHILOSOPHY
OF THE UNIVERSITY OF ST. ANDREWS.

ProQuest LLC.
789 East Eisenhower Parkway
P.O. Box 1346
Ann Arbor, MI 48106 – 1346

I was admitted as a Research Student under Ordinance General No. 12 in October, 1976.

I was admitted under Resolution of the University Court, 1967, No. 1 as a candidate for the degree of Ph.D. in October, 1977.

I declare that the following thesis is a record of research work carried out by me, that the thesis is my own composition, and that it has not been accepted in any previous application for a higher degree.

A.R. Webb.

I certify that Andrew Webb has satisfied the conditions of the Ordinance and Regulations and is qualified to submit the accompanying application for the degree of Doctor of Philosophy.

B. Roberts.

ABSTRACT

The nature of motions in intense magnetic fields is investigated. For a flux tube in a uniform atmosphere a dispersion relation is derived for the modes of vibration and analytic approximations are obtained for a slender tube. In a stratified atmosphere an expansion procedure is used to derive an equation for the vertical velocity perturbation. The behaviour of motions within the flux tube is shown to depend upon a transition frequency ω_v, such that vertically propagating waves are possible only for frequencies greater than ω_v.

Also, the nature of convective instability in a slender magnetic flux tube is explored. A sufficient condition for stability is derived for the case of an arbitrary temperature profile in the external medium. For a tube of infinite depth, with a uniform temperature gradient inside the tube equal to that in the exterior, a necessary and sufficient condition for convective stability to occur inside the tube is derived. Under the assumptions of the model, intense flux tubes are convectively stable if sufficiently shallow (with depths $1 - 2 \times 10^3$ km or less). Tubes that extend deeper into the convection zone are potentially (convectively) unstable, but may be stabilised for sufficiently strong magnetic fields.

Radiative damping of waves is important in the upper photosphere and the effect of radiative relaxation on the propagation of waves in an intense flux tube is examined both for a uniform and stratified atmosphere. The cut-off frequency is generalized to include the effects of radiative relaxation. The phase-shift

between velocity oscillations at two different levels and the phase difference between temperature and velocity perturbations are derived and compared with the available observations.

Finally, the consequences of the observed steady downflow are discussed.

Acknowlegements

I am very grateful to Dr. B. Roberts for the help and encouragement he has given to me. I would also like to thank Dr. J. Adam, Dr. A. Hood, Dr. A. Milne and Dr. E. Priest for helpful discussions and advice.

I thank my sister, Janet, for typing this thesis.

I would like to acknowledge financial support from the University of St. Andrews.

CONTENTS

SOLAR INTENSE MAGNETIC FIELDS

Chapter 1 : INTRODUCTION

Studies of solar magnetic fields over the past decade have shown that most of the magnetic flux in the solar photosphere outside of sunspots occurs in the form of highly concentrated flux elements ('filaments', 'fluxules', 'intense fields') located in downdrafts at the junctions of supergranules (Stenflo, 1976a; Harvey, 1971, 1977a). These isolated flux tubes, embedded in a virtually field-free photosphere (e.g. Vrabec, 1971), occur both in active and quiet regions. Typically they have field strengths of 1 - 2 kG and diameters, at photospheric levels, of 100 - 300 km (Stenflo, 1973). As a preliminary to a more detailed description of the observations, it is of interest to outline the development of ideas and observations concerning the nature of the Sun's small-scale field.

Hale, who discovered the magnetic field in sunspots in 1908, recorded fields of up to 700 G in active regions outside sunspots as early as 1922 and concluded that fields of 200 - 500 G outside sunspots were not uncommon. Beggs and Von Klüber (1956) reported very small areas with rather strong fields, up to 100 G, in large numbers along the main sunspot belts, even when in white light nothing but undisturbed photosphere could be seen on the surface. These comparatively large fields frequently occurred at some distance from an apparently single spot. The fact that very small areas, only a few square seconds of arc in extent, sometimes revealed relatively strong magnetic fields led Beggs and Von Klüber to suggest that the magnetic structure of the Sun's surface may be appreciably finer than could be resolved at that time. Leighton (1959) recorded fields of 100 - 200 G in extensive areas throughout

plage regions and Howard (1959) measured fields greater than 75 G near sunspots and suggested that the magnetic field in the photosphere and chromosphere is in the form of more or less vertical columns, with the horizontal dimension of the magnetic field in the photosphere being so small as to escape detection on any direct photographs.

Following the discovery of supergranulation cells (Leighton et al, 1962), surrounded by the bright linear features of the chromospheric (Ca K232) network and associated with downdrafts, Leighton (1963, 1965) argued that the convective motions of the supergranules concentrate the magnetic fields at the boundaries. The correlation between supergranular cell boundaries and the magnetic field pattern was confirmed by Simon and Leighton (1964), who estimated the width of the magnetic network at about 700 km. Further observations of small-scale solar magnetic fields outside sunspots were made by Sheeley (1966, 1967), who measured field strengths of several hundred gauss, occurring in areas easily as small as 500 km in extent, in regions of the solar surface sometimes well removed from areas of sunspot activity. In addition, these fields were shown to correspond to the bright Ca K232 emission and to darkenings in the continuum, suggesting that the small-scale fields occur in the dark lanes of the granulation. This was later confirmed by Beckers and Schröter (1968) who measured 'magnetic knots' with strengths up to 1400 G and diameters of 1100 km. However, these strong fields were detected in the vicinity of sunspots and not observed outside an active region.

The close correlation between the longitudinal magnetic field and the chromospheric and photospheric networks was also demonstrated by Chapman and Sheeley (1968), who showed that the

bright photospheric network is cospatial with the network of photospheric magnetic fields and concluded that these magnetic regions are a few hundred degrees hotter than their surroundings.

Recent observations of photospheric magnetic fields have led to a more complete description of the structure of intense magnetic fields, whose prcperties have been reviewed by Stenflo (1976a) and Harvey (1977a) (see also Athay, 1976; Stenflo, 1976b). We shall now summarize these observations.

1.1 General Description

More than 90% of the magnetic flux in the photosphere is concentrated into intense isolated kilogauss flux tubes ('filaments') (Howard and Stenflo, 1972), and this percentage is even higher in quiet regions (Frazier and Stenflo, 1972). The interfilamentary field is very weak (less than 3G according to Howard and Stenflo, 1972; less than 10 G according to Stenflo, 1976a) having a polarity opposite to that of the filamentary field (in the immediate vicinity of the filaments), with a strength of 2 - 5 G for active regions and about 1 G for quiet regions (Frazier and Stenflo, 1972).

Estimates of the field strengths of these small-scale magnetic elements have gradually increased (with a corresponding decrease in size) as improvements in magnetographs and telescopes have been made (Chapman, 1974). Presently, the magnetic field strength is estimated to be 1000 - 2000 G, for fields inside as well as outside active regions (Frazier, 1974; Frazier and Stenflo, 1978; Tarbell and Title, 1975, 1977; Stenflo, 1973, 1976a; Chapman, 1974), with a diameter of 100 - 300 km (Stenflo, 1973, 1976a; Athay, 1976) at photospheric levels. Livingston and Harvey (1969) argue that variations in the measured values of the field result from an

inability to resolve the individual elemental fields. Weak fields are observed only because fields are confined to regions much smaller than resolution (Tarbell and Title, 1977).

As there is strong evidence for a unique field strength distribution characterizing all magnetic elements in the quiet region network and active region plages, the question of flux quantization arises. Livingston and Harvey (1969) presented observational evidence for quantization in photospheric magnetic flux and concluded that for an elemental area 1 $(\text{arc-sec})^2$ the elemental field strength is 525 G. This gives the value 2.8×10^{10} Wb for the flux quantum. Further estimates have been given by Mehltretter (1974) and Stenflo (1973), who both give values of the flux quantum $\phi_0 \sim 5 \times 10^9$ Wb.

Estimates of the lifetimes of the flux elements vary. The lifetime depends upon the size of the structure. Mehltretter (1974) finds that his bright facula points, which he postulates are identical with magnetic flux tubes, are present generally for intervals of 5-15 minutes. A decay rate (Stenflo, 1976a)

$$\frac{d\phi}{dt} = -10^7 \text{ Wb s}^{-1} \qquad (1.1.1)$$

accounts for the observational results remarkably well. For a flux quantum of 5×10^9 Wb, (1.1.1) gives a lifetime of 8 min, in agreement with Mehltretter's observations. The lifetime is difficult to measure since the bright network shows transverse motions, as if being shuffled around by the solar granulation over distances of the order of 1000 km (Mehltretter, 1974).

The magnetic flux concentrations are located in both active and quiet regions. In the quiet regions of the photosphere the intense fields are situated at junctions of supergranules where strong downdrafts occur (Howard and Stenflo, 1972; Livingston, 1968;

Tanenbaum et al, 1969; Deubner, 1967). Flux concentrations always appear to be correlated with downflow of matter regardless of whether they occur in the quiet region network (Simon and Leighton, 1964; Tanenbaum et al, 1969; Frazier, 1970) or active region plages (Beckers and Schröter, 1968; Giovanelli and Ramsay, 1971; Sheeley, 1971; Howard, 1972). The magnitude of the flow is in the range 0.3 - 0.7 km s^{-1} (Stenflo, 1973; Tarbell and Title, 1977; Giovanelli and Brown, 1977) and appears to increase in magnitude with depth (Harvey, 1977a; Giovanelli and Slaughter, 1978). The flow may be a transient phenomenon or the result of an overstable oscillation (Spruit, 1979).

Very little is known about the exact height variation of the magnetic field, though it appears to diverge very rapidly with height (Howard and Stenflo, 1972; Frazier and Stenflo, 1972; Harvey, 1977a). This may be inferred from the fact that part of the strong field flux returns in the form of weak-field opposite polarity flux adjacent to the magnetic elements (Frazier and Stenflo, 1972) and also that the brightness structure becomes coarser with height (Reeves et al, 1974; Simon and Noyes, 1971) though it is not clear whether the diameter of a brightness element is strictly proportional to the diameter of a flux tube at all heights (Stenflo, 1976a).

The magnetic field concentrations in the photosphere appear to be strongly correlated with the bright photospheric and chromospheric networks and are associated with strong atmospheric heating (Simon and Leighton, 1964; Sheeley, 1967; Frazier, 1971; Sheeley and Engvold, 1970; Stenflo, 1973, 1976a).

The chromospheric network is a large-scale brightness pattern located at the borders of the photospheric supergranulation and coincides with the regions of local magnetic field enhancement (Beckers, 1977). It appears as a bright structure in the K line of Ca II and the centre of the Hα line, while the wings of Hα show a dark network. The photospheric network may be regarded as a downward extension of the chromospheric network and appears as a bright network in certain Fraunhofer lines. Near the solar limb the photospheric network becomes visible in continuum light as photospheric faculae. The network is closely correlated with the photospheric magnetic field distribution. Stenflo (1973) reports a one-to-one correspondence between flux concentrations and bright network points and finds that the brightness structures are somewhat larger than the magnetic field concentrations.

The number of bright points per supergranulation cell is approximately 100, which is also the number of spicules per cell, and so it has been suggested (Simon and Leighton, 1964; Parker, 1974b) that the magnetic field at the boundaries of supergranules is the birthplace of spicules. Beckers (1972) reported a direct relation between the presence of a photospheric magnetic field of 10 - 100 G and the occurrence of spicules. In fact, spicules do appear to shoot out from the bright points in the photospheric network (Stenflo, 1973) and Simon and Zirker (1974) have measured fields up to 1400 G in small structures at the centres of spicule bushes.

The relationship between the magnetic flux concentrations and other small-scale photospheric features has also been investigated. Observations provide strong evidence for the

concentration of solar magnetic fields in the subgranular structures called filigree (Beckers, 1975). Mehltretter's (1974) observations of faculae as consisting of bright point-like structures with typical dimensions of 100 - 200 km leads him to the view that faculae are identical with the solar filigree (Dunn and Zirker, 1973; Dunn et al, 1974) and may be the site of intense photospheric flux tubes as suggested by Dunn and Zirker (1973). However, Simon and Zirker (1974) found that the magnetic structure is somewhat broader (1"-2") than the brightness structure (in contrast to Stenflo's observation). The filigree network is the 'crinkle' pattern of the bright photospheric network. The facula structure in the wings of the Ca II K line appears almost exclusively to be made up of bright facula points sitting in intergranular lanes - singly or associated in chains. Bruzek (1977) identifies this facula structure with the filigree pattern. The width of the facula points (0.25") is similar to that of the filigree and to the dimensions of intense flux tubes. Facula granules, seen on the limb, probably correspond to clusters of unresolved facula points (Bruzek, 1977).

The magnetic elements tend to clump together to form larger magnetic features, which in turn are organised into still larger-scale complexes (Harvey, 1977b; Zwaan, 1967). Recently, Parker (1979a, b) has proposed that the sunspot itself may consist of many separate flux tubes, which form a single spot at the visible surface, but are distinct within the interior of the Sun.

1.2 Models of Flux Tubes

Models and theoretical ideas concerning magnetic flux tubes in the convection zone and photosphere have been reviewed recently by Spruit (1977b) and Weiss (1977). A number of facula models have been constructed (Rogerson, 1961; Kuz'minykh, 1965; Chapman, 1970; Stellmacher and Wiehr, 1971; Badalyan and Prudkovskii, 1973; Muller, 1975) identifying faculae as granular-type structures having a temperature excess of some hundreds of degrees at photospheric levels. More recently, models which assume different types of solar features as the origin of faculae have been proposed. A number of these consider faculae as small-scale structures with a high magnetic field strength (Stenflo, 1975; Frazier and Stenflo, 1978; Chapman, 1977, 1979). For example, Stenflo's (1975) model of the photospheric network is based on an element with field strength about 2 kG and a temperature enhancement which begins at about 180 km above $\tau_{5000} = 1$ and increases rapidly with height. Mehltretter (1974) and Stellmacher and Wiehr (1979) identify faculae with the filigree structure. Faculae, filigree and intense magnetic fields may simply be different manifestations of the same feature (Chapman, 1979). All the models give a significant temperature excess above the photosphere.

Spruit (1976) has presented models of axially symmetric flux tubes, ranging in size from facula points (150 km) to small pores (1000 km). He finds that in the continuum the structure looks like a depression in the photosphere (similar to the Wilson depression) and suggests that faculae seen on the limb may be a result of radiation from the bright wall.

A model of the photospheric network, including the effect of a downflow within the magnetic structure, has been put forward by Unno and Ribes (1979). This model, together with those mentioned briefly above, will be discussed in detail in Chapter 6.

1.3 Models of the Solar Atmosphere

In order to relate our results to observations, much of the work presented in later chapters will refer to models of the solar convection zone and models of the chromosphere. Therefore, in this section we shall discuss briefly some of the models available and, for the models adopted in this thesis, we present figures of the variation with height of some of the more important physical and mathematical quantities.

CHROMOSPHERE

The models we consider are homogeneous models, in which the atmosphere varies only with height and the physical conditions are assumed to be uniform over any one horizontal plane, i.e. parallel to the solar surface. To some extent, the concept of a homogeneous model is an artificial one since the real solar atmosphere contains a significant amount of non-uniform dynamic structure. A homogeneous model, therefore, represents physical conditions which may be intermediate to spicular and interspicular regions. Both the Bilderberg Continuum Atmosphere (BCA) (Gingerich and De Jager, 1968) and the Harvard-Smithsonian Reference Atmosphere (HSRA) (Gingerich et al, 1971) are homogeneous models.

The BCA is a model based on observed intensities and centre-to-limb observations of the solar continuous spectra.

The model is characterized by a flat temperature minimum of 4600 K (a value determined by the measurements of ultraviolet intensities) in the range $10^{-4} \lesssim \tau_{5000} \lesssim 10^{-2}$, where τ_{5000} is the optical depth at a wavelength of 5000Å. The extent of the temperature minimum is derived from infra-red limb-darkening measurements. A hydrogen/helium ratio of 10 by number is assumed.

The HSRA, which is the model of the atmosphere we shall adopt throughout this thesis, used the results of space observations in the ultra-violet (OSO-4) and airbourne observations in the infra-red. It differs from the BCA in the low chromosphere ($\tau_{5000} < 10^{-4}$) where deviations from local thermodynamic equilibrium in hydrogen and carbon have been taken into account. Also the temperature minimum (4170K) is lower than the BCA and is narrower in extent.

CONVECTION ZONE

Spruit's (1974, 1977a) models of the solar convection zone have been constructed to match the solar interior model of Abraham and Iben (1971) and a model of the solar atmosphere. Spruit (1974) developed a model consistent with the HSRA, by using abundances consistent with those used for the HSRA, while his later model (Spruit, 1977a) was constructed to fit the atmospheric model of Vernazza et al (1976). The behaviour of convection in the superadiabatic region is estimated by the use of a modified mixing-length formalism.

Since the atmospheric model we shall use in this thesis is the HSRA, we use the convection zone model of Spruit (1974).

PROFILES

The pressure, p, temperature, T and density, ρ are sketched as functions of height, z, in Figures 1.1 - 1.3 using the models of Spruit (1974) and the HSRA. The origin (z=0) is taken as $\tau_{5000} = 1.0$, where τ_{5000} is the optical depth at a wavelength of 5000Å. Note how rapidly both the pressure and density decrease above z=0. In contrast, the temperature does not vary greatly in the 1000 km above z=0, though just below z=0 there is a narrow region where the gradient is very steep.

Figure 1.4 shows the variation with height of the mean molecular weight, μ, and the ratio of specific heats, γ. We see that, for the height range plotted, both functions have a broad maximum above z=0. Above a height of about 200 km, γ takes the value of 5/3 up to a height of about 600 km and then decreases. Below 200 km, γ decreases rapidly with depth, at the top of the convection zone, to reach a broad minimum of approximately 1.06 before starting to increase with depth at z= -1000 km.

Also, it is convenient, at this stage, to plot the square of the Brunt - Väisälä frequency, N_0^2, defined by

$$N_0^2(z) = g\left(-\frac{1}{\rho}\frac{d\rho}{dz} - \frac{g\mu}{\gamma RT}\right),$$

where g is the acceleration due to gravity (274 ms^{-2}) and R is the gas constant (=8.26x$10^3 JK^{-1}kg^{-1}$). N_0^2 is shown in Figure 1.5. Note that the division between $N_0^2 > 0$ and $N_0^2 < 0$ takes place at approximately z=0. The importance of the Brunt - Väisälä frequency will be discussed in the following chapter.

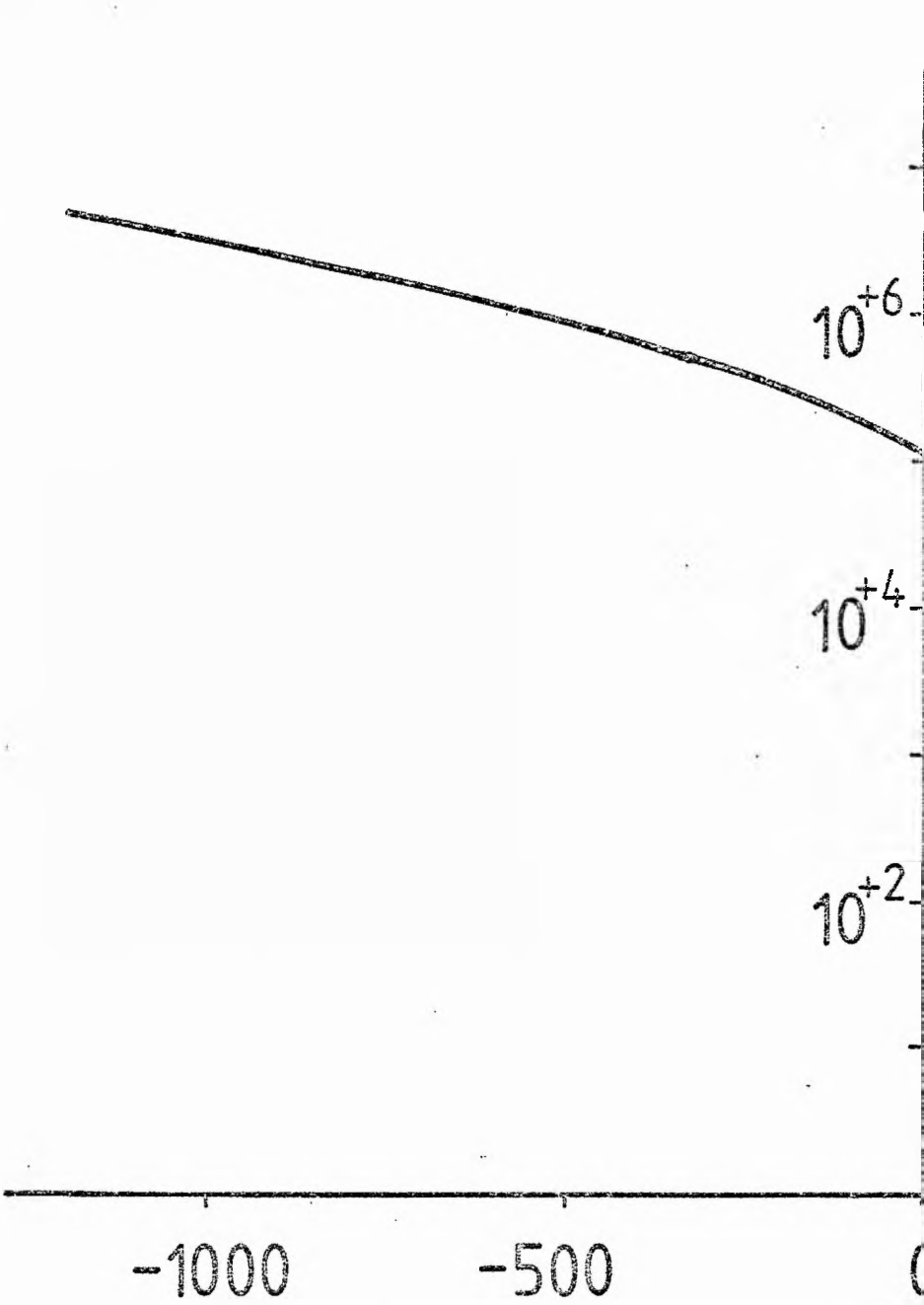

Figure 1.1 - The pressure, p , as a function of

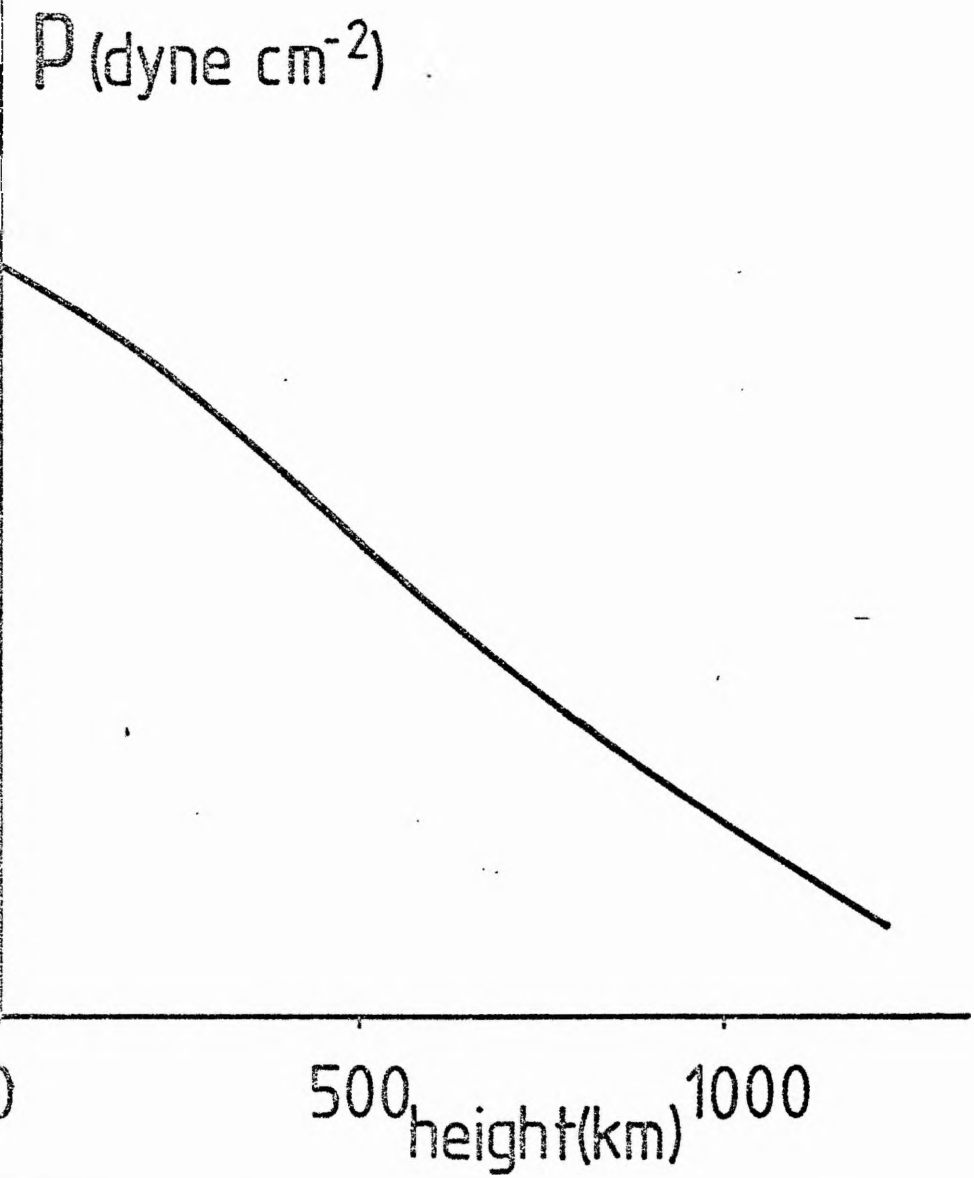

height in the solar atmosphere.

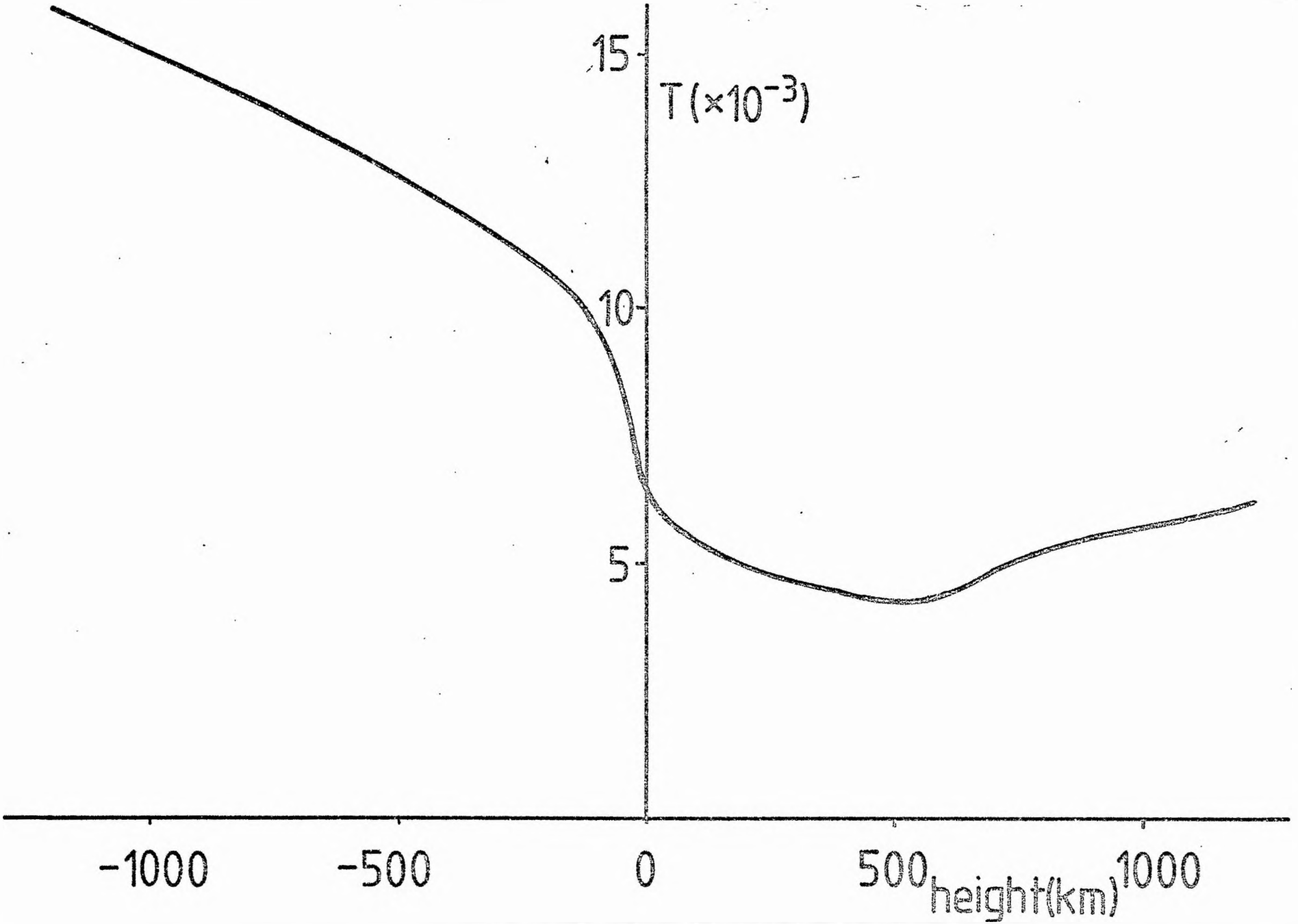

Figure 1.2 - The temperature, T, as a function of height in the solar atmosphere.

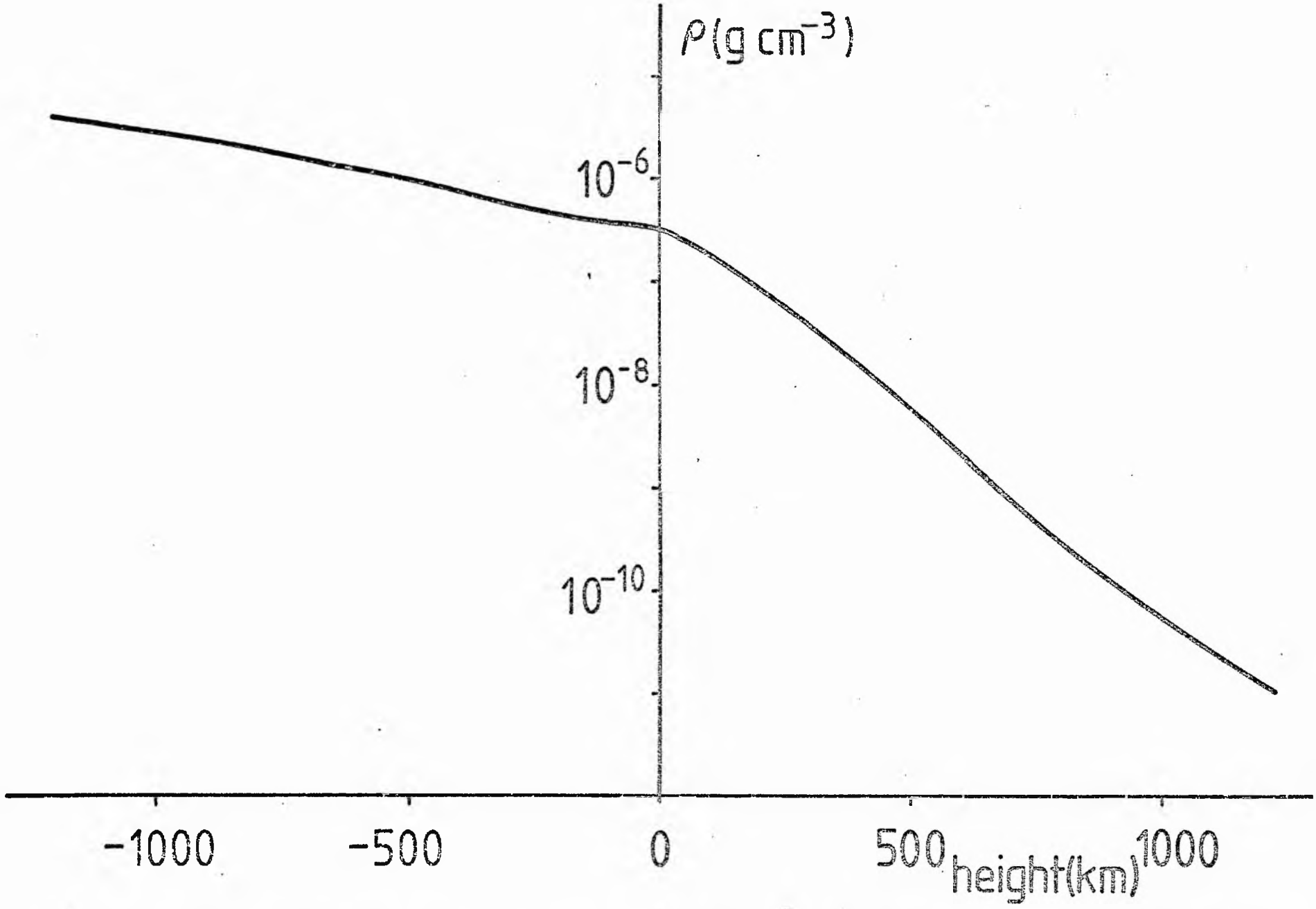

Figure 1.3 - The density, ρ, as a function of height in the solar atmosphere.

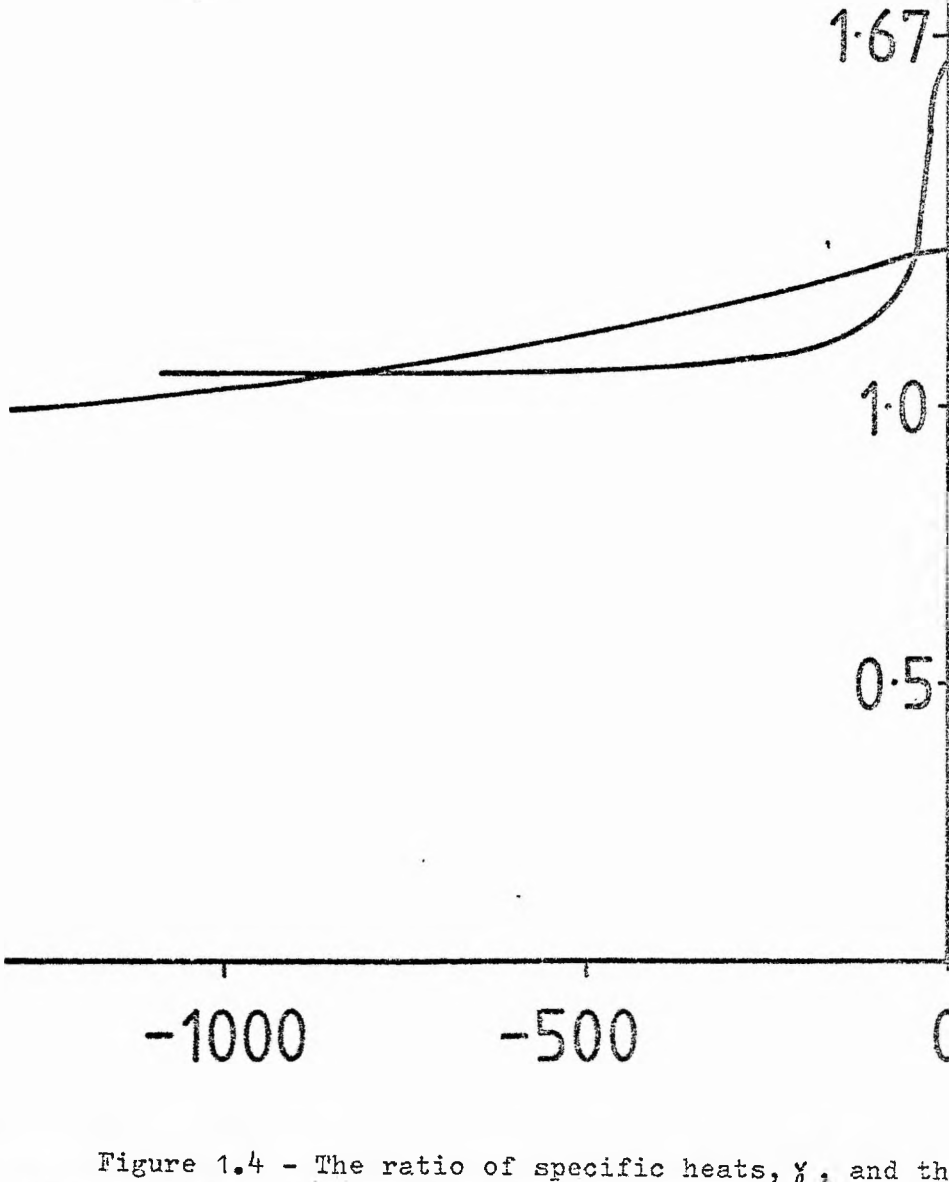

Figure 1.4 - The ratio of specific heats, γ, and th
as functions of height.

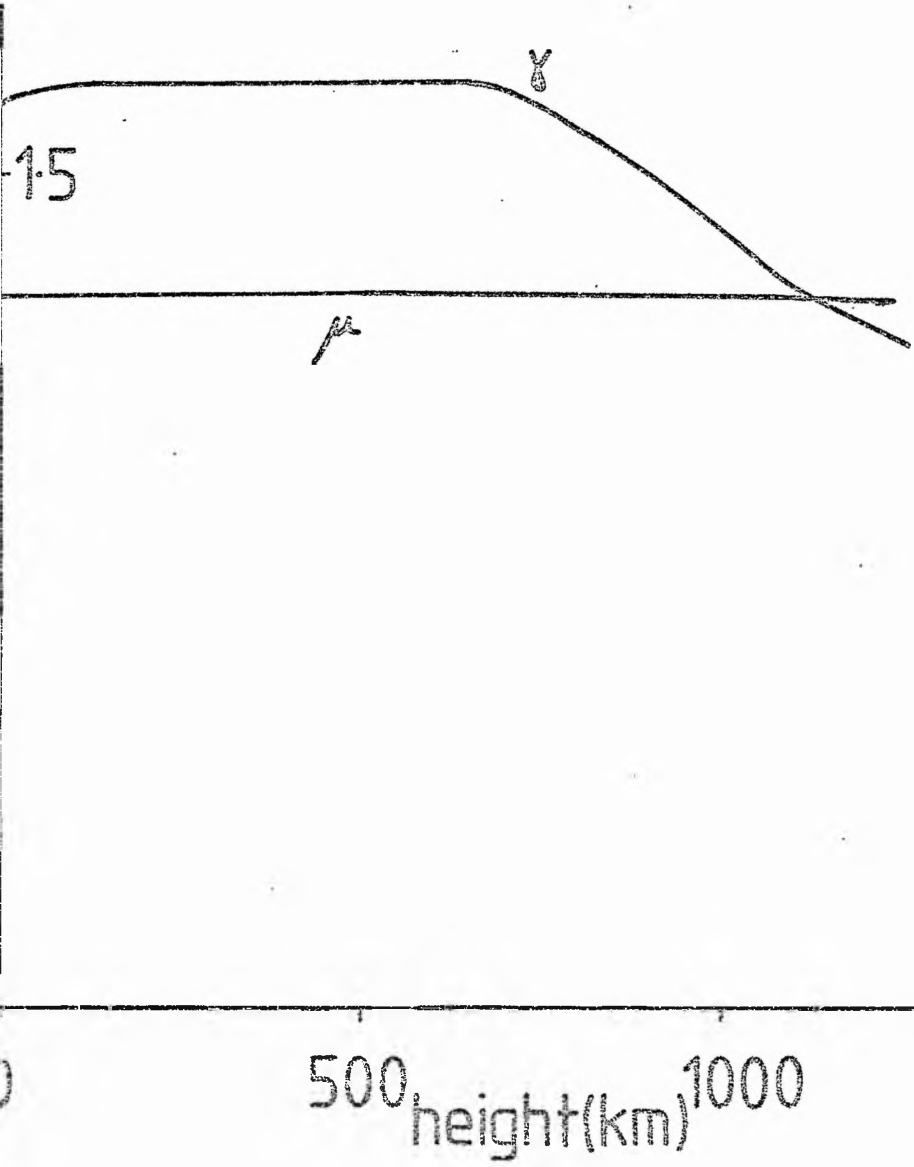

e mean molecular weight, μ,

Figure 1.5 - The square of the Brunt-Väisälä frequency, N_0^2, as a function of height.

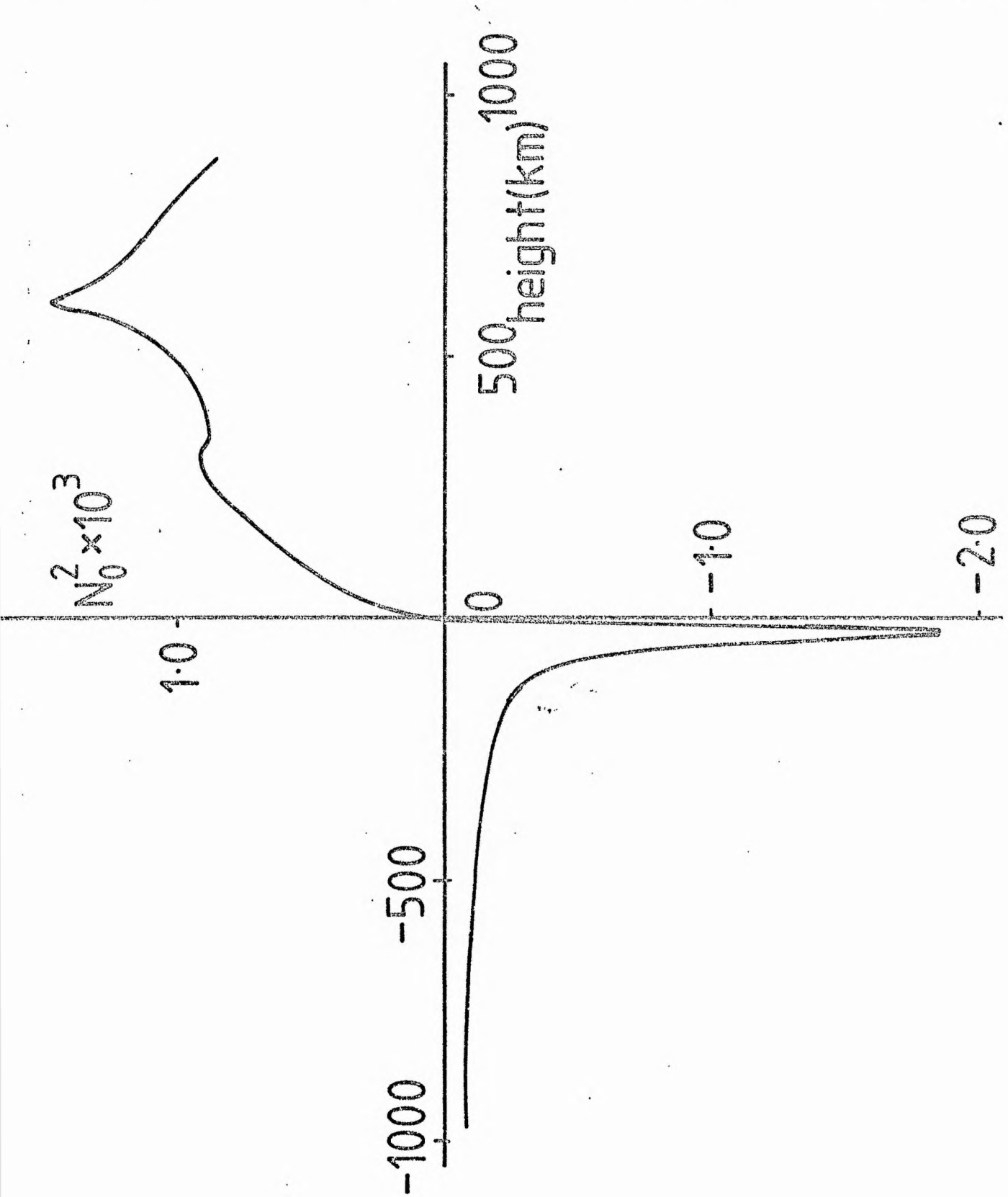

1.4 Basic Equations

In this section we present the basic equations of magnetohydrodynamics (M.H.D.) we use throughout this thesis. Unnecessary detail is omitted and further discussion may be found in some of the basic texts and reviews (e.g. Ferraro and Plumpton, 1966; Jeffrey, 1966; Roberts, 1967; Cowling, 1976).

1.4.1 Electromagnetic Equations

In an inertial frame the electric field, $\underline{E}$, and magnetic field, $\underline{H}$, satisfy Maxwell's equations

$$\nabla \wedge \underline{E} = -\frac{\partial \underline{B}}{\partial t}, \qquad (1.4.1)$$

$$\nabla \wedge \underline{H} = \underline{j} + \frac{\partial \underline{D}}{\partial t}, \qquad (1.4.2)$$

$$\nabla . \underline{D} = q, \qquad (1.4.3)$$

$$\nabla . \underline{B} = 0, \qquad (1.4.4)$$

where $\underline{j}(\underline{r},t)$ and $q(\underline{r},t)$ are the current and charge densities, $\underline{B}$ is the magnetic induction field and $\underline{D}$ is the electric displacement. In addition, for a linear homogeneous and isotropic medium, we have the two constitutive relations

$$\underline{D} = \varepsilon \underline{E}, \qquad (1.4.5)$$

$$\underline{B} = \mu \underline{H}, \qquad (1.4.6)$$

where ε and μ denote, respectively, the electrical permittivity and magnetic permeability. In general, ε and μ depend on the thermodynamic state of the medium, but for a large class of problems met in M.H.D. ε and μ may be considered constant. In a vacuum $\mu=\mu_0, \varepsilon=\varepsilon_0$ and $c=(\varepsilon_0\mu_0)^{-\frac{1}{2}}$ is the velocity of light.

The first approximation we make is the 'quasi-steady' approximation. If L is a characteristic length, and T is a

typical time-scale associated with the hydromagnetic flow, then Equations (1.4.1) and (1.4.6) give

$$\frac{|\underline{E}|}{L} \sim \mu_0 \frac{|\underline{H}|}{T} \quad . \tag{1.4.7}$$

Comparing $\frac{\partial \underline{D}}{\partial t}$ with $\nabla_\wedge \underline{H}$ in (1.4.2), and using the above relation together with Equation (1.4.5), we have

$$\left| \frac{\partial \underline{D}}{\partial t} \Big/ \nabla_\wedge \underline{H} \right| \sim \frac{\epsilon_0 |\underline{E}|}{T} \frac{L}{|\underline{H}|} \sim \mu_0 \epsilon_0 \frac{L^2}{T^2} \sim \frac{U^2}{c^2}$$

for a typical flow speed $U \sim L/T$. Thus, provided

$$\frac{U^2}{c^2} \ll 1 , \tag{1.4.8}$$

Equation (1.4.2) is replaced by Ampère's law:

$$\nabla_\wedge \underline{H} = \underline{j} , \tag{1.4.9}$$

which implies that electric currents flow in closed circuits.

An additional equation is required to establish a relationship between the current density $\underline{j}$ and electric field intensity $\underline{E}$. This is Ohm's Law. A unit electric charge moving at velocity $\underline{v}$ relative to a magnetic field $\underline{B}$ experiences a force $\underline{E} + \underline{v}_\wedge \underline{B}$, and Ohm's Law assumes the form

$$\underline{j} = \sigma (\underline{E} + \underline{v}_\wedge \underline{B}) , \tag{1.4.10}$$

where σ is the electrical conductivity of the fluid. The contribution $q\underline{v}$ to $\underline{j}$ may be neglected under the condition (1.4.8). This assumed form of Ohm's Law may require modifications and be replaced by generalized Ohm's Law (Boyd and Sanderson, 1969). However, the above form is valid provided the following conditions hold

$$\frac{1}{T\omega_p} \ll \frac{U}{c}\,,$$

$$\frac{\Omega_e}{T\omega_p^2} \ll \left(\frac{U}{c}\right)^2, \qquad (1.4.11)$$

$$\frac{1}{T\Omega_i} \ll \left(\frac{U}{c_s}\right)^2,$$

where Ω_e and Ω_i are the electron and ion cyclotron frequencies, ω_p is the plasma frequency and c_s the speed of sound.

1.4.2 Induction Equation

An important equation of M.H.D. is the induction equation, which follows from Equations (1.4.1), (1.4.6), (1.4.9) and (1.4.10):

$$\frac{\partial \underline{B}}{\partial t} = \nabla \wedge (\underline{v} \wedge \underline{B}) - \nabla \wedge (\eta \nabla \wedge \underline{B}), \qquad (1.4.12)$$

where

$$\eta = (\mu_0 \sigma)^{-1}, \qquad (1.4.13)$$

is the magnetic diffusivity. For η constant, Equation (1.4.12) may be written

$$\frac{\partial \underline{B}}{\partial t} = \nabla \wedge (\underline{v} \wedge \underline{B}) + \eta \nabla^2 \underline{B}. \qquad (1.4.14)$$

If we consider the relative magnitudes of the two terms on the right-hand side, then

$$\left| \frac{\nabla \wedge (\underline{v} \wedge \underline{B})}{\eta \nabla^2 \underline{B}} \right| \sim \frac{LU}{\eta} = R_m\,, \qquad (1.4.15)$$

where R_m is defined as the magnetic Reynolds number. For laboratory conditions R_m is generally small (for liquids like mercury or sodium in the laboratory $R_m < 1$, except for very high velocities) though in geophysical and astrophysical applications R_m is generally large.

For $R_m \ll 1$, the equation approximates to the diffusion equation:

$$\frac{\partial \underline{B}}{\partial t} = \eta \nabla^2 \underline{B}, \qquad (1.4.16)$$

and the magnetic field 'leaks' through the material and decays as oppositely-directed fields, initially at different points, leak together and neutralize each other (Cowling, 1976).

In the other extreme, $R_m \gg 1$, Equation (1.4.4) reduces to

$$\frac{\partial \underline{B}}{\partial t} = \nabla \wedge (\underline{v} \wedge \underline{B}), \qquad (1.4.17)$$

the induction equation for a perfect conductor. This resembles the equation governing vorticity in an inviscid fluid from which the Kelvin-Helmholtz vorticity theorem is derived. The corresponding result for a magnetic field is Alfvén's theorem, which states that the lines of magnetic induction are 'frozen in' the plasma.

When $R_m \gg 1$, the ratio of the terms on both sides of Ohm's Law (1.4.10) (if $E \sim UB$) is

$$\frac{j}{\sigma U B} \sim \frac{1}{R_m} \ll 1,$$

so that Ohm's Law reduces to

$$\underline{E} + \underline{v} \wedge \underline{B} = \underline{0}, \qquad (1.4.18)$$

i.e. the total electric field vanishes.

For this assumption of perfect conductivity to be valid, we require that

$$\frac{\nu_c}{T \omega_p^2} \ll \left(\frac{U}{c}\right)^2, \qquad (1.4.19)$$

where ν_c is the electron-proton collision frequency (Boyd and Sanderson, 1969).

In this thesis we make the assumption of perfect conductivity and adopt Equation (1.4.17) as the appropriate form of the induction equation.

1.4.3 Hydrodynamic Equations

i) Equation of Continuity

The first equation of hydrodynamics, the equation of continuity, expresses the conservation of mass and is written

$$\frac{\partial \rho}{\partial t} + \nabla.(\rho \underline{v}) = 0, \qquad (1.4.20)$$

where $\rho(\underline{r}, t)$ is the density.

ii) Conservation of Momentum Equation

The equation expressing conservation of momentum is

$$\rho\left(\frac{\partial \underline{v}}{\partial t} + \underline{v}.\nabla\underline{v}\right) = -\nabla p + \rho \underline{g} + \underline{F} + \rho\nu\nabla^2\underline{v} + \frac{1}{3}\rho\nu\nabla(\nabla.\underline{v}), \qquad (1.4.21)$$

where $p(\underline{r}, t)$ is the pressure, ν the kinematic viscosity, $\underline{g}$ is the acceleration due to gravity and $\underline{F}$ is the body force arising from electromagnetic and mechanical effects. For electromagnetic effects we take $\underline{F} = \underline{Fe}$ where

$$\underline{Fe} = \underline{j} \wedge \underline{B} + q\underline{E}, \qquad (1.4.22)$$

and is called the Lorentz Force. This equation represents the macroscopic form of the force produced by the electromagnetic field on a charge q, of velocity $\underline{v}$, in a vacuum. It is based on the Coulomb law for the electric field case and the Biot-Savart law for the magnetic field case. These are both experimentally established laws (Dragos, 1975). Under the quasi-static assumption (1.4.8) the electrostatic body force $q\underline{E}$ may be neglected and the Lorentz force is written

$$\underline{Fe} = \underline{j} \wedge \underline{B} \equiv (\underline{B}.\nabla)\frac{\underline{B}}{\mu_0} - \nabla\left(\frac{B^2}{2\mu_0}\right) \qquad (1.4.23)$$

The second term in the above identity for $\underline{j} \wedge \underline{B}$ represents a hydrostatic pressure of magnitude $B^2/2\mu_0$ and the first term represents a tension and pressure term, the tension being of magnitude B^2/μ_0 per unit area. So the Lorentz force has two effects; a shortening of the magnetic field lines by the tension term and a compression of the plasma by the pressure term.

Neglecting viscosity, and taking the body force $\underline{F}$ to be given by (1.4.23), the momentum equation may be written

$$\rho\left(\frac{\partial \underline{v}}{\partial t} + \underline{v}.\nabla\underline{v}\right) = -\nabla p + \rho\underline{g} + \underline{j} \wedge \underline{B}, \qquad (1.4.24)$$

which is the form we adopt in this thesis.

1.4.4 Gas Law

The equation of state for a perfect gas is

$$p = N k T, \qquad (1.4.25)$$

where T is the temperature, k Boltzmann's constant ($= 1.3807 \times 10^{-16}$ erg/K) and N represents the number of free particles per cubic centimetre. Equation (1.4.25) may be written in an alternative form by introducing the mean molecular weight, $\mu = \rho/Nm_H$, where m_H is the mass of the hydrogen atom (1.67×10^{-27}kg), thus

$$p = \frac{R}{\mu}\rho T, \qquad (1.4.26)$$

where $R = k/m_H = 8.26 \times 10^3$ JK^{-1} kg^{-1} is the gas constant.

1.4.5 The Energy Equation

The conservation of energy equation follows from the first law of thermodynamics. The change in internal energy per unit mass, e, of a fluid element is equal to the net heat added to it minus the work done by it:

$$\frac{de}{dt} = -\mathcal{L} - p\frac{d}{dt}\left(\frac{1}{\rho}\right), \qquad (1.4.27)$$

where $\mathcal{L}$ is the rate of energy loss minus the rate of energy gain per unit mass, including the effects of radiation, thermal conduction, ohmic and viscous dissipation. The quantity $p\frac{d}{dt}\left(\frac{1}{\rho}\right)$ represents the rate of working by the gas in expanding against its surroundings.

Introducing c_p and c_v, the specific heats of the gas at constant pressure and volume respectively, related by

$$c_p - c_v = \frac{R}{\mu} , \tag{1.4.28}$$

then the internal energy of an ideal gas may be written

$$e = c_v T , \tag{1.4.29}$$

$$= \frac{P}{(\gamma-1)\rho} \tag{1.4.30}$$

where $\gamma = c_p/c_v$ is the ratio of specific heats.

Equation (1.4.27) then becomes

$$\frac{\rho^\gamma}{\gamma-1}\frac{d}{dt}\left(\frac{P}{\rho^\gamma}\right) = -\rho\mathcal{L} . \tag{1.4.31}$$

When there is no heat exchange between different parts of the fluid, $\mathcal{L} \equiv 0$, and (1.4.31) reduces to

$$\frac{dP}{dt} = \frac{\gamma P}{\rho}\frac{d\rho}{dt} , \tag{1.4.32}$$

governing variations in the pressure and density of a gas under adiabatic conditions.

We shall not treat the form of $\mathcal{L}$ explicity, since for most of the discussion in this thesis, we take the perturbation of $\mathcal{L}$, to be zero in the linearized form of (1.4.31) (See Section 1.6). Thus, we shall consider for the most part a

gas undergoing adiabatic perturbations, However, in Chapter 5 we shall present a suitable form for the perturbation in $\mathcal{L}$ as appropriate for discussing the effects of radiative relaxation.

1.4.6 Discussion

Finally in this section, it is convenient to summarize the forms of the basic equations we use and to give some of the underlying assumptions and related consequences.

i) BASIC EQUATIONS

Equation of continuity:

$$\frac{\partial \rho}{\partial t} + \nabla.(\rho \underline{v}) = 0, \qquad (1.4.20)$$

Momentum Equation:

$$\rho\left(\frac{\partial \underline{v}}{\partial t} + \underline{v}.\nabla\underline{v}\right) = -\nabla p + \rho \underline{g} + \underline{j} \wedge \underline{B}, \qquad (1.4.24)$$

Induction Equation:

$$\frac{\partial \underline{B}}{\partial t} = \nabla \wedge (\underline{v} \wedge \underline{B}), \qquad (1.4.17)$$

Energy Equation:

$$\frac{\rho^{\gamma}}{\gamma - 1} \frac{d}{dt}\left(\frac{p}{\rho^{\gamma}}\right) = -\rho \mathcal{L}, \qquad (1.4.31)$$

Gas Law:

$$p = \frac{R}{\mu} \rho T, \qquad (1.4.26)$$

Ampere's Law:

$$\underline{j} = \frac{1}{\mu_0} \nabla \wedge \underline{B}, \qquad (1.4.9)$$

Solenoidal condition:

$$\nabla.\underline{B} = 0. \qquad (1.4.4)$$

ii) VALIDITY OF THE BASIC EQUATIONS

Firstly, we have made the quasi-static approximation: $(U/c)^2 \ll 1$, where U is a characteristic velocity of the system and c is the speed of light. The neglect of terms of order $(U/c)^2$ in Equations (1.4.22), (1.4.9) and (1.4.10) filters out the electromagnetic waves

Plasma oscillations are automatically excluded by taking Ohm's law (Equation (1.4.10) as the relationship between the current and the effective electric field (Acheson and Hide, 1973). The assumed form of Ohm's law may require modifications (Generalized Ohm's law).

We have treated the plasma as a continuum with the pressure as a scalar. The plasma is described by a single fluid and we have neglected the effects of viscosity and rotation.

The assumption of perfect conductivity is valid for $R_m \gg 1$. In the photosphere, $\eta \approx 3\times10^{8} T^{-3/2} m^{2} s^{-1}$ (Spitzer, 1962), and so for $T \approx 6\times10^{3}$K, L ≈ 150km and U ≈ 1km s^{-1}, we have $R_m \approx 2\times10^{5}$.

We shall consider the validity of the adiabatic law for the perturbations in Section 1.6. In the following section we discuss the appropriate boundary conditions.

1.5 Boundary Conditions

The relevant boundary conditions may be obtained from the integral forms of the appropriate equations, applying these forms at a boundary (Jeffrey, 1966). For a fluid-fluid interface the boundary conditions are (Bernstein et al, 1958; Jackson, 1975)

$$\left\langle p + \frac{B^2}{2\mu_0} \right\rangle = 0, \qquad (1.5.1)$$

$$\underline{n} \cdot \langle \underline{v} \rangle = 0, \qquad (1.5.2)$$

$$\underline{n} \wedge \langle \underline{E} \rangle = (\underline{n} \cdot \underline{v}) \langle \underline{B} \rangle \qquad (1.5.3)$$

$$\underline{n} \cdot \langle \underline{B} \rangle = 0, \qquad (1.5.4)$$

$$\underline{n} \wedge \langle \underline{B} \rangle = \underline{K}, \qquad (1.5.5)$$

where $\underline{n}$ is the unit normal to the surface, $\underline{K}$ is an idealised surface current density flowing exactly on the boundary surface and $\langle X \rangle$ denotes the jump across the boundary of the physical quantity X.

Equations (1.5.1), (1.5.2) and (1.5.4) express the continuity across the boundary of the total pressure and the normal components of the velocity and magnetic field. In Equation (1.5.5) it is understood that the surface current $\underline{K}$ has only components parallel to the surface at every point (Jackson, 1975) and this equation states that the tangential component of $\underline{B}$ is discontinuous by an amount whose magnitude is equal to K and whose direction is parallel to $\underline{K} \wedge \underline{n}$.

1.6 The Linearized Equations

Throughout this thesis we shall consider the propagation of waves governed by linear theory. The use of linear theory implies that we consider disturbances so weak that in the equations of motion we can view them as small quantities whose products are negligible. The governing equations are those listed in Section 1.4 and we linearize these equations by regarding as small quantities all departures from a basic state, where the magnetic field, pressure, density, temperature

and energy loss term are given by $\underline{B}_0(\underline{r})$, $p_0(\underline{r})$, $\rho_0(\underline{r})$, $T_0(\underline{r})$ and $\mathcal{L}_0$ respectively.

The basic state ($\underline{v} = 0$) satisfies the equations:

$$0 = -\nabla p_0(\underline{r}) + \rho_0(\underline{r})\underline{g} + \underline{j}_0(\underline{r}) \wedge \underline{B}_0(\underline{r}), \tag{1.6.1}$$

$$0 = \mathcal{L}_0, \tag{1.6.2}$$

$$p_0(\underline{r}) = \frac{R}{\mu} \rho_0(\underline{r}) T_0(\underline{r}), \tag{1.6.3}$$

$$\nabla . \underline{B}_0(\underline{r}) = 0, \quad \mu_0 \underline{j}_0(\underline{r}) = \nabla \wedge \underline{B}_0(\underline{r}). \tag{1.6.4}$$

Consider small amplitude perturbations $\underline{v}'(\underline{r},t)$, $\underline{b}'(\underline{r},t)$, $p'(\underline{r},t)$, $\rho'(\underline{r},t)$, $T'(\underline{r},t)$ and $\mathcal{L}'$ about the above basic state so that

$$\underline{B} = \underline{B}_0(\underline{r}) + \underline{b}'(\underline{r},t),$$

$$p = p_0(\underline{r}) + p'(\underline{r},t), \text{ etc.}$$

Then the equations of motion become

$$\frac{\partial \rho'}{\partial t} + \nabla . (\rho_0 \underline{v}') = 0, \tag{1.6.5}$$

$$\rho_0 \frac{\partial \underline{v}'}{\partial t} = -\nabla p' + \rho' \underline{g} + \underline{j}_0 \wedge \underline{b}' + \underline{j}' \wedge \underline{B}_0, \tag{1.6.6}$$

$$\frac{\partial \underline{b}'}{\partial t} = \nabla \wedge (\underline{v}' \wedge \underline{B}_0), \tag{1.6.7}$$

$$\frac{1}{\gamma - 1}\left\{\frac{dp'}{dt} - c_0^2 \frac{d\rho'}{dt}\right\} = -\rho_0 \mathcal{L}', \tag{1.6.8}$$

$$p' = \frac{R}{\mu}(\rho_0 T' + \rho' T_0), \tag{1.6.9}$$

$$\nabla . \underline{b}' = 0, \quad \mu_0 \underline{j} = \nabla \wedge \underline{b}', \tag{1.6.10}$$

where $c_0 = (\gamma p_0/\rho_0)^{\frac{1}{2}}$ is the adiabatic speed of sound and we have neglected second order quantities:

$$|\underline{v}'.\nabla\underline{v}'| \ll \left|\frac{\partial \underline{v}'}{\partial t}\right|, \quad |\underline{j}' \wedge \underline{b}'| \ll |\underline{j}_0 \wedge \underline{b}'|, \text{ etc.}$$

Apart from Chapter 5, where we discuss the effect of radiative relaxation on the waves propagating in an intense magnetic flux tube, we shall take $\mathcal{L}' \equiv 0$ in this thesis. The assumption that the waves propagate adiabatically is a good approximation in those layers of the convection zone where there is a large superadiabatic temperature gradient (a depth of 50 - 600 km below $\tau_{5000} = 1$), since the opacity of the gas is high there, but it fails near the surface ($\tau_{5000} = 1$) where radiative exchange is rapid (Spruit and Zweibel, 1979). Nevertheless the analysis is simplified considerably by neglecting heat exchange. The boundary conditions for the basic state described by (1.6.1) - (1.6.4) and for the linearized equations (1.6.5) - (1.6.10) follow from Section (1.5.1). In particular the basic state satisfies the condition

$$p_0 + \frac{B_0^2}{2\mu_0} \quad \text{continuous across the boundary,} \tag{1.6.11}$$

and the perturbations satisfy

$$\left.\begin{array}{l} p' + \dfrac{\underline{B}_0.\underline{b}'}{\mu_0} \\ \underline{v}'.\underline{n} \end{array}\right\} \quad \text{continuous across the boundary.} \tag{1.6.12, 1.6.13}$$

The above boundary conditions for the perturbations may be applied at the equilibrium position of the interface provided that the disturbance of the surface is sufficiently small (Lighthill, 1978).

1.7 Outline of the thesis

In this chapter we have given a general description of the small-scale solar magnetic field network found at the boundaries of the supergranular cells. Following a brief discussion of models of these tubes and of the mean solar atmosphere, the relevant equations of motion were presented. Finally, the linearized equations of motion describing small-amplitude disturbances were derived. The remainder of this thesis relies, on the whole, on this system of equations.

Before confining ourselves to a discussion of waves in tubes, we review, in the following chapter, some of the theory of waves in an unbounded atmosphere. Firstly, we give a discussion of waves arising when each of the restoring forces due to gravity, compressibility and the magnetic field acts separately. In the Sun, of course, these forces do not occur in isolation and so we proceed to consider waves resulting from the interaction of two of the forces. The chapter concludes with a discussion of magneto-acoustic-gravity waves.

Chapter 3 deals with waves in magnetic flux tubes and is divided into two main parts. The first considers propagation in a uniform tube and derives a dispersion relation for the modes of vibration. This is solved numerically for a tube of arbitrary radius, but of particular interest are the solutions for a slender tube and analytic approximations are obtained for these. For a slender tube two modes exist: a slow mode-type wave (tube wave) and a sound wave. In the second part the important effect of gravity is included and an equation for the vertical velocity perturbation is derived.

The behaviour of motions within the flux tube is shown to depend upon a transition frequency ω_v, such that vertically propagating waves are possible only for frequencies greater than ω_v. The results are applied to the solar atmosphere using Spruit's (1974) model and the HSRA.

In Chapter 4 the nature of convective instability in a slender magnetic flux tube is explored. A sufficient condition for stability is derived for the case of an arbitrary temperature profile in the external medium. The discussion allows for the possibility of a temperature difference between the interior and exterior of the tube. Special cases of the sufficiency condition reduce to Schwarzschild's criterion and its generalisation by Gough and Tayler (1966). The distribution of stable and unstable eigenvalues, for the particular case of a linear temperature profile, is discussed in detail. For a tube of infinite depth, with a uniform temperature gradient inside the tube equal to that in the ambient medium, a necessary and sufficient condition for convective stability to occur inside the tube is derived. The stable modes form a continuous spectrum; the unstable modes are discrete and infinite in number. In a tube of finite depth d, with a linear temperature profile, a necessary and sufficient condition for convective stability is derived. There exists a critical depth d* such that tubes of depth d are stable if and only if $d < d^*$. The critical depth d* is determined for a wide range of conditions, and the results applied to the Sun. Under the assumptions of the model, intense flux tubes are convectively stable if sufficiently shallow (with depths $1\text{-}2\times10^3$km or less).

Tubes that extend deeper into the solar convection zone are potentially (convectively) unstable, but may be stabilised for sufficiently strong magnetic fields (typically greater than about a kilogauss). The observed downdrafts inside intense flux tubes, if a manifestation of convective instability, are thus likely to be a transient phenomenon in which the field inside the tube is further intensified until hydrostatic equilibrium obtains. Convective instability in a flux tube is thus a possible means of achieving kilogauss field strengths.

Radiative damping of waves is important in the upper photosphere. It is thus of interest to examine the effect of radiative relaxation on the propagation of waves in an intense magnetic flux tube embedded in a uniform atmosphere. Assuming Newton's law of cooling, it is shown in Chapter 5 that the radiative energy loss leads to wave damping. Both the 'damping per wavelength' and the 'damping per period' reach maximum value when the sound and radiative timescales are comparable. The stronger the magnetic field the greater the damping. In a stratified atmosphere the radiative energy loss leads to a decrease in the vertical phase velocity of the waves, and to a damping of the amplitude for those waves with frequencies greater than the adiabatic value (ω_v) of the tube cut-off frequency. The cut-off frequency is generalized to include the effects of radiative relaxation, and allows the waves to be classified as 'mainly progressive' or 'mainly damped'. The phase-shift between velocity oscillations at two different levels and the phase-difference between temperature and velocity perturbations are compared with the available observations.

Chapter 6 discusses the consequences of the steady downflow observed within flux tubes. It is shown that for the flow to decrease in magnitude with height, as observed by Giovanelli and Slaughter (1978), then the interior of the tube must be significantly hotter than the exterior at photospheric levels. This temperature excess decreases with height. The results are compared with observations and models of faculae.

Finally, the main results of the thesis are summarized in Chapter 7 and suggestions for improvements and further work are made.

Chapter 2 : WAVES IN AN UNBOUNDED ATMOSPHERE

2.1 Introduction

The subject of wave propagation in an unbounded atmosphere has been widely treated in the fluid dynamics literature (see, for example, Tolstoy, 1973; Lighthill, 1978), and, in particular, wave propagation in the solar atmosphere has received considerable attention and has been reviewed by Schatzman and Souffrin (1967), Stein and Leibacher (1974) (See also Bray and Loughhead, 1974, chapter 6; Athay, 1976) and Michalitsanos (1973b), who considered the theoretical interpretations of the five-minute period oscillation. The theory of wave propagation is a complex one, particularly when restoring forces due to gravity, compressibility and a magnetic field are all important. Before we consider the nature of waves in magnetic flux tubes, we shall present in this chapter a summary of the propagation of waves in a compressible, gravitationally-stratified, but unbounded, atmosphere. Also, in Section 2.2 we derive some new results concerning propagation in a vertical magnetic field.

The three restoring forces arising in a compressible, gravitationally-stratified atmosphere with a magnetic field, are the buoyancy force due to gravitational stratification, the pressure force due to compressibility and magnetic forces due to the magnetic pressure and tension. With all three forces, the wave modes occurring (magneto-acoustic-gravity waves), are naturally very complex, though attempts to investigate these waves using the local dispersion relation of McLellan and Winterberg (1968) have been made by a number of authors (e.g. Bel and Mein, 1971; Michalitsanos, 1973a; Bel and Leroy, 1977).

However, in order to gain some understanding of the nature of waves under the action of three restoring forces, we shall discuss, initially, the wave modes which arise when only one of the forces acts. Then we shall consider the coupling of two types of wave. Firstly, though, we shall derive the general wave equation. We shall assume that variations are nearly adiabatic, which is valid in the chromosphere but not in the photosphere (see Chapter 5). The linearized equations of motion for an inviscid, perfectly-conducting gas undergoing adiabatic perturbations are Equations (1.6.5) - (1.6.10), with $\mathcal{L}' \equiv 0$, and we now denote the perturbations by p, ρ, $\underline{b}$ etc. Differentiating Equation (1.6.6) with respect to t and eliminating the time derivatives $\frac{\partial \underline{v}}{\partial t}$, $\frac{\partial p}{\partial t}$ and $\frac{\partial \underline{b}}{\partial t}$ using (1.6.5), (1.6.7) and (1.6.8) we obtain the wave equation (Bray and Loughhead, 1974)

$$\frac{\partial^2 \underline{v}}{\partial t^2} = c_0^2 \nabla(\nabla.\underline{v}) + (\gamma-1)\underline{g}\nabla.\underline{v} + \nabla(\underline{v}.\underline{g}) - \frac{1}{\mu_0 \rho_0} \underline{B}_0 \wedge \left\{\nabla \wedge [\nabla \wedge (\underline{v} \wedge \underline{B}_0)]\right\} , \quad (2.1.1)$$

governing the propagation of waves through a compressible, horizontally-stratified fluid with magnetic field $\underline{B}_0$, pressure p_0 and density ρ_0.

2.1.1 Sound Waves

Perhaps the simplest type of motion of an atmosphere takes place when locally a compression occurs. The result is known as a sound wave. With $\underline{g} \equiv \underline{0}$ and $\underline{B}_0 \equiv \underline{0}$, Equation (2.1.1) gives the result that $\nabla.\underline{v}$ is propagated at the sound speed c_0:

$$\frac{\partial^2}{\partial t^2} \nabla.\underline{v} = c_0^2 \nabla^2 (\nabla.\underline{v}) \quad , \quad (2.1.2)$$

while $\nabla \wedge \underline{v}$ remains unchanged with time. The macroscopic motions

of the gas are in the direction of propagation, so we say this is a longitudinal wave. For a harmonic wave of frequency ω and wavenumber $\underline{K} = (k_x, k_y, k_z)$, $\underline{v}(\underline{r},t) = \underline{v} \exp i(\omega t - \underline{K}.\underline{r})$, the dispersion relation is

$$\omega^2 = K^2 c_0^2 \quad . \tag{2.1.3}$$

The phase velocity, or wave speed (velocity of propagation of a given phase of a sinusoidal wave such as the crest in the direction of the wave vector $\underline{K}$) is given by

$$\frac{\omega}{K} = c_0 \ , \tag{2.1.4}$$

whilst the group velocity (the velocity of wave energy propagation) is

$$\frac{\partial \omega}{\partial \underline{K}} = c_0 \hat{\underline{K}} \ . \tag{2.1.5}$$

Thus phase and energy propagate in the same direction at the sound speed.

2.1.2 Internal Gravity Waves

When the restoring force is buoyancy, the waves are internal gravity waves, and a detailed discussion of these waves may be found in Lighthill (1978, chapter 4), whose treatment we follow closely (see also Schwarzschild, 1958).

Consider an equilibrium distribution of density, $\rho_0(z)$, continuously decreasing with height. The equilibrium distribution of pressure, $p_0(z)$, is given by the hydrostatic law

$$\frac{dp_0(z)}{dz} = - \rho_0(z) g. \tag{2.1.6}$$

Suppose that a particle of fluid is displaced from a height z to $z + \zeta$. Suppose also that the element remains in pressure equilibrium with its surroundings and that density changes within the element are adiabatic. The movement of the element brings it to a region where the equilibrium density takes the value

$$\rho_e = \rho_0(z) + \zeta \rho_0'(z), \quad \text{with} \quad \rho_0'(z) < 0 , \tag{2.1.7}$$

and where the pressure is reduced to

$$p_e = p_0(z) - \rho_0(z) g \zeta . \tag{2.1.8}$$

(A subscript e (i) will be used to denote equilibrium values outside (inside) the element at the height $z + \zeta$).

The pressure inside the element is also given by (2.1.8) since $p_i = p_e$ by our assumption of pressure equality, whilst the density is reduced to

$$\rho_i = \rho_0(z) - \frac{\rho_0(z) g \zeta}{c_0^2(z)} . \tag{2.1.9}$$

The element has an excess density over its surroundings of

$$\rho_i - \rho_e = - \left(\rho_0' + \frac{g \rho_0}{c_0^2}\right) \zeta , \tag{2.1.10}$$

and, hence, the fluid experiences a buoyancy force per unit volume

$$g(\rho_e - \rho_i) = \zeta g \left(\rho_0' + \frac{g \rho_0}{c_0^2}\right) . \tag{2.1.11}$$

If the buoyancy force alone acts on the element of fluid, its equation of motion is

$$\frac{\partial^2 \zeta}{\partial t^2} = - N_0^2 \zeta , \tag{2.1.12}$$

where N_0, the Brunt - Väisälä frequency, is given by

$$N_0^2 = -g\left(\frac{\rho_0'}{\rho_0} + \frac{g}{c_0^2}\right) . \qquad (2.1.13)$$

Provided the condition

$$N_0^2 > 0 \qquad (2.1.14)$$

is satisfied, the displaced element of fluid will oscillate with frequency N_0. The condition (2.1.14) is the criterion for convective stability (Schwarzschild, 1958). If $N_0^2 < 0$, the displaced element will not oscillate about its equilibrium position, but continue to move upwards. Gravity waves, therefore, can only propagate where the condition (2.1.14) is satisfied and so cannot propagate in the solar convection zone. Internal gravity waves and convection may be considered as stable and unstable manifestations of the same mode (Stein and Leibacher, 1974). Gravity waves are transverse waves and cannot propagate vertically, since the buoyancy force is an interaction between elements of different density situated at the same level, a situation precluded by vertical propagation (Schatzman and Souffrin, 1967).

The dispersion relation for internal gravity waves may be derived using the Boussinesq approximation, in which the term $\frac{\partial \rho}{\partial t}$ is neglected in the equation of continuity, which then becomes

$$\nabla.(\rho_0 \underline{v}) = 0 . \qquad (2.1.15)$$

This equation, together with the linearized equation of momentum (1.6.6) and the value of the excess density (2.1.10) leads to an equation for q, the z-component of $\rho_0 \underline{v}$ (Lighthill, 1978)

$$\nabla^2\left(\frac{\partial^2 q}{\partial t^2}\right) = -N_0^2(z)\left(\frac{\partial^2 q}{\partial x^2} + \frac{\partial^2 q}{\partial y^2}\right) . \qquad (2.1.16)$$

For $N_0^2(z)$ constant, we may seek plane wave solutions of the form

$$q = q_1 \exp i(\omega t - \underline{K}.\underline{r}),$$

from which the dispersion relation is

$$\omega^2 = N_0^2 \frac{k_x^2 + k_y^2}{k_x^2 + k_y^2 + k_z^2} , \qquad (2.1.17)$$

or

$$\omega^2 = N_0^2 \sin^2\theta , \qquad (2.1.17)'$$

where $\theta = \cos^{-1}(\frac{\underline{K}.\hat{z}}{K})$ is the angle between the direction of propagation and the z-axis. Equation (2.1.17)' shows immediately that gravity waves can propagate only with frequencies $\omega \leq N_0$.

The velocity $\underline{v}$ may be expressed in terms of q by

$$\underline{v} = \frac{1}{\rho_0}\left[- \frac{k_x k_z}{k_x^2 + k_y^2} , - \frac{k_y k_z}{k_x^2 + k_y^2} , 1 \right] q , \qquad (2.1.18)$$

and so we have

$$\underline{v}.\underline{K} \equiv 0 . \qquad (2.1.19)$$

Thus, for purely vertical motion, so that the direction of propagation lies in the horizontal plane by Equation (2.1.19), Equation (2.1.17) gives $\omega^2 = N_0^2$, in agreement with our parcel of fluid argument.

The group velocity, $\underline{V}g$, is given by (Lighthill, 1978)

$$\underline{V}g = (\frac{\partial\omega}{\partial k_x}, \frac{\partial\omega}{\partial k_y}, \frac{\partial\omega}{\partial k_z}) = \frac{N_0 k_z}{k_x^2 + k_y^2 + k_z^2}\left[\frac{k_x k_z, k_y k_z, - k_x^2 - k_y^2}{(k_x^2 + k_y^2)^{\frac{1}{2}}(k_x^2 + k_y^2 + k_z^2)^{\frac{1}{2}}} \right], \qquad (2.1.20)$$

where the factor in square brackets is the unit vector perpendicular to $\underline{K}$, and so

$$\underline{V}g.\underline{K} = 0 . \qquad (2.1.21)$$

That is, the group velocity is perpendicular to the phase velocity. Equation (2.1.20) shows that the vertical component of the group velocity has the opposite sign to the vertical component of the phase velocity and therefore for waves whose phase is upward propagating, the energy propagation has a downward component and vice versa.

2.1.3 Alfvén Waves

When magnetic tension is the restoring force, the resulting waves are Alfvén waves (see Cowling (1976, Chapter 3)). Using the analogy with elastic strings, Alfvén recognised that transverse waves propagating along the lines of force might be generated by 'plucking' the tubes of force (Boyd and Sanderson, 1969). If the analogy is valid, then the velocity, v_A, of these waves would be $(T/\rho)^{\frac{1}{2}}$, T being the tension in the 'magnetic string' and ρ the density of the fluid. In Chapter 1, we showed that the stresses, caused in a fluid by a magnetic field, give rise to a hydrostatic pressure $B_0^2/2\mu_0$ together with a tension B_0^2/μ_0 along the field lines. We would anticipate, then, that

$$v_A = B_0/(\mu_0\rho)^{\frac{1}{2}} .$$

Consider a uniform magnetic field $\underline{B} = B_0\hat{\underline{z}}$, permeating a uniform, incompressible fluid of pressure p_0 and density ρ_0. Suppose that this (static) equilibrium is disturbed in a certain region so that the magnetic field, velocity and pressure are given by

$$\underline{B} = \underline{B}_0 + \underline{b} , \qquad (2.1.22)$$

$$\underline{v} = \underline{v} , \qquad (2.1.23)$$

$$p = p_0 + p' , \qquad (2.1.24)$$

where $\left|\frac{b}{B_0}\right| \ll 1$, $\left|\frac{v}{c_0}\right| \ll 1$ and $\left|\frac{p'}{p_0}\right| \ll 1$ are the usual conditions for linearization. The linearized induction equation (1.6.7) becomes

$$\frac{\partial \underline{b}}{\partial t} = B_0 \frac{\partial \underline{v}}{\partial z} , \tag{2.1.25}$$

whilst the momentum equation may be written

$$\rho_0 \frac{\partial \underline{v}}{\partial t} = -\nabla\left(p' + \frac{B_0 b_z}{\mu_0}\right) + \frac{B_0}{\mu_0}\frac{\partial \underline{b}}{\partial z} . \tag{2.1.26}$$

Taking the divergence of (2.1.26) it follows, since $\nabla.\underline{v} = \nabla.\underline{b} = 0$, that

$$\nabla^2\left(p' + \frac{B_0 b_z}{\mu_0}\right) = 0 . \tag{2.1.27}$$

Now, away from the perturbed zone of the fluid, p' and b_z are zero. Therefore, since $p' + \frac{B_0 b_z}{\mu_0}$ is a solution of Laplace's equation which is constant outside the region of perturbation, it must be constant everywhere. So (2.1.26) becomes

$$\rho_0 \frac{\partial \underline{v}}{\partial t} = \frac{B_0}{\mu_0}\frac{\partial \underline{b}}{\partial z} . \tag{2.1.28}$$

Combining (2.1.25) and (2.1.28) gives

$$\frac{\partial^2 \underline{b}}{\partial t^2} = v_A^2 \frac{\partial^2 \underline{b}}{\partial z^2}$$

and

$$\frac{\partial^2 \underline{v}}{\partial t^2} = v_A^2 \frac{\partial^2 \underline{v}}{\partial z^2} , \tag{2.1.29}$$

where the Alfvén speed, v_A, is given by

$$v_A = B_0/(\mu_0\rho_0)^{\frac{1}{2}} . \tag{2.1.30}$$

For perturbations of the form $\exp i(\omega t - k_z z)$, Equation (2.1.29) gives the dispersion relation for Alfvén waves:

$$\omega^2 = k_z^2 v_A^2 . \qquad (2.1.31)$$

The phase speed ω/K is therefore

$$\frac{\omega}{K} = v_A \cos\theta , \qquad (2.1.32)$$

where $\theta = \cos^{-1}(\hat{\underline{z}}.\frac{\underline{K}}{K})$, and the group velocity, $\underline{V}g$, is given by

$$\underline{V}g = \frac{\partial\omega}{\partial\underline{K}} = (0,0,v_A) . \qquad (2.1.33)$$

The group velocity is along the magnetic field and is equal to the Alfvén speed, while the phase velocity is always less than or equal to v_A.

2.1.4 Acoustic-gravity Waves

The previous sections have considered the wave modes resulting from each of the restoring forces in turn: the pressure force (sound waves), buoyancy (gravity waves) and magnetic tension (Alfvén waves). We now investigate waves arising from the combined action of pressure and gravity. These are known as acoustic-gravity waves. The governing wave equation is (2.1.1) with $\underline{B}_0 \equiv \underline{0}$:

$$\frac{\partial^2\underline{v}}{\partial t^2} = c_0^2\nabla(\nabla.\underline{v}) + (\gamma-1)\underline{g}\nabla.\underline{v} + \nabla(\underline{v}.\underline{g}) , \qquad (2.1.34)$$

derived, for example, by Lamb (1945).

We shall consider waves whose wave vector, $\underline{K}$, lies in the x - z plane ($k_y \equiv 0$) and, writing $\underline{v} = (v_x, v_y, v_z)$, Equation (2.1.34) gives $v_y = 0$ and two coupled equations for v_x and v_z:

$$(-g + c_0^2(z)\frac{\partial}{\partial z})\frac{\partial v_z}{\partial x} = (-c_0^2(z)\frac{\partial^2}{\partial x^2} + \frac{\partial^2}{\partial t^2})v_x , \qquad (2.1.35)$$

and

$$\left(\frac{\partial^2}{\partial t^2} + \gamma g \frac{\partial}{\partial z} - c_0^2(z)\frac{\partial^2}{\partial z^2}\right) v_z = \left(-(\gamma-1)g + c_0^2(z)\frac{\partial}{\partial z}\right)\frac{\partial v_x}{\partial x} . \quad (2.1.36)$$

For perturbations of the form

$$v_z = \hat{v}_z(z)e^{i\omega t - ik_x x} , \quad v_x = \hat{v}_x(z)e^{i\omega t - ik_x x} ,$$

Equations (2.1.35) and (2.1.36) may be combined to give (e.g. Uchida, 1965)

$$A_0\frac{d^2\hat{v}_z}{dz^2} - \left(\frac{A_0}{\Lambda_0} + A_0'\right)\frac{d\hat{v}_z}{dz} + \left(\frac{A_0^2}{c_0^2} + (\gamma-1)\frac{k_x^2 g^2}{\omega^2 c_0^2}A_0 + \frac{gk_x^2}{\omega^2}A_0'\right)\hat{v}_z = 0 , \quad (2.1.37)$$

where

$$A_0 = \omega^2 - k_x^2 c_0^2 , \quad (2.1.38)$$

and $\Lambda_0 = RT_0/\mu g$ is the temperature scale-height.

Note that Equation (2.1.37) has a regular singularity at $z = z_c$, where $A_0(z_c) = 0$. We shall discuss this further but firstly, we shall consider a number of special cases of Equation (2.1.37).

INCOMPRESSIBILITY

An incompressible fluid can sustain gravitational waves but not acoustic waves. The adiabatic law is replaced by the condition

$$\nabla\cdot\underline{v} = 0 , \quad (2.1.39)$$

and we may derive an equation for $\hat{v}_z$ (Jones, 1976)

$$\frac{d^2\hat{v}_z}{dz^2} + \frac{1}{\rho_0}\frac{d\rho_0}{dz}\frac{d\hat{v}_z}{dz} - k_x^2\left(1 + \frac{g}{\omega^2\rho_0}\frac{d\rho_0}{dz}\right)\hat{v}_z = 0 , \quad (2.1.40)$$

which may also be obtained by allowing γ to tend to infinity in Equation (2.1.37).

BOUSSINESQ APPROXIMATION

This approximation assumes not only that the fluid is incompressible, but also that density variations may be ignored except insofar as they influence buoyancy. The resulting equation for $\hat{v}_z$ is

$$\frac{d^2\hat{v}_z}{dz^2} - k_x^2\left(1 + \frac{g}{\omega^2\rho_0}\frac{d\rho_0}{dz}\right)\hat{v}_z = 0 \ , \qquad (2.1.41)$$

which, for $\frac{1}{\rho_0}\frac{d\rho_0}{dz}$ constant, gives

$$\omega^2 = -\frac{\frac{g}{\rho_0}\frac{d\rho_0}{dz}k_x^2}{k_x^2 + k_z^2} \ . \qquad (2.1.42)$$

for plane wave solutions $v_z \sim e^{i\omega t - ik_z z - ik_x x}$.

VERTICAL PROPAGATION

For purely vertical propagation, $k_x = 0$, Equation (2.1.37) describes sound waves in a stratified atmosphere:

$$\frac{d^2\hat{v}_z}{dz^2} - \frac{1}{\Lambda_0}\frac{d\hat{v}_z}{dz} + \frac{\omega^2}{c_0^2}\hat{v}_z = 0 \ , \qquad (2.1.43)$$

and, for an isothermal atmosphere (Λ_0, c_0 constant), this has solutions

$$\hat{v}_z \sim \exp\left(\frac{z}{2\Lambda_0} \pm iKz\right) \ ,$$

where

$$K^2 = \frac{\omega^2 - \omega_a^2}{c_0^2} \qquad (2.1.44)$$

The frequency, $\omega_a = c_0/2\Lambda_0$, is the cut-off frequency for vertical propagation, since propagation ($K^2 > 0$) occurs only for $\omega > \omega_a$. Note that for propagation, the amplitude of v_z e-folds in two scale heights.

ACOUSTIC-GRAVITY WAVES IN AN ISOTHERMAL ATMOSPHERE

In an isothermal atmosphere, the sound speed c_0 in Equation (2.1.37) is constant. A possible solution is $A_0 \neq 0$, i.e.

$$\omega^2 = k_x^2 c_0^2 ,$$

for which the Lamb wave solution is given by

$$v_z \equiv 0 ,$$

$$v_x \sim \exp((\gamma-1)gz/c_0^2 + ik_x(c_0 t \pm x))$$

and

$$p \sim \exp(-gz/c_0^2 + ik_x(c_0 t \pm x))$$

These equations represent a system of waves (Lamb wave) spreading horizontally with constant velocity c_0 (Lamb, 1945, Chapter X). The velocity increases with height while the pressure perturbation decreases.

For $A_0 \neq 0$ (i.e. $\omega^2 \neq k_x^2 c_0^2$), Equation (2.1.37) can be written in canonical form:

$$\frac{d^2V}{dz^2} + \left[\left(\frac{\omega^2 - \omega_a^2}{c_0^2}\right) - \frac{k_x^2}{\omega^2}(\omega^2 - \omega_g^2)\right] V = 0 , \qquad (2.1.45)$$

where

$$\hat{v}_z = V \rho_0^{-\frac{1}{2}} , \qquad (2.1.46)$$

and the two critical frequencies, ω_a and ω_g, are given by

$$\omega_a = \frac{\gamma g}{2c_0} \quad \text{- the acoustic cut-off frequency,} \qquad (2.1.47)$$

$$\omega_g = (\gamma-1)^{\frac{1}{2}} \frac{g}{c_0} \quad \text{- the Brunt-Väisälä (or buoyancy) frequency for an isothermal atmosphere.} \qquad (2.1.48)$$

Solutions of (2.1.45) are of the form $V \sim \exp(ik_z z)$, where

$$k_z^2 = \frac{\omega^2 - \omega_a^2}{c_0^2} - \frac{k_x^2}{\omega^2}(\omega^2 - \omega_g^2) \qquad (2.1.49)$$

is the dispersion relation for acoustic-gravity waves.

For $1 < \gamma \leq 5/3$, $\omega_a > \omega_g$ (for example, with $\gamma = 5/3$ $\omega_a \sim 1.02\,\omega_g$). Therefore, for frequencies in the range $\omega_g < \omega < \omega_a$, k_z is imaginary and hence vertical propagation is not possible.

The solution of Equation (2.1.49) may be represented graphically on a diagnostic diagram (Figure 2.1), where the lines $k_z = 0$ are plotted on a $\omega - k_x$ domain. There are three regions. One lies above the lines $\omega = \omega_a$ and $\omega = k_x c_0$ and has real values of k_z. These are sound waves modified by the effects of gravity. A second region with real k_z, and hence vertically propagating waves, lies below the lines $\omega = \omega_g$ and $\omega = k_x c_0/\omega_a$. This is the internal gravity wave domain. The intermediate region has solutions with imaginary values of k_z, so that the wave solutions either grow or decay with height. These (non-propagating) waves are said to be evanescent.

For high frequencies, $\omega \gg \omega_a$, the waves are essentially sound waves, and for vertical propagation ($k_x \equiv 0$) only the modified acoustic waves are present, with ω_a being the low-frequency cut-off for propagation.

Solving Equation (2.1.49) for ω^2 gives

$$\omega^2 = \tfrac{1}{2}\left\{\omega_a^2 + c_0^2K^2 \pm \left[(\omega_a^2 + c_0^2K^2)^2 - 4c_0^2k_x^2\omega_g^2\right]^{\frac{1}{2}}\right\}, \qquad (2.1.50)$$

where $K^2 = k_x^2 + k_z^2$. This has two real positive roots for ω^2,

Figure 2.1 - Boundaries in the ω-k_x plane, dividing regions of vertically propagating waves ($k_z^2 > 0$) and evanescent waves ($k_z^2 < 0$). The two frequencies Ω_a and Ω_g are defined by: $\Omega_a = \omega_a \Lambda_0 / c_0$ and $\Omega_g = \omega_g \Lambda_0 / c_0$; and we have taken $\gamma = 5/3$. The line $\omega = k_x c_0$ is the Lamb mode.

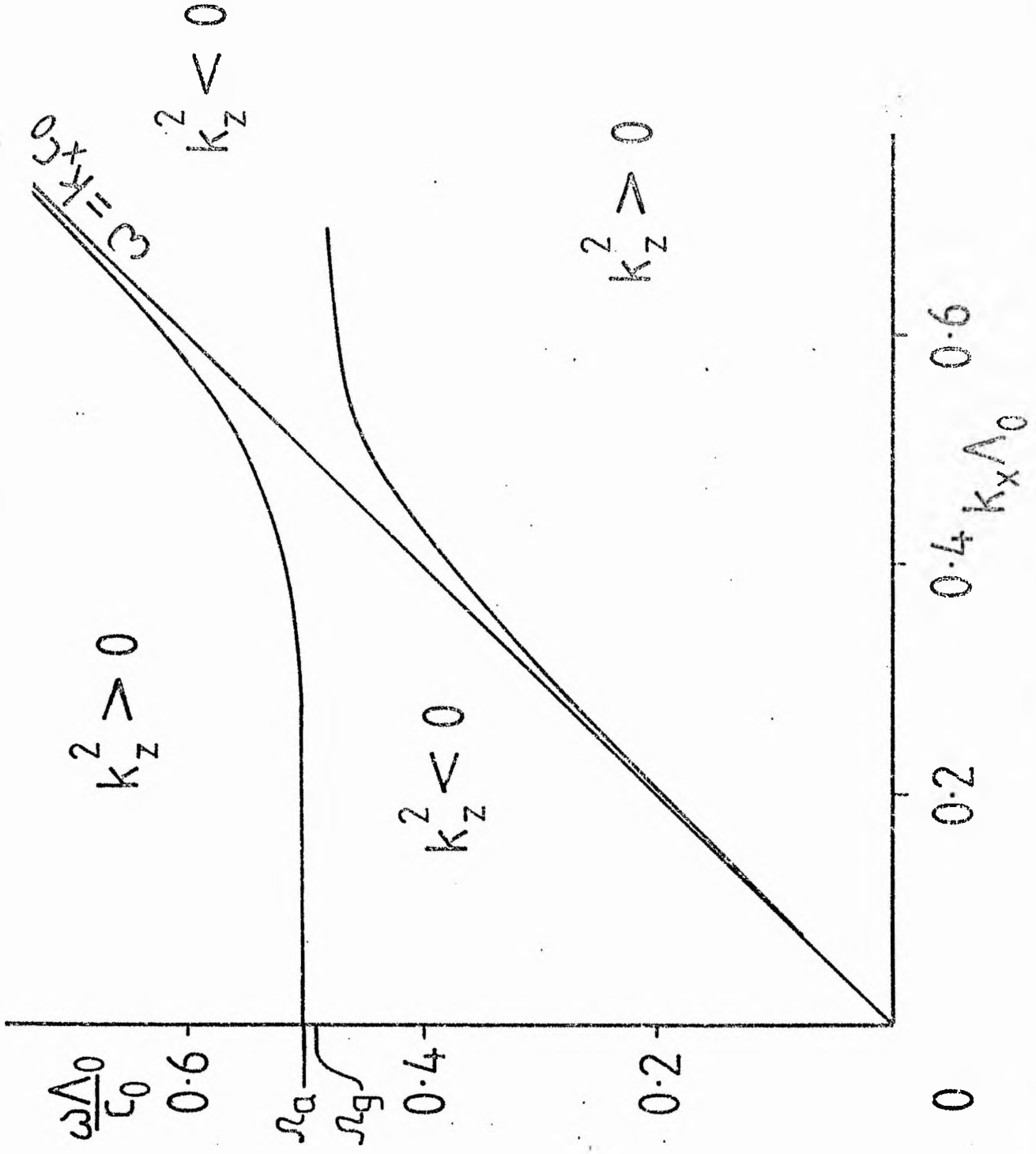

the positive sign giving a root greater than ω_a^2 and thus corresponding to acoustic waves, and the negative sign giving a root less than ω_g^2 and corresponding to gravity modes.

The phase speed, $V_p = \omega/K$, is given by

$$V_p^2 = \tfrac{1}{2}\left[\frac{\omega_a^2}{K^2} + c_0^2 \pm \left[\left(\frac{\omega_a^2}{K^2} + c_0^2\right)^2 - 4\frac{c_0^2}{K^2}\omega_g^2 \sin^2\phi\right]^{\frac{1}{2}}\right], \qquad (2.1.51)$$

where ϕ is the angle of phase propagation relative to the vertical direction. When $\phi = 0$ or π, the phase speed for gravity waves is zero, showing that these waves connot propagate vertically (see section 2.1.2). It may also be shown that the phase velocity of gravity waves is always less than the velocity of sound, whereas the phase velocity of modified acoustic waves is greater than the velocity sound.

It follows from Equation (2.1.50) that the velocity of energy propagation, the group velocity, $\underline{V}_g \equiv \frac{\partial\omega}{\partial \underline{K}}$, has components (Bray and Loughhead, 1974)

$$V_{gx} = \frac{\partial\omega}{\partial k_x} = \frac{c_0^2 k_x(\omega^2 - \omega_g^2)}{(2\omega^2 - \omega_a^2 - c_0^2K^2)} \quad ,$$

and (2.1.52)

$$V_{gz} = \frac{\partial\omega}{\partial k_z} = \frac{c_0^2\omega^2 k_z}{(2\omega^2 - \omega_a^2 - c_0^2K^2)} \quad .$$

For gravity waves, the quantity $2\omega^2 - \omega_a^2 - c_0^2K^2$ is negative and so the vertical component of the group velocity vector is opposite in sign to the vertical component of the phase velocity. Therefore the upward transfer of energy is accomplished by waves whose phase propagates downwards (see Section 2.1.2).

ACOUSTIC-GRAVITY WAVES IN A TEMPERATURE - STRATIFIED ATMOSPHERE

Many situations occur where the assumption of an isothermal atmosphere cannot be justified and we must use the general equation for $\hat{v}_z$ (2.1.37). This equation has a regular singularity at $z = z_c$ given by $A_0(z_c) = 0$, i.e.

$$\omega^2 - k_x^2 c_0^2(z_c) = 0 \,. \tag{2.1.53}$$

Using the method of Frobenius, the solutions for $\hat{v}_z$ in the neighbourhood of $z = z_c$ are

$$\hat{v}_{z1} \sim (z - z_c)^2, \quad \hat{v}_{z2} \sim \text{constant}, \tag{2.1.54}$$

showing that $\hat{v}_z$ is well-behaved in the region of $z = z_c$.

We may note that the equation for the pressure perturbation, $p(z)$, is

$$A_1 \frac{d^2p}{dz^2} - \left(A_1' + A_1 \frac{\rho_0'}{\rho_0}\right)\frac{dp}{dz} + \left[-\frac{k_x^2}{\omega^2} A_1^2 + \frac{A_1}{c_0^2}\left(\omega^2 - \frac{g\Lambda_0'}{\Lambda_0}\right) - A_1' \frac{g}{c_0^2}\right] p = 0, \tag{2.1.55}$$

where

$$A_1(z) = \omega^2 - N_0^2(z) \,. \tag{2.1.56}$$

The equation for the pressure has a regular singularity at $z = z_c^*$ given by $A_1(z_c^*) = 0$, and the solutions for the pressure in the neighbourhood of $z = z_c^*$ are

$$p_1 \sim (z - z_c^*)^2 \,, \quad p_2 \sim \text{constant}. \tag{2.1.57}$$

Thus, both the equations for the velocity and pressure exhibit singularities, though at different levels in the atmosphere, and across these levels the perturbations change continuously. This is in contrast to the solution of the magnetoatmospheric

wave equation for motion in the presence of a horizontal magnetic field (Adam, 1977), where a logarithmic singularity occurs and waves are captured as they approach the singular level from either side and are constrained to propagate along the field line.

The Lamb mode does not occur if the atmosphere is not isothermal. The propagation of waves in an atmosphere with uniform temperature gradient has been studied by Lamb (1945), who obtained solutions for v_z in terms of the confluent hypergeometric function. Further studies of waves in a temperature-stratified atmosphere have been made by Bahng and Schwarzschild (1963), Moore and Spiegel (1964) and Uchida (1965).

2.1.5 Magneto-acoustic Waves

In the presence of a magnetic field there is an additional restoring force and in this section we consider waves under the combined action of pressure and a magnetic field only, with gravity neglected.

The governing equation (2.1.1) takes the form

$$\frac{\partial^2 \underline{v}}{\partial t^2} = c_0^2 \nabla(\nabla.\underline{v}) - \frac{1}{\mu_0 \rho_0} \underline{B}_0 \wedge \left(\nabla \wedge [\nabla \wedge (\underline{v} \wedge \underline{B}_0)] \right). \qquad (2.1.58)$$

Taking the magnetic field $\underline{B}_0$ to be parallel to the z-axis, $\underline{B}_0 = B_0 \hat{\underline{z}}$, and writing $\underline{v} = (v_x, v_y, v_z)$, (2.1.58) leads to the two equations (Lighthill, 1960)

$$\frac{\partial^2 \Gamma}{\partial t^2} = v_A^2 \frac{\partial^2 \Gamma}{\partial z^2} \quad , \qquad (2.1.59)$$

and

$$\frac{\partial^2}{\partial t^2}\left[\frac{\partial^2}{\partial t^2} - (c_0^2 + v_A^2)\nabla^2\right]\Delta + c_0^2 v_A^2 \frac{\partial^2}{\partial z^2}\nabla^2\Delta = 0 , \quad (2.1.60)$$

where $\Delta = \nabla.\underline{v}$ and Γ is the z component of vorticity,

$$\Gamma = (\nabla \wedge \underline{v})_z = \frac{\partial v_y}{\partial x} - \frac{\partial v_x}{\partial y} . \quad (2.1.61)$$

Γ is propagated one-dimensionally along $\underline{B}_0$ at the Alfvén speed, v_A.

For plane-wave solutions of the form $e^{i\omega t - i\underline{K}.\underline{r}}$, (2.1.59) and (2.1.60) give the dispersion relations

$$\omega^2 = k_z^2 v_A^2, \quad (2.1.62)$$

and

$$\omega^4 - (c_0^2 + v_A^2)K^2\omega^2 + c_0^2 v_A^2 k_z^2 K^2 = 0 . \quad (2.1.63)$$

Equation (2.1.62) describes <u>generalized Alfvén waves</u>. The density variation is zero and the fluid behaves as if it were incompressible (Cowling, 1976). The phase velocity, V_p, is

$$V_p = \frac{\omega}{K} = v_A \cos\theta , \quad (2.1.64)$$

where $\theta = \cos^{-1}(k_z/K)$ is the angle between the wave propagation vector and the magnetic field. The group velocity, $\underline{V}_g$, is directed along the magnetic field:

$$\underline{V}_g = (0,0,v_A) , \quad (2.1.65)$$

and is of magnitude v_A.

Equation (2.1.63) is the dispersion relation for <u>magneto-acoustic waves</u>, which may be written in the alternative form

$$\omega^4 - \omega^2(c_0^2 + v_A^2)K^2 + c_0^2 v_A^2 K^2 \cos^2\theta = 0 . \quad (2.1.66)$$

The waves are characterized as fast or slow modes according to the magnitude of the phase velocity. Solving (2.1.66) for ω^2, we obtain

$$\omega^2 = \tfrac{1}{2}(c_0^2 + v_A^2)K^2 \pm \tfrac{1}{2}K^2\left[(c_0^2 + v_A^2)^2 - 4c_0^2 v_A^2 \cos^2\theta\right]^{\frac{1}{2}},$$

and hence it follows that the phase velocity, V_p, is given by

$$V_p^2 = \frac{\omega^2}{K^2} = \tfrac{1}{2}(c_0^2 + v_A^2) \pm \tfrac{1}{2}\left[(c_0^2 + v_A^2)^2 - 4c_0^2 v_A^2 \cos^2\theta\right]^{\frac{1}{2}}. \quad (2.1.67)$$

The positive sign characterizes fast-mode waves and the negative sign slow-mode waves. The fluid velocity for the fast and slow modes always lies in the $\underline{K} - \underline{B}_0$ plane. The magnetic field perturbation also lies in this plane but it is perpendicular to $\underline{K}$. The phase velocity for the fast mode exceeds the greater of c_0 and v_A. For $c_0 \gg v_A$, the fast mode will be acoustical in character (longitudinal fluid motion), while for $c_0 \ll v_A$ it becomes magnetic in character (transverse fluid motion). The slow mode assumes the opposite behaviour in that the phase velocity is less than the smaller of c_0 and v_A. It follows from Equation (2.1.67) that the fast mode can propagate in all directions whereas the slow mode cannot propagate at right angles to the magnetic field (for further discussion see Bray and Loughhead, 1974).

It is convenient to note here the solutions for $c_0^2 \ll v_A^2$. In this limit, Equation (2.6.9) has solutions

$$\omega^2 \sim k_z^2 c_0^2 \quad \text{and} \quad \omega^2 \sim (k_x^2 + k_y^2 + k_z^2)v_A^2 . \quad (2.1.68)$$

The slow mode is a sound wave with group velocity c_0 in the direction of the magnetic field and the fast mode is an Alfvén wave with group velocity v_A in the direction of propagation.

In general, the group velocity, $\underline{V}_g$, has components

$$\left.\begin{aligned} V_{gx} &= \frac{\partial\omega}{\partial k_x} = \frac{\omega^4 k_x}{K^2\omega(2\omega^2 - (c_0^2 + v_A^2)K^2)}, \\ V_{gy} &= \frac{\partial\omega}{\partial k_y} = \frac{\omega^4 k_y}{K^2\omega(2\omega^2 - (c_0^2 + v_A^2)K^2)}, \\ V_{gz} &= \frac{\partial\omega}{\partial k_z} = \frac{(\omega^4 - K^2 c_0^2 v_A^2)k_z}{K^2(2\omega^2 - (c_0^2 + v_A^2)K^2)}. \end{aligned}\right\} \qquad (2.1.69)$$

If $c_0 \gg v_A$, the group velocity c_0 is perpendicular to the wave fronts for the fast wave, and v_A parallel to $\underline{B}_0$ for the slow wave, so that we get the usual sound and Alfvén waves. If $v_A \gg c_0$, the group velocity is v_A perpendicular to the wave fronts for the fast wave, and c_0 parallel to $\underline{B}_0$ for the slow. The slow wave must then be regarded as a sound wave constrained to be propagated along the field lines, the fast wave, though propagated magnetically with velocity v_A, is not a true Alfvén wave, magnetic pressures affecting the propagation as much as magnetic tensions (Cowling, 1976).

2.1.6 Magneto-Acoustic-Gravity Waves

Wave motions arising from the combined effects of compressibility, gravity and a magnetic field have been investigated under various approximations by a number of workers. Propagation in a horizontal magnetic field has been considered by Yu (1965), Chen and Lykoudis (1972), Nye and Thomas (1976) and Adam (1977a,b). An exact solution to the governing wave equation for propagation in an isothermal atmosphere was obtained by Nye and Thomas (1976) and Adam, who also investigated the nature of the singularity

occurring in the magnetoatmospheric wave equation. McLellan and Winterberg (1968) analysed wave motions in a uni-directional magnetic field and derived a local dispersion relation, which gave three wave modes, each of which was found to be strongly coupled to each of the three kinds of motion: acoustic, gravity and hydromagnetic. One of the modes, the Alfvén mode, is independent of incompressibility and gravity. The local dispersion relation of McLellan and Winterberg has been studied further by Bel and Mein (1971), and Bel and Leroy (1977), who considered vertical propagation only, Michalitsanos (1973a) who considered the effect of an inclined magnetic field on the critical sonic and internal gravity cut-off frequencies (assuming propagation in the $\underline{g}$ - $\underline{B}$ plane), and Nakagawa *et al* (1973), who examined the necessary and sufficient conditions of trapped magnetoatmospheric waves.

In this section, we shall briefly re-derive the results of McLellan and Winterberg (1968) and those of Michalitsanos. We are interested primarily in wave propagation in a vertical magnetic field, as may be found in regions overlying the borders of supergranules, and we shall derive a general equation for the vertical component of the velocity perturbation in the following section.

LOCAL ANALYSIS

Mclellan and Winterberg consider the full wave equation (2.1.1):

$$\frac{\partial^2 \underline{v}}{\partial t^2} = c_0^2 \nabla(\nabla.\underline{v}) + (\gamma-1)\underline{g}\nabla.\underline{v} + \nabla(\underline{v}.\underline{g}) - \frac{1}{\mu_0 \rho_0} \underline{B}_0 \wedge [\nabla \wedge (\nabla \wedge (\underline{v} \wedge \underline{B}_0))] \quad (2.1.1)$$

It is not possible to obtain exact solutions of Equation (2.1.1) in which $\rho_0(z)$, $\underline{B}_0(z)$ and $c_0(z)$ take a quite general form.

However, for a uniform magnetic field, $\underline{B}_0$, in an isothermal atmosphere (c_0 constant) much can be found out about wavelike solutions to the equations from the local dispersion relation. This is a relationship

$$\omega = \omega(k_x, k_y, k_z; z) \ , \tag{2.1.70}$$

varying with the height z, between the frequency and the three components of wave number, in solutions that vary locally as

$$\underline{v} = \underline{V} \exp i(\omega t - k_x x - k_y y - k_z z) \ . \tag{2.1.71}$$

The local dispersion relation is calculated by ignoring the rates of change of the amplitudes $\underline{V}$ with position, compared with the rate of change of the sinusoidally fluctuating factor (Lighthill, 1978).

Substituting (2.1.71) into (2.1.1) we find that the equation possesses non-trivial solutions provided (Bray and Loughhead, 1974)

$$\omega^6 - \omega^4\left[(c_0^2 + v_A^2)K^2 + \frac{(\underline{B}_0\cdot\underline{K})^2}{\mu_0\rho_0} - i\gamma g k_z\right] + \omega^2\left[g^2(\gamma-1)(K^2 - k_z^2)\right.$$

$$\left. - i\gamma g\left(\frac{(\underline{B}_0\cdot\underline{K})^2}{\mu_0\rho_0}k_z + B_{0z}\frac{\underline{B}_0\cdot\underline{K}}{\mu_0\rho_0}K^2\right) + 2c_0^2\frac{(\underline{B}_0\cdot\underline{K})^2}{\mu_0\rho_0}K^2 + B_0^2\frac{(\underline{B}_0\cdot\underline{K})^2}{(\mu_0\rho_0)^2}K^2\right]$$

$$- g^2(\gamma-1)\frac{(\underline{B}_0\cdot\underline{K})^2}{\mu_0\rho_0}(K^2 - k_z^2) + i\gamma g B_{0z}\frac{(\underline{B}_0\cdot\underline{K})^3}{(\mu_0\rho_0)^2}K^2 - c_0^2\frac{(\underline{B}_0\cdot\underline{K})^4}{(\mu_0\rho_0)^2}K^2 = 0 \ , \tag{2.1.72}$$

which may be factorized to give

$$\omega^2 - \frac{(\underline{B}_0\cdot\underline{K})^2}{\mu_0\rho_0} = 0 \ , \tag{2.1.73}$$

and

$$\omega^4 - \omega^2\left[(c_0^2+v_A^2)K^2 - i\gamma g k_z\right] + g^2(\gamma-1)(K^2-k_z^2) + c_0^2\frac{(\underline{B}_0\cdot\underline{K})^2}{\mu_0\rho_0}K^2$$

$$- i\gamma g B_{0z}\frac{(\underline{B}_0\cdot\underline{K})}{\mu_0\rho_0}K^2 = 0 \,. \qquad (2.1.74)$$

Equation (2.1.73) represents the propagation of a generalized Alfvén wave. The second equation (2.1.74) is the dispersion relation for magneto-gravity waves. For a vertical magnetic field, $\underline{B} = B_0\hat{\underline{z}}$, Equation (2.1.74) becomes

$$\omega^4 - \omega^2\left[(c_0^2+v_A^2)K^2 - i\gamma g k_z\right] + g^2(\gamma-1)(K^2-k_z^2) + c_0^2 v_A^2 K^2 k_z^2 - i\gamma g v_A^2 k_z K^2 = 0 \,, \qquad (2.1.74)'$$

which, for vertical propagation ($K = k_z$), reduces to

$$(\omega^2 - k_z^2 v_A^2)(\omega^2 + i\gamma g k_z - k_z^2 c_0^2) = 0 \,, \qquad (2.1.75)$$

describing Alfvén waves and vertically propagating sound waves (see Equation (2.1.43)).

The effect of an inclined magnetic field on the cut-off frequencies ω_a and ω_g (see Section 2.1.4) has been examined by Michalitsanos (1973) who gives the generalisation of the diagnostic diagram when a magnetic field is present and finds that the frequency range in which vertical propagation is not possible in the non-magnetic atmosphere becomes smaller as the inclined field is introduced, with the cut-off frequency for magnetically-coupled internal gravity waves increasing as the strength of the field increases.

2.2 Propagation in a Stratified Atmosphere with Uniform Vertical Field

In this section we present some new results concerning the propagation of waves in a stratified atmosphere permeated by a uniform vertical magnetic field. The equations for the vertical and horizontal velocity perturbations are derived and solutions are obtained for a number of special cases. In particular, we consider the situation when the Alfvén speed is much greater than the sound speed, and investigate the recent claim by Hollweg (1979) for a resonance in the solar atmosphere.

The basic state is described by

$$\underline{B} = B_0 \hat{\underline{z}} \ , \tag{2.2.1}$$

$$\frac{dp_0(z)}{dz} = - \rho_0(z) g, \tag{2.2.2}$$

$$p_0(z) = \rho_0(z) g \Lambda_0(z) \ . \tag{2.2.3}$$

For linear perturbations about this basic state, the governing wave equation is (2.1.1) and since the magnetic field is vertical we may put $\frac{\partial}{\partial y} \equiv 0$ without loss of generality. The equation for v_y decouples, being

$$\frac{\partial^2 v_y}{\partial t^2} - v_A^2(z) \frac{\partial^2 v_y}{\partial z^2} = 0 \ , \tag{2.2.4}$$

and the corresponding equation for b_y is

$$\frac{\partial^2 b_y}{\partial t^2} - \frac{\partial}{\partial z}\left(v_A^2(z) \frac{\partial b_y}{\partial z} \right) = 0 \ . \tag{2.2.5}$$

Equation (2.2.4) describes the propagation of Alfvén waves vertically.

In addition, there are two coupled equations for v_x and v_z:

$$\left(c_0^2 \frac{\partial}{\partial z} - g\right)\frac{\partial v_z}{\partial x} + \left(v_A^2 \frac{\partial^2}{\partial z^2} + (c_0^2 + v_A^2)\frac{\partial^2}{\partial x^2} - \frac{\partial^2}{\partial t^2}\right) v_x = 0 , \quad (2.2.6)$$

and

$$\left(c_0^2 \frac{\partial^2}{\partial z^2} - \gamma g \frac{\partial}{\partial z} - \frac{\partial^2}{\partial t^2}\right)v_z + \left(c_0^2 \frac{\partial}{\partial z} - (\gamma - 1)g\right)\frac{\partial v_x}{\partial x} = 0 . \quad (2.2.7)$$

In the absence of a magnetic field, these simply reduce to Equations (2.1.35) and (2.1.36). For vertical propagation ($\frac{\partial}{\partial x} \equiv 0$) we have

$$\left(\frac{\partial^2}{\partial t^2} - v_A^2 \frac{\partial^2}{\partial z^2}\right)v_x = 0 , \quad (2.2.6)'$$

and

$$\left(\frac{\partial^2}{\partial z^2} - \frac{1}{\Lambda_0}\frac{\partial}{\partial z} - \frac{1}{c_0^2}\frac{\partial^2}{\partial t^2}\right)v_z = 0 , \quad (2.2.7)'$$

describing vertically propagating Alfvén and sound waves, as given by the local analysis of McLellan and Winterberg (Equation (2.1.75)).

For perturbations of the form

$$v_x(x,z;t) = \hat{v}_x(z)\exp i(\omega t - k_x x), \; v_z(x,z;t) = \hat{v}_z(z)\exp i(\omega t - k_x x), \quad (2.2.8)$$

Equations (2.2.6) and (2.2.7) may be combined to give a single equation for the amplitudes $\hat{v}_x(z)$ and $\hat{v}_z(z)$. The equation for $\hat{v}_x(z)$ is

$$L_0 \frac{d^4\hat{v}_x}{dz^4} + L_1 \frac{d^3\hat{v}_x}{dz^3} + L_2 \frac{d^2\hat{v}_x}{dz^2} + L_3 \frac{d\hat{v}_x}{dz} + L_4 \hat{v}_x = 0 , \quad (2.2.9)$$

where

$$L_0(z) = \omega^2 - N_0^2 , \qquad (2.2.10)$$

$$L_1(z) = (N_0^2)' + (\omega^2 - N_0^2)\left(\frac{N_0^2}{g} + \frac{g}{c_0^2}\right) ,$$

$$L_2(z) = \frac{(\omega^2-N_0^2)}{v_A^2}\left(\frac{v_A^2}{c_0^2}(\omega^2-N_0^2) + \omega^2-k_x^2v_A^2 + \frac{gv_A^2}{c_0^2}\left(\frac{\gamma-1}{\gamma\Lambda_0}\right)\right) + \frac{(N_0^2)'}{\gamma\Lambda_0} ,$$

$$L_3(z) = -(\omega^2-N_0^2)\frac{(\omega^2+k_x^2v_A^2)}{v_A^2}\left(\frac{N_0^2}{g} + \frac{g}{c_0^2}\right) + (N_0^2)'\left(\frac{\omega^2-k_x^2v_A^2}{v_A^2}\right),$$

$$L_4(z) = \frac{(\omega^2-N_0^2)}{v_A^2}\left[\frac{(\omega^2-N_0^2)}{c_0^2}\left[\omega^2-k_x^2(c_0^2+v_A^2)\right] + \frac{\omega^2}{g}\left(\frac{N_0^2}{\gamma\Lambda_0} - (N_0^2)'\right) - \frac{k_x^2v_A^2}{\gamma\Lambda_0}\frac{\gamma-1}{\gamma\Lambda_0}\right] ,$$

and $\hat{v}_z$ is related to $\hat{v}_x$ by

$$\hat{v}_z = \frac{-1}{(\omega^2-N_0^2)ik_x}\left[v_A^2\frac{d^3\hat{v}_x}{dz^3} + \frac{v_A^2}{\gamma\Lambda_0}\frac{d^2\hat{v}_x}{dz^2} + (\omega^2-k_x^2v_A^2)\frac{d\hat{v}_x}{dz} - \left(\frac{\omega^2N_0^2}{g} + \frac{k_x^2v_A^2}{\gamma\Lambda_0}\right)\hat{v}_x\right] \quad (2.2.1$$

N_0 is the Brunt-Väisälä frequency given by (2.1.13)

The corresponding equation for $\hat{v}_z$ is

$$M_0\frac{d^4\hat{v}_z}{dz^4} + M_1\frac{d^3\hat{v}_z}{dz^3} + M_2\frac{d^2\hat{v}_z}{dz^2} + M_3\frac{d\hat{v}_z}{dz} + M_4\hat{v}_z = 0 , \qquad (2.2.12)$$

where

$$M_0(z) = \frac{c_0^2}{v_A^2}\left[\omega^2-k_x^2(c_0^2+v_A^2)\right] + g(1-\gamma)\left(\frac{N_0^2}{g} + 2.\frac{1-\gamma}{\gamma\Lambda_0}\right), \qquad (2.2.13)$$

$$M_1(z) = -M_0' + M_0\left(\frac{N_0^2}{g} - \frac{\gamma-1}{\gamma\Lambda_0} - \frac{1}{\Lambda_0}\right) ,$$

$$M_2(z) = \frac{M_0^2}{c_0^2} + \frac{M_0}{c_0^2}\left[\omega^2 + k_x^2 \frac{c_0^4}{v_A^2} + \gamma g\left(\frac{N_0^2}{g} - 2.\frac{\gamma-1}{\gamma\Lambda_0} - \frac{(1-\gamma)}{\gamma^2\Lambda_0}\right)\right] + \frac{M_0'}{\gamma\Lambda_0},$$

$$M_3(z) = -\frac{\gamma g}{c_0^4} M_0^2 + \frac{M_0}{c_0^2}\left[\frac{k_x^2 c_0^4}{v_A^2}\left(\frac{N_0^2}{g} - \frac{3}{\Lambda_0} + \frac{1}{\gamma\Lambda_0}\right) + \gamma g\left(\frac{N_0^2}{g}\right)' + \frac{\gamma-1}{\Lambda_0} N_0^2 \right.$$

$$\left. - \omega^2\left(\frac{N_0^2}{g} - \frac{\gamma-1}{\gamma\Lambda_0}\right)\right] - \frac{M_0'}{c_0^2}\left[\omega^2 + \frac{k_x^2 c_0^4}{v_A^2} + \gamma g\left(\frac{N_0^2}{g} + 2.\frac{1-\gamma}{\gamma\Lambda_0}\right)\right],$$

$$M_4(z) = \frac{M_0^2\omega^2}{c_0^4} - \frac{M_0}{c_0^2}\left[\frac{gk_x^2 c_0^2}{v_A^2}\left(-\frac{1}{\Lambda_0} + \frac{1-\gamma}{\gamma\Lambda_0}\right) + \frac{\omega^2}{g}(N_0^2)' + \omega^2 \frac{\gamma-1}{\gamma\Lambda_0}\frac{N_0^2}{g}\right]$$

$$+ \frac{M_0'}{c_0^2}\left[\frac{gk_x^2 c_0^2}{v_A^2} + \omega^2\left(\frac{N_0^2}{g} + 2.\frac{(1-\gamma)}{\gamma\Lambda_0}\right)\right],$$

and $\hat{v}_x$ is related to $\hat{v}_z$ by

$$\hat{v}_x = \frac{-1}{ik_x\left[\frac{c_0^2}{v_A^2}\left(\omega^2 - k_x^2(c_0^2+v_A^2)\right) - (\gamma-1)g\left(\frac{N_0^2}{g} + 2.\frac{1-\gamma}{\gamma\Lambda_0}\right)\right]}\left\{c_0^2\frac{d^3\hat{v}_z}{dz^3} - \frac{c_0^2}{\gamma\Lambda_0}\frac{d^2\hat{v}_z}{dz^2} + \right.$$

$$\left. + \left[\omega^2 + k_x^2\frac{c_0^4}{v_A^2} + \gamma g\left(\frac{N_0^2}{g} + 2.\frac{1-\gamma}{\gamma\Lambda_0}\right)\right]\frac{d\hat{v}_z}{dz} - \left[g\frac{k_x^2 c_0^2}{v_A^2} + \omega^2\left(\frac{N_0^2}{g} + 2.\frac{1-\gamma}{\gamma\Lambda_0}\right)\right]\hat{v}_z\right\}. \quad (2.2.14)$$

Note that both the equation for $\hat{v}_x$ and that for $\hat{v}_z$ have regular singularities. In Equation (2.2.9), the singularity is at $z = z_c$ given by $L_0(z_c) = 0$, i.e.

$$\omega^2 - N_0^2(z_c) = 0, \quad (2.2.15)$$

and so the position of singularity in the $\hat{v}_x$ equation is <u>independent of magnetic field strength</u>. The solutions for $\hat{v}_x$ about $z = z_c$ are (see Ince, 1956 chapter XVI)

$$v_{x1} \sim (z - z_c)^4,\ v_{x2} \sim (z - z_c)^2,\ v_{x3} \sim (z - z_c),\ v_{x4} \sim \text{constant}. \quad (2.2.16)$$

Similarly, we may show that the solutions for $\hat{v}_z$ are well-behaved about the singularity $z = z_c^*$ given by $M_0(z_c^*) = 0$:

$$\frac{c_0^2(z_c^*)}{v_A^2(z_c^*)}\left[\omega^2 - k_x^2(c_0^2(z_c^*)+v_A^2(z_c^*))\right] - g(\gamma-1)\left(\frac{N_0^2(z_c^*)}{g} - 2.\frac{\gamma-1}{\gamma\Lambda_0(z_c^*)}\right) = 0 \ . \qquad (2.2.17)$$

In general, it is not possible to obtain solutions to Equations (2.2.9) and (2.2.12). Therefore we shall consider some special cases of the system (2.2.6) and (2.2.7). The isothermal atmosphere has been widely treated in the literature, using the local analysis of McLellan and Winterberg (see Section 2.1.6) and is a good approximation for the mid-chromosphere. Another case of interest is that of small horizontal wavelength ($k_x\Lambda_0 >> 1$) which arises in a slender flux tube as we shall see in the following chapter. We also consider the extreme when the Alfvén speed is much greater than the sound speed.

ISOTHERMAL ATMOSPHERE

Consider an isothermal atmosphere, so that Λ_0, c_0 and N_0 are constant and the density and Alfvén speed vary as

$$\rho_0(z) = \rho_0(0)e^{-z/\Lambda_0} \ , \ v_A(z) = v_A(0)e^{z/2\Lambda_0} \ .$$

For variations of the form (2.2.8) we may eliminate $\hat{v}_z$ between Equations (2.2.6) and (2.2.7) to give ($\omega^2 \neq N_0^2$)

$$v_A^2(z)\frac{d^4\hat{v}_x}{dz^4} + v_A^2(z)\left(\frac{2}{H(z)} - \frac{\gamma g}{c_0^2}\right)\frac{d^3\hat{v}_x}{dz^3} + \left[\omega^2\left(1+\frac{v_A^2(z)}{c_0^2}\right) - k_x^2 v_A^2(z) + \frac{1}{H(z)}\left(\frac{1}{H(z)} - \frac{g\gamma}{c_0^2}\right)v_A^2(z)\right]\frac{d^2\hat{v}_x}{dz^2} +$$

$$+\left[-\frac{\gamma g}{c_0^2}\omega^2 - k_x^2 v_A^2(z)\left(\frac{2}{H(z)} - \frac{\gamma g}{c_0^2}\right)\right]\frac{d\hat{v}_x}{dz} + \left[\frac{\omega^4}{c_0^2} - \frac{\omega^2 k_x^2}{c_0^2}(c_0^2+v_A^2(z)) - (\gamma-1)\frac{g^2k_x^2}{c_0^2}\right]\hat{v}_x = 0, \qquad (2.2.18)$$

where H(z) is the density scale-height defined by

$$\frac{1}{H(z)} = -\frac{1}{\rho_0(z)}\frac{d\rho_0(z)}{dz} .$$

Since the atmosphere is isothermal

$$\frac{1}{H(z)} = \frac{\gamma g}{c_0^2} \equiv \frac{1}{\Lambda_0} , \qquad (2.2.19)$$

and Equation (2.2.18) reduces to

$$v_A^2(z)\frac{d^4\hat{v}_x}{dz^4} + \frac{\gamma g}{c_0^2}v_A^2(z)\frac{d^3\hat{v}_x}{dz^3} + \left[\omega^2\left(1+\frac{v_A^2(z)}{c_0^2}\right) - k_x^2 v_A^2(z)\right]\frac{d^2\hat{v}_x}{dz^2} - \frac{\gamma g}{c_0^2}\left[\omega^2 + k_x^2 v_A^2(z)\right]\frac{d\hat{v}_x}{dz}$$

$$+\left[\frac{\omega^4}{c_0^2} - \frac{\omega^2 k_x^2}{c_0^2}(c_0^2+v_A^2(z)) + (\gamma-1)\frac{g^2 k_x^2}{c_0^2}\right]\hat{v}_x = 0 . \qquad (2.2.18)'$$

Writing $\hat{v}_x(z) = \hat{v}_x^* e^{-ik_z z}$, we may derive a <u>local</u> dispersion relation

$$\omega^4 - \omega^2\left[(c_0^2+v_A^2)K^2 - i\gamma g k_z\right] + g^2(\gamma-1)k_x^2 + c_0^2 v_A^2 K^2 k_z^2 + i\gamma g v_A^2 K^2 k_z = 0 . \quad (2.2.20$$

where $K^2 = k_x^2 + k_z^2$.

Note that the above equation differs from the local dispersion relation of McLellan and Winterberg for a vertical magnetic field (Equation (2.1.74)') by the sign of the final term. This is because density variations have been neglected in the derivation of (2.1.74)', and therefore the terms involving $H^{-1}(z)$ in (2.2.18) are also neglected.

In fact, we may obtain series solutions of Equation (2.2.18)' in $x = e^{-z/\Lambda_0}$. These solutions may be expressed in terms of the generalized hypergeometric function ${}_2F_3$(Slater, 1966):

$${}_2F_3\left[b_1(\alpha_1), b_2(\alpha_1); a_{21}, a_{31}, a_{41}; x\right] ,$$

$${}_2F_3\left[b_1(\alpha_2), b_2(\alpha_2); a_{12}, a_{32}, a_{42}; x\right] ,$$

$$ {}_2F_3\left[b_1(\alpha_3),\ b_2(\alpha_3);\ a_{13},\ a_{23},\ a_{43};\ x\right], \qquad (2.2.21) $$

$$ {}_2F_3\left[b_1(\alpha_4),\ b_2(\alpha_4);\ a_{14},\ a_{24},\ a_{34};\ x\right], $$

with $x = e^{-z/\Lambda_0}$ and $a_{ij} = \alpha_i - \alpha_j + 1$, where the α_j are the roots of the indicial equation

$$ \alpha^4 - \alpha^3 + \alpha^2\left(\frac{\omega^2\Lambda_0^2}{c_0^2} - k_x^2\Lambda_0^2\right) + \alpha k_x^2\Lambda_0^2 - \omega^2\frac{k_x^2\Lambda_0^4}{c_0^2} = 0, \qquad (2.2.22) $$

and we have assumed the a_{ij} are not integers. The quantities $b_{1,2}$ are roots of the quadratic

$$ b^2\frac{\omega^2\Lambda_0^2}{v_A^2(0)} + b(2\alpha+1)\frac{\omega^2\Lambda_0^2}{v_A^2(0)} + \alpha(\alpha+1)\frac{\omega^2\Lambda_0^2}{v_A^2(0)} + \frac{\omega^4\Lambda_0^4}{c_0^2v_A^2(0)} - \frac{\omega^2k_x^2\Lambda_0^4}{v_A^2(0)} + k_x^2\Lambda_0^4\frac{\gamma-1}{\gamma\Lambda_0}\frac{g}{v_A^2(0)} = 0. \qquad (2.2.23) $$

We note that in the absence of gravity Equation (2.2.18) has constant coefficients and so admits solutions of the form $\exp(ik_z z)$ satisfying

$$ k_z^4v_A^2 - \left[\omega^2\left(1+\frac{v_A^2}{c_0^2}\right) - k_x^2v_A^2\right]k_z^2 + \frac{\omega^2}{c_0^2}\left[\omega^2 - k_x^2(c_0^2+v_A^2)\right] = 0, \qquad (2.2.24) $$

which is the usual dispersion relation for magneto-acoustic waves (Equation (2.1.66)). The Alfvén wave follows from Equation (2.2.4) which gives

$$ \omega^2 = k_z^2v_A^2. $$

SMALL HORIZONTAL WAVELENGTH

We have seen that the limit of vertical propagation ($k_x\Lambda_0 \to 0$) gives two modes: Alfvén waves and sound waves (Equations (2.2.6)' and (2.2.7)'). In the opposite extreme of $k_x\Lambda_0 \to \infty$, Equation

(2.2.13) for $\hat{v}_z$ gives

$$\frac{d^2\hat{v}_z}{dz^2} - \frac{\gamma g v_A^2(z)}{c_0^2(z)(c_0^2(z)+v_A^2(z))}\frac{d\hat{v}_z}{dz} + \left(\frac{\omega^2}{c_T^2(z)} - \frac{g}{v_A^2(z)}\frac{\Lambda_0'}{\Lambda_0} - \right.$$

$$\left. - \frac{g}{\Lambda_0 v_A^2(z)}\left(\frac{\gamma-1}{\gamma} + \frac{v_A^2(z)}{c_0^2(z)+v_A^2(z)}\right)\right)\hat{v}_z = 0 . \qquad (2.2.25)$$

Note that the order of the differential equation (2.2.13) is reduced.

The above equation may be written in the form

$$\frac{d}{dz}\left(\sigma(z)\frac{d\hat{v}_z}{dz}\right) + \left[\omega^2 r(z) - s(z)\right]\hat{v}_z = 0 , \qquad (2.2.26)$$

where

$$\sigma(z) = \frac{\left(1 + \frac{c_0^2(z)}{v_A^2(z)}\right)}{\rho_0(z)\Lambda_0(z)} , \qquad r(z) = \frac{\sigma(z)}{c_T^2(z)}$$

and

$$s(z) = \sigma(z)\left[\frac{g}{v_A^2(z)}\frac{\Lambda_0'}{\Lambda_0} + \frac{g}{\Lambda_0 v_A^2(z)}\left(\frac{\gamma-1}{\gamma} + \frac{v_A^2(z)}{c_0^2(z)+v_A^2(z)}\right)\right]$$

Equation (2.2.26), together with boundary conditions of the form

$$a_1\hat{v}_z(z_1) + a_2\hat{v}_z'(z_1) = 0,$$

$$b_1\hat{v}_z(z_2) + b_2\hat{v}_z'(z_2) = 0,$$

(for constants a_1, a_2, b_1 and b_2), imposed at levels $z = z_1$ and $z = z_2$, forms a Sturm-Liouville system, with real eigenvalues ω^2. Equation (2.2.25) arises in the flux tube problem examined in Chapter 3 and the Sturm-Liouville system above will be looked at in more detail in Chapter 4. In fact, Equation (2.2.25) has

been discussed by Syrovat-skii and Zhugzhda (1968) for the case $v_A^2 >> c_0^2$ and solutions for $\hat{v}_z$ obtained for a polytropic atmosphere.

STRONG MAGNETIC FIELD

The propagation of waves in regions where the magnetic field is strong is of interest since the limit $v_A^2 >> c_0^2$ is valid in the upper chromosphere (and above) for the quiet Sun and at lower altitudes in the regions of high magnetic field strengths associated with sunspots. This limit has been considered recently by Hollweg (1979), who neglects the term $\partial p/\partial x$ in the x component of the momentum equation and arrives at the two coupled equations for $\hat{v}_x$ and $\hat{v}_z$:

$$\frac{d^2\hat{v}_x}{dz^2} + \left(\frac{\omega^2}{v_A^2(z)} - k_x^2 \right) \hat{v}_x = 0 , \qquad (2.2.27)$$

and

$$c_0^2 \frac{d^2\hat{v}_z}{dz^2} - \gamma g \frac{d\hat{v}_z}{dz} + \omega^2 \hat{v}_z - ik_x c_0^2 \frac{d\hat{v}_x}{dz} + ik_x(\gamma - 1) g \hat{v}_x = 0 . \qquad (2.2.28)$$

Hollweg presents his analysis for an isothermal atmosphere only, though in fact Equations (2.2.27) and (2.2.28) are valid even if the temperature is non-uniform. Equation (2.2.28) is identical to (2.2.7) while (2.2.27) is equivalent to (2.2.6) under the limit of $v_A^2 >> c_0^2$ and $v_A^2 k_z^2 \hat{v}_x^* >> c_0^2 k_z k_x \hat{v}_z^*$, $v_A^2 k_z^2 \hat{v}_x^* \gg g k_x \hat{v}_z^*$, where k_z is the (local) vertical wavenumber and $\hat{v}_x^*$ and $\hat{v}_z^*$ are the amplitudes of $\hat{v}_x$ and $\hat{v}_z$.

For an <u>isothermal</u> atmosphere ($\Lambda_0' \equiv 0$, $\rho_0 = \rho_0(0) e^{-z/\Lambda_0}$, $v_A^2 = v_A^2(0) e^{z/\Lambda_0}$) Equations (2.2.27) and (2.2.28) combine to

give

$$\left[A_0 \frac{d^2}{dz^2} - A_0' \frac{d}{dz} - \frac{A_0^2}{ik_x} - \frac{\gamma-1}{\gamma\Lambda_0} A_0' - A_0\left(\frac{\gamma-1}{\gamma\Lambda_0}\right)^2\right]\left(\frac{d^2\hat{v}_z}{dz^2} - \frac{1}{\Lambda_0}\frac{d\hat{v}_z}{dz} + \frac{\omega^2}{c_0^2}\hat{v}_z\right) = 0, \tag{2.2.29}$$

where

$$A_0 = -ik_x\left[\frac{\omega^2}{v_A^2} - k_x^2 + \left(\frac{\gamma-1}{\gamma\Lambda_0}\right)^2\right] \tag{2.2.30}$$

Equation (2.2.29) is a special case of (2.2.12) and has a regular singularity at z_c, where $A_0(z_c) = 0$.
Solving (2.2.27) for $\hat{v}_x$ yields

$$\hat{v}_x = AJ_\nu\left(\frac{2\omega\Lambda_0}{v_A(0)}\, e^{-z/2\Lambda_0}\right) + BJ_{-\nu}\left(\frac{2\omega\Lambda_0}{v_A(0)}\, e^{-z/2\Lambda_0}\right), \tag{2.2.31}$$

where A and B are arbitrary constants and J_ν is the Bessel function of the first kind of order $\nu = |2k_x\Lambda_0|$. If ν is an integer then $Y_{-\nu}$ replaces $J_{-\nu}$ as the second solution. The solution for $\hat{v}_z$ is then obtained from (2.2.28) with the result that

$$\hat{v}_z = (Ce^{qz} + De^{-qz})e^{z/2\Lambda_0} + \frac{(e^{qz}G_1(z) - e^{-qz}G_2(z))\Lambda_0}{(1-4\omega^2\Lambda_0^2/c_0^2)^{\frac{1}{2}}}\, e^{z/2\Lambda_0}, \tag{2.2.32}$$

where q (assumed non-zero) satisfies

$$q^2 + \frac{\omega^2 - \omega_a^2}{c_0^2} = 0, \tag{2.2.33}$$

with $\omega_a = c_0/2\Lambda_0$, the cut-off frequency for vertical propagation (see Section 2.1). The two functions $G_1(z)$ and $G_2(z)$ are given by the integrals

$$G_1(z) = \int_0^z r(z')\exp\left[-(q+\frac{1}{2\Lambda_0})z'\right]dz' \; ; \; G_2(z) = \int_0^z r(z')\exp\left[-(-q+\frac{1}{2\Lambda_0})z'\right]dz', \tag{2.2.34}$$

where

$$r(z) = ik_x \left(\frac{d}{dz} - \frac{\gamma-1}{\gamma\Lambda_0} \right) \hat{v}_x . \qquad (2.2.35)$$

Now we have seen in Section 2.1 that under the circumstances of $v_A^2 \gg c_0^2$ the fast and slow modes in a gravity-free medium ($\Lambda_0 \to \infty$, $\omega_a \to 0$) are given by the dispersion relations

$$\omega^2 \sim k_z^2 c_0^2 \qquad \text{and} \qquad \omega^2 \sim (k_x^2 + k_z^2) v_A^2,$$

representing sound waves propagating energy along the magnetic field and Alfvén waves. With gravity present, we see from (2.2.32) there are again two modes. The first term in Equation (2.2.32) represents vertically-propagating sound waves (see Equations (2.1.45) and (2.1.46)) and the second term corresponds to the Alfvén mode since it depends on the form of $\hat{v}_x$ which is propagated as an Alfvén wave.

It is possible to obtain exact solutions for $G_1(z)$ and $G_2(z)$. Writing $x=\exp(-z/2\Lambda_0)$, the integral for $G_1(x)(l = 1,2)$ may be expressed in the form

$$G_1(x) = ik_x 2\Lambda_0 \left[\left(\frac{x^{2\Lambda_0\alpha_1}}{2\Lambda_0} \hat{v}_x(x) - \frac{\hat{v}_x(1)}{2\Lambda_0} \right) + \left(\frac{\gamma-1}{\gamma\Lambda_0} - \alpha_1 \right) \int_1^x x'^{2\Lambda_0\alpha_1 - 1} \hat{v}_x(x')dx' \right], \quad (2.2.$$

where $\alpha_1 = q + \frac{1}{2\Lambda_0}$, $\alpha_2 = -q + \frac{1}{2\Lambda_0}$.

The integral in Equation (2.2.36) comprises of terms of the form

$$\int_1^x x'^{\mu} J_\lambda(ax')dx', \qquad (2.2.37)$$

where $\mu = 2\Lambda_0\alpha_1 - 1$ $(l=1,2)$, $\lambda = \pm\nu$, and $a = 2\omega\Lambda_0/v_A(0)$.

The above integral may be evaluated using the result (Magnus and Oberhettinger, 1949)

$$\frac{d}{dz}\left[(\mu+\lambda-1)\,z\,C_\lambda(z)\,S_{\mu-1,\lambda-1}(z) - z\,C_{\lambda-1}(z)S_{\mu,\lambda}(z)\right] = z^\mu C_\lambda(z), \quad (2.2.38)$$

where $C_\nu(z)$ is any cylindrical function and $S_{\mu,\nu}$ is one of the Lommel functions, whose properties and relation to the hypergeometric function are outlined in the appendix, where also the solution for $G_1(x)$ is given.

An approximate solution may be obtained for frequencies $\omega \leq \omega_a$, when the solution (2.2.31) for $\hat{v}_x$(2.2.31) may be written

$$\hat{v}_x = A\left(\frac{2\omega\Lambda_0}{v_A(0)}\right)^\nu \exp(-\nu z/2\Lambda_0) + B\left(\frac{2\omega\Lambda_0}{v_A(0)}\right)^{-\nu} \exp(\nu z/2\Lambda_0), z \geq 0. \quad (2.2.39)$$

The integral $G_1(z)$ then becomes

$$G_1(z) = ik_x \left\{ A\left(\frac{2\omega\Lambda_0}{v_A(0)}\right)^\nu \left(\frac{\nu}{2\Lambda_0} + \frac{\gamma-1}{\gamma\Lambda_0}\right) \left[\frac{\exp\left[-\left(q+\frac{1}{2\Lambda_0}+\frac{\nu}{2\Lambda_0}\right)\right] - 1}{q + \frac{1}{2\Lambda_0} + \frac{\nu}{2\Lambda_0}}\right] \right.$$

$$\left. -B\left(\frac{2\omega\Lambda_0}{v_A(0)}\right)^{-\nu} \left(\frac{\nu}{2\Lambda_0} - \frac{\gamma-1}{\gamma\Lambda_0}\right) \left[\frac{\exp\left[-\left(q+\frac{1}{2\Lambda_0}+\frac{\nu}{2\Lambda_0}\right)\right] - 1}{q + \frac{1}{2\Lambda_0} - \frac{\nu}{2\Lambda_0}}\right] \right\}, \quad (2.2.40)$$

with q replaced by -q for $G_2(z)$. We investigate the above solution further in the following section.

2.2.1 Resonant Response

The response of an atmosphere to a given source has been considered by many authors, and in particular attempts have been made to interpret the observed solar motions as a resonant effect. In resonant models of the atmosphere, the results are very dependent on the choice of the parameters of the models and on the

boundary conditions (Provost, 1975). In these models the assumption is made that the convection zone acts as an 'oscillating lower boundary' and the dependence of a physical quantity, $X(\underline{x},t)$, on space and time is prescribed at the base of the atmosphere. There exist different choices for X : the vertical velocity (Lamb, 1945; Stix, 1970); pressure perturbation (Worrall, 1972; Moore, 1974). Resonance occurs provided that there exists a non-trivial solution of the governing system of equations which has a zero value of X. On the other hand, the response of an atmosphere to a non-resonant excitation has been studied by Provost (1975), who prescribed the energy (which cannot be zero) at the oscillating lower boundary, and consequently resonance is not generated. More recently, Hollweg (1979) has derived the equations (2.2.27) and (2.2.28) and claimed that a resonance exists between the (driving) fast wave and the (driven) gravity-modified acoustic wave. In this final section, we investigate Hollweg's claim further.

As an introduction, we give an illustration of resonance by considering the analysis of Roberts (1979, 1980), who has discussed resonance in the context of spicules. Roberts (1979) investigates the effect of forced vibrations and considers a flux tube in a uniform atmosphere with a prescribed pressure at the boundary, $\delta p_e^{(bdy)}$, of the form

$$\delta p_e^{(bdy)} = \tfrac{1}{2}\rho_e u_e^2 \sin\omega t \cos kz, \qquad (2.2.41)$$

for prescribed velocity u_e, frequency ω and wavenumber k.

The equation for the vertical velocity perturbation is (in a slender flux tube (Roberts, 1980))

$$\frac{\partial^2 v_z}{\partial t^2} - c_T^2 \frac{\partial^2 v_z}{\partial z^2} = - \frac{c_T^2}{\rho_0 v_A^2} \frac{\partial^2 \delta p_e^{(bdy)}}{\partial z \partial t} . \qquad (2.2.42)$$

A particular integral of (2.2.42) is

$$v_z(z,t) = V_0 \cos\omega t \sin kz \qquad (2.2.43)$$

where the amplitude V_0 is given by

$$V_0 = \frac{\frac{1}{2}\left(\frac{\rho_e}{\rho_0}\right) u_e^2 c_0^2 \omega k}{(c_0^2 + v_A^2)(k^2 c_T^2 - \omega^2)} , \qquad (2.2.44)$$

and so 'resonance' may occur when the wavenumber is such that

$$k^2 c_T^2 - \omega^2 = 0 , \qquad (2.2.45)$$

and V_0 becomes infinite.

In practice, the velocity amplitude will not become infinite because of applied boundary conditions. The presence of zero denominator suggests, however, large amplitude possibilities, since for a wavenumber k such that $k = \omega/c_T$, the particular integral of Equation (2.2.42) is (for a given frequency ω)

$$V_{pI} = \frac{c_T}{\rho_0 v_A^2} \frac{\rho_e u_e^2}{8} \left(\frac{\omega z}{c_T} \cos \frac{\omega z}{c_T} \cos\omega t + \omega t \sin\frac{\omega z}{c_T} \sin\omega t\right) \qquad (2.2.46)$$

and the amplitude of the vertical velocity is always finite, though again it is large for z (or t) large.

We return now to the problem of resonance between the (driving) fast wave and the (driven) gravity-modified acoustic wave, considered by Hollweg (1979). We consider possible situations when resonance may occur and then outline Hollweg's analysis and discuss his claim for a resonance.

The governing equations for the velocity amplitudes are (2.2.27) and (2.2.28). The solution for $\hat{v}_z$ is Equation (2.2.32) and may be written in the form

$$\hat{v}_z = (Ce^{qz} + De^{-qz})e^{z/2\Lambda_0} + \frac{(e^{qz}G_1(z) - e^{-qz}G_2(z))}{2q} e^{z/2\Lambda_0}, \quad (2.2.47)$$

where q, G_1 and G_2 are given by Equations (2.2.33), (2.2.34) and (2.2.35). It would appear from the above that a resonance occurs when $q = 0$ i.e. for a given horizontal velocity at some level (such as prescribed granular motion at the photosphere) then large vertical velocities may result when

$$\omega^2 = \omega_a^2 = \frac{c_0^2}{4\Lambda_0^2} . \quad (2.2.48)$$

For $\omega \sim \omega_a$, we may use the approximate solution (2.2.40) for the integrals G_1 and G_2 and substituting into (2.2.47) we have the solution for $\hat{v}_z$

$$\hat{v}_z = (Ce^{qz}+De^{-qz})e^{z/2\Lambda_0} + \frac{ik_x e^{z/2\Lambda_0}}{2q} \left\{ A\left(\frac{2\omega\Lambda_0}{v_A(0)}\right)^{\nu}\left(\frac{\nu}{2\Lambda_0} + \frac{\gamma-1}{\gamma\Lambda_0}\right) \times \right.$$

$$\times \left[\frac{e^{qz}\left(\exp\left[-(q+\frac{1}{2\Lambda_0}+\frac{\nu}{2\Lambda_0})z\right] -1\right)}{q + \frac{1}{2\Lambda_0} + \frac{\nu}{2\Lambda_0}} - \frac{e^{-qz}\left(\exp\left[-(-q+\frac{1}{2\Lambda_0}+\frac{\nu}{2\Lambda_0})z\right] -1\right)}{-q + \frac{1}{2\Lambda_0} + \frac{\nu}{2\Lambda_0}} \right] - B\left(\frac{2\omega\Lambda_0}{v_A(0)}\right)^{-\nu} \times$$

$$\left. \times\left(\frac{\nu}{2\Lambda_0} - \frac{\gamma-1}{\gamma\Lambda_0}\right)\left[\frac{e^{qz}\left(\exp\left[-(q+\frac{1}{2\Lambda_0}+\frac{\nu}{2\Lambda_0})z\right] -1\right)}{q + \frac{1}{2\Lambda_0} - \frac{\nu}{2\Lambda_0}} - \frac{e^{-qz}\left(\exp\left[-(-q+\frac{1}{2\Lambda_0}+\frac{\nu}{2\Lambda_0})z\right] -1\right)}{-q + \frac{1}{2\Lambda_0} - \frac{\nu}{2\Lambda_0}} \right] . \right.$$

(2.2.49)

As an illustration we consider $\hat{v}_z/\hat{v}_x(z = 0)$, as a function of frequency ω, for the particular integral only ($C = D = 0$) adopting (arbitrarily) the J_ν solution for $\hat{v}_x$ ($B = 0$). The ratio

$\hat{v}_z/\hat{v}_x(z = 0)$ is then given by

$$\frac{\hat{v}_z}{\hat{v}_x(z=0)} = \frac{ik_x e^{z/2\Lambda_0}}{2q}\left(\frac{\nu}{2\Lambda_0}+\frac{\gamma-1}{\gamma\Lambda_0}\right)\left[\frac{e^{qz}\left(\exp\left[-(q+\frac{1}{2\Lambda_0}+\frac{\nu}{2\Lambda_0})z\right]-1\right)}{q+\frac{1}{2\Lambda_0}+\frac{\nu}{2\Lambda_0}}\right.$$

$$\left. - \frac{e^{-qz}\left(\exp\left[-(-q+\frac{1}{2\Lambda_0}+\frac{\nu}{2\Lambda_0})z\right]-1\right)}{-q+\frac{1}{2\Lambda_0}+\frac{\nu}{2\Lambda_0}}\right]. \qquad (2.2.50)$$

Closer examination of the magnitude of the above expression reveals that it does not have a peak in the region of $\omega = \omega_a$. The solution for $|\hat{v}_z/\hat{v}_x(z = 0)|$, using the approximate form above, with B = C = D = 0 is sketched in Figure 2.2 as a function of ω/ω_a . We have taken $\gamma=1$ and $2k_x\Lambda_0=1$. Each curve is labelled by its value of e^{+z/Λ_0}. We conclude therefore that <u>there is no resonance for frequencies $\omega \sim \omega_a$ for the vertical velocity driven by the horizontal velocity component</u>.

Another possibility for resonance for frequencies $\omega \lesssim \omega_a$ (so that the approximate solution (2.2.40) is valid) is when

$$\pm q + \frac{1}{2\Lambda_0} - \frac{\nu}{2\Lambda_0} = 0 \qquad (2.2.51)$$

i.e.

$$k_x\Lambda_0 = \tfrac{1}{2} \pm \tfrac{1}{2}\left(1 - \frac{4\omega^2\Lambda_0}{g}\right)^{\frac{1}{2}}, \qquad (2.2.52)$$

which occurs for the $J_{-\nu}$ solution only. For (2.2.52) to be satisfied we must have $\omega \lesssim \omega_a$. We sketch in Figure 2.3 the ratio $|\hat{v}_z/\hat{v}_x(0)|$ as a function of ω/ω_a for the particular integral with A = 0. We take $k_x\Lambda_0 = \frac{1}{4}$, $\gamma = 5/3$ and use the approximate

Figure 2.2 - The ratio of the amplitude of the vertical velocity perturbation, at height z, to the horizontal velocity perturbation at z = 0, sketched for two heights z and for frequencies in the neighbourhood of the acoustic cut-off frequency ω_a (Equation (2.2.50)).

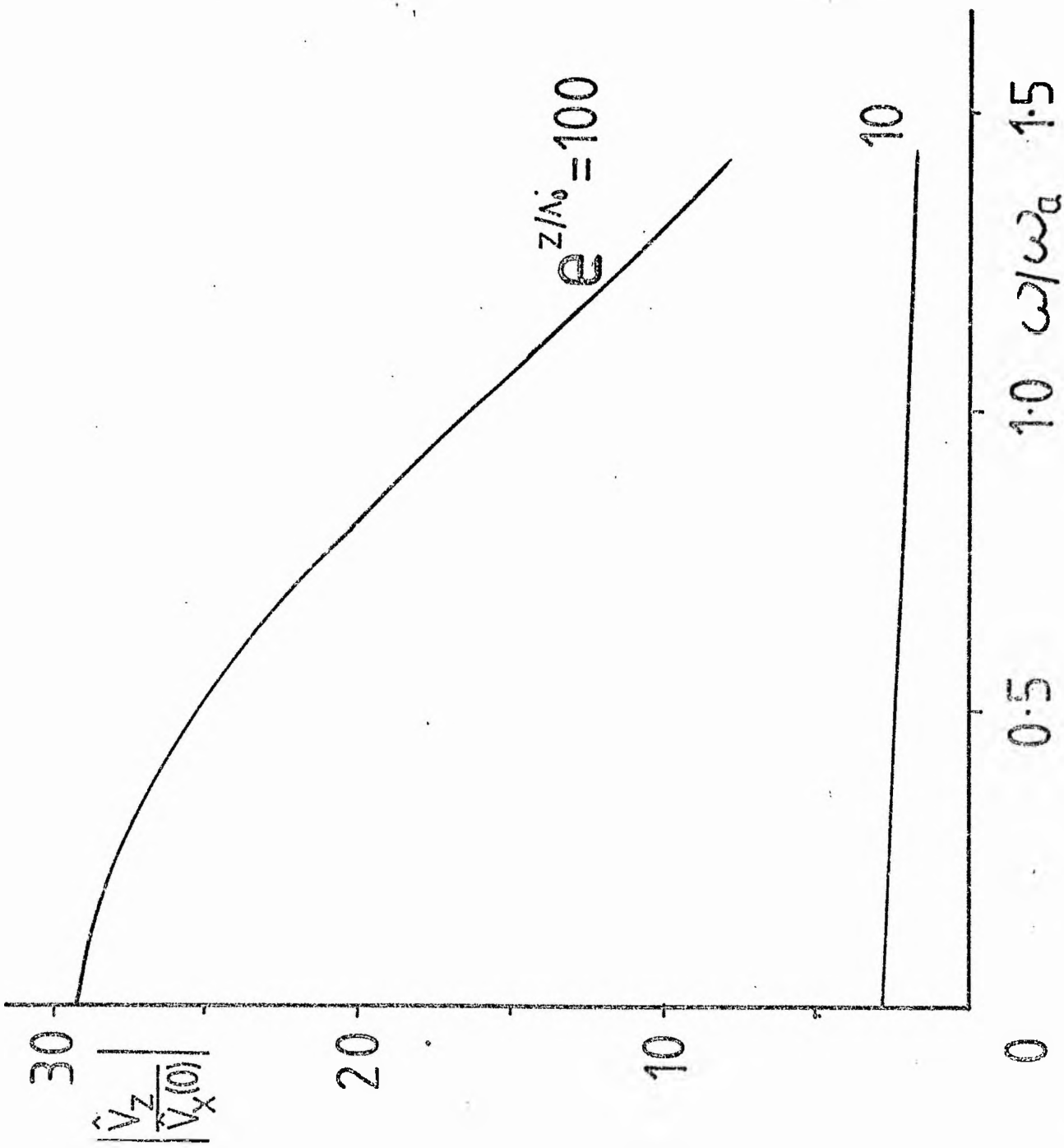

Figure 2.3 - The ratio of the amplitude of the vertical velocity perturbation, at height z, to the horizontal velocity perturbation at z = 0, sketched for two heights z. We have adopted the $J_{-\nu}$ solution for $\hat{v}_x$.

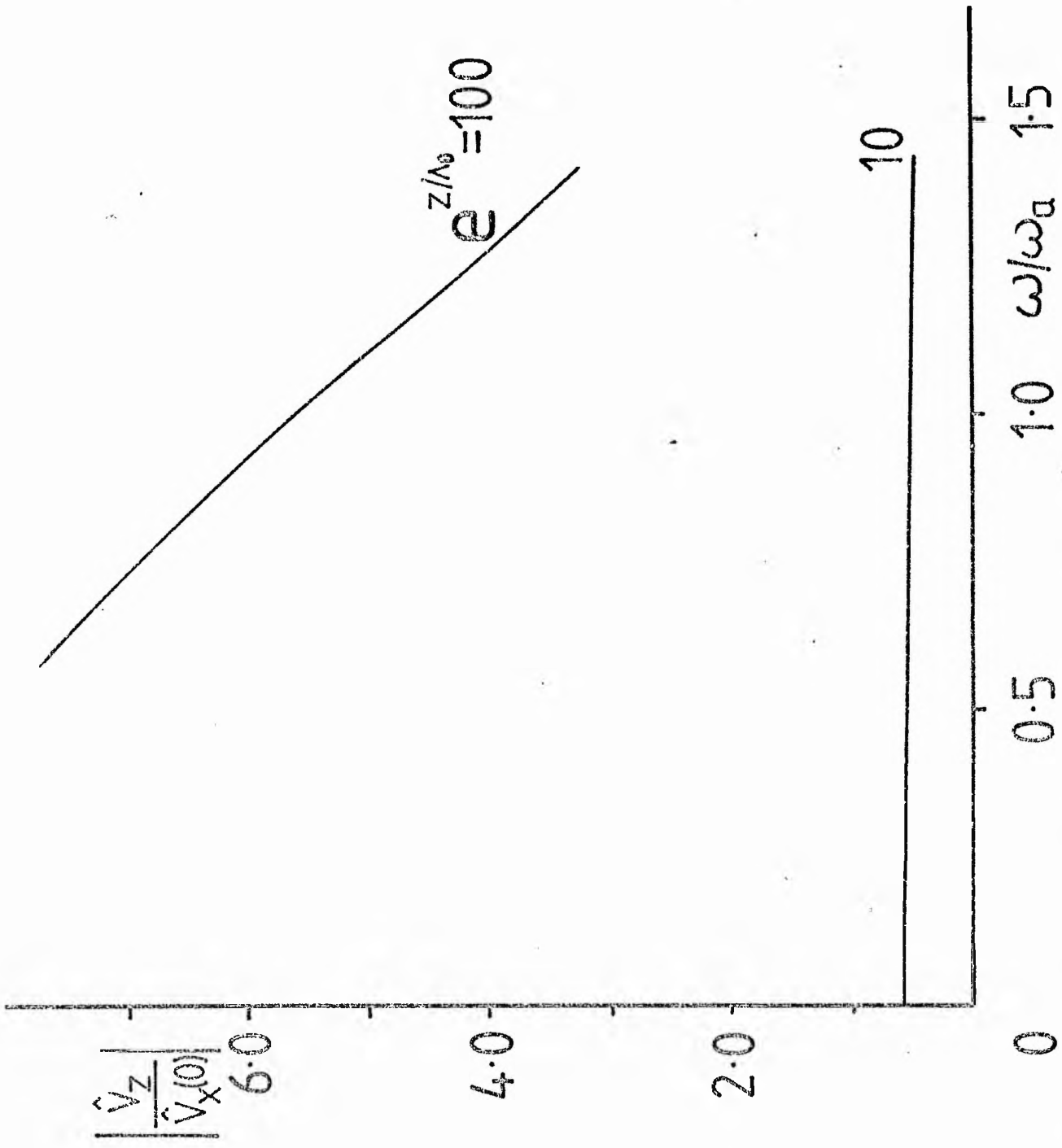

solution (2.2.49). Again, we see that there is no resonant effect for wavelengths and frequencies satisfying (2.2.52).

We now consider Hollweg's claim for resonant behaviour. For the sake of clarity it is convenient to reproduce here a small section of Hollweg's analysis. For simplicity we take $\gamma = 1$ in (2.2.35). Writing $y = \frac{2\omega\Lambda_0 e^{-z/2\Lambda_0}}{v_A(0)}$, Hollweg substitutes the series expansions for $J_\nu(y)$ and $J_{-\nu}(y)$ into the integrals (2.2.34) so that the particular integral of (2.2.32) is given by

$$v_z = \Lambda_0\left(1-\frac{4\omega^2\Lambda_0^2}{c_0^2}\right)^{-\frac{1}{2}}\left\{y^{-(2\Lambda_0 q+1)}\, ik_x \int y^{(2\Lambda_0 q+1)}\frac{d}{dy}\left[A\sum_{k=0}\frac{(-1)^k(\frac{y}{2})^{2k+\nu}}{k.\ (\nu+k+1)}+\right.\right.$$

$$\left.\left. B\sum_{k=0}\frac{(-1)^k(\frac{y}{2})^{2k-\nu}}{k!\,\Gamma(-\nu+k+1)}\right]dy \;-\; (q \leftrightarrow -q)\right\}, \qquad (2.2.53)$$

where $(q \leftrightarrow -q)$ indicates that q and -q are to be interchanged. Integrating Equation (2.2.53) term by term then gives

$$v_z = \Lambda_0\left(1-\frac{4\omega^2\Lambda_0^2}{c_0^2}\right)^{-\frac{1}{2}}\left\{ik_x\left[A\sum_{k=0}\frac{(-1)^k\, 2^{-2k-\nu}(2k+\nu)y^{2k+\nu}}{k!\,\Gamma(\nu+k+1)(2k+\nu+2\Lambda_0 q+1)}\right.\right.$$

$$\left.\left. + B\sum_{k=0}\frac{(-1)^k\, 2^{-2k+\nu}(2k-\nu)y^{2k-\nu}}{k!\,\Gamma(-\nu+k+1)(2k-\nu+2\Lambda_0 q+1)}\right] - (q \leftrightarrow -q)\right\}. \qquad (2.2.54)$$

Hollweg argues that the velocity amplitude may become infinite when

$$(2k \pm \nu + 2\Lambda_0 q + 1) = 0 \quad \text{or} \quad (2k \pm \nu - 2\Lambda_0 q + 1) = 0, \qquad (2.2.55)$$

and since both k and ν are real and positive, q must be real, i.e. $\omega < \omega_a$. In this case $1 \pm 2\Lambda_0 q > 0$, and so 'resonance' can

only occur for the solution $J_{-\nu}$ and the condition becomes

$$\nu = |2k_x\Lambda_0| = 2k + 1 \pm 2\Lambda_0 q \,, \qquad (2.2.56)$$

that is,

$$k_x\Lambda_0 = k + \tfrac{1}{2} \pm \tfrac{1}{2}\left(1 - \frac{4\omega^2\Lambda_0}{g}\right), \quad k = 0, 1, \ldots \qquad (2.2.56)'$$

However the integrals (2.2.34) are always finite for any combination of ω and k_x and so <u>infinite velocity amplitudes do not occur</u>. Condition (2.2.56)', with k = 0, is that given by (2.2.52), and we have seen that this does not correspond to resonance. It is interesting to note that the condition for resonance (2.2.56) is simply the condition that in the Lommel function solution, $S_{\mu,\nu}$, $\mu \pm \nu$ is a negative odd integer (see the Appendix).

The condition for resonance given by Hollweg is simply that the series solution (after applying boundary conditions) contains a term $\log_e y$. For y small, this is large in magnitude but for $k \gg 1$ it is not the dominant term, and for k = 0 we have seen there may be no resonant effect.

In conclusion, then, we consider that Hollweg's claim for a resonance between the vertical velocity perturbation and the (driving) horizontal perturbation to be misleading.

Appendix

The differential equation

$$z^2 \frac{d^2y}{dz^2} + z\frac{dy}{dz} + (z^2 - \lambda^2)y = z^{\mu+1} , \qquad (2.A.1)$$

has the solution

$$y = s_{\mu,\lambda}(z),$$

where

$$s_{\mu,\lambda}(z) = \frac{z^{\mu+1}}{(\mu-\lambda+1)(\mu+\lambda+1)}\ {}_1F_2\left(1; \frac{\mu-\lambda+3}{2}, \frac{\mu+\lambda+3}{2}; \frac{-z^2}{4}\right), \qquad (2.A.2)$$

provided that $\mu \pm \lambda$ is not a negative odd integer (Magnus and Oberhettinger, 1949). The function ${}_1F_2$ is a generalized hypergeometric series.

For arbitrary values of μ and ν the function (Erdélyi et al, 1954)

$$S_{\mu,\nu}(z) = s_{\mu,\lambda}(z) + 2^{\mu-1}\Gamma\left(\frac{\mu-\lambda+1}{2}\right)\Gamma\left(\frac{\mu+\lambda+1}{2}\right)\left[\sin\left(\frac{\mu-\lambda}{2}\pi\right) J_\lambda(z) - \cos\left(\frac{\mu-\lambda}{2}\pi\right) Y_\lambda(z)\right]$$

is a solution of (2.A.1), since the expression on the right-hand side remains meaningful when $\mu \pm \nu$ approaches a negative odd integer.

The functions $s_{\mu,\nu}(z)$ and $S_{\mu,\nu}(z)$ are known as Lommel functions. The solution for $G_1(x)$ is then given by Equations (2.2.31), (2.2.36) and (2.2.38):

$$q_L(x) = 2ik_x\Lambda_0\Big\{A\Big[\frac{x^{\mu+1}}{2\Lambda_0}J_\nu(ax) - \frac{1}{2\Lambda_0}J_\nu(a) +$$

$$+\frac{1}{\Lambda_0}\Big(\frac{\gamma-1}{\gamma}-\frac{\mu+1}{2}\Big)a^{-\mu-1}\Big((\mu+\nu-1)ax\,J_\nu(ax)S_{\mu-1,\nu-1}(ax) - ax\,J_{\nu-1}(ax)S_{\mu,\nu}(ax)$$

$$-(\mu+\nu-1)a\,J_\nu(a)S_{\mu-1,\nu-1}(a) + a\,J_{\nu-1}(a)S_{\mu,\nu}(a)\Big)\Big]$$

$$+B\Big[\frac{x^{\mu+1}}{2\Lambda_0}J_{-\nu}(ax) - \frac{1}{2\Lambda_0}J_{-\nu}(a) +$$

$$+\frac{1}{\Lambda_0}\Big(\frac{\gamma-1}{\gamma}-\frac{\mu+1}{2}\Big)a^{-\mu-1}\Big((\mu-\nu-1)ax\,I_\nu(ax)S_{\mu-1,-\nu-1}(ax) - ax\,I_{-\nu-1}(ax)S_{\mu,-\nu}(ax)$$

$$-(\mu-\nu-1)a\,I_{-\nu}(a)S_{\mu-1,-\nu-1}(a) - a\,I_{-\nu-1}(a)S_{\mu,-\nu}(a)\Big)\Big]\Big\},$$

where $a = 2\omega\Lambda_0/v_A(0)$ and $\mu = 2\Lambda_0\alpha_1 - 1$.

Chapter 3 : WAVE PROPAGATION IN A MAGNETIC FLUX TUBE

3.1 Introduction

In this chapter we consider the possible wave modes present in a structured magnetic field, namely an isolated magnetic flux tube, and in particular we are concerned with a slender flux tube in a stratified atmosphere, as appropriate to the solar context. Firstly, however, we shall consider a uniform medium.

Cram and Wilson (1975) have discussed the possible modes of vibration of a two-dimensional Cartesian magnetic flux sheath and Wilson (1978a, 1978b) has presented a discussion of hydromagnetic modes in structured magnetic fields for both the flux sheath and flux tube geometries. Wilson's analysis differs somewhat from our own (Wilson, 1979a, b), and we shall briefly consider the discrepancy in Section 3.2. Defouw (1976) was the first to consider the propagation of waves in a slender flux tube in a stratified compressible atmosphere, though his treatment is for an isothermal atmosphere only.

The governing equations are those presented in Chapter 1 (Equations (1.6.5) - (1.6.10)), and it is useful to restate them here in component form in cylindrical geometry for an axi-symmetric flux tube $\underline{B}_0(r,z) = (B_{0r}, 0, B_{0z})$, and basic state $\rho_0 = \rho_0(r,z)$ etc.

The equations for the basic state are

$$0 = -\nabla p_0 + \underline{j}_0 \wedge \underline{B}_0 - \rho_0 \underline{g} ,$$

$$0 = \nabla \cdot \underline{B}_0 , \qquad \underline{j}_0 = \frac{\nabla \wedge B_0}{\mu_0}$$

For adiabatic perturbations (i.e. $\mathcal{L}' \equiv 0$) in velocity and magnetic field of the form

$$\underline{v} = (v_r, v_\theta, v_z) \qquad \underline{b} = (b_r, b_\theta, b_z)$$

the components of the perturbation equations are

$$\frac{\partial \rho}{\partial t} + v_r \frac{\partial \rho_0}{\partial r} + v_z \frac{\partial \rho_0}{\partial z} + \rho_0 \left(\frac{1}{r} \frac{\partial}{\partial r}(r v_r) + \frac{1}{r} \frac{\partial v_\theta}{\partial \theta} + \frac{\partial v_z}{\partial z} \right) = 0, \tag{3.1.1}$$

$$\rho_0 \frac{\partial v_r}{\partial t} = -\frac{\partial p}{\partial r} - \frac{B_{0z}}{\mu_0} \left(\frac{\partial b_z}{\partial r} - \frac{\partial b_r}{\partial z} \right) - \frac{b_z}{\mu_0} \left(\frac{\partial B_{0z}}{\partial r} - \frac{\partial B_{0r}}{\partial z} \right), \tag{3.1.2}$$

$$\rho_0 \frac{\partial v_\theta}{\partial t} = -\frac{1}{r} \frac{\partial p}{\partial \theta} - \frac{B_{0z}}{\mu_0} \left(\frac{1}{r} \frac{\partial b_z}{\partial \theta} - \frac{\partial b_\theta}{\partial z} \right) + \frac{B_{0r}}{\mu_0} \left(\frac{1}{r} \frac{\partial}{\partial r} r b_\theta - \frac{\partial b_r}{\partial \theta} \right), \tag{3.1.3}$$

$$\rho_0 \frac{\partial v_z}{\partial t} = -\frac{\partial p}{\partial z} - \rho g + \frac{B_{0r}}{\mu_0} \left(\frac{\partial b_z}{\partial r} - \frac{\partial b_r}{\partial z} \right) + \frac{b_r}{\mu_0} \left(\frac{\partial B_{0z}}{\partial r} - \frac{\partial B_{0r}}{\partial z} \right), \tag{3.1.4}$$

$$\frac{\partial p}{\partial t} + v_r \frac{\partial p_0}{\partial r} + v_z \frac{\partial p_0}{\partial z} = c_0^2 \left(\frac{\partial \rho}{\partial t} + v_r \frac{\partial \rho_0}{\partial r} + v_z \frac{\partial \rho_0}{\partial z} \right), \tag{3.1.5}$$

$$\frac{\partial b_r}{\partial t} = -\frac{B_{0r}}{r} \frac{\partial v_\theta}{\partial \theta} - \frac{\partial}{\partial z} \left(v_z B_{0r} - v_r B_{0z} \right), \tag{3.1.6}$$

$$\frac{\partial b_\theta}{\partial t} = \frac{\partial}{\partial r} \left(v_\theta B_{0r} \right) + \frac{\partial}{\partial z} \left(v_\theta B_{0z} \right), \tag{3.1.7}$$

$$\frac{\partial b_z}{\partial t} = \frac{1}{r} \frac{\partial}{\partial r} \left[r \left(v_z B_{0r} - v_r B_{0z} \right) \right] - B_{0z} \frac{\partial v_\theta}{\partial \theta}, \tag{3.1.8}$$

$$\frac{1}{r} \frac{\partial}{\partial r} (r b_r) + \frac{1}{r} \frac{\partial b_\theta}{\partial \theta} + \frac{\partial b_z}{\partial z} = 0. \tag{3.1.9}$$

3.2 Uniform Atmosphere

The purpose of this section is to investigate waves in a uniform vertical column of magnetic field and to determine the resulting form of the dispersion relation for a flux tube as it becomes slender. Then, we shall present an *ab initio* approximation for waves in a slender flux tube, and compare the results with the more general analysis.

Consider the basic state of a uniform medium of pressure p_0, density ρ_0 and magnetic field $\underline{B} = B_0\hat{\underline{z}}$. The linearized equations describing adiabatic perturbations about this static ($\underline{v}_0 \equiv \underline{0}$) state are those given above (Equations (3.1.1) - (3.1.9)), with $g=0$, $B_{0r}=0$, $B_{0z}=B_0$ and p_0, ρ_0 and c_0^2 constants. In a cylindrical coordinate system (r, θ, z), with perturbations in velocity and magnetic field

$$\underline{v} = (v_r, v_\theta, v_z) \quad , \qquad \underline{b} = (b_r, b_\theta, b_z),$$

the governing system of equations may be reduced to two equations, namely

$$\frac{\partial^2}{\partial t^2}\left(\frac{\partial^2}{\partial t^2} - (c_0^2 + v_A^2)\nabla^2\right)\Delta + c_0^2 v_A^2 \frac{\partial^2}{\partial z^2}\nabla^2\Delta = 0, \qquad (3.2.1)$$

where

$$\nabla^2 \equiv \frac{\partial^2}{\partial r^2} + \frac{1}{r}\frac{\partial}{\partial r} + \frac{1}{r^2}\frac{\partial^2}{\partial \theta^2} + \frac{\partial^2}{\partial z^2}, \quad \Delta = \nabla.\underline{v}, \qquad (3.2.2)$$

and

$$\left(\frac{\partial^2}{\partial t^2} - v_A^2 \frac{\partial^2}{\partial z^2}\right)\Gamma = 0, \qquad (3.2.3)$$

with

$$\Gamma = \left(\nabla \wedge \underline{v}\right)_z = \frac{1}{r}\frac{\partial}{\partial r}(r v_\theta) - \frac{1}{r}\frac{\partial v_r}{\partial \theta} \quad . \qquad (3.2.4)$$

Here $c_0 = (\gamma p_0/\rho_0)^{\frac{1}{2}}$ and $v_A = B_0/(\mu_0\rho_0)^{\frac{1}{2}}$ are the sound and Alfvén speeds respectively.

For a basic state of a cylindrical column of field of radius r_0, embedded in a field-free medium of density ρ_e and pressure p_e,

$$\underline{B} = \begin{cases} B_0\hat{\underline{z}} \quad , & r < r_0 \, , \\ 0 \quad , & r > r_0 \, , \end{cases} \qquad (3.2.5)$$

and lateral pressure balance implies

$$p_0 + \frac{B_0^2}{2\mu_0} = p_e . \qquad (3.2.6)$$

Thus the interior and exterior densities are related by

$$\rho_e c_e^2 = \rho_0 (c_0^2 + \frac{\gamma}{2} v_A^2) \qquad (3.2.7)$$

where $c_e = (\gamma p_e/\rho_e)^{\frac{1}{2}}$ is the sound speed of the exterior.

Consider the interior region. Writing

$$\Delta = R(r) e^{i\omega t + il\theta + ikz} ,$$

Equation (3.2.1) reduces to a form of Bessel's equation

$$\frac{d^2R}{dr^2} + \frac{1}{r}\frac{dR}{dr} - (\frac{l^2}{r^2} + m_0^2)R = 0, \qquad (3.2.8)$$

where

$$m_0^2 = \frac{(k^2c_0^2 - \omega^2)(k^2v_A^2 - \omega^2)}{(k^2c_T^2 - \omega^2)(c_0^2 + v_A^2)} , \qquad (3.2.9)$$

and the speed c_T is defined by

$$c_T^2 = \frac{c_0^2 v_A^2}{c_0^2 + v_A^2} . \qquad (3.2.10)$$

Equation (3.2.8) has solution

$$R(r) = \begin{cases} A_0 I_1(m_0 r) + A_1 K_1(m_0 r), & m_0^2 > 0 \\ A_0 J_1(n_0 r) + A_1 Y_1(n_0 r), & m_0^2 < 0 \end{cases} \quad (r < r_0), \qquad (3.2.11)$$

where $n_0^2 = -m_0^2$, and J_1, Y_1, I_1 and K_1 are Bessel functions of order 1 (Abramowitz and Stegun, 1967). A_0 and A_1 are arbitrary constants.

The perturbations in velocity, magnetic field, density and pressure are then given by

$$v_r = \frac{(c_0^2 + v_A^2)(k^2c_T^2 - \omega^2)}{-\omega^2(k^2v_A^2 - \omega^2)} \frac{dR(r)}{dr} e^{i\omega t+il\theta+ikz} ,$$

$$v_\theta = \frac{l(k^2c_0^2 - \omega^2)}{i\omega^2 m_0^2} \frac{R(r)}{r} e^{i\omega t+il\theta+ikz} , \quad (l\neq 0)$$

$$v_z = \frac{1}{ik} \frac{k^2c_0^2}{\omega^2} R(r) e^{i\omega t+il\theta+ikz} ,$$

$$b_r = \frac{B_0k(c_0^2 + v_A^2)(k^2c_T^2 - \omega^2)}{\omega^3(k^2v_A^2 - \omega^2)} \frac{dR}{dr} e^{i\omega t+il\theta+ikz} ,$$

$$b_\theta = \frac{B_0kl}{i\omega^3} \frac{(k^2c_0^2 - \omega^2)}{m_0^2} \frac{R(r)}{r} e^{i\omega t+il\theta+ikz} , (l\neq 0)$$

$$b_z = (k^2c_0^2 - \omega^2) \frac{B_0}{i\omega^3} R(r) e^{i\omega t+il\theta+ikz} ,$$

$$\rho = -\frac{\rho_0}{i\omega} R(r) e^{i\omega t+il\theta+ikz} ,$$

$$p = -\frac{c_0^2\rho_0}{i\omega} R(r) e^{i\omega t+il\theta+ikz} ,$$

$(0 \leq r < r_0)$ (3.2.1

For axisymmetric perturbations ($\frac{\partial}{\partial\theta} \equiv 0$), the equations for v_θ and b_θ uncouple from the rest of the system; disturbances v_θ and b_θ are propagated as Alfvén waves.

In this chapter we shall consider only axisymmetric perturbations. The solution (3.2.11) for R(r) is then

$$R(r) = \begin{cases} A_0 I_0(m_0 r) , & m_0^2 > 0 \\ A_0 J_0(n_0 r) , & m_0^2 < 0 \end{cases} , \quad (r < r_0), \qquad (3.2.13)$$

where we have now applied the condition that the perturbations are finite at the origin.

In the exterior region, the governing equation (with $\frac{\partial}{\partial\theta} \equiv 0$) for R(r) is

$$\frac{d^2R}{dr^2} + \frac{1}{r}\frac{dR}{dr} - m_e^2 R = 0 , \qquad (r > r_0) \qquad (3.2.14)$$

where

$$m_e^2 = \frac{k^2 c_e^2 - \omega^2}{c_e^2} . \qquad (3.2.15)$$

Note that m_e^2 may be positive or negative accordingly as the vertical phase-speed ω/k is subsonic or supersonic with respect to the sound speed in the external medium. The solutions of (3.2.14) are

$$R(r) = \begin{cases} A_3 K_0(m_e r), & m_e^2 > 0 \\ A_2 J_0(n_e r) + A_3 Y_0(n_e r), & m_e^2 < 0 \end{cases} \quad (r > r_0), \qquad (3.2.16)$$

where A_3 and A_2 are arbitrary constants and we have applied the boundary condition that the solutions be finite at infinity.

3.2.1 The Dispersion Relation

In addition to the boundary conditions at the origin and infinity, the interior and exterior regions are related by the boundary conditions (See Chapter 1)

$$v_r, \text{ and } p + \frac{B_0 b_z}{\mu_0} \text{ continuous across } r = r_0. \qquad (3.2.17)$$

For ω^2 and k^2 real, there are four cases to consider: $m_0^2 \gtrless 0$, $m_e^2 \lessgtr 0$; $m_0^2 > 0$ ($m_e^2 > 0$) corresponds to decaying, exponential-type solutions in the interior (exterior); $m_0^2 < 0$ corresponds to oscillatory solutions inside the tube. We note that in general there is also the possibility of solutions with complex frequencies.

The possible combinations of c_0, c_e and v_A giving rise to the different cases may be easily visualized in terms of a modification to a diagram of Cram and Wilson (1975). Figure 3.1a, b, c gives the regions of $m_0^2 \gtrless 0$, $m_e^2 \gtrless 0$, in the plane $(\frac{\omega}{kc_0}, \frac{v_A}{c_0})$ for a) $c_0 = c_e$, b) $c_e > c_0$, c) $c_0 > c_e$. The areas labelled A are for $m_e^2 > 0$ and those labelled B are for $m_e^2 < 0$.

3.2.1(i) Evanescent Modes in the exterior

We shall consider firstly the case of evanescent modes in the exterior ($m_e^2 > 0$ -- regions A in Figure 3.1) with m_0^2 being either positive (giving evanescent solutions) or negative (giving oscillatory solutions in the interior). With the appropriate solution of (3.2.16), the solutions for the velocity, pressure and density in the exterior are

$$\left.\begin{aligned} v_r^{(e)} &= \frac{c_e^2}{\omega^2} m_e A_e K_1(m_e r) e^{i\omega t + ikz}, \\ v_z^{(e)} &= \frac{1}{ik}\frac{k^2 c_e^2}{\omega^2} A_e K_0(m_e r) e^{i\omega t + ikz}, \\ p^{(e)} &= -\frac{c_e^2 \rho_e}{i\omega} A_e K_0(m_e r)\, e^{i\omega t + ikz}, \\ \rho^{(e)} &= -\frac{\rho_e}{i\omega} A_e K_0(m_e r) e^{i\omega t + ikz}, \end{aligned}\right\} \quad (r > r_0) \quad (3.2.18)$$

where A_e is an arbitrary constant.

Suppose that m_0^2 is positive (regions A1, A3 and A5). Applying the boundary conditions (3.2.17) gives the dispersion relation

$$\frac{I_0(m_0 r_0)}{I_1(m_0 r_0)} = \frac{m_0}{m_e}\frac{\rho_e}{\rho_0}\frac{\omega^2}{(k^2 v_A^2 - \omega^2)}\frac{K_0(m_e r_0)}{K_1(m_e r_0)}, \quad (3.2.19)$$

valid for $m_0^2 > 0$, $m_e^2 > 0$.

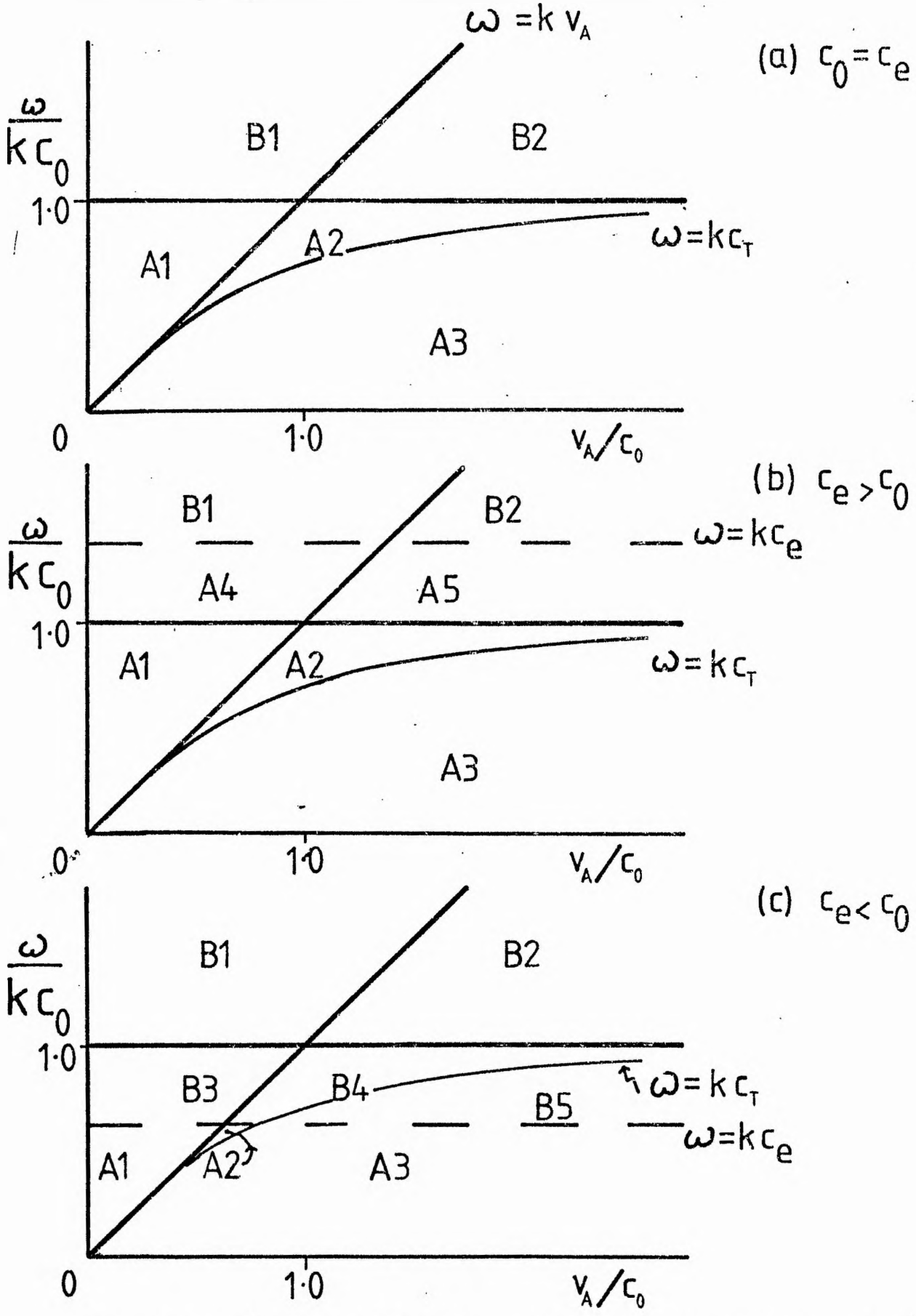

Figure 3.1 - Regions in the ω/kc_0 - v_A/c_0 plane for $m_0^2 \gtrless 0$ and $m_e^2 \gtrless 0$. The regions labelled B are those where $m_e^2 < 0$ and those labelled A where $m_e^2 > 0$. Regions A1, A3 and A5 have $m_0^2 > 0$. a) $c_0 = c_e$ (See Cram and Wilson (1975)). b) $c_e > c_0$. c) $c_e < c_0$. The dashed line in Figures b) and c) is the line $\omega^2 = k^2 c_e^2$.

It is obvious from Equation (3.2.19) that there are no solutions in the regions A1 of Figure 3.1. Therefore, the solutions of interest lie only in the regions A3 and A5.

Now, we are interested in the solutions for a slender tube, which we shall define, at this stage, to correspond to $kr_0 \ll 1$. Thus, a tube is slender if its circumference is very much less than the vertical wavelength of a disturbance. Assuming that as $kr_0 \to 0$, both $m_0 r_0 \to 0$ and $m_e r_0 \to 0$, which must be verified a posteriori, and noting that

$$I_0(m_0 r_0) \sim 1 , \quad I_1(m_0 r_0) \sim \frac{1}{2} m_0 r_0 \quad \text{as } m_0 r_0 \to 0,$$

and

$$K_0(m_e r_0) \sim -\log(m_e r_0), \; K_1(m_e r_0) \sim (m_e r_0)^{-1} \text{ as } m_e r_0 \to 0 ,$$

then Equation (3.2.19) reduces to

$$\rho_0(k^2 c_T^2 - \omega^2)(c_0^2 + v_A^2) + \frac{1}{4}(k^2 c_0^2 - \omega^2)\omega^2 \rho_e r_0^2 \log(m_e r_0)^2 = 0. \tag{3.2.20}$$

Equation (3.2.20) gives rise to two solutions for ω^2. The first solution, given by Roberts (Roberts and Webb , 1978), is

$$\omega^2 \approx k^2 c_T^2 + \frac{1}{4}\frac{\rho_e}{\rho_0} c_T^2 \frac{(c_0^2 - c_T^2)}{c_0^2 + v_A^2} k^4 r_0^2 \log(k^2 r_0^2) ; \tag{3.2.21}$$

thus, in a slender tube we have the result $\omega^2 \approx k^2 c_T^2$. Substituting the expression (3.2.21) for ω^2 into those for m_0^2 and m_e^2, we find that both $m_0 r_0$ and $m_e r_0$ tend to zero as $kr_0 \to 0$. The solution is consistent with our assumptions that $m_0^2 > 0$ and $m_e^2 > 0$ provided that $c_T^2 < c_e^2$. Therefore the solutions lie in the region A3 in Figures 3.1a, b and A3 for $(v_A/c_0) < (v_A/c_0)_c$ in Figure 3.1c.

The second solution is

$$\omega^2 \approx k^2 c_e^2 - \frac{c_e^2}{r_0^2} \exp \frac{-4}{(kr_0)^2} \left[\frac{(c_T^2 - c_e^2)(c_0^2 + v_A^2)}{(c_0^2 + \frac{\gamma}{2} v_A^2)(c_0^2 - c_e^2)} \right], \quad (3.2.22)$$

provided $c_e < c_T$ or $c_e > c_0$. This solution lies in the region A5 in Figure 3.1 b and in A3 for $(v_A/c_0) > (v_A/c_0)_c$ in Figure 3.1 c. So in a slender tube we also have the solution $\omega^2 \approx k^2 c_e^2$. This solution also satisfied the consistency requirement that $m_0 r_0 \to 0$ and $m_e r_0 \to 0$ as $kr_0 \to 0$.

Combining the above results, for a slender flux tube in a uniform atmosphere, with $m_e^2 > 0$ and $m_0^2 > 0$, for $c_e > c_0$ there are two approximate solutions

$$\left.\begin{aligned} \omega^2 &\approx k^2 c_e^2 \\ \omega^2 &\approx k^2 c_T^2 \end{aligned}\right\} \quad c_e > c_0, \quad (3.2.23)$$

whilst for $c_e \leq c_0$

$$\omega^2 \approx \min (k^2 c_T^2, k^2 c_e^2), \quad c_e < c_0, \quad (3.2.24)$$

The dispersion relation (3.2.19) has been solved numerically and the solutions sketched in Figures (3.2 a, b) and (3.3 a, b).

In addition to the two approximate solutions given above, there is an exact solution $\omega^2 = k^2 c_0^2$, for $c_0 = c_e$. The motions are longitudinal ($v_r = v_r^{(e)} = 0$) and the magnetic field is undisturbed ($\underline{b} \equiv \underline{0}$).

The solution for the mode $\omega^2 \approx k^2 c_T^2$ is plotted in Figure 3.2a for various values of c_0^2/v_A^2 and for $c_0 = c_e$. We see that for $kr_0 \ll 1$, the approximation $\omega^2 \approx k^2 c_T^2$ is a good one. This mode has phase speed that is both subsonic and sub-Alfvénic and

Figure 3.2a - The solution of the dispersion relation (3.2.19) for the wave. for various values of the parameter c_0/v_A and the tube 'radius' kr_0, with $c_e = c_0$ and $\gamma = 5/3$. Notice that $\omega^2 \approx k^2 c_T^2$ for kr_0 not too large (e.g. $kr_0 \lesssim 1$) in agreement with our weaker claim that agreement is obtained for $kr_0 \ll 1$.

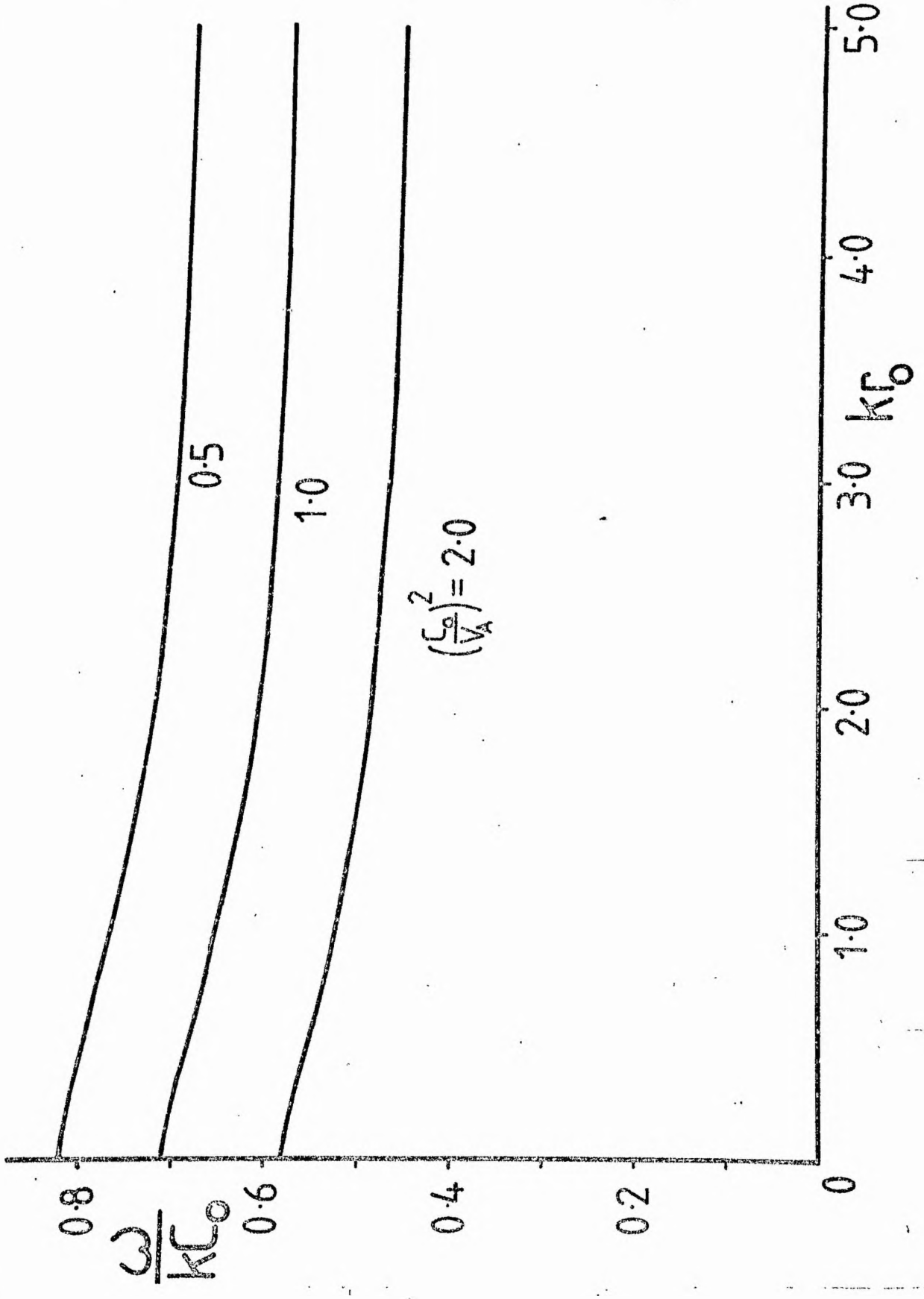

Figure 3.2b - The solution of the dispersion relation (3.2.19) for the sound wave solution for $c_0^2/v_A^2 = 0.4$ and $c_0^2/c_e^2 = 0.5$. Note that for $kr_0 \ll 1$ the solution tends to $\omega^2 = k^2 c_e^2$ (labelled — — -- — —) very rapidly as described by Equation (3.2.22).

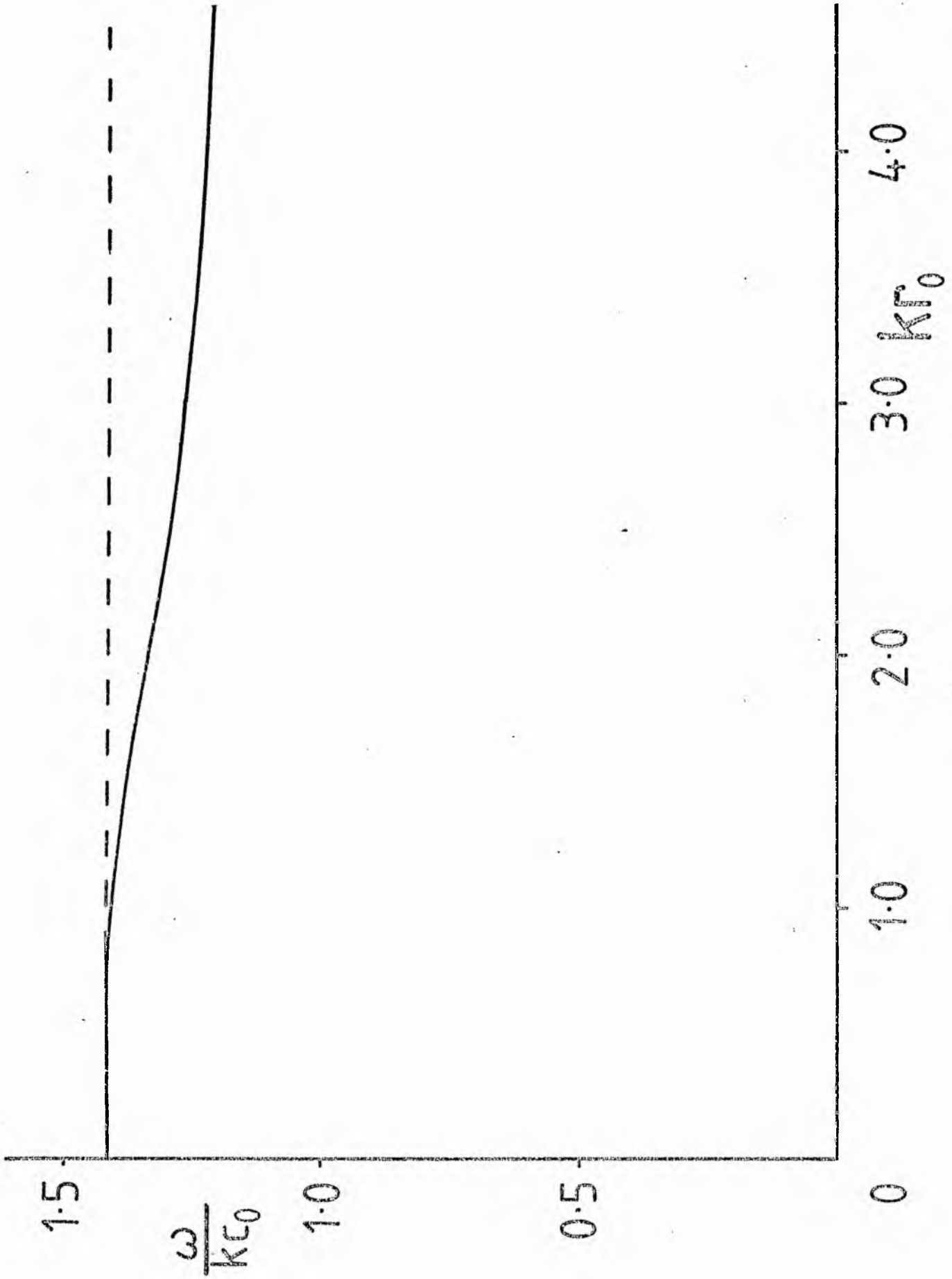

Figure 3.3a - The solutions for the vertical velocity v_z, normalized to unity at the origin (continuous curve), total pressure p_T (labelled - - -), and gas pressure p (labelled — - — - —) as a function of r/r_0 for the tube-wave solution. We have taken $c_0 = c_e$, $c_0 = v_A$, $\gamma = 5/3$ and have sketched for two values of kr_0.

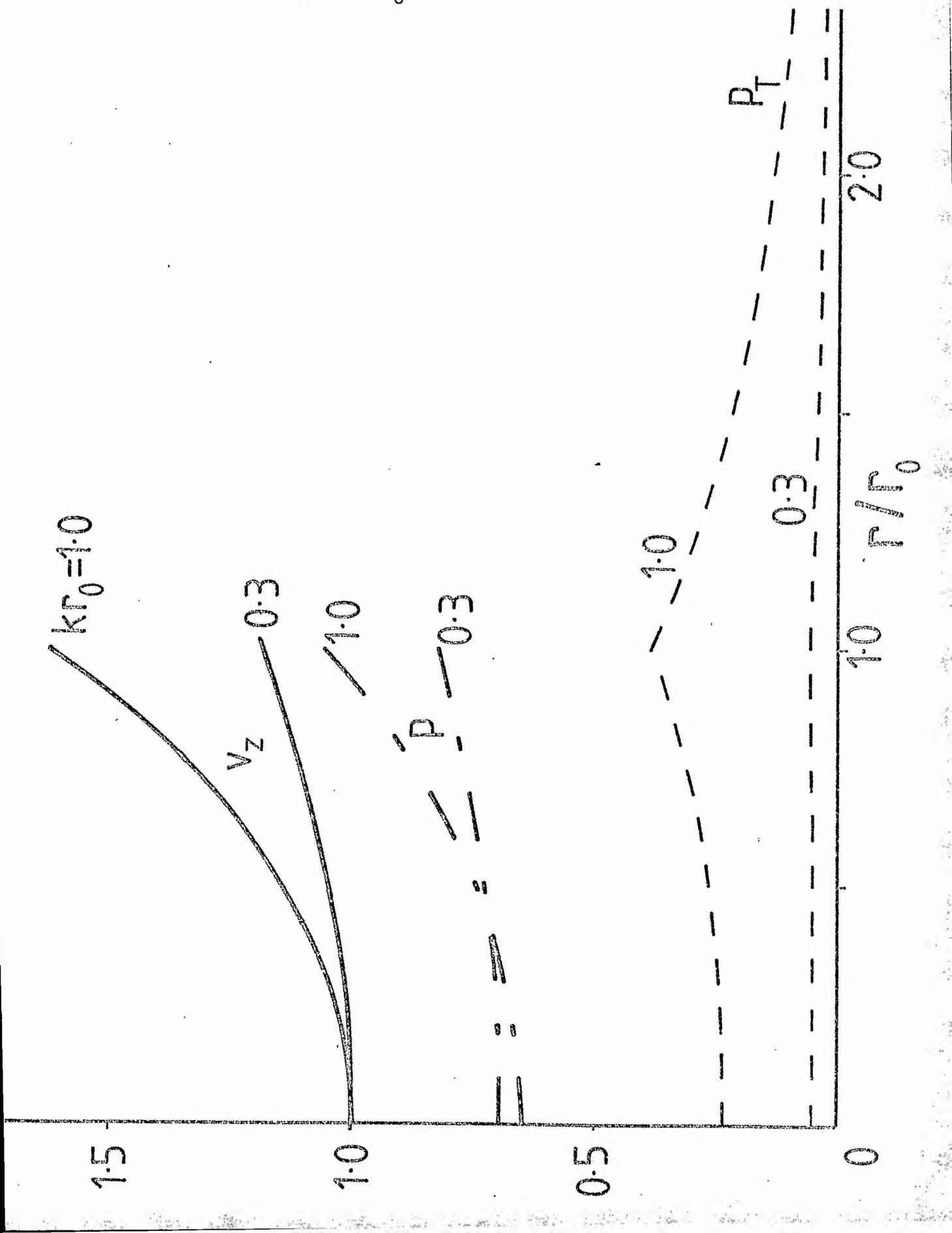

Figure 3.3b - The solutions for the vertical velocity v_z, total pressure p_T, and gas pressure p as a function of r/r_0. We have taken $c_0^2/v_A^2 = 0.4$, $c_0^2/c_e^2 = 0.5$, $\gamma = 5/3$ and $kr_0 = 1$.

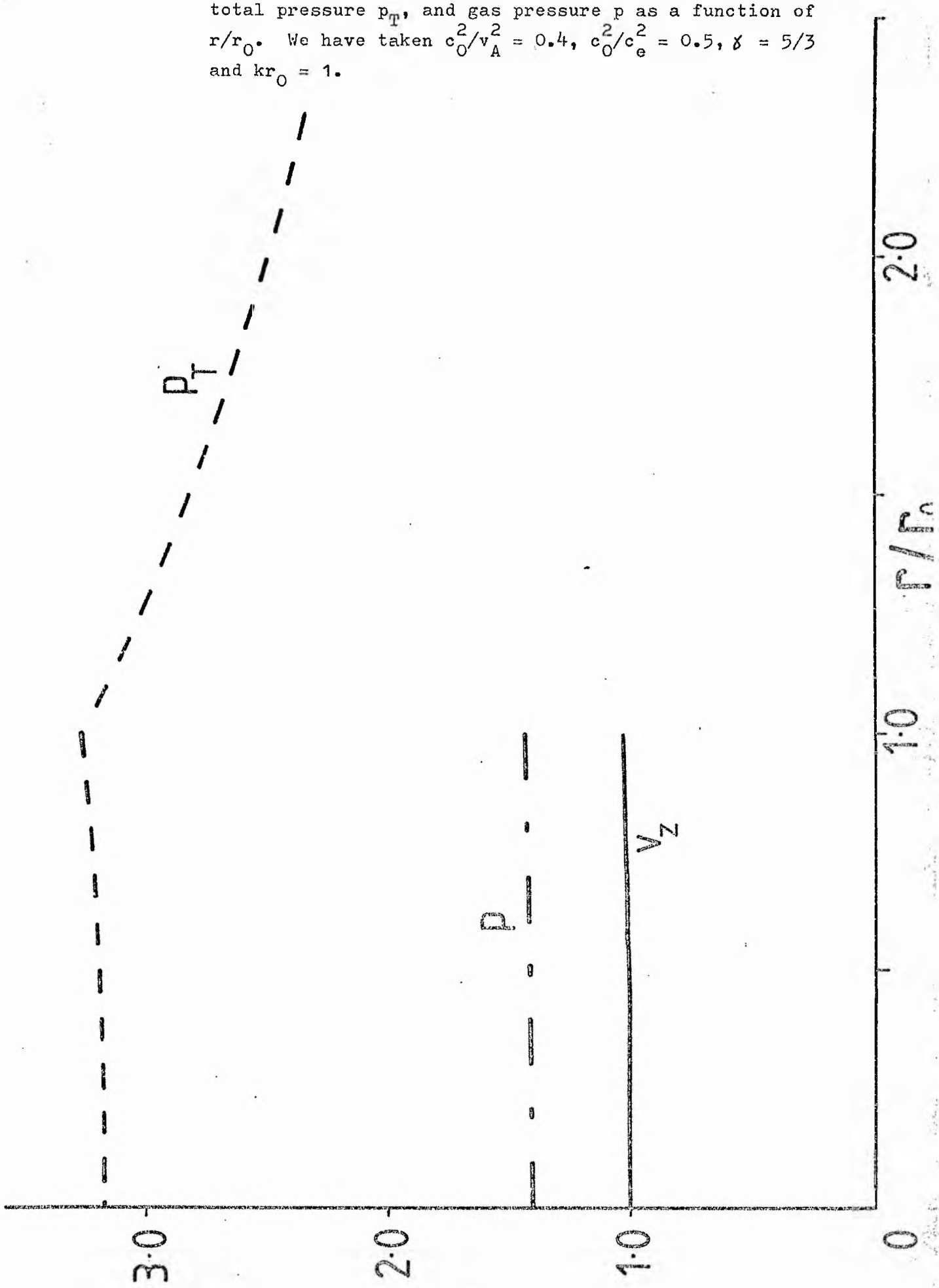

so it is a slow-mode-type wave. The total pressure, radial velocity, internal gas pressure and vertical component of velocity inside the tube are sketched in Figure 3.3a as functions of r/r_0. From the figure we see that as $kr_0 \to 0$ the total pressure (and hence the external gas pressure) becomes small compared to the internal gas pressure. Indeed, it follows from Equation (3.2.12) that

$$\frac{p + B_0 b_z/\mu_0}{p} = \frac{(\omega^2 - k^2 c_T^2)(c_0^2 + v_A^2)}{\omega^2 c_0^2} \quad . \qquad (3.2.25)$$

Thus, for the solution (3.2.21),

$$\left(\frac{p_e}{p}\right)_{r_0} = \frac{p+B_0 b_z/\mu_0}{p} = \frac{1}{4}\frac{\rho_e}{\rho_0}\left(1 - \frac{c_T^2}{c_0^2}\right) k^2 r_0^2 \log(k^2 r_0^2), \qquad (3.2.26)$$

$$\to 0 \quad \text{as } kr_0 \to 0.$$

Therefore the solution $\omega^2 \approx k^2 c_T^2$ for a slender flux tube corresponds to <u>negligible perturbations in the exterior</u>.

The solutions for the second mode are sketched in Figures 3.2b and 3.3b. The pressure fluctuations in the exterior are no longer negligible for small kr_0 for this mode, as may be seen from Equation (3.2.25) which gives

$$\frac{p + B_0 b_z/\mu_0}{p} = \frac{(c_e^2 - c_T^2)(c_0^2 + v_A^2)}{c_e^2 c_0^2} \quad . \qquad (3.2.27)$$

The second mode is a sound wave, with phase speed equal to the sound speed in the exterior, propagating along the tube.

Consider now the case of $m_0^2 < 0$, corresponding to oscillatory solutions inside the tube. The relevant parameter ranges are those defined by regions A2 and A4 of Figure 3.1.

We adopt the second solution of 3.2.13, and the resulting dispersion relation is

$$\frac{J_0(n_0 r_0)}{J_1(n_0 r_0)} + \frac{n_0 \rho_e}{m_e \rho_0} \frac{\omega^2}{k^2 v_A^2 - \omega^2} \frac{K_0(m_e r_0)}{K_1(m_e r_0)} = 0 \quad . \qquad (3.2.28)$$

Again, we look for solutions satisfying the requirement that $n_0 r_0 \to 0$ and $m_e r_0 \to 0$ as $k r_0 \to 0$. Using the approximations

$$J_0(n_0 r_0) \sim 1 \ , \quad J_1(n_0 r_0) \sim \tfrac{1}{2} n_0 r_0 \text{ as } n_0 r_0 \to 0 \ .$$

Equation (3.2.28) reduces to the approximate dispersion relation

$$1 - \frac{n_0^2}{4} \frac{\rho_e}{\rho_0} \frac{\omega^2}{(k^2 v_A^2 - \omega^2)} r_0^2 \log (m_e r_0)^2 = 0 \ . \qquad (3.2.29)$$

Substituting for n_0^2 then gives Equation (3.2.20) and, as we have seen, this has the approximate solutions given by (3.2.21) and (3.2.22). However, (3.2.29) shows that the approximate solution $\omega^2 \approx k^2 c_T^2$ no longer satisfies the requirement that $n_0^2 > 0$, and so the only solution for a slender flux tube is the sound wave solution,(3.2.22), which satisfies the conditions $n_0^2 > 0$, $m_e^2 > 0$ provided $c_e > c_0$. Therefore, for $n_0^2 > 0$, the only solution satisfying $|n_0 r_0| \to 0$ as $k r_0 \to 0$ lies in region A4 of Figure 3.1.

It is convenient to summarize the results obtained so far in this subsection. In a slender flux tube ($k r_0 << 1$) the solutions satisfying the requirements that $|m_0 r_0| \to 0$ and $|m_e r_0| \to 0$ as $k r_0 \to 0$ (i.e. that the perturbations vary slowly across the tube, so that the motions are essentially <u>longitudinal</u>), and that the disturbances in the exterior are evanescent ($m_e^2 > 0$), are

$$\left.\begin{aligned} \omega^2 &\approx k^2 c_e^2 \\ \omega^2 &\approx k^2 c_T^2 \end{aligned}\right\} \quad c_e > c_0$$

$$\omega^2 \approx \min\,(k^2 c_e^2,\ k^2 c_T^2), \quad c_e < c_0 \qquad (3.2.30)$$

The mode $\omega^2 \approx k^2 c_T^2$ corresponds to solutions with negligible variation in the exterior and the solution $\omega^2 \approx k^2 c_e^2$ corresponds to ordinary sound waves propagating in the field-free gas (Defouw, 1976).

Continuing with our investigation, we note that there may be other solutions of the dispersion relations (3.2.19) and (3.2.28), for $kr_0 \ll 1$, which are not admitted by the approximation $|m_0 r_0| \to 0$ as $kr_0 \to 0$. However, closer examination of (3.2.19) shows that the only solutions for $kr_0 \ll 1$ are those given by (3.2.23) and (3.2.24).

The dispersion relation (3.2.28) does, however, possess solutions for which $n_0 r_0 \to$ constant $\neq 0$ as $kr_0 \to 0$. To see this, suppose that $n_0 r_0 \to \nu_i$ as $kr_0 \to 0$, where ν_i is a constant for each root ω_i ($i = 1,2,\ldots$). Then we may show from (3.2.28) that $\nu_i = j_{1,i}$, where $j_{1,i}$ are the roots of the Bessel function J_1. Thus the solutions for ω, as $kr_0 \to 0$, are

$$\omega^2 = \omega_i^2 \approx k^2 c_T^2 + \frac{k^4 c_T^4 r_0^2}{\left(c_0^2 + v_A^2\right) j_{1,i}^2} \qquad (3.2.31)$$

There are an infinite number of modes, each one being characterized by an integer i. The accuracy of the approximation $\omega^2 \approx k^2 c_T^2$ is greater for larger i. The two modes with largest frequency ($i = 1,2$) are sketched in Figure 3.4.

In Table 3.1 we present, in summary, the above described modes and their approximate dispersion relations as $kr_0 \to 0$.

Figure 3.4 - The solutions of the dispersion relations for modes in an evanescent environment. We have taken $c_e = c_0 = v_A$ and $\gamma = \frac{5}{3}$, and plotted frequency as a function of 'radius' kr_0. The continuous lines (————) refer to modes that are oscillatory inside the tube and correspond to the first two (i = 1,2) modes in order of descending frequency. The dashed line (— — — —) corresponds to the mode that is evanescent inside the tube and is shown for comparison. Notice that all of the modes give $\omega^2 \approx k^2 c_T^2$ for $kr_0 \ll 1$.

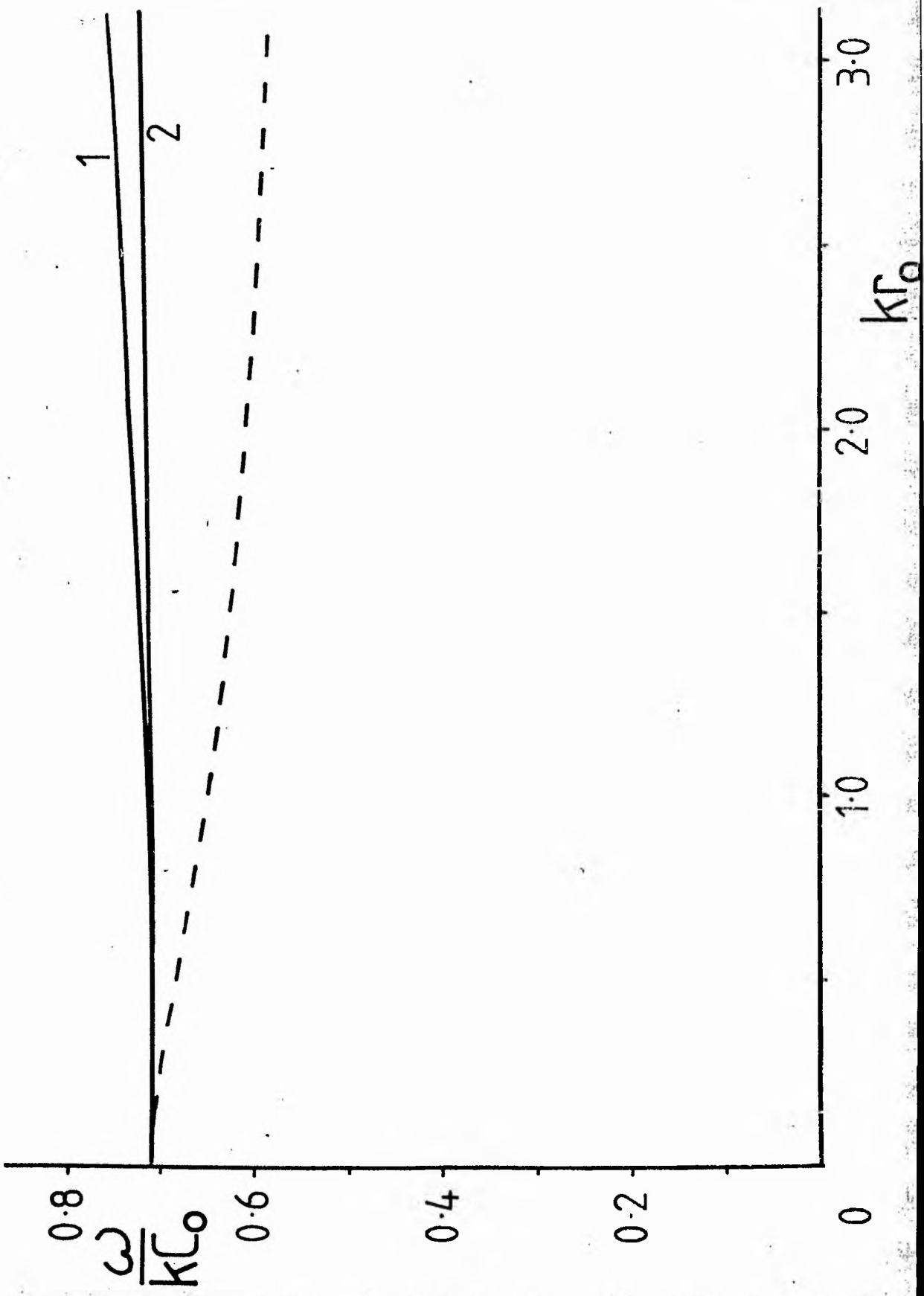

In addition, we have indicated the limiting behaviour of $|m_0 r_0|$ and $|p_e/p|$.

Table 3.1

Solution	Equation	limit $m_0 r_0$ as $kr_0 \to 0$	Regions in Fig 3.1	Validity	limit $kr_0 \to 0$ $\lvert p_e/p \rvert$
$\omega^2 = k^2 c_T^2 -$	3.2.21	$m_0^2 > 0, m_0 r_0 \to 0$	A3	$c_T < c_e$	0
$\omega^2 = k^2 c_T^2 +$	3.2.31	$m_0^2 < 0$ $n_0 r_0 \to j_{1,i}$	A2	$c_T < c_e$	0
$\omega^2 = k^2 c_e^2 -$	3.2.22	$m_0^2 > 0 \lvert m_0 r_0 \rvert \to 0$	A5	$c_e > c_0$	$\lvert c_e^2 - c_T^2 \rvert \dfrac{(c_0^2 + v_A^2)}{c_e^2 c_0^2}$
			A3	$c_e < c_T$	
		$m_0^2 < 0$ $n_0 r_0 \to 0$	A4	$c_e > c_0$	

Solutions of the dispersion relations (3.2.19) and (3.2.28) as $kr_0 \to 0$.

3.2.1(ii) Waves in the Exterior

In the previous section we considered only solutions evanescent in the exterior ($m_e^2 > 0$). The perturbations decayed away from a maximum on the boundary (Figures 3.3a,b). Consider now the case $m_e^2 < 0$, for which the solution in the exterior region is

$$R(r) = A_2 J_0(n_e r) + A_3 Y_0(n_e r), \quad (r > r_0) , \qquad (3.2.32)$$

where $n_e^2 = -m_e^2$ and A_2, A_3 are arbitrary constants.

For m_e^2 real and negative both the solutions J_0 and Y_0 satisfy the boundary condition at infinity and so the solution we adopt in the exterior depends upon the physical situation we are modelling. We may write the solution (3.2.32) as a linear combination of two Hankel functions

$$R(r) = A\, H_0^{(1)}(n_e r) + B\, H_0^{(2)}(n_e r) , \quad (r > r_0), \qquad (3.2.33)$$

representing incoming ($H_0^{(1)}$) and outgoing ($H_0^{(2)}$) waves (assuming that the real parts of ω and n_e are positive). Allowing n_e

to be complex requires that, for only outgoing waves far from the tube, solutions with the imaginary part of n_e negative are chosen, since we require the perturbations finite at infinity. The dispersion relation for such a wave is (Roberts and Webb, 1979)

$$\rho_0(k^2c_T^2-\omega^2)(c_0^2+v_A^2)m_0n_e=\rho_e\omega^2(k^2c_0^2-\omega^2)\,\frac{I_1(m_0r_0)}{I_0(m_0r_0)}\,\frac{H_0^{(2)}(n_er_0)}{H_1^{(2)}(n_er_0)}\,. \quad (3.2.34)$$

The solutions are expected to have the imaginary part of ω positive (giving a decay), so that the outgoing wave represents a sink of energy.

The general form of the solution (3.2.32) shows that standing waves may arise provided that n_e^2 is real. For example, the J mode is generated by the addition of an outgoing and ingoing wave of equal phase and amplitude. Wilson's (1979a,b) analysis differs from our own in that he considers the standing mode only and chooses (arbitrarily) the J solution, giving the dispersion relation (Roberts and Webb, 1979)

$$\rho_0(k^2c_T^2-\omega^2)(c_0^2+v_A^2)m_0n_e=\rho_e\omega^2(k^2c_0^2-\omega^2)\,\frac{I_1(m_0r_0)}{I_0(m_0r_0)}\,\frac{J_0(n_er_0)}{J_1(n_er_0)}\,, \quad (3.2.35)$$

for m_0, n_e positive.

For small kr_0, the dispersion relation (3.2.35) reduces to

$$(k^2c_e^2-\omega^2)(k^2c_T^2-\omega^2)(c_0^2+v_A^2)+\omega^2(k^2c_0^2-\omega^2)(c_0^2+\tfrac{\gamma}{2}v_A^2)=0\,, \quad (3.2.36)$$

assuming m_0r_0 and $n_er_0 \to 0$ as $kr_0 \to 0$. For the special case of $c_0=c_e$ (i.e. interior and exterior temperatures equal), (3.2.36) gives $\omega^2=k^2c_0^2$ and $\omega^2=k^2c_0^2/(1-\gamma/2)$, both of which are in excess of $k^2c_T^2$. The solution $\omega^2=k^2c_0^2$ corresponds to a degenerate mode in that $\omega^2=k^2c_0^2$ gives $m_0=0$ and is a solution of (3.2.35) for all kr_0, corresponding to purely longitudinal motion.

Apart from the solution of (3.2.35) satisfying $\omega^2 \approx k^2 c_0^2/(1-\gamma/2)$ as $kr_0 \to 0$, there are an infinite number of other solutions, all of which satisfy $\omega^2 \to \infty$ as $kr_0 \to 0$. The solution for general kr_0 is shown in Figure 3.5. The solutions for the Y mode are also sketched in Figure 3.5 (for $c_0 = c_e = v_A$).

In this section we have discussed the dispersion relation for wave modes in a uniform magnetic flux tube. We have considered in detail modes evanescent in the external medium, with phase speeds less than the sound speed. For these modes we have derived two solutions appropriate for a slender flux tube, namely $\omega^2 \approx k^2 c_T^2$ and $\omega^2 \approx k^2 c_e^2$.

As a preliminary to the discussion of wave modes in a slender flux tube in a stratified atmosphere, we shall develop, in the next section, a slender flux tube approximation for a uniform tube and compare the results with the exact solutions obtained above. This approximation, first given for a non-uniform medium by Roberts (see Roberts and Webb, 1978) allows a solution of the system, without the necessity of solving for the radial dependence of the perturbations inside the tube.

3.2.2 The Slender Flux Tube Approximation in a Uniform Medium

In this section we shall apply an expansion procedure to the linearized equations governing perturbations in a slender flux tube in a uniform atmosphere. Applying approximate boundary conditions, we derive a general dispersion relation which gives, as a special case, depending on the assumed form of the external pressure variations, the relations (3.2.20) and (3.2.36), valid

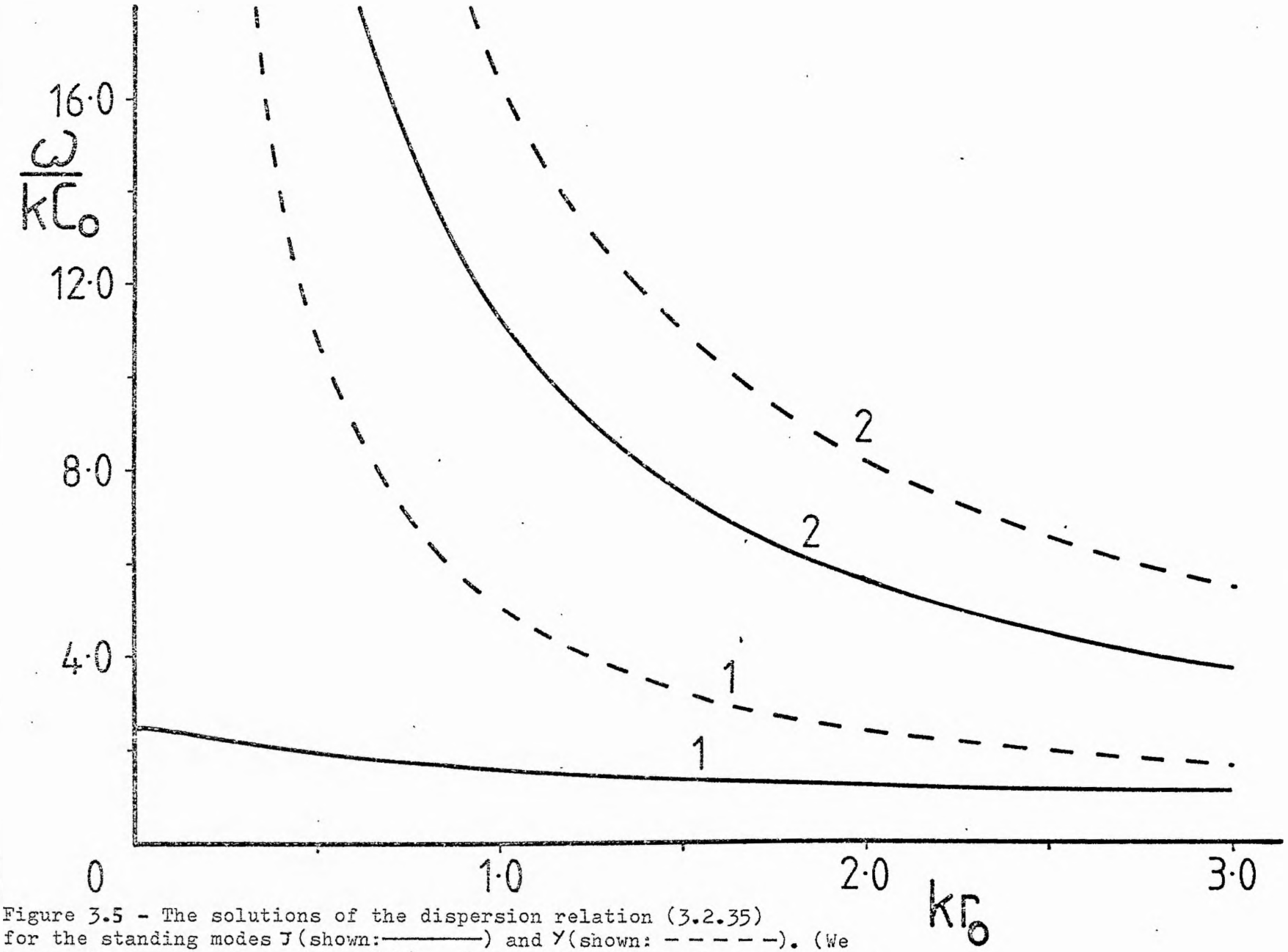

Figure 3.5 - The solutions of the dispersion relation (3.2.35) for the standing modes J (shown: ————) and Y (shown: – – – – –). (We have set $c_0 = c_e = v_A$ and $\gamma = 5/3$). The J-mode corresponds to that investigated by Wilson (1979a). We have numbered the modes (i=1,2) in order of ascending frequency.

when the horizontal scale of variations inside the tube is large compared to the radius.

The linear equations are those presented in section 3.1. Each perturbed quantity is expanded in a MacLaurin series about $r = 0$. We write

$$\left.\begin{aligned} v_z(r,z,t) &= v_z(0,z,t) + \frac{r}{R} v_z^1(0,z,t)(1+O(\tfrac{r}{R})) \\ v_r(r,z,t) &= \frac{r}{R} v_r^1(0,z,t)(1+O(\tfrac{r}{R})) \\ b_z(r,z,t) &= b_z(0,z,t) + \frac{r}{R} b_z^1(0,z,t)(1+O(\tfrac{r}{R})) \\ b_r(r,z,t) &= \frac{r}{R} b_r^1(0,z,t)(1+O(\tfrac{r}{R})) \\ p(r,z,t) &= p(0,z,t) + \frac{r}{R} p^1(0,z,t)(1+O(\tfrac{r}{R})) \\ \rho(r,z,t) &= \rho(0,z,t) + \frac{r}{R} \rho^1(0,z,t)(1+O(\tfrac{r}{R})) \end{aligned}\right\} \quad (r < r_0), \qquad (3.2.37)$$

where R is the length-scale over which perturbations vary inside the tube. For example, for wave motions inside the tube R may be taken to be $(m_0)^{-1}$, where m_0 is the horizontal wave number. The quantity $v_z^1(0,z,t)$ is given by

$$v_z^1(0,z,t) = \left[R\frac{\partial v}{\partial r}z\right]_{r=0}, \qquad (3.2.38)$$

and $v_z^1(0,z,t)/v_z(0,z,t)$ is assumed $O(1)$. Similar relations hold for v_r^1, b_r^1, v_r^2, etc. The expansion is valid for $r \ll R$. Thus, in particular, if $r_0 \ll R$, i.e. if the length-scale of perturbations inside the tube is large compared to the radius of the tube, then the expansion is valid for all $r < r_0$.

Substituting the expressions (3.2.37) into the linearized equations we arrive at the following system of governing equations (Roberts and Webb, 1979)

$$\frac{\partial \hat{\rho}}{\partial t} + \rho_0 \hat{\Delta} = 0, \tag{3.2.39}$$

$$\rho_0 \frac{\partial \hat{v}_z}{\partial t} + \frac{\partial \hat{p}}{\partial z} = 0, \tag{3.2.40}$$

$$\frac{1}{\rho_0}\frac{\partial \hat{\rho}}{\partial t} - \frac{1}{B_0}\frac{\partial \hat{b}_z}{\partial t} + \frac{\partial \hat{v}_z}{\partial z} = 0, \tag{3.2.41}$$

$$\frac{\partial \hat{p}}{\partial t} - C_0^2 \frac{\partial \hat{\rho}}{\partial t} = 0, \tag{3.2.42}$$

where $\hat{p}$, $\hat{\rho}$, $\hat{b}_z$ and $\hat{v}_z$ now refer to the perturbations of the pressure, density, vertical component of magnetic field and vertical component of velocity, as measured on the tube's axis r=0. In addition the radial component of momentum gives (to zeroth order)

$$p^1 + \frac{B_0 b_z^1}{\mu_0} = 0 \quad . \tag{3.2.43}$$

The quantity $\hat{\Delta}$ in Equation (3.2.39) is the value of $\nabla.\underline{v}$ on the z-axis and is given by

$$\hat{\Delta} = (\nabla.\underline{v})_{r=0} = \frac{\partial v}{\partial z}_z + \left[\frac{1}{r}\frac{\partial}{\partial r}(rv_r)\right]_{r=0} ,$$

which may be reduced further for a slender tube, $r_0 \ll R$, by using (3.2.37):

$$v_r(r,z,t) \approx \frac{r}{R} v_r^1(0,z,t) \quad , \tag{3.2.44}$$

where $v_r^1(0,z,t) = R\left(\frac{\partial v_r}{\partial r}\right)_{r=0}$, and so

$$= \frac{\partial v_z}{\partial z} + 2\left[\frac{\partial v_r}{\partial r}\right]_{r=0} . \tag{3.2.45}$$

In the external region, the governing equations (see Equations (1.6.5), (1.6.6) and (1.6.8)) are

$$\frac{\partial \rho^{(e)}}{\partial t} + \rho_e \nabla . \underline{v}^{(e)} = 0, \tag{3.2.46}$$

$$\rho_e \frac{\partial \underline{v}^{(e)}}{\partial t} + \nabla p^{(e)} = 0, \tag{3.2.47}$$

$$\frac{\partial p^{(e)}}{\partial t} - c_e^2 \frac{\partial \rho^{(e)}}{\partial t} = 0, \tag{3.2.48}$$

where $p^{(e)}=p^{(e)}(r,z,t)$, etc.

As in Section 3.2.1, the interior and exterior of the tube are related by requiring that the radial velocity component and total pressure be continuous across the boundary $r=r_0$:

$$v_r(r=r_0) = v_r^{(e)}(r=r_0) \tag{3.2.49a}$$

and

$$p(r=r_0) + \frac{1}{\mu_0} B_0 b_z(r=r_0) = p^{(e)}(r=r_0). \tag{3.2.49b}$$

In addition we shall require the disturbances to tend to zero as r tends to infinity.

Now, since the tube is slender, we may approximate the radial component of velocity <u>inside</u> the tube by (3.2.44), and using (3.2.47) to relate the radial component of velocity outside the tube to the external pressure field, the boundary condition (3.2.49a) is approximated by

$$r_0 \left(\frac{\partial v_r}{\partial r}\right)_{r=0} = -\frac{1}{i\omega\rho_e}\left(\frac{\partial p^{(e)}}{\partial r}\right)_{r=r_0}, \tag{3.2.49a}'$$

for perturbations of the form $e^{i\omega t+ikz}$.

The second boundary condition may be treated similarly by

noting that

$$\left[p + \frac{B_0 b_z}{\mu_0}\right]_{r=r_0} = \hat{p} + \frac{B_0 \hat{b}_z}{\mu_0} + O\left(\left(\frac{r_0}{R}\right)^2\right) ;$$

which follows from (3.2.43). Thus (3.2.49b) becomes

$$\hat{p} + \frac{B_0 \hat{b}_z}{\mu_0} = p^{(e)}(r_0) . \qquad (3.2.49b)'$$

Equations (3.2.39) - (3.2.42) and the boundary conditions (3.2.49a,b)' provide a closed system once $p^{(e)}(r)$ is determined. Combining Equations (3.2.39), (3.2.40), (3.2.42), (3.2.45) and the boundary condition (3.2.49a)' gives

$$(\omega^2 - k^2 c_0^2)\hat{v}_z - \frac{2}{r_0}\frac{c_0^2 k}{\omega \rho_e}\left(\frac{\partial p^{(e)}}{\partial r}\right)_{r=r_0} = 0 . \qquad (3.2.50)$$

A second equation relating $\hat{v}_z$ and $p^{(e)}$ may be obtained from Equations (3.2.40) - (3.2.42) and the second boundary condition (3.2.49b)':

$$(c_0^2 + v_A^2)(\omega^2 - k^2 c_T^2)v_z + \frac{\omega k}{\rho_0} c_0^2 \, p^{(e)}(r_0) = 0 . \qquad (3.2.51)$$

Finally, eliminating $\hat{v}_z$ gives the <u>dispersion relation</u>

$$(c_0^2+v_A^2)(\omega^2-k^2c_T^2)+\omega^2(\omega^2-k^2c_T^2)\left(\frac{\rho_e}{\rho_0}\right)\frac{r_0 p^{(e)}(r_0)}{2\left(\partial p^{(e)}/\partial r\right)_{r=r_0}} = 0, \qquad (3.2.52)$$

valid for a slender ($r_0/R \ll 1$) tube in which the motions vary only weakly across the cross-section of the tube.

The form of the dispersion relation (3.2.52) depends upon the form of the pressure perturbation in the exterior. Now, Equations (3.2.46) - (3.2.48) may be combined to give

$$\left(\frac{\partial^2}{\partial t^2} - c_e^2 \nabla^2\right) p^{(e)}(r,z,t) = 0 ; \qquad (3.2.53)$$

where

$$\nabla^2 \equiv \frac{\partial^2}{\partial r^2} + \frac{1}{r}\frac{\partial}{\partial r} + \frac{\partial^2}{\partial z^2} \quad .$$

With $p^{(e)}(r,z,t) = P^{(e)}(r)e^{i\omega t+ikz}$, Equation (3.2.53) becomes

$$\frac{d^2p^{(e)}(r)}{dr^2} + \frac{1}{r}\frac{d}{dr}P^{(e)}(r) - m_e^2 P^{(e)}(r) = 0 \ , \qquad (3.2.54)$$

where $m_e^2 = (k^2c_e^2 - \omega^2)/c_e^2$. For k and ω real, m_e^2 is real and the form of the solution of (3.2.54) depends upon the sign of m_e^2. Applying the boundary condition at infinity, the solutions to (3.2.54) are

$$P^{(e)}(r) = \begin{cases} A_0K_0(m_er) \ , & m_e^2 > 0, \\ A_1J_0(n_er) + A_2Y_0(n_er), & m_e^2 = -n_e^2 < 0, \end{cases} \qquad (r > r_0) \quad (3.2.55)$$

where A_0, A_1 and A_2 are arbitrary constants.

Consider first the case of $m_e^2 > 0$. Assuming for $r_0/R \ll 1$ that $m_er_0 \ll 1$, then the dispersion relation (3.2.52) becomes on substituting for $P^{(e)}(r)$ from (3.2.55)

$$\rho_0(c_0^2 + v_A^2)(\omega^2 - k^2c_T^2) + \tfrac{1}{4}(k^2c_0^2 - \omega^2)\omega^2\rho_e r_0^2 \log(m_er_0)^2 = 0, \quad (3.2.56)$$

valid for $r_0/R \ll 1$ and $m_er_0 \ll 1$. This is simply Equation (3.2.20), which was derived under the assumptions that $m_0r_0 \ll 1$ and $m_er_0 \ll 1$, where m_0 is the horizontal wavenumber. As we have seen, (3.2.56) has solutions

$$\omega^2 \approx k^2c_T^2 + \frac{1}{4}\frac{\rho_e}{\rho_0}c_T^2\frac{(c_0^2 - c_T^2)}{c_0^2 + v_A^2}k^4r_0^2\log(k^2r_0^2),$$

and

$$\omega^2 \approx k^2c_e^2 - \frac{c_e^2}{r_0^2}\exp\frac{-4}{(kr_0)^2}\left\{\frac{(c_T^2 - c_e^2)(c_0^2 + v_A^2)}{(c_0^2 + \frac{\gamma}{2}v_A^2)(c_0^2 - c_e^2)}\right\} .$$

If $c_e > c_0$, then both solutions are possible. However, if $c_e < c_0$ there is only one solution : $\omega^2 \approx \min (k^2 c_e^2, k^2 c_T^2)$. Thus, the expansion procedure gives the solutions for which the scale of variation of the perturbations across the tube is small. Note that it does not reproduce the solutions (3.2.31) for which $|m_0 r_0|$ is large for kr_0 small. So, in order for the more general analysis (of Section 3.2.1) to be consistent with the approximation of this section, the definition of a slender flux tube we must adopt is $|m_0 r_0| \ll 1$.

As we have shown in Section 3.2.1, the solution $\omega^2 \approx k^2 c_T^2$ corresponds to negligible pressure perturbations in the exterior, since

$$\frac{p^{(e)}(r_0)}{P(r_0)} \approx \frac{\hat{P} + B_0 \hat{b}_z/\mu_0}{p} = \frac{(c_0^2 + v_A^2)(\omega^2 - k^2 c_T^2)}{\omega^2 c_0^2} , \qquad (3.2.57)$$

which follows from Equations (3.2.51) and (3.2.40). The approximate solution ($\omega^2 \approx k^2 c_T^2$) may be derived by setting $p^{(e)} = 0$ in the exterior and ignoring (3.2.49a)(Defouw, 1976). The use of the equation

$$\hat{p} + \frac{B_0 \hat{b}_z}{\mu_0} = 0 , \qquad (3.2.58)$$

leads to considerable simplification and, in the stratified case discussed in the next section, allows a relatively straightforward investigation of the effects of gravity on the 'tube wave'.

For $m_e^2 < 0$, we see from Equation (3.2.55) that an additional constraint must be imposed on the disturbance at infinity, in order that (3.2.52) be reduced further. For example, if we suppose that the standing wave $J_0(n_e r)$ is selected (so that $A_2 = 0$) (Wilson, 1979a), the dispersion relation (3.2.52) gives

$$(k^2c_e^2-\omega^2)(k^2c_T^2-\omega^2)(c_0^2+v_A^2) + \omega^2(k^2c_0^2-\omega^2)(c_0^2+\tfrac{\gamma}{2}v_A^2) = 0 , \qquad (3.2.59)$$

which is the relation obtained in Section 3.2.1(ii) for solutions which satisfied the condition $|n_0 r_0| \to 0$ as $kr_0 \to 0$.

In conclusion, the slender flux tube approximation outlined in this section reproduces the solutions for which the perturbations vary only weakly across the tube. In the following section, we shall devevelop this method for a flux tube in a stratified atmosphere.

3.3 Stratified Atmosphere

The expansion procedure developed in this section for the basic state and the perturbations follows closely that given by Roberts (Roberts and Webb, 1978). We extend the work of Defouw (1976) and derive an equation for the vertical component of the velocity perturbation and, as a special case, we recover the results of Defouw's analysis of waves in a flux tube in a stratified, isothermal atmosphere.

3.3.1 The Equilibrium State of a Slender Flux Tube

The equilibrium is that of a flux tube in which the density, $\rho_0(r,z)$, the magnetic field $\underline{B}_0(r,z)$ and the pressure $p_0(r,z)$ vary weakly across the tube. Gravity acts in the negative z direction and the magnetic field is discontinuous at $r = r_0$ (which may be a function of z) and is zero outside $r = r_0$. The equilibrium configuration is sketched in Figure 3.6.

In a cylindrical co-ordinate system, for a basic state which does not vary greatly across the tube, each of the physical variables is expanded in a MacLaurin series about $r = 0$:

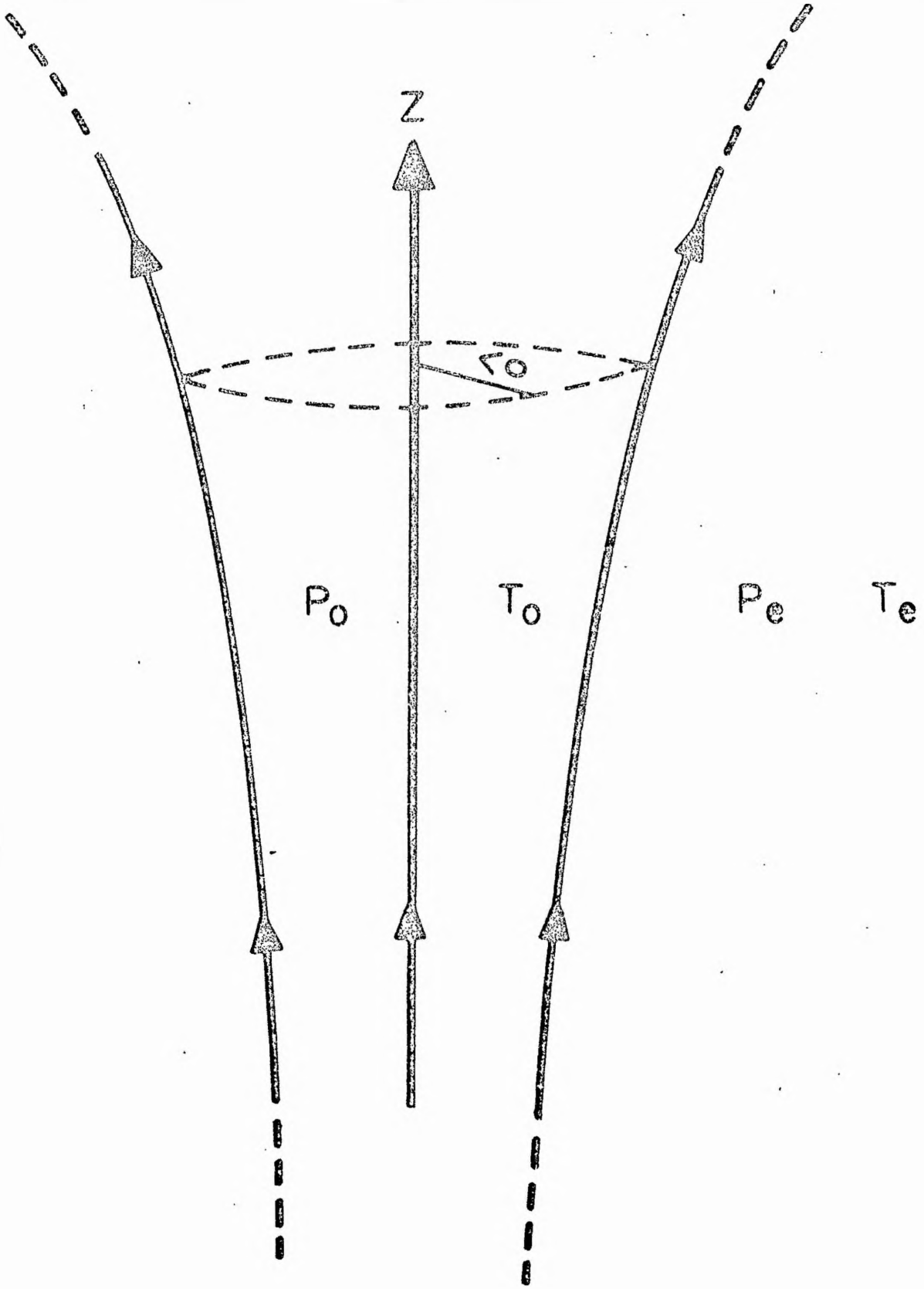

Figure 3.6 - The Equilibrium of a slender flux tube.

$$
\left.
\begin{aligned}
p_0(r,z) &= p_0^0(z) + \frac{r}{L}\, p_0^1(z)(1+O(\tfrac{r}{R})), \\
\rho_0(r,z) &= \rho_0^0(z) + \frac{r}{L}\, \rho_0^1(z)(1+O(\tfrac{r}{R})), \\
B_{0z}(r,z) &= B_{0z}^0(z) + \frac{r}{L}\, B_{0z}^1(z)(1+O(\tfrac{r}{R})), \\
B_{0r}(r,z) &= \frac{r}{L}\, B_{0r}^1(z)(1+O(\tfrac{r}{R})),
\end{aligned}
\right\} \quad (r < r_0) \qquad (3.3.1)
$$

where $p_0^0(z)$, $\rho_0^0(z)$ and $B_{0z}^0(z)$ denote equilibrium values of the pressure, density and vertical component of magnetic field as measured on the tube's axis $r = 0$; L is the length-scale over which the basic state quantities vary inside the tube, i.e.

$$
L \sim \left(\frac{1}{p_0}\frac{\partial p_0}{\partial r}\right)^{-1} \qquad (3.3.2)
$$

and is determined by the structure of the tube. For example, in the previous section, where we discussed a uniform basic state, L would be infinite.

The term $p_0^1(z)$ is given by

$$
p_0^1(z) = L\left(\frac{\partial p_0(r,z)}{\partial r}\right)_{r=0} ,
$$

and similar expressions hold for $\rho_0'(z)$, $B_{0z}^1(z)$, etc., and we assume $\mu_0 p_0^0/B_{0z}^{0\,2} \sim \mu_0 p_0^1/B_{0z}^{0\,2} \sim 1$ etc.

For this expansion to be valid for $0 \leqslant r < r_0$, we require $r_0 \ll L$.

The basic state is governed by Equations (1.6.1) and (1.6.4), namely

$$
\nabla \cdot \underline{B}_0 = 0 , \qquad (3.3.3)
$$

and

$$
-\nabla p_0 + \rho_0 \underline{g} + \underline{j}_0 \wedge \underline{B}_0 = 0 . \qquad (3.3.4)
$$

Equation (3.3.3) becomes, on substituting for B_{0r} and B_{0z} from (3.3.1),

$$\frac{dB^0_{0z}}{dz} + \frac{2B^1_{0r}}{L} + O(\frac{r}{L}) = 0 \ , \qquad (3.3.3)'$$

giving

$$\frac{1}{B^0_{0z}} \frac{dB^0_{0z}}{dz} \sim \frac{1}{L} \qquad (3.3.5)$$

We also specify the temperature as $T_0(r,z) = T_0(z)$.

Note that in addition to the length-scale L, which is a measure of the variation on a horizontal scale, we have the scale heights, Λ_0 and Λ_e, inside and outside the flux tube defined by

$$\Lambda_0(z) = \frac{RT_0(z)}{\mu_i g} \ , \quad \Lambda_e(z) = \frac{RT_e(z)}{\mu_e g} \ , \qquad (3.3.6)$$

where μ_i and μ_e are the mean molecular weights of the internal and external regions respectively, and T_e is the temperature in the exterior.

Integrating Equation (3.3.3) over a volume bounded by the walls of the tube and the two planes $z = z_1$, $z = z_2$ gives

$$r_0^2(z_1)\ B^0_{0z}(z_1) = r_0^2(z_2)\ B^0_{0z}(z_2);$$

thus, to zeroth order, the conservation of magnetic flux equation is

$$r_0^2(z)\ B^0_{0z}(z) = \text{constant.} \qquad (3.3.7)$$

Two further equations for the basic state inside the tube may be obtained by substituting for p_0, ρ_0 and B_0 from (3.3.1) into (3.3.4). The radial component of momentum gives

$$p_0^1(z) + \frac{B^0_{0z}(z)\ B^1_{0z}(z)}{\mu_0} = 0 \ , \qquad (3.3.8)$$

whilst the vertical component gives

$$\frac{dp_0^0(z)}{dz} + \rho_0^0(z)g = 0 \ . \qquad (3.3.9)$$

The external atmosphere is also in hydrostatic equilibrium, and so

$$\frac{dp_e}{dz} = -\rho_e(z)g, \tag{3.3.10}$$

where $\rho_e(z)$ is the density in the exterior.

The interior and exterior are related by the pressure balance condition (1.5.1)

$$p_0(r_0 z) + \frac{B_0^2(r_0,z)}{2\mu_0} = p_e(z) ,$$

which reduces (as a consequence of (3.3.1) and (3.3.8)) to

$$p_0^0(z) + \frac{B_{0z}^{0\,2}(z)}{2\mu_0} + O(\frac{r}{R})^2 = p_e(z) . \tag{3.3.11}$$

Differentiating (3.3.11), it follows, using (3.3.9) and (3.3.10) that (Parker, 1955)

$$\frac{d}{dz}\left(\frac{B_{0z}^{0\,2}(z)}{2\mu_0}\right) = g(\rho_0^0(z) - \rho_e(z)) , \tag{3.3.12}$$

which may be written in terms of the scale heights Λ_0 and Λ_e as

$$\frac{d}{dz}\left(\frac{B_{0z}^{0\,2}(z)}{2\mu_0}\right) = \frac{p_0^0(z)}{\Lambda_0(z)} - \frac{p_e(z)}{\Lambda_e(z)} \tag{3.3.13}$$

Equations (3.3.13) and (3.3.11) may now be combined to give

$$\frac{1}{B_{0z}^0}\frac{dB_{0z}^0}{dz} = -\frac{1}{2\Lambda_0(z)} + \frac{1}{\Lambda_0(z)}\left(1 - \frac{\Lambda_0(z)}{\Lambda_e(z)}\right)\frac{p_e(z)}{B_{0z}^{0\,2}/\mu_0} , \tag{3.3.14}$$

which may be written

$$\frac{1}{B_{0z}^0}\frac{dB_{0z}^0}{dz} = \frac{1}{\Lambda_0(z)}\left[\frac{-1}{2} + \frac{1}{\gamma}\left(1 - \frac{c_0^2}{c_e^2}\right)\left(\frac{c_0^2}{v_A^2} + \frac{\gamma}{2}\right)\right] , \tag{3.3.14}'$$

for sound speed c_e in the exterior. Thus, if the tube is in temperature balance with its surroundings (and $\mu_i = \mu_e$ so that

$\Lambda_0 = \Lambda_e$), Equation (3.3.14) gives

$$\frac{1}{B^0_{0z}(z)} \frac{dB^0_{0z}(z)}{dz} = -\frac{1}{2\Lambda_0(z)} \quad . \tag{3.3.15}$$

In view of this result and (3.3.5), we take L to be equal to the local scale height of the atmosphere for $\Lambda_0 \equiv \Lambda_e$.

On the other hand, if $L \gg \Lambda_0(z)$, so that the field is approximately uniform and vertical ($\frac{1}{B^0_{0z}} \frac{dB^0_{0z}}{dz} \Lambda_0(z) \ll 1$), then Equation (3.3.14) implies that the tube cannot be in temperature balance with its surroundings. In fact, the tube must be cooler. For a vertical field, (3.3.14)' gives

$$\tfrac{1}{2} = \left(1 - \frac{c_0^2(z)}{c_e^2(z)}\right)\left(\frac{c_0^2(z)}{\gamma v_A^2(z)} + \tfrac{1}{2}\right) , \tag{3.3.16}$$

which implies $c_e > c_0$; i.e. $\Lambda_e > \Lambda_0$, and so Λ_0 satisfies

$$\Lambda_0(z) = \Lambda_e(z)\left(1 - \frac{B_0^2/2\mu_0}{p_e(z)}\right) ,$$

which is simply a restatement of $\rho_o = \rho_e$.

In the remaining discussion of the equilibrium we shall be concerned with the case of $\Lambda_0 = \Lambda_e$ only and so $L = \Lambda_0$ and the condition for validity of the expansion for $0 \leqslant r < r_0$ is

$$r_0(z)/\Lambda_0(z) \ll 1 \quad . \tag{3.3.17}$$

The equilibrium configuration of $\Lambda_0 \neq \Lambda_e$ has been considered by Roberts (1976) and is discussed further in the following chapter.

A consequence of Equations (3.3.15), (3.3.9) and (3.3.10) is that

$$B^{0\,2}_{0z}(z) = B^{0\,2}_{0z}(0) \frac{p_e(z)}{p_e(0)} = B^{0\,2}_{0z}(0) \frac{p^0_0(z)}{p^0_0(0)} , \tag{3.3.18}$$

and so $B_0(z) \sim p_e^{\frac{1}{2}}(z)$. From the conservation of magnetic flux (Equation 3.3.7), we then have that $r_0 \sim p_e^{-\frac{1}{4}}(z)$ (Parker, 1955).

Also, as a result of (3.3.17), it follows that the sound speed, $c_0(z) = (\gamma p_0/\rho_0)^{\frac{1}{2}}$, and the Alfvén speed, $v_A(z) = B_{0z}^0/(\mu_0\rho_0)^{\frac{1}{2}}$ are related by

$$\frac{c_0^2(z)}{\gamma(z)v_A^2(z)} = \frac{c_0^2(0)}{\gamma(0)v_A^2(0)} ,$$

and so $c_0/\gamma^{\frac{1}{2}} \sim v_A$ at every level z.

A further parameter which naturally arises is the Brunt-Väisälä frequency (see Chapter 1) given by

$$N_0^2 = \frac{g}{H_0(z)} - \frac{g^2}{c_0^2(z)} , \quad \frac{1}{H_0(z)} = \frac{-1}{\rho_0(z)} \frac{d\rho_0(z)}{dz} , \qquad (3.3.19)$$

where $H_0(z)$ is the density scale-height.

For a tube <u>in temperature balance with its surroundings</u>, the equilibrium is completely characterized by the scale-height $\Lambda_0(z)$ (Roberts, 1978; see Roberts and Webb, 1978):

$$\left.\begin{aligned} p_0(z) &= p_0(0)e^{-n(z)} , \quad B_{0z}^0 = B_{0z}^0(0)e^{-\frac{1}{2}n(z)} , \\ \rho_0(z) &= \rho_0(0)\frac{\Lambda_0(0)}{\Lambda_0(z)} e^{-n(z)} , \end{aligned}\right\} \qquad (3.3.20)$$

where

$$n(z) = \int_0^z \frac{dz'}{\Lambda_0(z')} ,$$

while the parameters are given by

$$\left.\begin{aligned} c_0^2(z) &= \gamma g\Lambda_0(z) , \quad v_A^2(z) = v_A^2(0)\frac{\Lambda_0(z)}{\Lambda_0(0)} , \\ \frac{1}{H_0(z)} &= \frac{1+\Lambda_0'(z)}{\Lambda_0(z)} , \quad N_0^2(z) = \frac{g}{\Lambda_0(z)}\left(\frac{\gamma-1}{\gamma} + \Lambda_0'(z)\right). \end{aligned}\right\} \qquad (3.3.21)$$

We regard $\Lambda_0(z)$ ($=\Lambda_e(z)$) as a prescribed function of z (though in the Sun $\Lambda_e(z)$ is determined by the energetics) that we may choose from a model atmosphere (See Chapter 1).

For <u>axisymmetric</u> perturbations about a basic state given by $\underline{B}_0(r,z) = (B_{0r}(r,z),\ 0,\ B_{0z}(r,z))$, $p_0(r,z)$ and $\rho_0(r,z)$, the equations for v_θ and b_θ uncouple from the rest of the system; disturbances v_θ and b_θ are propagated as Alfvén waves, with the equation for v_θ being

$$\rho_0(r,z)\frac{\partial^2 v_\theta}{\partial t^2} = \left(\frac{B_{z0}}{\mu_0}\frac{\partial}{\partial z} + \frac{B_{r0}}{\mu_0}\frac{1}{r}\frac{\partial}{\partial r}\,r\right)\left(\frac{\partial}{\partial r}(v_\theta B_{r0}) + \frac{\partial}{\partial z}(v_\theta B_{r0})\right)$$

However, it is not possible to derive an equation for the vertical velocity perturbation (for example) for a general basic state. Therefore, in this section, we consider axisymmetric perturbations ($\frac{\partial}{\partial\theta} \equiv 0$) about the basic state described in the previous section. The linearized equations are Equations (3.1.1) - (3.1.8) and the perturbations are expanded in a MacLaurin series about r=0:

$$\left.\begin{aligned}
v_z(r,z,t) &= v_z^0(z,t) + \frac{r}{R}\,v_z^1(z,t)\left(1 + O\left(\tfrac{r}{R}\right)\right),\\
v_r(r,z,t) &= \frac{r}{R}\,v_r^1(z,t)\left(1 + O\left(\tfrac{r}{R}\right)\right),\\
b_z(r,z,t) &= b_z^0(z,t) + \frac{r}{R}\,b_z^1(z,t)\left(1 + O\left(\tfrac{r}{R}\right)\right),\\
b_r(r,z,t) &= \frac{r}{R}\,b_r^1(z,t)\left(1 + O\left(\tfrac{r}{R}\right)\right),\\
p(r,z,t) &= p^0(z,t) + \frac{r}{R}\,p^1(z,t)\left(1 + O\left(\tfrac{r}{R}\right)\right),\\
\rho(r,z,t) &= \rho^0(z,t) + \frac{r}{R}\,\rho^1(z,t)\left(1 + O\left(\tfrac{r}{R}\right)\right),
\end{aligned}\right\}\quad (r < r_0) \qquad (3.3.22)$$

where R is the length-scale over which the perturbations vary inside the tube. The terms v_z^0, b_z^0, p^0 and ρ^0 are the values

of the perturbations in the vertical component of velocity, vertical component of magnetic field, pressure and density as measured on the tube's axis r=0. The term v_z^1 is given by

$$v_z^1 = R\left(\frac{\partial v_z}{\partial r}(r,z,t)\right)_{r=0} , \qquad (3.3.23)$$

and similar relations hold for $p^1(z,t)$, $\rho^1(z,t)$ etc.

The expansion for the perturbations is valid throughout the region $0 \leq r < r_0$ provided $r_0/R \ll 1$.

We substitute the expressions (3.3.1) for the basic state and (3.3.22) for the perturbations into the linearized system of equations (3.1.1 - 3.1.8) to arrive at the following system of equations, valid throughout $0 \leq r < r_0$ for $r_0/L \ll 1$ and $r_0/R \ll 1$:

$$\frac{\partial \hat{\rho}}{\partial t} + \hat{v}_z \rho_0' + \rho_0 \hat{\Delta} = 0 , \qquad (3.3.24)$$

$$\rho_0 \frac{\partial \hat{v}_z}{\partial t} + \frac{\partial \hat{p}}{\partial z} + \hat{\rho} g = 0 , \qquad (3.3.25)$$

$$\frac{1}{\rho_0}\frac{\partial \hat{\rho}}{\partial t} - \frac{1}{B_0}\frac{\partial \hat{b}_z}{\partial t} + \frac{\partial \hat{v}_z}{\partial z} + \hat{v}_z\left(\frac{\rho_0'}{\rho_0} - \frac{B_0'}{B_0}\right) = 0 , \qquad (3.3.26)$$

$$\frac{\partial \hat{p}}{\partial t} + \hat{v}_z p_0' = c_0^2\left(\frac{\partial \rho}{\partial t} + \hat{v}_z \rho_0'\right), \qquad (3.3.27)$$

where $p_0(z)$, $\rho_0(z)$ and $B_0(z)$ are the values of the equilibrium pressure, density and vertical component of magnetic field evaluated at r = 0 and $\hat{p}$, $\hat{\rho}$, $\hat{b}_z$ and $\hat{v}_z$ now refer to the perturbations of the pressure, density, vertical component of magnetic field and vertical component of velocity as measured on the tube's axis r = 0; a dash is used to denote differentiation with respect to z and $\hat{\Delta}$ denotes the value of $\nabla.\underline{v}$ on the z-axis, and for a

'slender' tube ($r_0/R \ll 1$) (see Equation 3.2.45)

$$\hat{\Delta} = \frac{\partial v_z}{\partial z} + 2\left(\frac{\partial v_r}{\partial r}\right)_{r=0} \qquad (3.3.28)$$

Note that Equations (3.3.24) - (3.3.27) are valid ($o \leq r < r_0$) provided $r_0/R \ll 1$ and $r_0/L \ll 1$; and not, as Wilson (1978b) has suggested, only if the linearized terms are large compared to r_0/L.

The interior and exterior of the tube are related by the conditions that the normal component of velocity and the total pressure be continuous across the boundary $r = r_0$:

$$v_n(r=r_0) = v_n^{(e)}(r=r_0) \ , \qquad (3.3.29)$$

and

$$p(r=r_0) + \frac{1}{\mu_0}\underline{B}_0(r=r_0).\underline{b}\ (r=r_0) = p^{(e)}(r=r_0) \ , \qquad (3.3.30)$$

where v_n and $v_n^{(e)}$ are the velocities normal to the boundary in the interior and exterior respectively.

In the exterior, the governing equations are

$$\frac{\partial p^{(e)}}{\partial t} + \nabla.(\rho_e \underline{v}^{(e)}) = 0 \ , \qquad (3.3.31)$$

$$\rho_e \frac{\partial \underline{v}^{(e)}}{\partial t} + \nabla p^{(e)} - \rho_e \underline{g} = 0 \ , \qquad (3.3.32)$$

$$\frac{\partial p^{(e)}}{\partial t} + \underline{v}^{(e)}.\nabla p_e = c_e^2\left(\frac{\partial \rho^{(e)}}{\partial t} + \underline{v}^{(e)}.\nabla \rho_e\right) \ , \qquad (3.3.33)$$

where $c_e(z)$ is the external sound speed, and $p^{(e)}(r,z,t)$, $\rho^{(e)}(r,z,t)$ and $\underline{v}^{(e)}(r,z,t)$ are the perturbations in pressure density and velocity.

For perturbations having a time-dependence of the form $e^{i\omega t}$ (i.e. $p^{(e)} = p^{(e)}(r,z)e^{i\omega t}$) Equations (3.3.31) - (3.3.33) admit separable solutions, with separation constant K^2, of the form

$p^{(e)}(r,z) = p_r^{(e)}(r)\, p_z^{(e)}(z)$ where

$$\frac{d^2 p_r^{(e)}(r)}{dr^2} + \frac{1}{r}\frac{dp_r^{(e)}(r)}{dr} - K^2 p_r^{(e)}(r) = 0 , \qquad (3.3.34)$$

and

$$(\omega^2 - N_e^2)\frac{d^2 p_z^{(e)}(z)}{dz^2} + \left[N_e^{2'} - (\omega^2 - N_e^2)\frac{\rho_e'}{\rho_e} \right] \frac{dp_z^{(e)}(z)}{dz}$$

$$+ \left[\frac{K^2}{\omega^2}(\omega^2 - N_e^2)^2 + \frac{1}{c_e^2}(\omega^2 - N_e^2)\left(\omega^2 - \frac{g\Lambda_e'}{\Lambda_e}\right) + \frac{g}{c_e^2} N_e^{2'} \right] p_z^{(e)}(z) = 0. \qquad (3.3.35)$$

where N_e is the Brunt-Väisälä frequency in the exterior. Note that Equation (3.3.35) is identical to (2.1.55) with k_x^2 replaced by $-K^2$. Equation (3.3.34) has solution

$$p_r^{(e)}(r) = A_1 I_0(Kr) + A_2 K_0(Kr) ,$$

where A_1 and A_2 are arbitrary constants, and for $g \to 0$ Equation (3.3.35) has solution $e^{\pm ikz}$ where

$$K^2 = \frac{k^2 c_e^2 - \omega^2}{c_e^2} .$$

Returning to the boundary condition (3.3.29), we may write v_n, the velocity inside the tube in the direction of the outward unit normal, $\hat{\underline{n}}$, as

$$v_n = \underline{v}.\hat{\underline{n}} = \underline{v}.\ (\cos\theta,\ 0,\ -\sin\theta)$$

$$= v_r \cos\theta - v_z \sin\theta , \qquad (3.3.36$$

where $\theta = \cos^{-1}(\hat{\underline{n}}.\hat{\underline{r}})$ is the angle between the unit normal and the horizontal. This may be simplified further by noting that $\tan\theta = \frac{dr_0}{dz} \ll 1$, thus

$$v_n = v_r(r_0,z) - \frac{dr_0}{dz} v_z(r_0,z) . \qquad (3.3.37)$$

Finally, for a slender tube ($r_0/R \ll 1$, $r_0/L \ll 1$) Equation (3.3.37) gives

$$v_n \approx r_0\left(\frac{\partial v}{\partial r}r\right)_{r=0} - \frac{dr_0}{dz}\, v_z \,. \tag{3.3.38}$$

The velocity component normal to the surface in the exterior may also be written in a similar form to (3.3.37) for $\frac{dr_0}{dz} \ll 1$,

$$v_n^{(e)} = v_r^{(e)}(r_0,z) - \frac{dr_0}{dz}\, v_z^{(e)}(r_0,z) \,, \tag{3.3.39}$$

and using the relations (3.3.31) - (3.3.33), this may be expressed in terms of the pressure perturbation as

$$v_n^{(e)} \approx \frac{1}{i\omega\rho_e}\left[-\frac{\partial p^{(e)}}{\partial r} + \frac{dr_0}{dz}\,\frac{\omega^2}{N_e^2-\omega^2}\left(\frac{\partial p^{(e)}}{\partial z} + \frac{g}{c_e^2}\,p^{(e)}\right)\right]_{r=r_0} \tag{3.3.40}$$

Combining (3.3.38) and (3.3.40), the boundary condition (3.3.29) may be written

$$r_0\left(\frac{\partial v}{\partial r}r\right)_{r=0} - \frac{dr_0}{dz}\, v_z = \frac{1}{i\omega\rho_e}\left[-\frac{\partial p^{(e)}}{\partial r} + \frac{dr_0}{dz}\,\frac{\omega^2}{N_e^2-\omega^2}\left(\frac{\partial p^{(e)}}{\partial z} + \frac{g}{c_e^2}\,p^{(e)}\right)\right]_{r=r_0} . \tag{3.3.41}$$

For a straight tube, $\frac{dr_0}{dz} = 0$, this condition reduces to (3.2.49a).

We may approximate the second boundary condition (3.3.30) by

$$p + B_0\,\frac{\hat{b}_z}{\mu_0} = p^{(e)}(r_0,z) \,. \tag{3.3.42}$$

Equations (3.3.24) - (3.3.27), (3.3.41) and (3.3.42) provide a closed system once the form of $p^{(e)}$ is determined. Equations (3.3.25) - (3.3.27) and (3.3.42) may be combined to give an equation for the velocity $\hat{v}_z$ in terms of $p^{(e)}$:

$$\frac{d^2\hat{v}_z}{dz^2} + \left(\frac{\rho_0'}{\rho_0} + \frac{c_T^{2\prime}}{c_T^2} - \frac{B_0'}{B_0}\right)\frac{d\hat{v}_z}{dz} + \left[\frac{\omega^2-N_0^2}{c_T^2} - \frac{d}{dz}\left(\frac{B_0'}{B_0}+\frac{g}{c_0^2}\right) - \left(\frac{B_0'}{B_0}+\frac{g}{c_0^2}\right)\left(\frac{\rho_0'}{\rho_0}+\frac{c_T^{2\prime}}{c_T^2}+\frac{g}{c_0^2}\right)\right]\hat{v}_z =$$

$$= \frac{i\omega}{\rho_0 v_A^2}\left[\frac{d}{dz}P^{(e)}(r_0,z) + \left(\frac{g}{c_0^2} + \frac{c_T^{2'}}{c_T^2} + \frac{\rho_0'}{\rho_0} - 2\frac{B_0'}{B_0}\right)P^{(e)}(r_0,z)\right] . \quad (3.3.43)$$

In the limit of $g \to 0$, this reduces to the Equation (3.2.50) for variations of the form $e^{\pm ikz}$. Another special case of interest is when the tube is in temperature balance with its surroundings when (3.3.43) becomes

$$\frac{d^2\hat{v}_z}{dz^2} - \frac{1}{2\Lambda_0}\frac{d\hat{v}_z}{dz} + \left[\frac{\omega^2}{c_T^2} - \frac{N_0^2}{c_0^2}\left(\frac{\gamma}{2} + \frac{c_0^2}{v_A^2}\right)\right]\hat{v}_z = \frac{i\omega}{\rho_0 v_A^2}\left(\frac{dP^{(e)}}{dz} + \frac{g}{c_0^2}P^{(e)}\right). \quad (3.3.44)$$

Using the expression (3.3.28) for $\hat{\Delta}$ in Equation (3.3.24), together with Equations (3.3.26) and (3.3.27) the boundary condition (3.3.42) may be arranged to give

$$2\left(\frac{\partial v_r}{\partial r}\right)_{r=0}\left(1 + \frac{c_0^2}{v_A^2}\right) + \left(\frac{B_0'}{B_0} - \frac{g}{v_A^2}\right)\hat{v}_z + \frac{c_0^2}{v_A^2}\frac{d\hat{v}_z}{dz} + \frac{i\omega}{\rho_0 v_A^2}P^{(e)}(r_0,z) = 0 . \quad (3.3.45)$$

Writing $P^{(e)}(r_0,z) = P_r^{(e)}(r_0)P_z^{(e)}(z)$, the two Equations (3.3.43) and (3.3.45) may be combined with the boundary condition (3.3.41) to give a single equation for $\hat{v}_z$ involving the radial dependence of the external pressure perturbation, $P_r^{(e)}$, only.

3.3.3 Derivation of the Velocity Equation

i UNIFORM VERTICAL FIELD

As an introduction to this section, we shall consider a uniform vertical magnetic field, $\underline{B} = B_0\hat{\underline{z}}$, so that the terms involving $\frac{dr_0}{dz}$ in Equation (3.3.41) are absent, and $\frac{d}{dz}P^{(e)}(r_0,z)$ may be replaced by $P_r^{(e)}(r_0)\frac{d}{dz}P_z^{(e)}(z)$ in (3.3.43). Note that for this equilibrium the tube is not in temperature balance with its surroundings (see Equation (3.3.16)).

The three governing equations (3.3.41), (3.3.43) and (3.3.45) become

$$r_0\left(\frac{\partial v_r}{\partial r}\right)_{r=0} = -\frac{1}{i\omega\rho_e}\left(\frac{\partial p_r^{(e)}}{\partial r}\right)_{r=r_0} p_z^{(e)}(z) , \qquad (3.3.46)$$

$$\frac{d^2\hat{v}_z}{dz^2} - \frac{v_A^2}{\Lambda_0(c_0^2+v_A^2)}\frac{d\hat{v}_z}{dz} + \left[\frac{\omega^2}{c_T^2} - \frac{g}{v_A^2}\frac{\Lambda_0'}{\Lambda_0} - \frac{g}{\Lambda_0 v_A^2}\left(\frac{\gamma-1}{\gamma} + \frac{v_A^2}{c_0^2+v_A^2}\right)\right]\hat{v}_z =$$

$$\frac{i\omega}{\rho_0 v_A^2}\left[\frac{dp_z^{(e)}}{dz} + \left(\frac{g}{v_A^2} - \frac{v_A^2}{\Lambda_0(c_0^2+v_A^2)}\right)p_z^{(e)}(z)\right] p_r^{(e)}(r_0) , \qquad (3.3.47)$$

and

$$2\left(\frac{\partial v_r}{\partial r}\right)_{r=0}\left(1+\frac{c_0^2}{v_A^2}\right) - \frac{g}{v_A^2}\hat{v}_z + \frac{c_0^2}{v_A^2}\frac{d\hat{v}_z}{dz} + \frac{i\omega}{\rho_0 v_A^2} p_r^{(e)}(r_0)p_z^{(e)}(z) = 0 . \qquad (3.3.48)$$

Eliminating $\left(\frac{\partial v_r}{\partial r}\right)_{r=0}$ between Equations (3.3.46) and (3.3.48), and substituting for $p_z^{(e)}(z)$ from the resulting equation into (3.3.47) gives

$$\left(1-\frac{i\omega}{\rho_0 v_A^2}\beta(z)\right)\frac{d^2\hat{v}_z}{dz^2} + \left[-\frac{v_A^2}{\Lambda_0(c_0^2+v_A^2)} - \frac{i\omega}{\rho_0 v_A^2}\left[\beta'(z)+\alpha(z)+\left(\frac{g}{c_0^2} - \frac{v_A^2}{\Lambda_0(c_0^2+v_A^2)}\right)\beta(z)\right]\right]\frac{d\hat{v}_z}{dz}$$

$$+\left[\frac{\omega^2}{c_T^2} - \frac{g}{v_A^2}\frac{\Lambda_0'}{\Lambda_0} - \frac{g}{\Lambda_0 v_A^2}\left(\frac{\gamma-1}{\gamma} + \frac{v_A^2}{c_0^2+v_A^2}\right) - \frac{i\omega}{\rho_0 v_A^2}\left[\alpha'(z)+\left(\frac{g}{c_0^2} - \frac{v_A^2}{\Lambda_0(c_0^2+v_A^2)}\right)\alpha(z)\right]\right]\hat{v}_z = 0 , \qquad (3.3.49$$

where

$$\alpha(z) = \frac{-i\omega\rho_e g J}{\omega^2\left[2\left(1+\frac{c_0^2}{V_A^2}\right) + \frac{\rho_e}{\rho_0} J\right]} ,$$

$$\beta(z) = \frac{i\omega\rho_e c_0^2 J}{\omega^2\left[2\left(1+\frac{c_0^2}{V_A^2}\right) + \frac{\rho_e}{\rho_0} J\right]} ,$$

and

$$J = \frac{\omega^2 r_0 p_r^{(e)}(r_0)}{V_A^2\left(\frac{\partial p_r^{(e)}}{\partial r}\right)_{r=r_0}}$$

Equation (3.3.49) describes vertical motions in a straight flux tube in a stratified atmosphere, and is valid for $r_0/R \ll 1$. In the absence of gravity the solution for $\hat{v}_z$ is $\hat{v}_z = \hat{v}_z(0)e^{ikz}$ where

$$(\omega^2-k^2c_T^2)(c_0^2+v_A^2)+\omega^2(\omega^2-k^2c_0^2)\frac{\rho_e}{\rho_0}\frac{1}{2}\frac{r_0 P_r^{(e)}(r_0)}{\left(\frac{\partial P_r^{(e)}}{\partial r}(r)\right)_{r_0}} = 0 , \qquad (3.3.50)$$

which is the dispersion relation (3.2.52), obtained for a slender tube ($r_0/R \ll 1$) in a uniform atmosphere, and has solutions $\omega^2 \approx k^2c_T^2$, and $\omega^2 \approx k^2c_e^2$ if $r_0/R \ll 1$. In the non-stratified case, the 'tube wave' solution $\omega^2 \approx k^2c_T^2$ corresponds to the condition $\zeta \ll 1$ being valid; the horizontal wavelength in the exterior remains finite as $kr_0 \to 0$ and, for $P_r^{(e)} \sim K_0(m_e r)$, we find

$$\zeta \sim k^2\frac{c_T^2}{v_A^2} r_0^2 \log m_e r_0 \ll 1 .$$

The second solution is a sound-wave solution. The condition $\zeta \ll 1$ does not hold since $m_e/k \to 0$ as $kr_0 \to 0$ (the waves propagate in the z-direction).

In the stratified atmosphere we also have solutions for the radial dependence of the pressure perturbation in the exterior of the form $P_r^{(e)} \sim K_0(Kr)$ (see Equation 3.3.34). If we confine our attention to the tube-wave solution, i.e. we do not admit the possibility of vertically propagating sound waves so that K does not $\to 0$ as $r_0/R \to 0$, then we find that

$$\zeta \ll 1 \qquad \text{for} \qquad r_0/R \ll 1 ,$$

and Equation (3.3.49) approximates to

$$\frac{d^2\hat{v}_z}{dz^2} - \frac{v_A^2}{\Lambda_0(c_0^2+v_A^2)}\frac{d\hat{v}_z}{dz} + \left[\frac{\omega^2}{c_T^2} - \frac{g}{v_A^2}\frac{\Lambda_0'}{\Lambda_0} - \frac{g}{\Lambda_0 v_A^2}\left(\frac{\gamma-1}{\gamma}+\frac{v_A^2}{c_0^2+v_A^2}\right)\right]\hat{v}_z = 0 . \qquad (3.3.51)$$

Note that the above solution is equivalent to Equation (3.3.47) with $P^{(e)} \equiv 0$, and so it may be derived by replacing the boundary conditions (3.3.29) and (3.3.30) by the boundary condition

$$\hat{p} + \frac{B_0 \hat{b}_z}{\mu_0} = 0 \ . \qquad (3.3.52)$$

The solution of Equation (3.3.51) is valid therefore for a flux tube in a stratified atmosphere for which the pressure perturbations in the exterior are negligible. Also, Equation (3.3.51) is identical to Equation (2.2.25), which was derived for a uniform vertical field with horizontal wavelength small compared to vertical scale height.

ii FIELD VARYING WITH HEIGHT

If the magnetic field varies with height, the term involving $\frac{dr_0}{dz}$ in the boundary condition (3.3.41) may not necessarily be neglected. However, if we adopt the solution for the pressure in the exterior which decays rapidly from the boundary (i.e. the Bessel function K_0), the second term on the right hand side of (3.3.41) is small compared to the first (for $r_0/\Lambda_0 \ll 1$) and the condition approximates to

$$r_0 \left(\frac{\partial v_r}{\partial r}\right)_{r=0} - \frac{dr_0}{dz} \hat{v}_z = \frac{-1}{i\omega\rho_e} \left(\frac{\partial p_r^{(e)}}{\partial r}\right)_{r=r_0} p_z^{(e)}(z) \ , \qquad (3.3.53)$$

while the second condition (3.3.45) may be written

$$2\left(\frac{\partial v_r}{\partial r}\right)_{r=0}\left(1 + \frac{c_0^2}{v_A^2}\right) + \left(\frac{B_0'}{B_0} - \frac{g}{v_A^2}\right)\hat{v}_z + \frac{c_0^2}{v_A^2}\frac{d\hat{v}_z}{dz} + \frac{i\omega}{\rho_0 v_A^2} p_r^{(e)}(r_0)\, p_z^{(e)}(z) = 0 \ . \qquad (3.3.54)$$

The final condition (3.3.43) is

$$\frac{d^2\hat{v}_z}{dz^2} + \left(\frac{\rho_0'}{\rho_0} + \frac{c_T^{2\prime}}{c_T^2} - \frac{B_0'}{B_0}\right)\frac{d\hat{v}_z}{dz} + \left[\frac{\omega^2 - N_0^2}{c_T^2} - \frac{d}{dz}\left(\frac{B_0'}{B_0} + \frac{g}{c_0^2}\right) - \left(\frac{B_0'}{B_0} + \frac{g}{c_0^2}\right)\left(\frac{\rho_0'}{\rho_0} + \frac{c_T^{2\prime}}{c_T^2} + \frac{g}{c_0^2}\right)\right]\hat{v}_z =$$

$$\frac{i\omega}{\rho_0 v_A^2} P_r^{(e)}(r_0)\left[\frac{dP_z^{(e)}(z)}{dz}+\left(\frac{-g}{c_0^2}+\frac{c_T^{2\prime}}{c_T^2}+\frac{\rho_0'}{\rho_0}-\frac{2B_0'}{B_0}\right)P_z^{(e)}(z)\right] . \quad (3.3.55)$$

Eliminating $P_z^{(e)}(z)$ and $\left(\frac{\partial v_r}{\partial r}\right)_{r=0}$ between (3.3.53), (3.3.54) and (3.3.55) and applying the condition $\zeta << 1$ ('tube wave'), then gives

$$\frac{d^2\hat{v}_z}{dz^2}+\left(\frac{\rho_0'}{\rho_0}+\frac{c_T^{2\prime}}{c_T^2}-\frac{B_0'}{B_0}\right)\frac{d\hat{v}_z}{dz}+\left[\frac{\omega^2-N_0^2}{c_T^2}-\frac{d}{dz}\left(\frac{B_0'}{B_0}+\frac{g}{c_0^2}\right)-\left(\frac{B_0'}{B_0}+\frac{g}{c_0^2}\right)\left(\frac{\rho_0'}{\rho_0}+\frac{c_T^{2\prime}}{c_T^2}+\frac{g}{c_0^2}\right)\right]\hat{v}_z=0 . \quad (3.3.56)$$

This equation describes essentially vertical motion in a 'slender' flux tube, where the perturbations in the exterior are negligible; it may be obtained more directly by replacing the boundary conditions (3.3.29) and (3.3.30) by the 'reduced' boundary condition (3.3.52). In addition, there will be a mode coupled to the sound wave in the exterior. In this thesis we shall concentrate, for simplicity, on a flux tube in a 'quiescent' atmosphere and adopt the above equation for the vertical velocity perturbation $\hat{v}_z$. This applies only if the motions within the flux tube occur in isolation to the motions in the exterior. As we shall see in Section 3.3.6, observations are inconclusive as to whether or not there is a strong coupling between the interior and exterior.

3.3.4 Discussion

The purpose of the previous section was to derive an equation for the vertical velocity perturbation. The equation we derived (3.3.56) governs motions in a slender flux tube in a compressible atmosphere with negligible pressure perturbations in the exterior (tube wave). We did not assume temperature balance between the tube and its surroundings or that γ is constant with height. However a number of special cases of Equation (3.3.56) are readily treated.

Firstly, consider a uniform atmosphere with magnetic field $\underline{B}_0 = B_0 \hat{\underline{z}}$. Equation (3.2.53) has solutions $\hat{v}_z \sim e^{\pm ikz}$, where

$$\omega^2 = k^2 c_T^2 .$$

Thus, as expected, we recover the dispersion relation (3.2.21), valid provided $K^2 > 0$, i.e. $c_T^2 < c_e^2$.

For the interior and exterior of equal temperature, ($\Lambda_0 = \Lambda_e$ so that $c_0^2/\gamma v_A^2$ is constant) and constant γ, Equation (3.3.56) may be written

$$\frac{d^2 v_z}{dz^2} - \frac{1}{2\Lambda_0(z)} \frac{d\hat{v}_z}{dz} + \left[\frac{\omega^2 - N_0^2(z)}{c_T^2(z)} + \left(1 - \frac{\gamma}{2}\right) \frac{N_0^2(z)}{c_0^2(z)} \right] \hat{v}_z = 0 \quad , \qquad (3.3.57)$$

which becomes (using 3.3.21)

$$\frac{d^2 v_z}{dz^2} - \frac{1}{2\Lambda_0(z)} \frac{d\hat{v}_z}{dz} + \left[\frac{\omega^2 \Lambda_0(0)}{c_T^2(0)\Lambda_0(z)} - \frac{1}{\gamma \Lambda_0^2(z)} \left(\frac{\gamma - 1}{\gamma} + \Lambda_0'(z) \right) \left(\frac{\gamma}{2} + \frac{c_0^2(0)}{v_A^2(0)} \right) \right] \hat{v}_z = 0 . \qquad (3.3.57)'$$

Equation (3.3.57) may be written in canonical form by writing

$$V = \hat{v}_z \exp\left(-\frac{1}{4} \int_0^z \frac{dz'}{\Lambda_0(z')} \right) ,$$

and then $V(z)$ satisfies

$$\frac{d^2 V}{dz^2} + \left(\frac{\omega^2 - \omega_v^2}{c_T^2} \right) V = 0 , \qquad (3.3.58)$$

where the frequency, $\omega_v(z)$, satisfies

$$\omega_v^2(z) = N_0^2(z) + \frac{c_T^2(z)}{\Lambda_0^2(z)} \left(\frac{3}{4} - \frac{1}{\gamma} \right) \left(\frac{3}{4} - \frac{1}{\gamma} + \Lambda_0' \right) . \qquad (3.3.59)$$

The solutions of Equation (3.3.58) are oscillatory in character for $\omega^2 > \omega_v^2$, and for $\omega^2 < \omega_v^2$ the solutions are (locally) exponential in nature. Thus, the equation

$$\omega^2 - \omega_v^2 = 0 ,$$

may be considered as defining a critical value of ω^2, i.e. ω_v^2, giving the transition frequency between vertically-propagating waves and vertically evanescent modes. The critical frequency, ω_v, given by Equation (3.3.59), is plotted as a function of height in the solar atmosphere in Figure 3.7 using Spruit's (1974) model and the H.S.R.A. for the temperature profile. We take $\gamma = 5/3$ and $c_0 = v_A$. The variation of the critical frequency with height is determined by the scale height of the atmosphere. Equation (3.3.59) gives

$$\omega_v^2 = \frac{c_T^2(0)}{c_0^2(0)} \frac{\gamma g}{\Lambda_0(z)} \left[\frac{3}{4} \Lambda_0'(z) + \frac{9}{16} - \frac{1}{2\gamma} + \frac{1}{\gamma} \left(\frac{\gamma - 1}{\gamma} + \Lambda_0'(z) \right) \frac{c_0^2(0)}{v_A^2(0)} \right] . \qquad (3.3.59)'$$

The transition period τ_v (corresponding to frequency $\omega_v = 2\pi/\tau_v$) is plotted in Figure 3.8.

From Figures 3.7 and 3.8 we see that in the region $-110\text{km} \lesssim z \lesssim 12\text{km}$ the motions are oscillatory in character for all $\omega > 0$, whilst outside this region the motions are (locally) oscillatory for $\omega > \omega_v$. Below z = -110km, ω_v increases from zero to a maximum of 0.0143 s^{-1} (corresponding to a period of 438s) at about 370km below $\tau_{5000} = 1$, and gradually decreases below this level. Above z=0, ω_v increases from zero at $z \approx 12$km to a local maximum of 0.032 s^{-1} (corresponding to a period of 195s) at 410km above $\tau_{5000}=1$.

Allowing for the variation with height of the ratio of specific heats, γ, which, as we have seen in Chapter 1, varies significantly over the range of interest, then the critical frequency $\omega = \omega_v^*$ is given by

$$\frac{\omega_v^{*2}}{c_T^2} = \frac{N_0^2}{c_T^2} + \frac{1}{\Lambda_0^2}\left(\frac{3}{4} - \frac{1}{\gamma}\right)\left(\frac{3}{4} - \frac{1}{\gamma} + \Lambda_0'\right) + \frac{\gamma'}{\gamma}\left[\frac{-1}{\gamma\Lambda_0} + \frac{\gamma(0)}{\gamma(0)+\gamma}\left(\frac{1}{\gamma\Lambda_0} - \frac{3}{4\Lambda_0}\right)\right]$$

$$+\left(\frac{\gamma'}{\gamma}\right)^2\left[\left(\frac{\gamma(0)}{\gamma(0)+\gamma}\right)^2\left(\frac{1}{4} - \frac{1}{2}\frac{\gamma}{\gamma(0)}\right) - \frac{1}{2}\left(\frac{\gamma(0)}{\gamma(0)+\gamma}\right)\right] + \frac{\gamma''}{2\gamma}\left(\frac{\gamma(0)}{\gamma(0)+\gamma}\right) . \qquad (3.3.60)$$

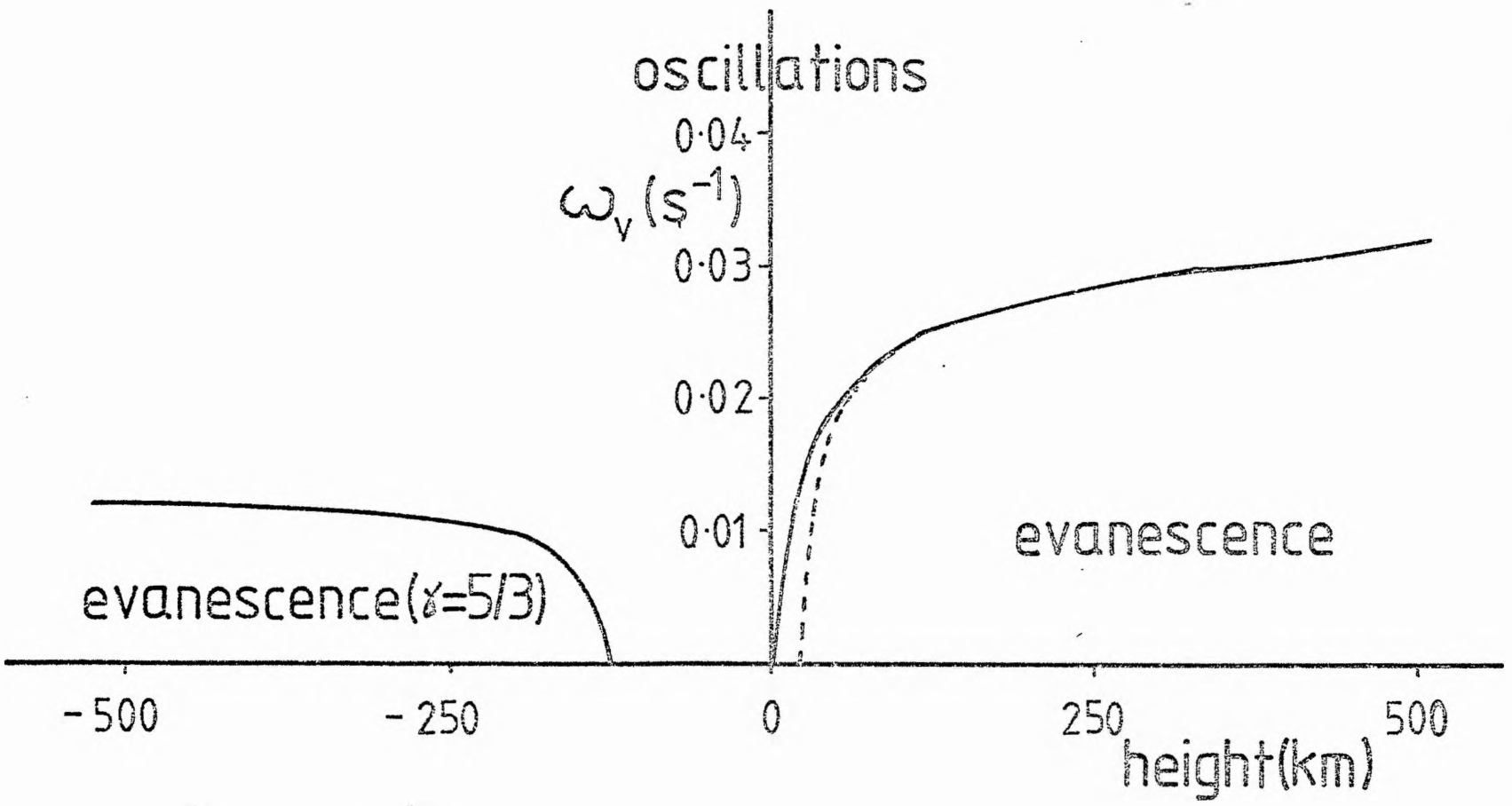

Figure 3.7 $-\omega_v^2$ as a function of height in the solar atmosphere. We have taken $c_0 = v_A$. Above the curve corresponds to oscillatory solutions, below the curve exponential modes. The continuous curve is for $\gamma = 5/3$ and the dashed line is the modification due to the variation of the ratio of specific heats, γ.

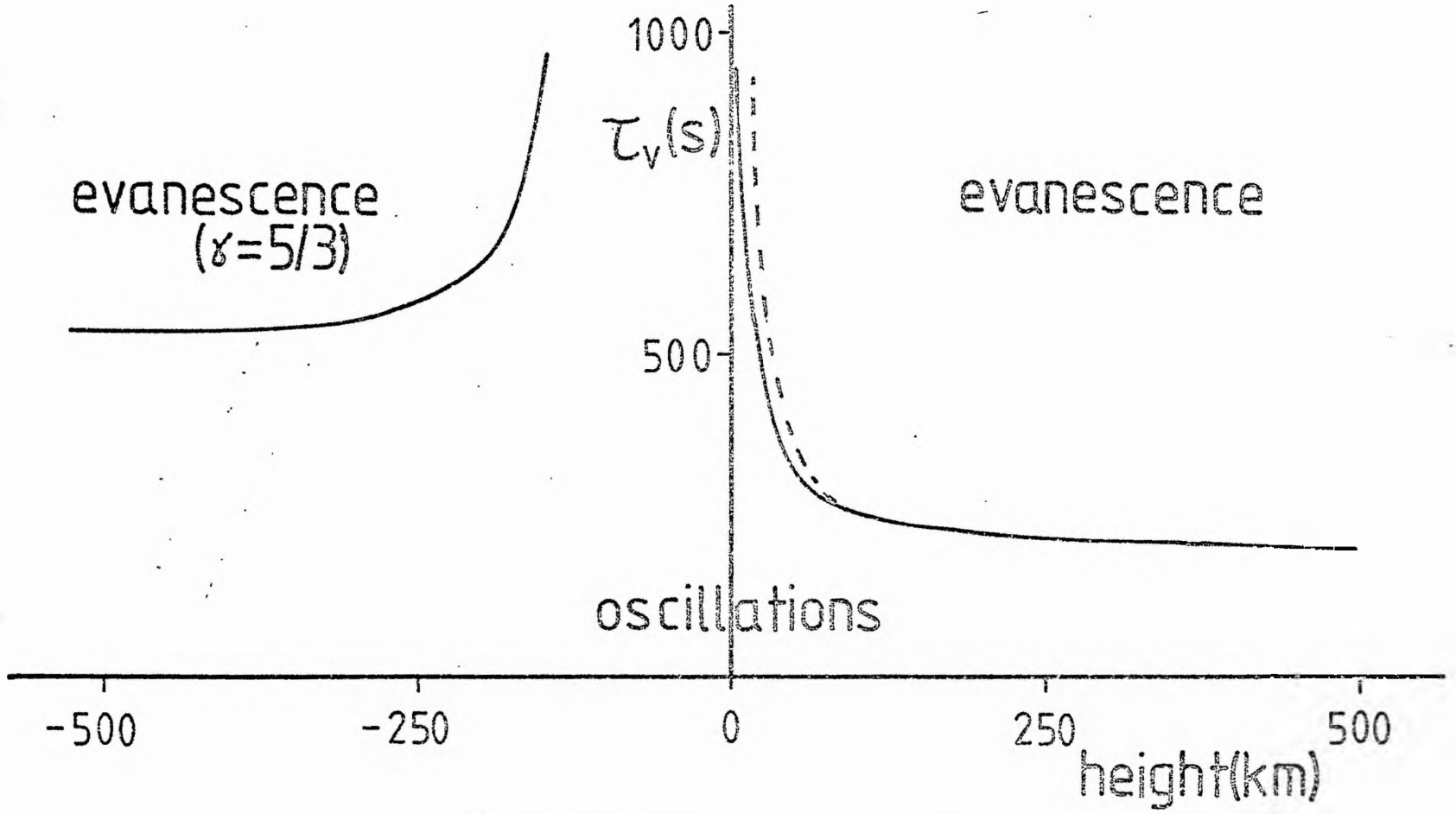

Figure 3.8 - The transition period τ_v as a function of height. We have taken $c_0 = v_A$ and the solid line corresponds to $\gamma = 5/3$, while the dashed line allows for the variation of γ.

The curve $\omega = \omega_v^*$ is sketched as a dashed line in Figure 3.7. The solutions of Equation (3.3.58) are now oscillatory for all z less than about 20 km above $\tau_{5000} = 1$ (at least, up to depth of 1000km below $\tau_{5000} = 1$). Above z=0, ω_v^* increases from zero at $z \approx 20$ km to a maximum of $0.032 s^{-1}$ (corresponding to a period of 195s) at $z \approx 410$km. The behaviour of ω_v^* in the range $0 \lesssim z \lesssim 500$km is very similar to that of ω_v. The effect of ionization is to allow waves to propagate in the convection zone, as Figure 3.7 shows.

It is of interest to compare the critical frequency given by (3.3.59) with those cut-off frequencies obtained in Chapter 2 for internal-gravity waves and sound waves. Since the waves described by Equation (3.3.58) propagate for frequencies greater than some cut-off frequency, it is not unreasonable to identify the waves with sound waves, modified due to the effect of gravity and a magnetic field. However, the waves are not purely acoustic in nature, since, whereas the acoustic cut-off frequency, $\gamma g/2c_0$, tends to infinity as γ tends to infinity, the limit of ω_v is finite, given by

$$\omega_v^2 \to \omega_{v\infty}^2 = g\left(\frac{1}{\Lambda_0} + \Lambda_0'\right) + \frac{V_A^2}{\Lambda_0^2}\frac{3}{4}\left(\frac{3}{4} + \Lambda_0'\right), \quad \text{as } \gamma \to \infty$$

and so the 'tube wave' is still present in the incompressible limit for $\omega > \omega_{v\infty}$.

3.3.5 The Pressure Equation

So far in this chapter we have dealt with the equation for the velocity perturbation only. We may perform similar analysis to Section 3.3.3 to derive an equation for the pressure perturbation,

$\hat{p}(z)$. This equation is

$$(\omega^2-N_0^2)\frac{d^2\hat{p}}{dz^2} + \alpha(\omega;z)\frac{d\hat{p}}{dz} + \beta(\omega;z)\hat{p} = 0 \ , \qquad (3.3.62)$$

where

$$\alpha(\omega;z) = (\omega^2-N_0^2)\left(\frac{1}{H_0} - \frac{B_0'}{B_0}\right) + (N_0^2)' ,$$

$$\beta(\omega;z) = (\omega^2-N_0^2)\left[\left(\omega^2-\frac{g}{H_0}\right)\left(\frac{1}{c_0^2}+\frac{1}{v_A^2}\right)+\frac{g^2}{c_0^2v_A^2}+\frac{g}{c_0^2\Lambda_0} - \frac{g}{c_0^2}\frac{B_0'}{B_0} - \frac{g}{c_0^2}\frac{\gamma'}{\gamma}\right] + \frac{g}{c_0^2}(N_0^2)' \ .$$

The pressure perturbation equation was derived by Roberts (see Roberts and Webb, 1978; Equation 29) for the case of constant ratio of specific heats.

Writing $\hat{p} = fq$ where

$$\frac{f'}{f} = -\frac{\alpha}{2(\omega^2-N_0^2)} \ , \qquad \omega^2 \neq N_0^2$$

i.e.

$$f = \left[\rho_0 B_0 \left|\omega^2-N_0^2\right|\right]^{\frac{1}{2}} ,$$

Equation (3.3.62) may be expressed in the canonical form

$$q'' + f_0(z;\omega)q = 0 \ , \qquad (3.3.63)$$

where

$$f_0 = \frac{1}{c_T^2(\omega^2-N_0^2)}\left[(\omega^2-N_0^2)^3 + A(\omega^2-N_0^2)^2 + B(\omega^2-N_0^2) + C\right] ,$$

and

$$A = \left[\left(\frac{3}{2}\gamma - 1\right)\frac{g^2}{c_0^2} + \frac{1}{2}\left(\frac{m'}{m}\right)' - \frac{1}{4}\left(\frac{m'}{m}\right)^2 - \frac{\gamma' g}{\gamma c_0^2}\right]c_T^2 \ ,$$

$$B = \left[\left(\frac{1}{2}\frac{m'}{m} + \frac{g}{c_0^2}\right)(N_0^2)' - \frac{(N_0^2)''}{2}\right]c_T^2 \ ,$$

$$C = -\frac{3}{4}\left[(N_0^2)'\right]^2 c_T^2 \ .$$

The length m is defined by

$$\frac{m'}{m} = \frac{-\Lambda_0'}{\Lambda_0} - \frac{3}{2\Lambda_0} \quad .$$

The nature of the pressure perturbations depends upon a critical 'transition' frequency, $\omega = \omega_p$ defined by the equation

$$P_0(z; \omega_p^2) = 0 \quad . \tag{3.3.64}$$

ω_p is also dependent on the basic state of the tube.

The critical frequency is sketched in Figure 3.9 for both the cases of γ constant (=5/3) and γ varying with height (dashed line). For $\gamma = 5/3$ the function ω_p has a peak of $5.1 \times 10^{-2} s^{-1}$ at $z \approx -25$ km. Below $z \approx -100$ km, ω_p is approximately constant up to a depth of 500 km, so that wave-like pressure perturbations occur for frequencies greater than $1.2 \times 10^{-2} s^{-1}$ (that is periods greater than 524 s). Above the convection zone, ω_p is constant for 100 km $\lesssim z \lesssim$ 450 km and wave-like pressure perturbations occur for periods greater than about 256s. There is a narrow region around the temperature minimum where the cubic equation (3.3.64) has three positive real roots for ω^2. For γ not constant, wave like pressure perturbations occur at depths below $z \approx -100$ km for all frequencies.

3.3.6 Observations

Having described the basic state of the flux tube in Section 3.3.1 and derived the equations describing vertical motions (3.3.56) and (3.3.62) we now consider the application of the above analysis to the Sun. We assume that the basic state of the tube is a static one and that the equations presented describe, at least approximately, motions in an intense magnetic flux tube. For a tube in temperature

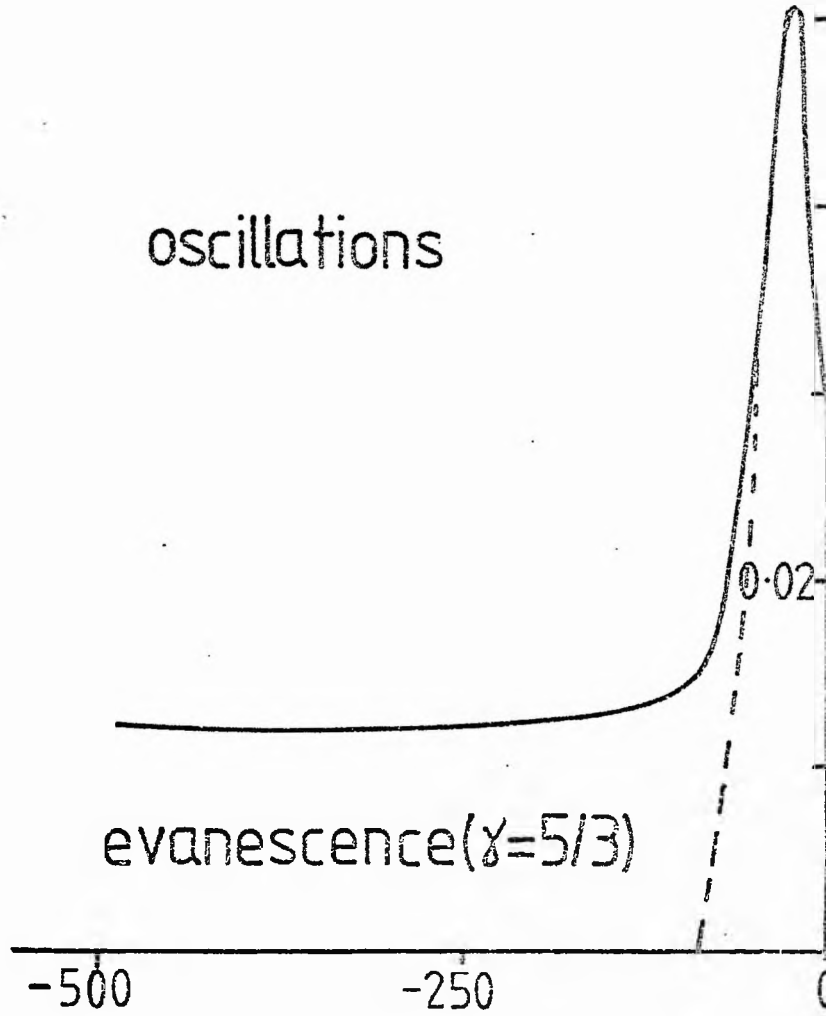

Figure 3.9 - ω_p^2 as a function of h
height (dashed line)

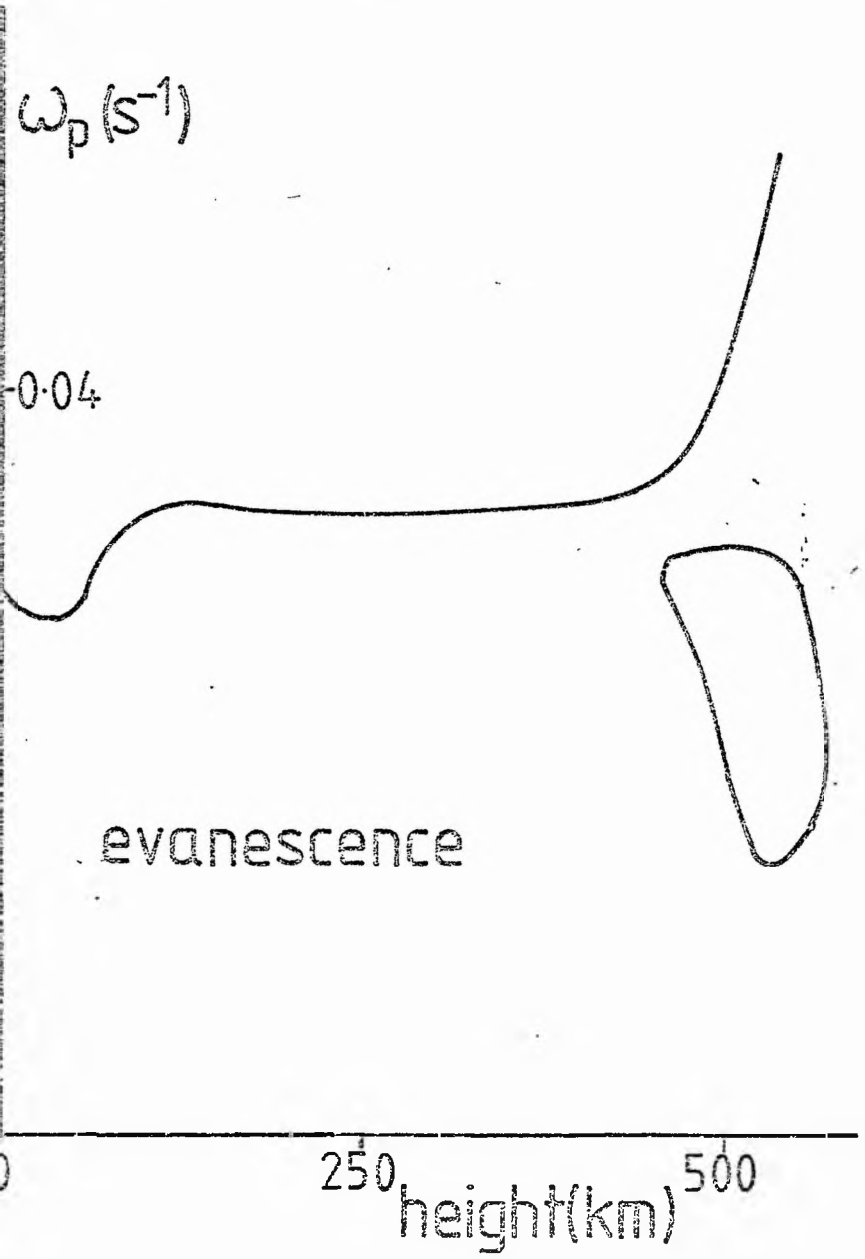

eight for $\gamma = 5/3$ and γ varying with

balance with its surroundings we must therefore assume that the condition $r_0 \ll \Lambda_0$ (3.3.17) holds. As we have described in Chapter 1, observations indicate that the radius of the tube at photospheric levels is about 100km, which is of the same order as the scale height, Λ_0. However, as depth increases, the radius of the tube decreases (see Equation (3.3.18)) and the scale height increases, so the approximation (3.3.17) improves with depth. Above the photosphere the tube fans out and our results may only be indicative of a more detailed analysis. Also, we have neglected the effect of radiation on the waves propagating in the tube. The adiabatic energy equation for the perturbations may be a reasonable approximation in the convection zone (see Chapter 1) but in the photosphere radiation has a significant effect and is discussed in Chapter 5. Further, we have considered only the 'tube wave'. That is, we have neglected the interaction of the tube with its surroundings, taking Equation (3.3.52) as the approximate boundary condition, and we have not considered the sound wave solution in the exterior. Observations are presently inconclusive as to whether or not there is a strong interaction between the tube and its surroundings.

The observations by Giovanelli et al (1978) of waves in magnetic flux tubes in the photosphere and low chromosphere show upward propagation, with closely-related but far from identical disturbances inside and outside the tube. This leads Giovanelli et al to two possible interpretations: i) a remote common source with negligible interaction between internal and external gas, or ii) strong interaction, so that the external and internal behaviours are closely related. The former case would correspond to our 'tube wave' solution for which perturbations in the exterior are negligible, and the latter is the modified sound wave solution.

The observed waves are upward propagating with average periods 275s in the lines 5250 Å and 5233 Å (formed, in the non-magnetic atmosphere at -25km below τ_{5000}= 1 and 195km above τ_{5000}= 1) and 290s in the lines 5166 Å and 5183 Å (formed at -25km and 540km). The main difference between the interior and the exterior is that outside the tube, there is an observed time difference of 7s for an estimated propagation distance of 600-700km yielding a phase velocity approaching 100kms^{-1}, whilst inside the time delay is 19s. The phase velocity is supersonic and in the absence of dissipation such waves are likely to be evanescent. Figure 3.8 predicts that waves with periods 275-290s are evanescent in the region above $z \approx 100$km.

In this chapter we have discussed wave propagation in a flux tube in a uniform atmosphere. We developed a slender flux tube approximation and extended this to a stratified atmosphere. In the following chapter we use this approximation and consider the nature of convectively unstable motions in a magnetic flux tube.

Chapter 4 CONVECTIVE INSTABILITY

4.1 Introduction

Observations of the quiet regions of the solar photosphere have shown that the magnetic field is made up of intense flux tubes, located in the boundaries of supergranules (see Chapter 1). The field in these flux tubes is estimated to be in the range 1-2kG and their diameters 100-300km.

Observations suggest that the average solar magnetic field is swept to supergranular cell boundaries and concentrated there (Simon and Leighton, 1963). Theoretical models illustrating the growth of magnetic fields around the boundaries of supergranulation cells have been developed, and the results demonstrate the tendency of the field to accumulate at these boundary points where the flow is most strongly converging (Leighton et al, 1962; Leighton, 1963; Parker, 1963; Weiss, 1964; Clark, 1965, 1966; Clark and Johnson, 1967). However, some other means is required for compressing fields to the very high pressures of kilogauss fields. Parker (1976) reviews the hydrodynamic effects that might contribute to the enhancement of the magnetic field and concludes that only cooling of the gas within the field can produce the high field densities inferred from observation. He suggests that the generation and emission of overstable Alfvén waves (Roberts, 1976a) is the only way to account for the cooling and subsequent field intensification. More recently, Parker (1978) has suggested, as an alternative explanation, that the reduced heat transport in the kinematically compressed magnetic field (of a few hundred gauss) leads to an almost adiabatic temperature gradient inside the tube so that the temperature inside the thermally insulated tube is cooler than its surroundings.

This then leads to an enhancement of the already existing downdraft in the tube and, as a result, the field is compressed further to reach, eventually, the observed kilogauss values. Zwaan (1978) has argued that the field is concentrated into bundles in the deep convection zone by differential rotation, but after a loop has surfaced, subsequent convective downflow reduces the temperature at the top of the flux tubes, which then contract to field strengths well above the local equilibrium value. A further possibility has been suggested by Galloway et al (1977, 1978), who have shown that convection in a Boussinesq fluid can compress magnetic fields to strengths beyond equipartition values.

By whatever means the Sun actually achieves the compression of magnetic fields into intense flux tubes, the fact remains that such fields exist. Given, then, the existence of such a slender kilogauss flux tube, what motions are likely to occur inside the tube? Additionally, under what circumstances will motions radically change the structure of the flux tube?

In Chapter 3 we considered the nature of wave motions inside a flux tube. For a slender flux tube in a stratified atmosphere, we presented a system of linearized zeroth order equations and applied boundary conditions to determine the equations for the vertical component of velocity, $\hat{v}_z$ (3.3.56) and the pressure $\hat{p}$ (3.3.62). In this chapter we consider the nature of convectively unstable motions in a magnetic flux tube. We investigate the role of the magnetic field in preventing such instability, including the effect of the splaying of the field lines with height. We should note that distinct from the convective instability is the tendency for the surface of the flux tube to be unstable to fluting (interchange instability) (Meyer et al (1977)).

It turns out that we are able to obtain sufficient conditions for stability against the tendency towards convection for a flux tube with an arbitrary temperature profile. In the special case of a linear profile we are able to describe in detail both the velocity field and its instability boundaries. Finally, we argue that convective instability may be a means of achieving intense fields (see also Spruit, 1979; Spruit and Zweibel, 1979).

4.2 The Equilibrium State in a Slender Flux Tube

The equilibrium has been described in general terms in Chapter 3. For the sake of completeness, and in order to make additional observations, we shall discuss the equilibrium state of a slender flux tube once more. The internal pressure $p_0(z)$ and density $\rho_0(z)$ are related by the barometric relation

$$\frac{dp_0}{dz} = -\rho_0 g \; ; \tag{4.2.1}$$

while the ideal gas equation determines the internal temperature $T_0(z)$:

$$p_0(z) = \frac{k}{\hat{m}} \rho_0(z) T_0(z) \; , \tag{4.2.2}$$

where k is Boltzmann's constant, $\hat{m}$ is the mean particle mass and g is the acceleration due to gravity. Lateral pressure balance demands that the external confining gas pressure $p_e(z)$ satisfy

$$p_0(z) + \frac{B_0^2(z)}{2\mu_0} = p_e(z) \; , \tag{4.2.3}$$

where $B_0(z)\hat{\mathbf{z}}$ is the zeroth-order (induction) field of the flux tube. The external atmosphere is also in hydrostatic equilibrium, and so

$$\frac{dp_e}{dz} = -\rho_e g \; , \tag{4.2.4}$$

where $\rho_e(z)$ is the density in the exterior region.

From (4.2.3) it follows that

$$\frac{d}{dz}\left(\frac{B_0^2(z)}{2\mu_0}\right) = g(\rho_0 - \rho_e) . \qquad (4.2.5)$$

Introduce the scale-heights $\Lambda_0 \equiv kT(z)/\hat{m}g$ and $\Lambda_e \equiv kT_e(z)/\hat{m}g$, of the internal and external atmospheres, and write

$$\Lambda_0(z) + \lambda(z) = \Lambda_e(z) , \qquad (4.2.6)$$

where $\lambda(z)$ is a measure of the temperature difference between the two regions. Then (4.2.5) may be combined with (4.2.2) and the corresponding equation for the exterior region to give

$$\frac{d}{dz}\left(\frac{B_0^2(z)}{2\mu_0}\right) = -\frac{1}{\Lambda_0(z)}\left(\frac{B_0^2(z)}{2\mu_0} - \frac{\lambda(z)}{\Lambda_e(z)}\, p_e(z)\right) . \qquad (4.2.7)$$

Now, in the presence of a strong magnetic field, we may expect a temperature difference to exist between the interior and the exterior of the tube, despite the natural tendency for thermal conduction to smooth out such a difference. There are strong theoretical reasons (Parker, 1955, 1976, 1978; Roberts, 1976a, b; Spruit, 1976) for believing this conjecture; indeed, if the flux tube is not cooler than its surroundings it is difficult to imagine how such intense fields occur. The observational evidence is presently inconclusive; in fact, the tubes appear as bright dots (Frazier, 1970) against the surrounding photosphere. They appear bright because they are less dense than their surroundings, so that one sees deeper into the Sun where the ambient temperature is higher than at the surface (Spruit, 1977).

Now the effect of a magnetic field upon the energetics of the basic-state is not well understood, so it is necessary to model the likely behaviour of the field in creating a temperature

difference. There are clearly several possibilities. For example, it is reasonable to suppose that the stronger the field (relative to the confining pressure), the larger the temperature difference the field creates.

Introduce

$$\tau(z) = \frac{\Lambda_e(z) - \Lambda_0(z)}{\Lambda_e(z)} , \qquad (4.2.8)$$

the ratio of the temperature difference between the internal and external media to the external temperature. Then, to model the behaviour of the magnetic field, we may suppose that $\tau(z)$ is proportional to the ratio of the magnetic pressure to the external gas pressure, and write

$$\tau(z) = \theta \left(\frac{B_0^2(z)}{2\mu_0 p_e(z)} \right) , \qquad (4.2.9)$$

where θ is a constant of proportionality. It is assumed that θ is less than or equal to one; also, for a cool interior θ is positive.

With the above form of $\tau(z)$, Equation (4.2.7) gives

$$\frac{1}{B_0} \frac{dB_0}{dz} = \frac{-(1-\theta)}{2\Lambda_0(z)} . \qquad (4.2.10)$$

Combined with (4.2.1) and (4.2.2) this gives

$$B_0^2(z) \sim (p_0(z))^{1-\theta} . \qquad (4.2.11)$$

Flux conservation implies that $r_0^2(z)B_0(z) = r_0^2(0)B_0(0)$, where $r_0(z)$ is the radius of the tube at the height z above the arbitrary reference level z = 0 (chosen to correspond to optical depth $\tau_{5000} = 1$ in the solar atmosphere). Thus

$$r_0(z) \sim (p_0(z))^{-\frac{1}{4}(1-\theta)} . \qquad (4.2.12)$$

Much of the subsequent discussion will be given in terms of the function $c_0^2(z)/v_A^2(z)$, where $c_0(z) = (\gamma p_0(z)/\rho_0(z))^{\frac{1}{2}}$ is the sound speed and $v_A(z) = B_0(z)/(\mu_0\rho_0(z))^{\frac{1}{2}}$ is the Alfvén speed inside the flux tube. (γ is the ratio of specific heats, which may be a function of z.)

It may be noted that the parameter c_0^2/v_A^2 is related to the plasma beta inside the tube by

$$\frac{c_0^2(z)}{v_A^2(z)} = \tfrac{1}{2}\gamma\beta_0(z) ,$$

where $\beta_0(z) = 2\mu_0 p_0(z)/B_0^2(z)$.

Now the parameter c_0^2/v_A^2 satisfies (from (4.2.1), (4.2.2) and (4.2.10)) the equation

$$\frac{\gamma v_A^2}{c_0^2}\frac{d}{dz}\left(\frac{c_0^2}{\gamma v_A^2}\right) = \frac{-\theta}{\Lambda_0(z)} , \qquad (4.2.13)$$

and so (for $\theta > 0$) $c_0^2/\gamma v_A^2$ increases with depth (-z) in a cool tube in such a way that

$$\frac{c_0^2(z)}{\gamma v_A^2(z)} \sim (p_0(z))^{\theta} . \qquad (4.2.14)$$

In particular, if $\theta = 0$ (so that the temperatures inside and outside the tube are equal), then $\frac{1}{\gamma}c_0^2(z) \sim v_A^2(z)$ and

$$B_0^2(z) \sim p_0(z) , \quad r_0(z) \sim p_0^{-\frac{1}{4}}(z) . \qquad (4.2.15)$$

The relation in (4.2.15) was first given by Parker (1955) in his discussion of magnetic buoyancy and the formation of sunspots.

4.3 Vertical Motions in a Slender Flux Tube

The equations governing motions of a perfectly-conducting, inviscid, ideal gas embedded in a magnetic field have been presented in Chapter 1. In a cylindrical coordinate system (r,θ,z),

in which there is no azimuthal dependence, both the basic state variables and the perturbations are expanded in a Maclaurin series about r=0. The resulting system of linear equations describing perturbations about the basic state (described in Section 4.2) is (See Equations (3.3.25) - (3.3.27))

$$\frac{\partial \hat{v}_z}{\partial t} + \frac{\partial \hat{p}}{\partial z} + \hat{\rho} g = 0 \ , \tag{4.3.1}$$

$$\frac{1}{\rho_0}\frac{\partial \hat{\rho}}{\partial t} - \frac{1}{B_0}\frac{\partial \hat{b}_z}{\partial t} + \frac{\partial \hat{v}_z}{\partial z} + \hat{v}_z\left(\frac{\rho_0'}{\rho_0} - \frac{B_0'}{B_0}\right) = 0 \ , \tag{4.3.2}$$

$$\frac{\partial \hat{p}}{\partial t} + \hat{v}_z p_0' = c_0^2\left(\frac{\partial \hat{\rho}}{\partial t} + \hat{v}_z \rho_0'\right) \ , \tag{4.3.3}$$

where $p_0(z)$, $\rho_0(z)$ and $B_0(z)$ are the values of the equilibrium pressure, density and vertical component of magnetic field evaluated at r=0, and $\hat{p}$, $\hat{\rho}$, $\hat{b}_z$ and $\hat{v}_z$ refer to the perturbations of pressure, density, vertical component of magnetic field and vertical component of velocity as measured on the tube's axis r=0. A dash denotes differentiation with respect to z.

In addition the flux tube is related to its surroundings by the two boundary conditions

$$v_n(r=r_0) = v_n^{(e)}(r=r_0) \ , \tag{4.3.4}$$

and

$$p(r=r_0) + \frac{1}{\mu_0} B_0(r=r_0) b_z(r=r_0) = p^{(e)}(r=r_0) \ , \tag{4.3.5}$$

where v_n and $v_n^{(e)}$ are the perturbation velocities normal to the boundary in the interior and exterior respectively and $p^{(e)}$ is the pressure perturbation in the exterior. If we adopt the solution for which pressure perturbations in the exterior are negligible then the above boundary conditions may be replaced

by the 'reduced boundary condition' (see Chapter 3)

$$\hat{p} + B_0 \frac{\hat{b}_z}{\mu_0} = 0 \ . \qquad (4.3.5)$$

Therefore we are not considering motions driven by the external medium.

Assuming a time-dependence of the form $e^{i\omega t}$, Equations (4.3.1) - (4.3.3) may be combined to give a second order ordinary differential equation for the velocity, valid for a negligible pressure perturbation in the exterior,

$$\frac{d^2\hat{v}}{dz^2} + \left(\frac{c_T^{2\prime}}{c_T^2} - \frac{B_0'}{B_0} - \frac{1}{H_0} \right) \frac{d\hat{v}}{dz} + \left[\frac{\omega^2 - N_0^2}{c_T^2} - \frac{d}{dz}\left(\frac{B_0'}{B_0} + \frac{g}{c_0^2} \right) - \left(\frac{B_0'}{B_0} + \frac{g}{c_0^2} \right) \left(\frac{c_T^{2\prime}}{c_T^2} - \frac{N_0^2}{g} \right) \right] \hat{v} = 0 \ , \qquad (4.3.6)$$

where $c_T^2 = \dfrac{c_0^2 v_A^2}{(c_0^2 + v_A^2)}$. The Brunt-Väisälä frequency, $N_0(z)$, and the density scale-height, $H_0(z)$, are defined by

$$\frac{1}{H_0(z)} = - \frac{\rho_0'(z)}{\rho_0(z)} \ , \qquad N_0^2(z) = \frac{g}{H_0(z)} - \frac{g^2}{c_0^2(z)} \ .$$

Note that in deriving Equation (4.3.6) we have only made use of Equation (4.2.1) in the basic-state. The temperature inside and outside the tube may be unequal. However, for the special case $T_0(z) = T_e(z)$ the equilibrium state is completely characterized by the scale-height $\Lambda_0(z)$:

$$c_0^2(z) = \gamma g \Lambda_0(z), \quad v_A^2(z) = v_A^2(0) \frac{\Lambda_0(z)}{\Lambda_0(0)}, \quad c_T^2(z) = c_T^2(0) \frac{\Lambda_0(z)}{\Lambda_0(0)} \ ,$$

$$\frac{1}{H_0(z)} = \frac{1 + \Lambda_0'(z)}{\Lambda_0(z)} \ , \qquad N_0^2(z) = \frac{g}{\Lambda_0(z)} \left(\frac{\gamma - 1}{\gamma} + \Lambda_0'(z) \right) \ . \qquad (4.3.7)$$

Equation (4.3.6) for $T_0 = T_e$ and γ assumed constant, then reduces to

$$\frac{d^2\hat{v}}{dz^2} - \frac{1}{2\Lambda_0(z)}\frac{d\hat{v}}{dz} + \left(\frac{\omega^2 - N_0^2(z)}{c_T^2(z)} + (1-\frac{\gamma}{2})\frac{N_0^2(z)}{c_0^2(z)}\right)\hat{v} = 0 \,. \qquad (4.3.6)'$$

This is Equation (3.3.57) of Chapter 3.

4.4 Sufficient Conditions for convective stability

In order to discuss the stability of a slender flux tube, it is convenient to write Equation (4.3.6) in the canonical Sturm-Liouville form:

$$\frac{d}{dz}\left(\sigma(z)\frac{d\hat{v}}{dz}\right) + \left[\omega^2 r(z) - q(z)\right]\hat{v} = 0 \,, \qquad (4.4.1)$$

where

$$\sigma(z) = \frac{\rho_0(z)c_T^2(z)}{B_0(z)} \,, \quad r(z) = \frac{\rho_0(z)}{B_0(z)} \,,$$

and

$$q(z) = \frac{\rho_0 c_T^2}{B_0}\left[\frac{N_0^2}{c_T^2} + \frac{d}{dz}\left(\frac{B_0'}{B_0} + \frac{g}{c_0^2}\right) + \left(\frac{B_0'}{B_0} + \frac{g}{c_0^2}\right)\left(\frac{c_T^{2\prime}}{c_T^2} - \frac{N_0^2}{g}\right)\right]$$

Together with boundary conditions of the general type

$$\left.\begin{aligned} a_1\hat{v}(0) + a_2\hat{v}'(0) &= 0 \,, \\ b_1\hat{v}(-d) + b_2\hat{v}'(-d) &= 0 \,, \end{aligned}\right\} \qquad (4.4.2)$$

(for constants a_1, a_2, b_1 and b_2), imposed at levels $z = 0$ and $z = -d$, Equation (4.4.1) constitutes the standard form of the Sturm-Liouville boundary-value problem (see, for general theory, Ince, 1956; and, in the context of a stratified fluid, Yih, 1965). (Particular forms of these boundary conditions will be considered in the next section, with reference to the special case treated there.)

It follows from the general Sturm-Liouville theory that eigenvalues ω^2 are <u>real</u> and, provided d is finite, these eigenvalues form an <u>infinite</u> sequence that may be ordered in increasing magnitude; thus

$$\omega_1^2 < \omega_2^2 < \ldots < \omega_n^2 < \ldots$$

Furthermore, $\omega_n^2 \to \infty$ as $n \to \infty$ (Ince, 1956, ch X).

Thus, under the boundary conditions (4.4.2), with d finite, there are an infinite number of eigenmodes with eigenfrequencies $\omega_i (i = 1, 2, 3, \ldots)$. If $\omega_i^2 > 0$, then the i^{th} mode is <u>stable</u>. If $\omega_i^2 < 0$, then the i^{th} mode is <u>unstable</u>. Thus, in particular, the basic-state is <u>unstable</u> if $\omega_1^2 < 0$ and (since $\omega_1^2 < \omega_i^2$, $i > 1$) this will be the mode of maximum growthrate. Unfortunately, Sturm-Liouville theory does not provide us with a direct calculation of ω_1^2. However, we may elicit further information on ω^2 (in particular the sign of ω^2) by obtaining a first integral of equation (4.4.1).

Multiplying (4.4.1) by $\hat{v}^*$, the complex conjugate of $\hat{v}$, and integrating by parts, it follows that

$$\omega^2 = \frac{\int_{-d}^{0} (q(z)|\hat{v}|^2 + \sigma(z)|\hat{v}'|^2)dz - \left[\sigma(z)\hat{v}^*\hat{v}'\right]_{-d}^{0}}{\int_{-d}^{0} r(z)|\hat{v}|^2 dz} \qquad (4.4.3)$$

It is clear from the form of (4.4.3) that our earlier restriction that d be finite is now no longer necessary. Thus, in the subsequent discussion d may be infinite.

Suppose that the boundary conditions are such that

$$\left[\sigma(z)\hat{v}^*\hat{v}'\right]_{-d}^{0} = 0 \quad ,$$

then Equation (4.4.3) gives

$$\omega^2 = \frac{\int_{-d}^{0}(q(z)|\hat{v}|^2 + \sigma(z)|\hat{v}'|^2)dz}{\int_{-d}^{0} r(z)|\hat{v}|^2 dz} \quad . \tag{4.4.4}$$

The stationary values of this ratio are the eigenvalues of the associated Sturm-Liouville system and finding the extremum of the above ratio is equivalent to finding the extremum of

$$\int_{-d}^{0}(q(z)|\hat{v}|^2 + \sigma(z)|\hat{v}'|^2)dz \quad ,$$

subject to

$$\int_{-d}^{0} r(z)|\hat{v}|^2 dz = K \quad ,$$

where K is a constant.

Suppose, now, that the boundary conditions are such that

$$\left[\sigma(z)\hat{v}^*\hat{v}'\right]_{-d}^{0} \leqslant 0$$

(as are the special cases of (4.4.2) examined in subsequent sections). Then it follows from (4.4.3), on noting that $\sigma(z) > 0$ and $r(z) > 0$, that a sufficient condition for ω^2 to be positive, and thus a sufficient condition for stability, is

$$q(z) > 0 \quad . \qquad \text{for all } z, \quad -d \leqslant z \leqslant 0 \ .$$

Thus, under such boundary conditions, a <u>sufficient condition for stability</u> is

$$\frac{N_0^2}{c_T^2} + \frac{d}{dz}\left(\frac{B_0'}{B_0} + \frac{g}{c_0^2}\right) + \left(\frac{B_0'}{B_0} + \frac{g}{c_0^2}\right)\left(\frac{c_T^{2\prime}}{c_T^2} - \frac{N_0^2}{g}\right) > 0 \quad \text{throughout } -d \leqslant z \leqslant 0 \ . \tag{4.4.5}$$

It is of interest to examine the sufficiency condition (4.4.5), under the assumption that the interior of the flux tube is cooler than its surroundings, and γ constant. In terms of the function $\tau(z)$, introduced in Equation (4.2.8), (4.4.5) may

be written in the form

$$\left[\left(\frac{2-\gamma}{\gamma}\right)\left(1-\tau(z)\right)+\frac{\tau'(z)}{\tau(z)}\left(1+\frac{v_A^2(z)}{c_0^2(z)}\right)\Lambda_0(z)\right]\frac{\tau(z)c_0^2(z)}{(1-\tau(z))(c_0^2(z)+v_A^2(z))} > -\Lambda_0'(z)-\left(\frac{\gamma-1}{\gamma}\right), \tag{4.4.6}$$

to be satisfied throughout $-d \leqslant z \leqslant 0$.

In terms of the parameter θ, introduced in (4.2.9), the sufficient condition for stability, Equation (4.4.6), becomes

$$\frac{\frac{2}{\gamma}-(1-\theta)}{\frac{2}{\gamma}\frac{c_0^2}{v_A^2}+(1-\theta)}\left(\frac{c_0^2}{c_0^2+v_A^2}\right)\theta > -\Lambda_0'(z)-\left(\frac{\gamma-1}{\gamma}\right), \tag{4.4.7}$$

to be satisfied throughout the atmosphere.

There are two special cases of (4.4.7) of immediate interest. In the extreme circumstances where thermal conduction is so efficient as to remove the temperature difference, so that $\tau = \theta = 0$, (4.4.7) reduces to

$$0 > -\Lambda_0' - \left(\frac{\gamma-1}{\gamma}\right).$$

Thus, a sufficient condition for stability in a slender tube, which is in temperature balance with its surroundings (i.e. $\Lambda_0 = \Lambda_e$), is that

$$N_0^2(z) > 0 \qquad \text{throughout } -d \leqslant z \leqslant 0. \tag{4.4.8}$$

This is the usual condition for convective instability in the absence of a magnetic field (Schwarzschild, 1906).

In the special case for which $\theta = 1$, and $\tau(z) = B_0^2(z)/2\mu_0 p_e(z)$, it follows from Equation (4.2.10) that $B_0'(z) \equiv 0$ and $\rho_0 = \rho_e$. Thus, the case $\theta = 1$ corresponds to a uniform (vertical) column of magnetic field; in this case, the equation governing velocity

perturbations is (3.2.48) and so a sufficient condition for stability to convection in a uniform slender flux tube is

$$\frac{B_0^2/\mu_0}{B_0^2/\mu_0 + \gamma p_0(z)} > -\Lambda_0' - \left(\frac{\gamma-1}{\gamma}\right) \quad \text{throughout } -d \leq z \leq 0 .$$

This is in fact the sufficient condition for stability in the presence of a uniform, laterally unbounded, magnetic field, originally derived by Gough and Tayler (1966) using the energy principle of Bernstein et al. (1958). Our analysis shows that the above condition also holds in a slender flux tube, provided the magnetic field is uniform. In fact, we have seen in Chapter 3, that the equation governing the velocity perturbations in a uniform slender flux tube is identical to that governing motions in a laterally unbounded atmosphere where $k_x\Lambda_0 \gg 1$, i.e. where the horizontal wavelength is much less than the vertical scale height. Thus the stability of an unbounded atmosphere, undergoing motions where the condition $k_x\Lambda_0 \gg 1$ holds, may be readily analysed by Sturm-Liouville theory.

Returning to the general sufficiency condition (4.4.7), we sketch in Figure 4.1 the condition (4.4.7), plotting c_0^2/v_A^2 against Λ_0' for various values of θ in the range $0 \leq \theta \leq 1$, and for $\gamma = 1.2$. It is clear from the figure that the cooler the interior of the tube (i.e., the larger the value of θ), the more likely that the sufficient condition for stability is satisfied, for a fixed magnetic field. It may be noted (see Equation (4.2.13) that c_0^2/v_A^2 increases with depth for $\theta > 0$ (cool interior), and so for $\theta = 1$ the sufficient condition is simply

$$\frac{v_A^2(-d)}{c_0^2(-d)+v_A^2(-d)} > -\Lambda_0' - \left(\frac{\gamma-1}{\gamma}\right) ,$$

where d is the depth of the layer.

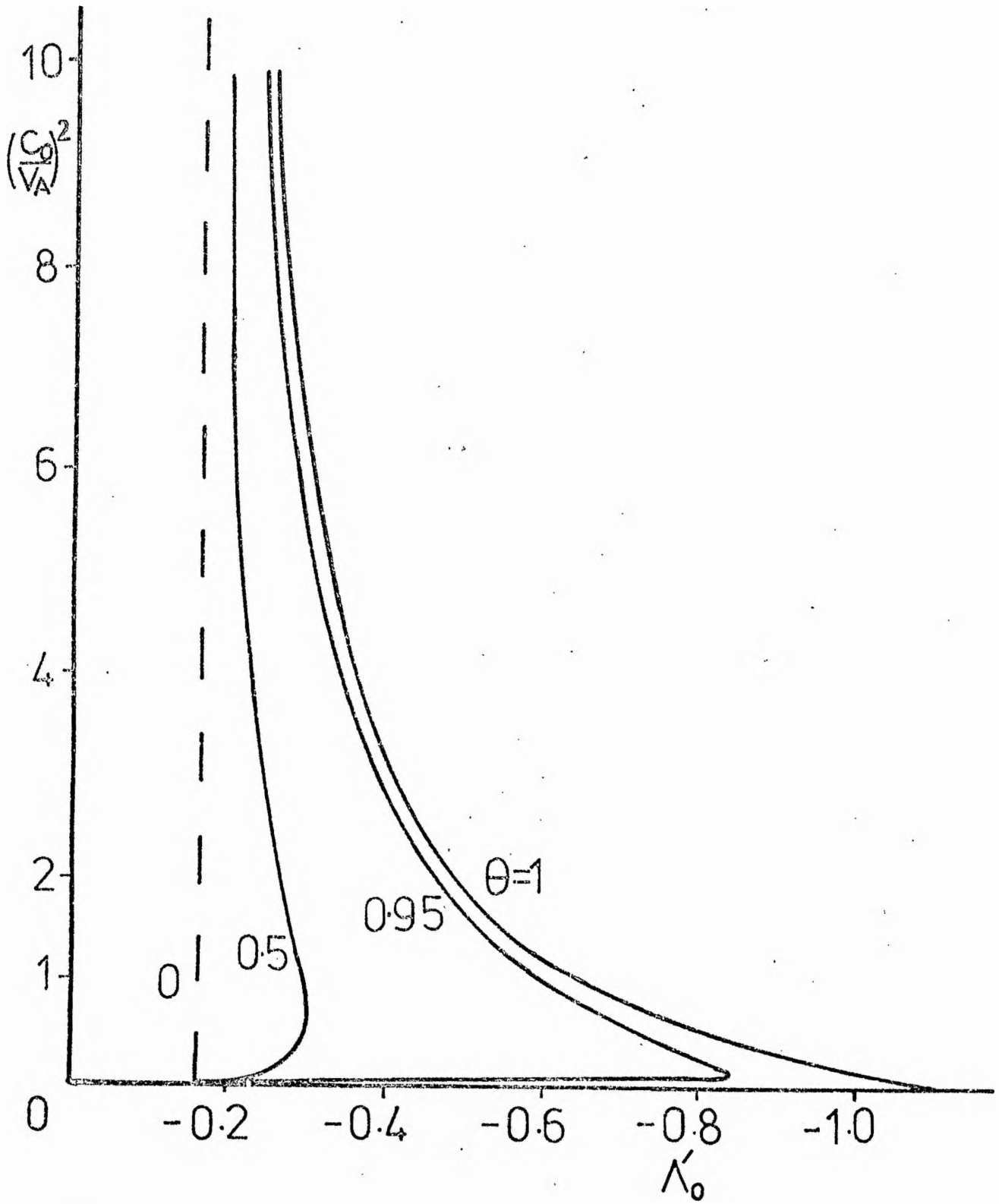

Figure 4.1 - Sufficient condition (Equation (4.4.7)) for stability in a flux tube with a cool interior. Stability is to the left of the curves. The larger the value of the parameter θ, the cooler the interior of the tube.

Finally, returning to (4.4.6), we may note that for the special case $\tau(z) = \tau_0$, a constant, considered in Parker (1976) and Roberts (1976b), the sufficient condition for stability reduces to

$$\left(\frac{2-\gamma}{\gamma}\right)\frac{c_0^2}{c_0^2 + v_A^2}\,\tau_0 \;>\; -\Lambda_0' - \left(\frac{\gamma-1}{\gamma}\right),$$

to be satisfied throughout the atmosphere.

The sufficiency conditions derived above provide useful information as to the prevention of instability in the tube. However, the criteria are clearly of somewhat limited value, simply by being only sufficient conditions: the conditions may be violated at some depth or indeed for all depths, and yet the tube be stable. Thus, in order to obtain a more precise condition for stability, we shall consider, in Section 4.6, the special case of a linear temperature profile inside the flux tube. We shall further assume, for the sake of simplicity, that temperatures inside and outside the tube are equal, so that $\tau = 0$. If the temperatures are different, then the tube is likely (as we have seen from the above sufficiency conditions) to be even more stable than the analysis in Section 4.6 reveals.

4.5 The Local Approximation

Before discussing, in the next Section, an exact solution to the velocity equation (4.3.6)', we shall consider the so-called 'local' approximation. This serves to illustrate many of the features of the more general analysis without the attendant complexity. We suppose that the coefficients of the velocity and its derivatives in Equation (4.3.6)' do not vary greatly with depth and, by way of illustration, we look for solutions

satisfying the simple boundary conditions:

$$\hat{v} = 0 \quad \text{at } z = 0 \; ; \tag{4.5.1}$$

and

$$\hat{v} = 0 \quad \text{at } z = -d \; , \tag{4.5.2a}$$

or

$$\hat{v} \to 0 \quad \text{as } z \to -\infty \tag{4.5.2b}$$

Of course, such a treatment is not directly applicable to the Sun. But the results are indicative of the more general case, and so serve to give a qualitative guide to the expected behaviour in the solar convection zone.

We may write Equation (4.3.6)' in the form

$$\hat{v}'' - \frac{1}{2\Lambda_0}\hat{v}' + \frac{1}{c_T^2}\left(\omega^2 - \Omega^2\right)\hat{v} = 0 \; , \tag{4.5.3}$$

where

$$\Omega^2(z) = N_0^2 \frac{c_T^2}{c_0^2}\left(\frac{\gamma}{2} + \frac{c_0^2}{v_A^2}\right) \; . \tag{4.5.4}$$

Note that Ω^2 has the same sign as N_0^2, and so may be positive or negative.

Assuming a locally constant atmosphere, the general solution of (4.5.3), satisfying the boundary condition (4.5.1), is

$$\hat{v} = A_1\left(e^{\lambda_1 z} - e^{\lambda_2 z}\right) , \tag{4.5.5}$$

where λ_1, λ_2 are the roots of the quadratic

$$\lambda^2 - \frac{1}{2\Lambda_0}\lambda + \left(\frac{\omega^2 - \Omega^2}{c_T^2}\right) = 0 \; , \tag{4.5.6}$$

and A_1 is an arbitrary constant. To discuss (4.5.5) further, it is convenient to consider the cases of finite and infinite depth separately.

Consider first the case of finite depth, for which the solution $\hat{v}$ of (4.5.5) satisfies the lower boundary condition (4.5.2a). This condition implies that

$$(\lambda_2 - \lambda_1)d = 2n\pi i \ , \qquad (4.5.7)$$

for integer n.

Now, since (4.5.5) may be rewritten in the form

$$\hat{v} = A_1 e^{\frac{1}{2}(\lambda_1+\lambda_2)z}\left[e^{\frac{1}{2}(\lambda_1-\lambda_2)z} - e^{-\frac{1}{2}(\lambda_1-\lambda_2)z}\right],$$

and from (4.5.6) we have

$$\lambda_1 + \lambda_2 = \frac{1}{2\Lambda_0} \ ,$$

the solution for the velocity is

$$\hat{v} = A e^{z/4\Lambda_0} \sin\left(\frac{n\pi z}{d}\right) \ ,$$

where A is an arbitrary constant.

Now solving (4.5.6) gives

$$(\lambda_1 - \lambda_2)^2 = 4\left[\frac{1}{16\Lambda_0^2} - \frac{(\omega^2 - \Omega^2)}{c_T^2}\right],$$

which, when combined with (4.5.7), determines the eigenvalues ω^2:

$$\omega^2 = \Omega^2 + \left(\frac{n^2\pi^2}{d^2} + \frac{1}{16\Lambda_0^2}\right)c_T^2 \ . \qquad (4.5.8)$$

Note that if

$$\Omega^2 + \frac{c_T^2}{16\Lambda_0^2} > 0 \ ,$$

i.e. if

$$\frac{\gamma/16}{\gamma/2 + c_0^2/v_A^2} > -\Lambda_0' - \left(\frac{\gamma-1}{\gamma}\right) \ ,$$

then all modes are stable, and we have an infinite sequence of positive eigenvalues ω_n^2.

However, if $-\Omega^2 < c_T^2/16\Lambda_0^2$, then unstable modes are permissible; but as $d \to 0$ Equation (4.5.8) implies that

$$\omega^2 \sim \frac{n^2\pi^2 c_T^2}{d^2} \quad ,$$

and so there exists a critical value d_n^* of the depth d, below which the basic-state is always stable. From(4.5.8), this critical depth d_n^* is given by

$$d_n^{*2} = \frac{-n^2\pi^2}{\frac{\Omega^2}{c_T^2} + \frac{1}{16\Lambda_0^2}} \qquad (4.5.9)$$

Thus, if $d < d_n^*$, there are no unstable modes. Note that the depth d_n^* is a function of n, the minimum value of which occurs for $n = 1$. Then $d_n^* = d_1^* \equiv d^*$, say, where

$$d^{*2} = \frac{-\pi^2}{\frac{\Omega^2}{c_T^2} + \frac{1}{16\Lambda_0^2}} \quad . \qquad (4.5.10)$$

Finally, we should note that there are no modes for which

$$\omega^2 < \Omega^2 + \frac{c_T^2}{16\Lambda_0^2} \quad .$$

For then λ_1 and λ_2 are real, and so cannot satisfy condition (4.5.9), i.e. $\hat{v}$ is non-zero everywhere, except at $z = 0$.

Consider now the case of infinite depth, for which the solutions of the velocity Equation (4.5.3) are subject to the boundary conditions (4.5.1) and (4.5.2b). The solution (4.5.5)

may now be written in the form

$$\hat{v} = A\, e^{z/4\Lambda_0} \sinh\left[\left(\frac{1}{16\Lambda_0^2} + \frac{\Omega^2 - \omega^2}{c_T^2}\right)^{\frac{1}{2}} z\right],$$

satisfying the condition $\hat{v} = 0$ at $z = 0$.

If $\frac{c_T^2}{16\Lambda_0^2} + \Omega^2 - \omega^2 < 0$, then condition (4.5.26) is satisfied for all ω^2, i.e. for $\omega^2 > \Omega^2 + \frac{c_T^2}{16\Lambda_0^2}$ the spectrum of eigenvalues ω^2 is <u>continuous</u> (i.e. no discrete eigenvalues exist).

For $\frac{c_T^2}{16\Lambda_0^2} + \Omega^2 - \omega^2 > 0$, $\hat{v} \to 0$ as $z \to -\infty$ provided $\omega^2 > \Omega^2$.

Therefore, if $\omega^2 > \Omega^2$, we again have a continuous spectrum; while if $\omega^2 < \Omega^2$, then there is no solution satisfying the boundary conditions.

The above illustration shows that for a finite depth, there is an infinite number of positive eigenvalues. There <u>may</u> exist a finite number of unstable modes provided Ω^2 is sufficiently negative; however, if the depth d is sufficiently small, no unstable modes exist. Qualitatively, these results agree with those to be presented in the following Sections. However, we should note that differences do arise for the case of a flux tube of infinite depth, in that, in the 'local' approximation, we find a continuous spectrum for $\omega^2 > \Omega^2$; whereas for the case to be presented in the next section, we find a continuous spectrum for $\omega^2 > 0$ and an infinite number of discrete eigenvalues for $\omega^2 < 0$.

4.6 The Linear Temperature Profile

Here we shall consider the special case of the linear profile

$$\Lambda_0(z) = \Lambda_0(0) + z\Lambda_0'(0) \quad , \tag{4.6.1}$$

for which Λ_0' is a constant. In order that the temperature and density increase monotonically with depth (see Equation (4.3.7)) it is necessary that the scale-height gradient, Λ_0', satisfy

$$-1 < \Lambda_0' < 0 \ .$$

Further, we shall suppose, for simplicity, that $\tau(z) \equiv 0$ (i.e. the temperatures inside and outside the tube are equal) and that γ is a constant. (Note that for $\tau = 0$ the ratio $c_0^2(z)/v_A^2(z)$ is a constant). Thus, as we have seen in Section 4.3, a sufficient condition for stability to convective motions is $N_0^2 > 0$. In particular, the isothermal atmosphere ($\Lambda_0' \equiv 0$) is always stable.

Under these assumptions, the governing equation for the velocity perturbation is Equation (4.3.6)', for which an exact solution is known (Roberts and Webb, 1978).

We use this solution here in order to investigate in detail the nature of motions in a linear temperature profile. To find the eigenvalues ω^2 using this solution we must, of course, specify appropriate boundary conditions on the velocity.

4.6.1 Boundary Conditions

We have considered two alternative forms of the lower boundary condition, namely

$$\hat{v} \to 0 \quad \text{as} \quad z \to -\infty \ ; \tag{4.6.2a}$$

$$\hat{v} = 0 \quad \text{at} \quad z = -d \ . \tag{4.6.2b}$$

Thus, we are requiring that the velocity $\hat{v}$ tend to zero at a depth d, which may be infinite. It is necessary to consider

the two cases separately, as the discussion in Section 4.5 indicates. We shall concentrate on the former condition, leaving the discussion of the case of finite depth to the end of this section.

In addition to the lower boundary condition (4.6.2a), we must specify the flow at (say) $z = 0$. We shall write this boundary condition in the general form

$$a_1 \hat{v}(0) + a_2 \hat{v}'(0) = 0 \ , \qquad (4.6.3)$$

where $a_1 \geqslant 0$ and $a_2 \geqslant 0$. Thus, with $a_1 = 0$ and $a_2 = 1$, we allow for the possibility that the vertical velocity is a maximum (or minimum) at the observed level $z = 0$; with $a_1 = 1$ and $a_2 = 0$, condition (4.4.3) imposes a top on the flux tube at $z = 0$, beyond which no flow penetrates. In fact, our results are not sensitive to the precise form of the constants a_1 and a_2. However, it should be noted that our results <u>are</u> sensitive to the alternative cases of the tube's depth being finite or infinite.

4.6.2 <u>The exact solution of the velocity equation</u>

Consider the case of equal temperatures ($T_0 = T_e$). for which Equation (4.3.6)' is applicable. We shall employ the boundary conditions (4.6.2a) and (4.6.3).

To find the solutions of (4.3.6)' it is convenient to introduce in place of z the new independent variable x, where

$$x = \frac{2\Lambda_0^{\frac{1}{2}}(0)}{c_T(0)} \left| \frac{\omega}{\Lambda_0'} \right| \Lambda_0^{\frac{1}{2}}(z) \ , \quad x > 0 \ . \qquad (4.6.4)$$

Then (4.3.6)' becomes

$$\frac{d^2\hat{v}}{dx^2} - \left(1 + \frac{1}{\Lambda_0'}\right) \frac{1}{x} \frac{d\hat{v}}{dx} + \left(\pm 1 - \frac{\left[s^2 - \left(1 + \frac{1}{2\Lambda_0'}\right)^2\right]}{x^2} \right) \hat{v} = 0 \ , \qquad (4.6.5)$$

where the + sign applies to <u>stable</u> solutions ($\omega^2 > 0$), and the

- sign to unstable solutions ($\omega^2 < 0$). The constant s^2 is defined by

$$s^2 = \frac{4}{\gamma(\Lambda_0')^2}\left(\frac{\gamma-1}{\gamma} + \Lambda_0'\right)\left(\frac{\gamma}{2} + \frac{c_0^2}{v_A^2}\right) + \left(1 + \frac{1}{2\Lambda_0'}\right)^2 . \qquad (4.6.6)$$

Note that s^2 may be positive or negative, but is positive if $N_0^2 > 0$.

In terms of the x variable, the boundary condition (4.6.2a) becomes

$$\hat{v} \to 0 \qquad \text{as} \qquad x \to \infty \; ; \qquad (4.6.2a)'$$

whilst condition (4.6.3) becomes

$$a_1 \hat{v} + \tfrac{1}{2}\Lambda_0' a_2 x \frac{d\hat{v}}{dx} = 0 \quad \text{at } x = x_0 \; , \qquad (4.6.3)'$$

where

$$x_0(\omega) = \frac{2\Lambda_0(0)}{c_T(0)}\left|\frac{\omega}{\Lambda_0'}\right| .$$

It is convenient to discuss the stable and unstable cases of (4.6.5) separately.

4.6.2(1) Stable solutions

Consider the velocity Equation (4.6.4) under the assumption that ω^2 is positive (so that the plus sign applies). The solutions of (4.6.5) are

$$\hat{v} \sim x^{1+1/2\Lambda_0'} J_s(x) \text{ and } x^{1+1/2\Lambda_0'} Y_s(x) \; , \qquad (4.6.7)$$

where J_s and Y_s are Bessel functions of the first and second kind (Abramowitz and Stegun, 1967). Note that s may be real or imaginary.

Now both of these solutions tend to zero as $x \to \infty$, provided $-1 < \Lambda_0' < 0$. Thus, since this condition on Λ_0' is satisfied both solutions (4.6.7) satisfy the lower boundary condition (4.6.2a)'. Furthermore, the upper boundary condition (4.6.3)' can be satisfied for any value of x_0 simply by choosing a suitable linear combination of the two independent solutions (4.6.7)'. Thus, the boundary conditions no longer determine a discrete set of eigenvalues $\omega^2 > 0$ (in contrast to the results found in Section 4.5 for a finite domain, $-d \leq z \leq 0$). Hence, for the infinite domain $z \leq 0$, there exists a continuous spectrum of eigenvalues $\omega^2 > 0$, whether s^2 is positive or negative.

4.6.2(2) Unstable solutions

Suppose, now, that ω^2 is negative, so that the minus sign applies in the velocity Equation (4.6.5). The solutions of (4.6.5) are now

$$\hat{v} \sim x^{1+1/2\Lambda_0'} I_s(x) \quad \text{and} \quad x^{1+1/2\Lambda_0'} K_s(x) \quad , \qquad (4.6.8)$$

where $I_s(x)$ and $K_s(x)$ are modified Bessel functions (of the first and second kind) of order s (which may be real or imaginary).

In order to satisfy the lower boundary condition (4.6.2a) we must reject the solution involving the modified Bessel function of the first kind, since it is unbounded as $x \to \infty$. So consider the second solution $x^{1+1/2\Lambda_0'} K_s(x)$. It is convenient to discuss the two cases $s^2 \geq 0$ and $s^2 < 0$ separately.

(a) $s^2 \geq 0$.

For this case $K_s(x)$ is a real positive, monotonically decreasing function of x. Also, we may show from (4.6.6) that

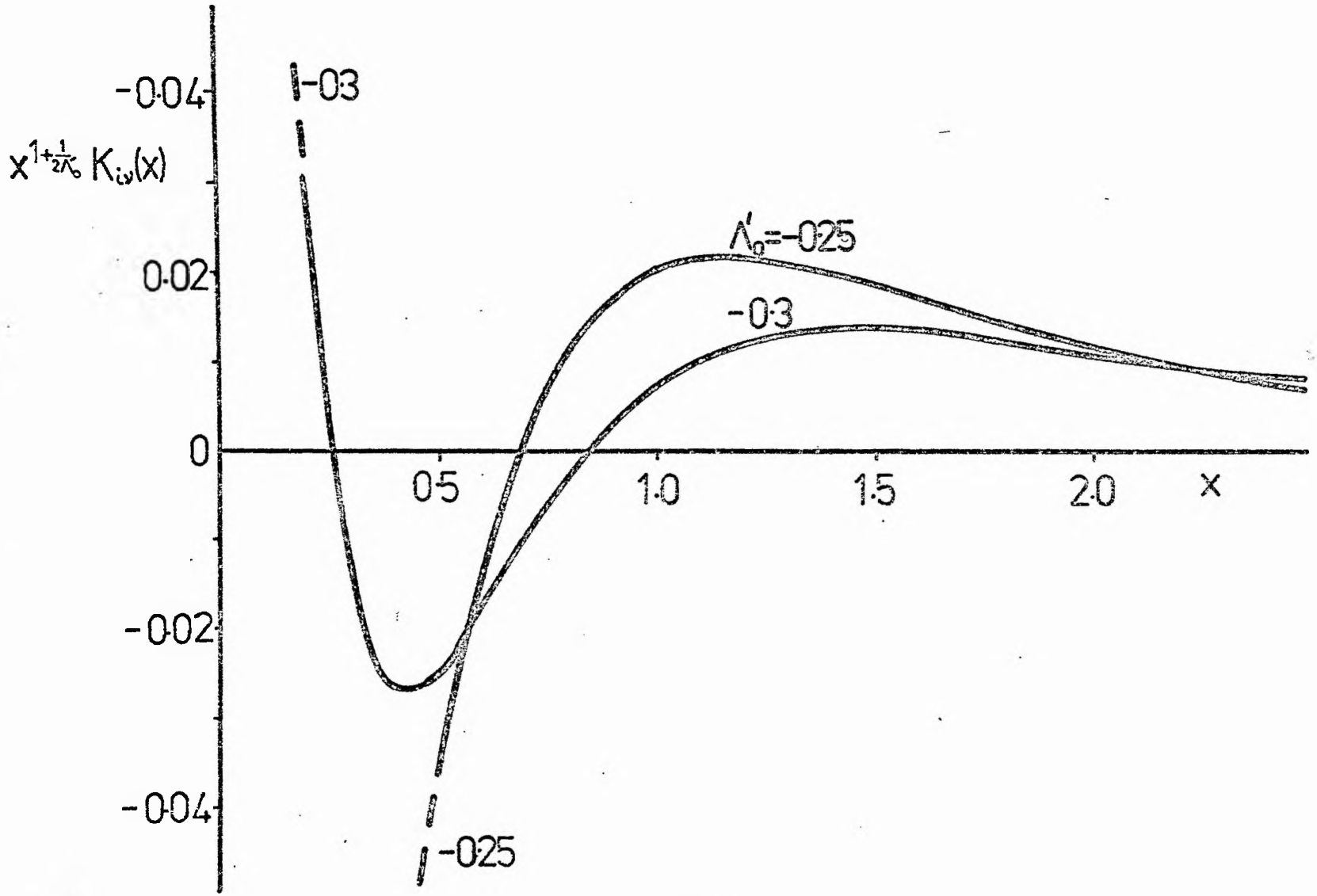

Figure 4.2 - The function $x^{1+1/2\Lambda_0'} K_{i\nu}(x)$ for $\gamma = 1.2$, $c_0 = v_A$ and two values of Λ_0'. For $0 > \Lambda_0' > \frac{1}{2}$ ($\Lambda_0' < -\frac{1}{2}$) the function oscillates infinitely with increasing (decreasing) amplitude as $x \to 0$.

(for $s^2 \geq 0$) we have

$$0 > \Lambda_0' > -\frac{3}{2} + \left(\frac{2}{\gamma}\right)^{\frac{1}{2}} .$$

Therefore, for γ in the range $1 < \gamma \leq 5/3$, $1+1/2\Lambda_0' < 0$ and $x^{1+1/2\Lambda_0'} K_s(x)$ is monotonically decreasing; so the boundary condition (4.6.3)' is not satisfied for any value of $\omega^2 < 0$, i.e. no unstable solutions exist for $s^2 \geq 0$. Hence, subject to the boundary conditions (4.6.2a)' and (4.6.3)', the fluid is stable if $s^2 \geq 0$. Note that this is consistent with the sufficiency condition for stability obtained in Section 4.4.

(b) $s^2 < 0$.

Writing $s^2 = -\nu^2$, where ν is real and positive, the solution for the velocity is

$$\hat{v} \sim x^{1+1/2\Lambda_0'} K_{i\nu}(x) . \qquad (4.6.9)$$

The velocity $\hat{v}$ as a function of x is sketched for various Λ_0' in Figure 4.2. For purposes of illustration, we have taken $c_0 = v_A$ and $\gamma = 1.2$.

It may be noted that $\hat{v}$ may be expressed in terms of the Whittaker function $W_{0,i\nu}$ by observing that

$$K_{i\nu}(x) = \left(\frac{\pi}{2x}\right)^{\frac{1}{2}} W_{0,i\nu}(2x) . \qquad (4.6.10)$$

(Gradshteyn and Ryzhik, (1965), p 1063).

Now the zeros of the Whittaker function $W_{\ell,m}(x)$ have been investigated by Dyson (1960), in relation to the stability of an idealized atmosphere with constant shear flow and exponentially decreasing density (see also Case, 1960). Dyson found that for ℓ real and m purely imaginary there are no complex zeros, and

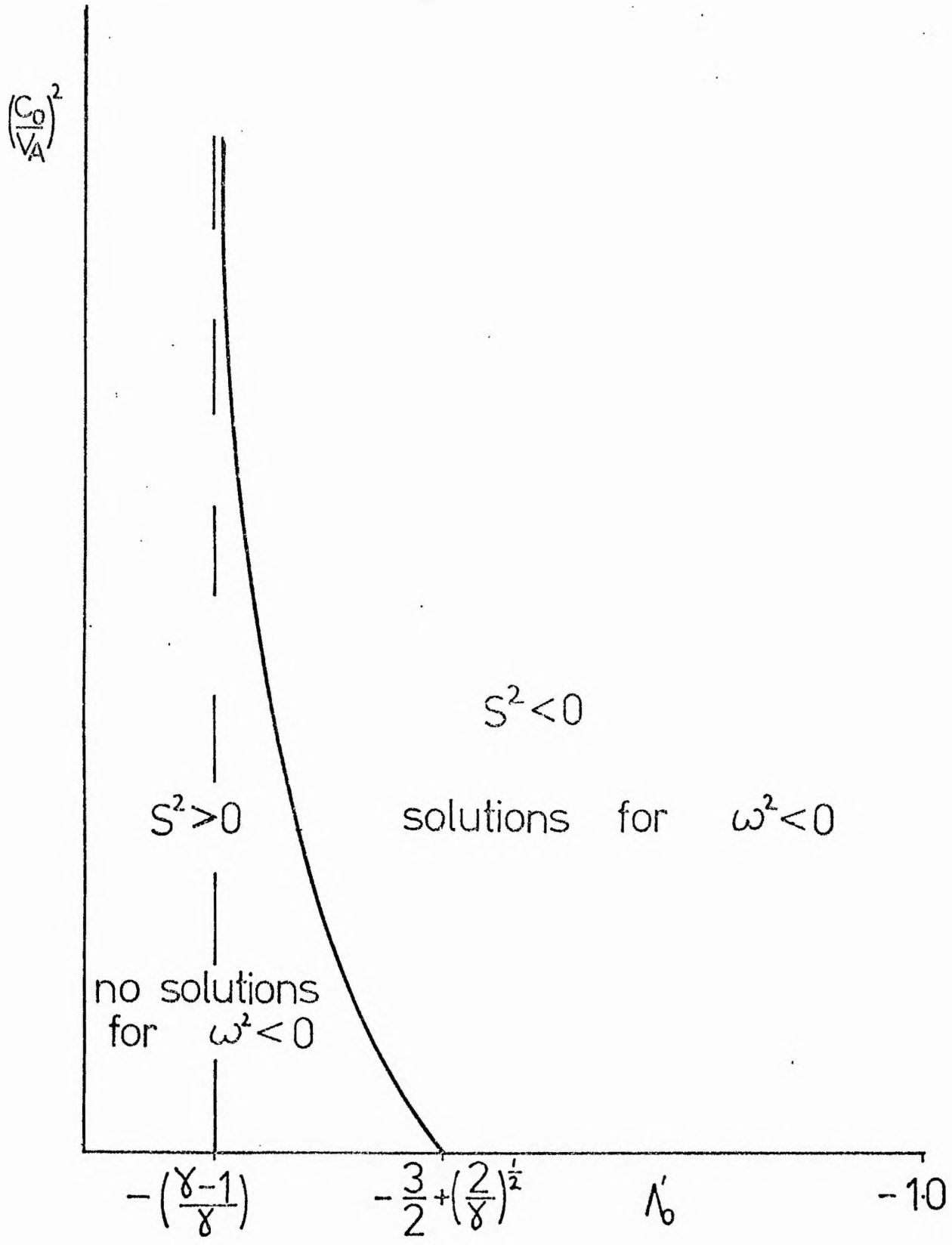

Figure 4.3 - The line $s^2 = 0$ (see Equation (4.6.6)), shown schematically in the (c_0^2/v_A^2) - Λ_0' plane, dividing the region with unstable modes ($s^2 < 0$) from that with only stable modes ($s^2 > 0$). The dashed line, $N_0^2 = 0$, is the asymptote for $s^2 = 0$ as $c_0^2/v_A^2 \to \infty$.

that there are an infinite number of simple zeros, on the positive real axis, which are bounded and have a point of accumulation at $x = 0$. In our problem, $\ell \equiv 0$, and $m = i\nu$ is purely imaginary.

Therefore, with boundary condition (4.6.2a) and (4.6.3), there are an infinite number of (negative) eigenvalues ω_i^2, with the property that

$$\omega_1^2 < \omega_2^2 < \ldots < \omega_n^2 < \ldots < 0; \qquad (4.6.11)$$

furthermore,

$$\omega_n^2 \to 0 \qquad \text{as} \qquad n \to \infty ,$$

and ω_1^2 is finite.

Thus there are unstable ($\omega^2 < 0$) solutions, satisfying the boundary conditions (4.6.2a)' and (4.6.3)', if and only if $s^2 < 0$, i.e. if and only if

$$\frac{4}{\gamma(\Lambda_0')^2}\left(\frac{\gamma-1}{\gamma} + \Lambda_0'\right)\left(\frac{\gamma}{2} + \frac{c_0^2}{v_A^2}\right) + \left(1 + \frac{1}{2\Lambda_0'}\right)^2 < 0 .$$

Hence, a <u>necessary and sufficient condition</u> for the <u>tube</u> to be (convectively) <u>stable</u> is

$$\frac{4}{\gamma(\Lambda_0')^2}\left(\frac{\gamma-1}{\gamma} + \Lambda_0'\right)\left(\frac{1}{2}\gamma + \frac{c_0^2}{v_A^2}\right) + \left(1 + \frac{1}{2\Lambda_0'}\right)^2 > 0 . \qquad (4.6.12)$$

The line $s^2 = 0$ is sketched in Figure 4.3 as a function of the parameters c_0^2/v_A^2 and Λ_0'. From (4.6.12) we see that a <u>sufficient</u> condition for $s^2 > 0$, and hence a sufficient condition for stability, is $N_0^2 > 0$, in agreement with the results obtained earlier (Equation (4.5.10)).

For $-\frac{3}{2}+(\frac{2}{\gamma})^{\frac{1}{2}} > \Lambda_0' > -1$, unstable solutions exist for all values of c_0^2/v_A^2. Note that $c_0^2/v_A^2 \to 0$ does not imply $B_0 \to \infty$ if $p_e(z)$ is fixed, because the magnetic pressure in the tube cannot exceed the confining external pressure. Thus, the limit $c_0^2/v_A^2 \to 0$ is achieved by allowing (see (4.2.3)) $B_0(z) \to (2\, p_e(z))^{\frac{1}{2}}$, for which $p_0(z)$ and $\rho_0(z)$ both tend to zero (and thus the tube is evacuated by the magnetic field).

For $-(\frac{\gamma-1}{\gamma}) > \Lambda_0' > -\frac{3}{2}+(\frac{2}{\gamma})^{\frac{1}{2}}$, there is a critical value of c_0^2/v_A^2, given by

$$\left(\frac{c_0^2}{v_A^2}\right)_{crit} = \frac{-\gamma}{4(\Lambda_0'+\frac{\gamma-1}{\gamma})}\,(\Lambda_0'+\tfrac{3}{2}+(\tfrac{2}{\gamma})^{\frac{1}{2}})(\Lambda_0'+\tfrac{3}{2}-(\tfrac{2}{\gamma})^{\frac{1}{2}}), \quad (4.6.13)$$

below which the solution is <u>stable</u>. So, provided the field is sufficiently strong, the gas in the flux tube is stable to convection.

Also, it may be noted from Figure 4.3, that the effect of increasing the ratio of specific heats, γ, is that the line $s^2 = 0$ is moved to the right, giving a greater region for stability. Thus, for certain values of c_0^2/v_A^2 and Λ_0', increasing γ may stabilise the perturbation.

Consider now the fastest growing eigenvalue ω_1^2, the existence of which for $s^2 < 0$ is guaranteed by (4.6.11). The values of ω_1^2 have been determined numerically for a range of values of the parameters c_0^2/v_A^2 and Λ_0'. For convenience, it was found simpler to use the form (4.6.9) for the velocity, and to solve numerically Bessel's equation for $K_{i\nu}(x)$, matching the numerical solution to the known asymptotic forms as $x \to 0$ and $x \to \infty$.

Figure 4.4 shows a plot of ω_1^2 (suitably non-dimensionlised) against c_0^2/v_A^2 for various Λ_0'. For the sake of illustration, we have taken the upper boundary condition as $\hat{v}' = 0$ at $z = 0$. (The results are similar for the general boundary condition (4.6.3).)

Now, as $c_0^2/v_A^2 \to \infty$, $\nu \to \infty$; and we may show (by considering the asymptotic form of $K_{i\nu}(x)$ as $\nu \to \infty$) that

$$\omega_1^2 \to N_0^2(0) \quad \text{as} \quad \frac{c_0^2}{v_A^2} \to \infty$$

Thus the behaviour of ω_1^2 at large c_0^2/v_A^2 indicated in Figure 4.4.

For $\Lambda_0' < -\frac{3}{2} + (\frac{2}{\gamma})^{\frac{1}{2}}$, the mode is unstable for all values of c_0^2/v_A^2, and

$$\omega_1^2 \to \frac{\gamma g \Lambda_0'^2}{4\Lambda_0(0)} x_{max}^2 \quad \text{as} \quad \frac{c_0^2}{v_A^2} \to 0 ,$$

where x_{max} is the largest value of x, for which the boundary condition (4.6.3)' is satisfied, with

$$\nu^2 = -\frac{1}{\Lambda_0'^2}(\Lambda_0' + \frac{3}{2} - (\frac{2}{\gamma})^{\frac{1}{2}})(\Lambda_0' + \frac{3}{2} + (\frac{2}{\gamma})^{\frac{1}{2}}).$$

For

$$-(\frac{\gamma-1}{\gamma}) > \Lambda_0' > -\frac{3}{2} + (\frac{2}{\gamma})^{\frac{1}{2}} ,$$

there is no unstable solution for $(c_0^2/v_A^2) < (c_0^2/v_A^2)_{crit}$, where $(c_0^2/v_A^2)_{crit}$ is given by (4.6.3). Figure 4.4 also shows that ω_1^2 is a monotonically increasing function of c_0^2/v_A^2; thus, the weaker the magnetic field, the faster the growthrate of the instability.

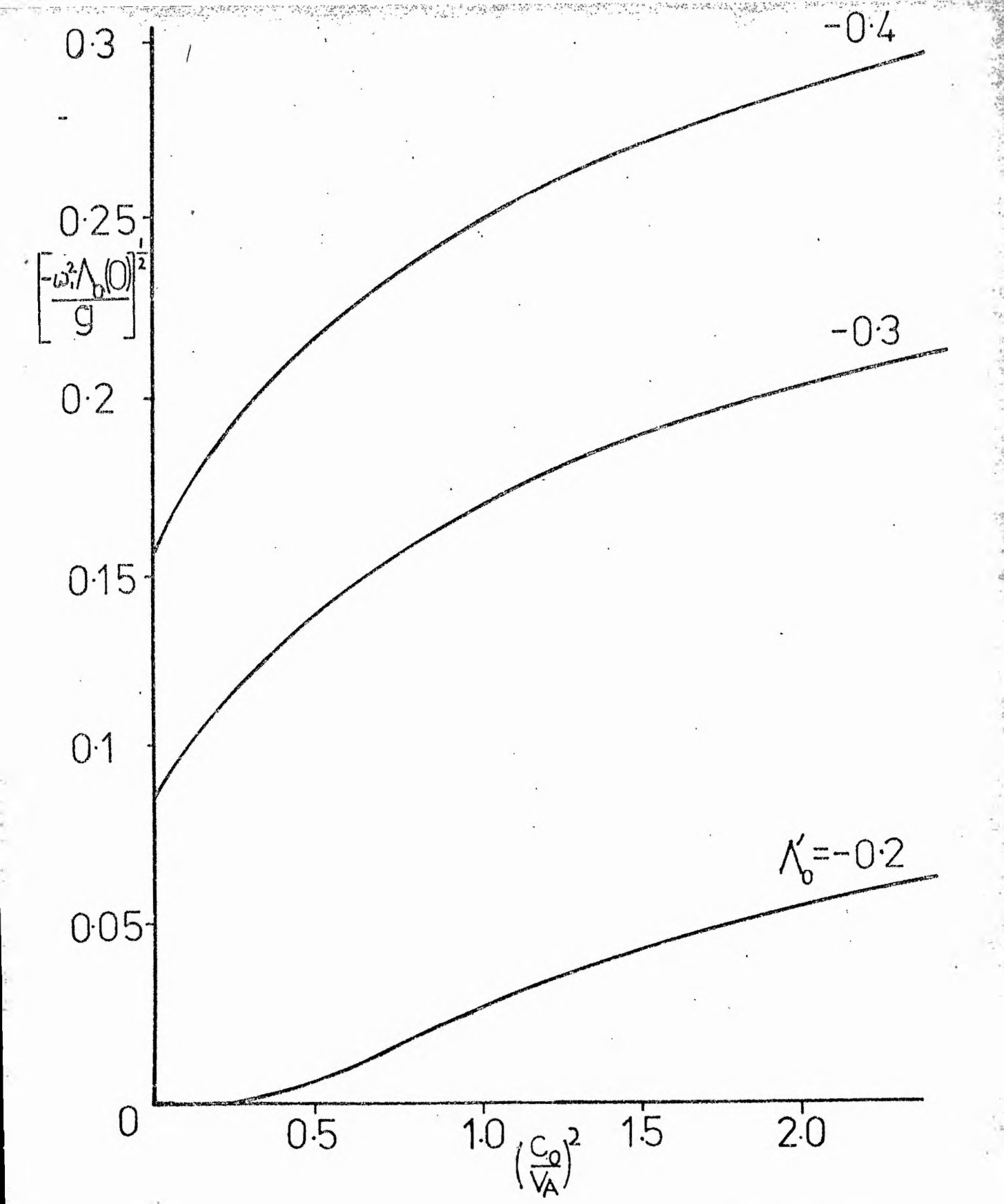

Figure 4.4 - The non-dimensional growthrate, $(-\omega_1^2\Lambda_0(0)/g)^{\frac{1}{2}}$, of the fastest-growing mode as a function of c_0^2/v_A^2 for several values of Λ_0'. We have taken $\gamma = 1.2$ and the upper boundary condition as $\hat{v}' = 0$ at $z = 0$.

In Figure 4.5 we have plotted ω_1^2 against Λ_0' for various values of c_0^2/v_A^2. We see that there is no solution for any value of c_0^2/v_A^2 if $0 > \Lambda_0' > -(\frac{\gamma-1}{\gamma})$, i.e. if $N_0^2 > 0$; and that for a given c_0^2/v_A^2, there is a minimum value of Λ_0', given by

$$\Lambda_{0_{crit}}' = -\left(\frac{3}{2} + \frac{2}{\gamma}\frac{c_0^2}{v_A^2}\right) + \frac{2}{\gamma}\left[\left(1 + \frac{c_0^2}{v_A^2}\right)\left(\frac{\gamma}{2} + \frac{c_0^2}{v_A^2}\right)\right]^{\frac{1}{2}}, \qquad (4.6.14)$$

for which the solution is stable if $0 > \Lambda_0' > \Lambda_{0_{crit}}'$.

We also find that, for given c_0^2/v_A^2 and Λ_0', the growth-rate of the fastest-growing mode is a decreasing function of γ.

4.6.3 Temperature and Pressure Perturbations

It is of interest to calculate the perturbations of the temperature and pressure as a function of the velocity perturbation $\hat{v}$, in order to determine whether cooling and field intensification result if the instability sets in as a downflow.

The pressure perturbation $\hat{p}$ and the temperature perturbation $\hat{\Lambda}$ (or, more precisely, the perturbation to the scale height Λ) may be expressed in terms of the velocity perturbation as

$$\hat{p} = \frac{1}{i\omega(1+c_0^2/v_A^2)}\left[(1 - \frac{\gamma}{2})\rho_0(z)g\hat{v}(z) - \rho_0(z)c_0^2(z)\frac{d\hat{v}}{dz}(z)\right], \qquad (4.6.15)$$

and

$$\hat{\Lambda} = \frac{-1}{i\omega\left(1+\frac{c_0^2}{v_A^2}\right)}\left[\left(\frac{\gamma}{2}+\frac{c_0^2}{v_A^2}\right)\left(\frac{\gamma-1}{\gamma}+\Lambda_0'\right)+\Lambda_0'\left(1 - \frac{\gamma}{2}\right)\right]\hat{v}(z) - \frac{(\gamma-1)\Lambda_0}{i\omega\left(1+\frac{c_0^2}{v_A^2}\right)}\frac{d\hat{v}(z)}{dz}. \qquad (4.6.16)$$

For boundary conditions of the form (4.6.3), then both the pressure perturbation $\hat{p}$ and the temperature perturbation $\hat{\Lambda}$ are negative near

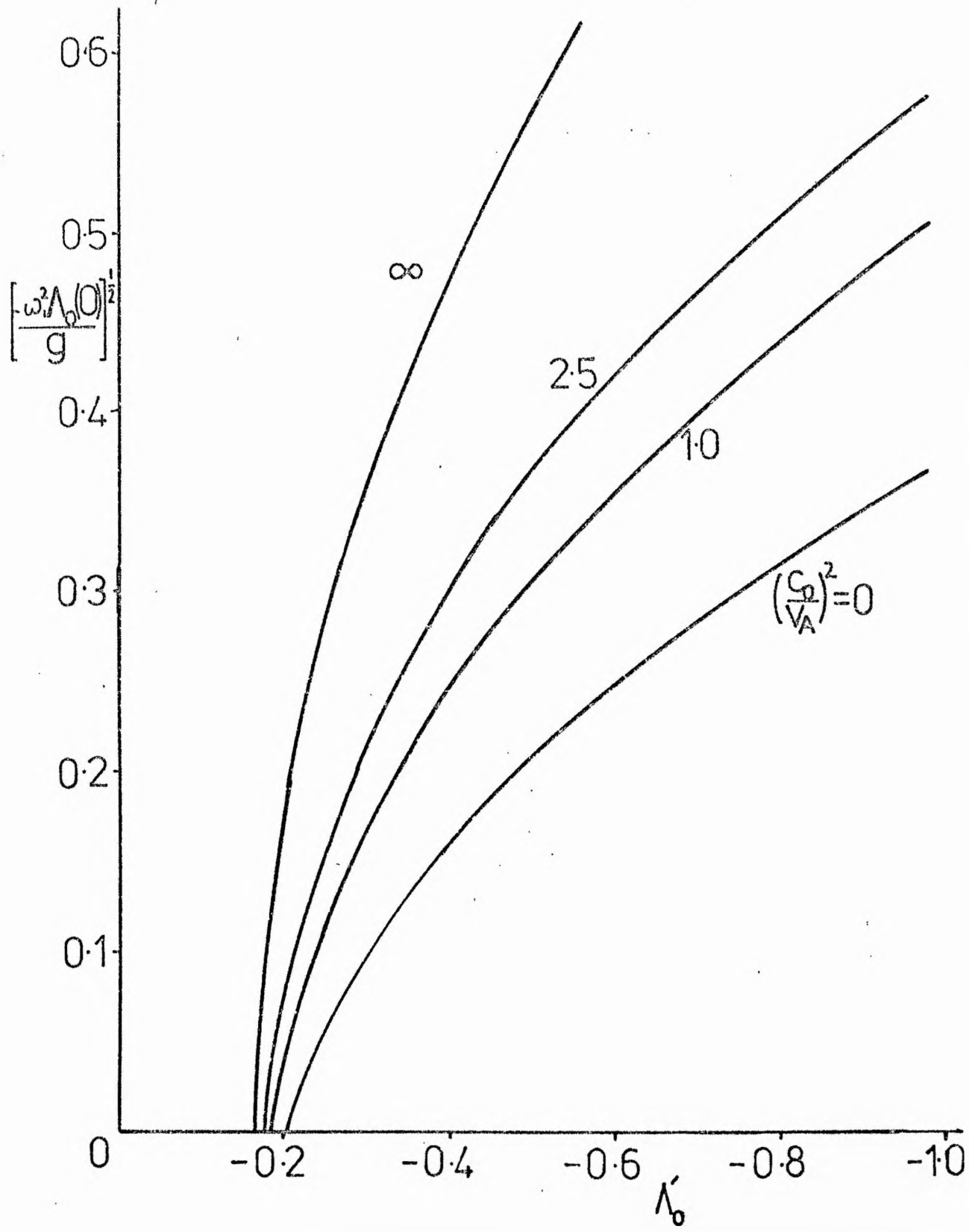

Figure 4.5 - The non-dimensional growthrate, $(-\omega_1^2 \Lambda_0(0)/g)^{\frac{1}{2}}$, of the fastest growing mode as a function of Λ_0', for various c_0^2/v_A^2. Again, for purposes of illustration, we have taken $\gamma = 1.2$ and the upper boundary condition as $\hat{v}' =$ at $z = 0$.

the surface for the instability setting in as a downflow. Equation (4.3.5)' then implies $\hat{b}_z$ is positive. Thus, a natural consequence of a downflow is a cooling of the gas within the tube and an increase in the field strength.

Writing $\hat{v}(z) = V x^{1+1/2\Lambda_0'} K_{i\nu}(x)$, we define the non-dimensional temperature and pressure perturbations $\overline{T}$ and $\overline{p}$ as

$$\overline{T} \equiv \frac{\hat{\Lambda}}{\Lambda_0(0)} \frac{i\omega\Lambda_0(0)}{V}, \qquad (4.6.17)$$

$$\overline{p} \equiv \frac{\hat{p}}{p_0(0)} \frac{i\omega\Lambda_0(0)}{V}. \qquad (4.6.18)$$

The variables $\hat{v}/V$, $\overline{p}$ and $\overline{T}$ are sketched in Figure 4.6 as a function of depth z. We have taken $\Lambda_0' = -0.25$, $\gamma = 1.2$ and $c_0 = v_A$, and we have adopted the boundary conditions $\hat{v}' = 0$ at $z = 0$ and $\hat{v} \to 0$ as $z \to -\infty$. We see that a downflow will lead to an increase of field up to a depth of $11.6\Lambda_0(0)$, below which the field will decrease. The temperature reduction takes place over a depth of $190\Lambda_0(0)$.

4.6.4 Finite depth

Finally, in this subsection, we consider the effect of applying the lower boundary condition (4.6.2b), so that the tube has a finite depth d.

The first important (though perhaps not surprising) point to emerge is that there no longer exists a continuous spectrum for $\omega^2 > 0$. This is because the velocity Equation (4.3.6)', together with the boundary conditions (4.6.2b) and (4.6.3), form a regular (Ince, 1956, ch. X) Sturm-Liouville system (see also Section 4.4), which, from the general theory, has discrete eigenvalues only.

Figure 4.6 - The non-dimensional velocity $\hat{v}/V$, pressure, $\bar{p}$, and temperature, $\bar{T}$, perturbations as functions of depth z. We have taken $\Lambda_0' = 0.25$, $\gamma = 1.2$ and $c_0 = v_A$ and applied the boundary conditions $\hat{v}' = 0$ at $z = 0$ and $\hat{v} \to 0$ as $z \to -\infty$. The velocity is normalized to unity at the origin.

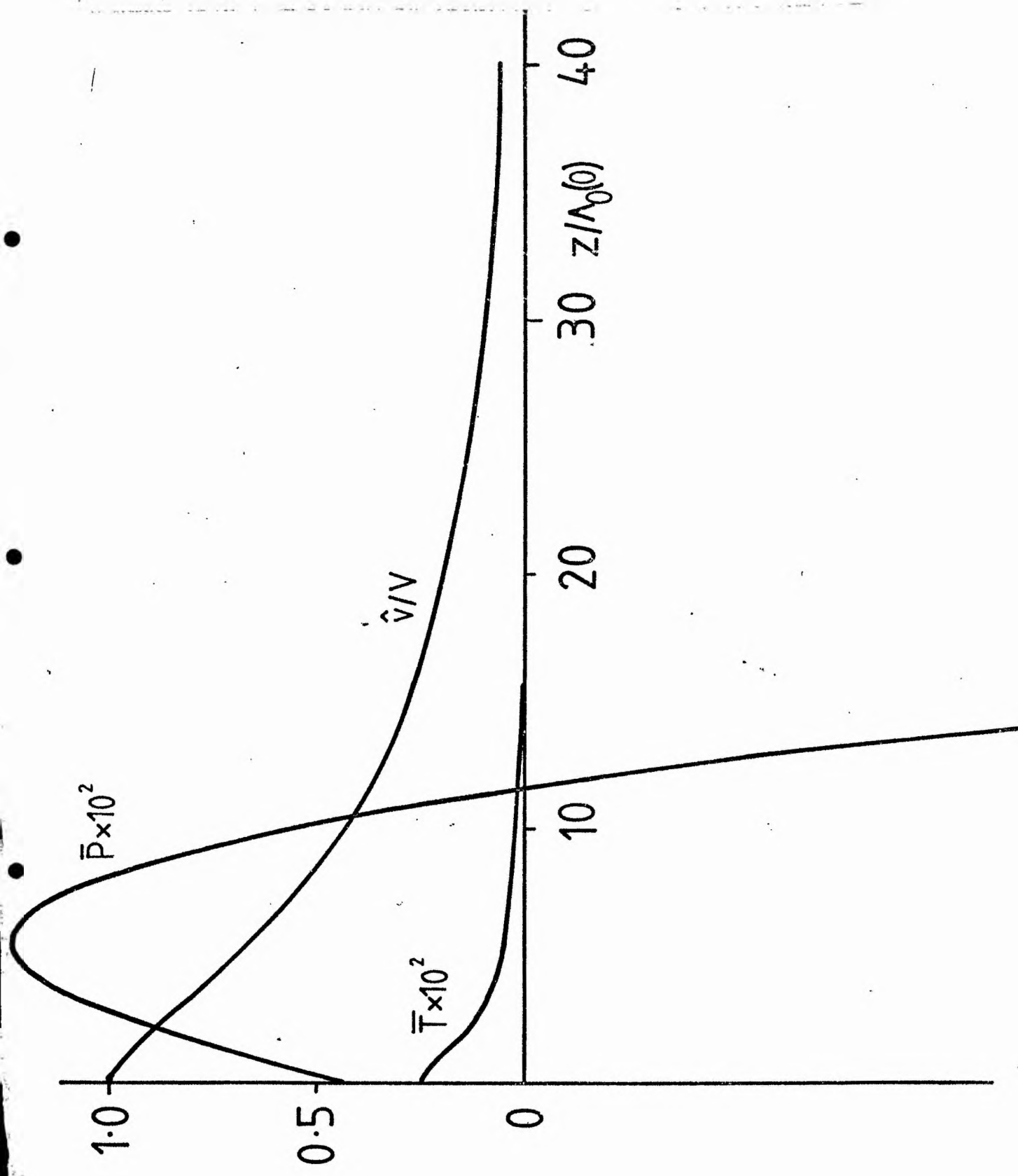

Again, for a given depth, we have a necessary and sufficient condition for the existence of unstable solutions. We find unstable solutions exist if and only if

$$e^{2\phi/\nu} < \frac{\Lambda_0(-d)}{\Lambda_0(0)} , \qquad (4.6.19)$$

where $\nu = \sqrt{(-s^2)}$, and ϕ depends on the coefficients a_1 and a_2 occurring in the boundary conditions (4.6.3). In general ϕ satisfies

$$\pi \geqslant \phi \geqslant \tan^{-1}\left(\frac{\nu}{1 + 1/2\Lambda_0'}\right)$$

For the special case $a_1 = 0$ (for which the upper boundary condition is $\hat{v}'(0) = 0$), we find that $\phi = \tan^{-1}\left(\frac{\nu}{1+1/2\Lambda_0'}\right)$; whilst for $a_2 = 0$ (for which $\hat{v}(0) = 0$), $\phi = \pi$.

The condition (4.6.19) is sketched for various $d/\Lambda_0(0)$ in Figure 4.7. In the region to the left of each curve, all the eigenvalues are positive; in the region to the right, there is at least one negative eigenvalue. Thus, for values of c_0^2/v_A^2 and Λ_0' lying to the right of the curve, there is an unstable mode of maximum growthrate.

Alternatively, from Figure 4.7, we see that for given c_0^2/v_A^2 and Λ_0' there exists a minimum depth d^*, such that for $d < d^*$, the perturbation is always stable. The critical value of d^* is determined (from (4.6.14) by

$$\Lambda_0(d^*) = \Lambda_0(0)\, e^{2\phi/\nu} \qquad (4.6.20)$$

The dependence of d^* on Λ_0' is sketched in Figure 4.8 for various values of the parameter c_0^2/v_A^2.

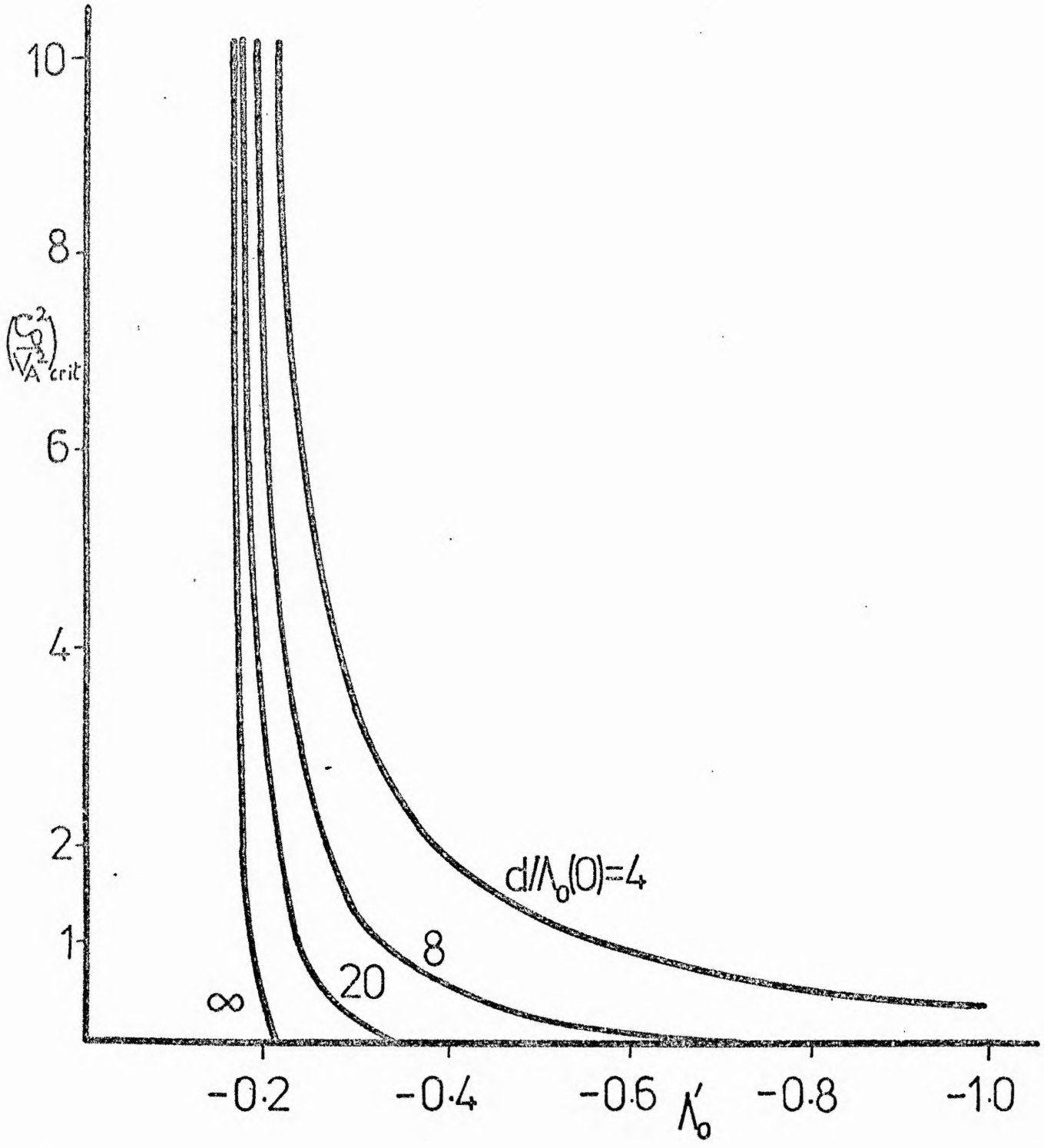

Figure 4.7 - Necessary and sufficient condition for instability in a tube of finite depth, d, sketched for various values of $d/\Lambda_0(0)$. For a given depth, to the left of the curve only stable modes exist and to the right there is at least one unstable mode. The upper boundary condition has been taken as $\hat{v}' = 0$ at $z = 0$, and $\gamma = 1.2$.

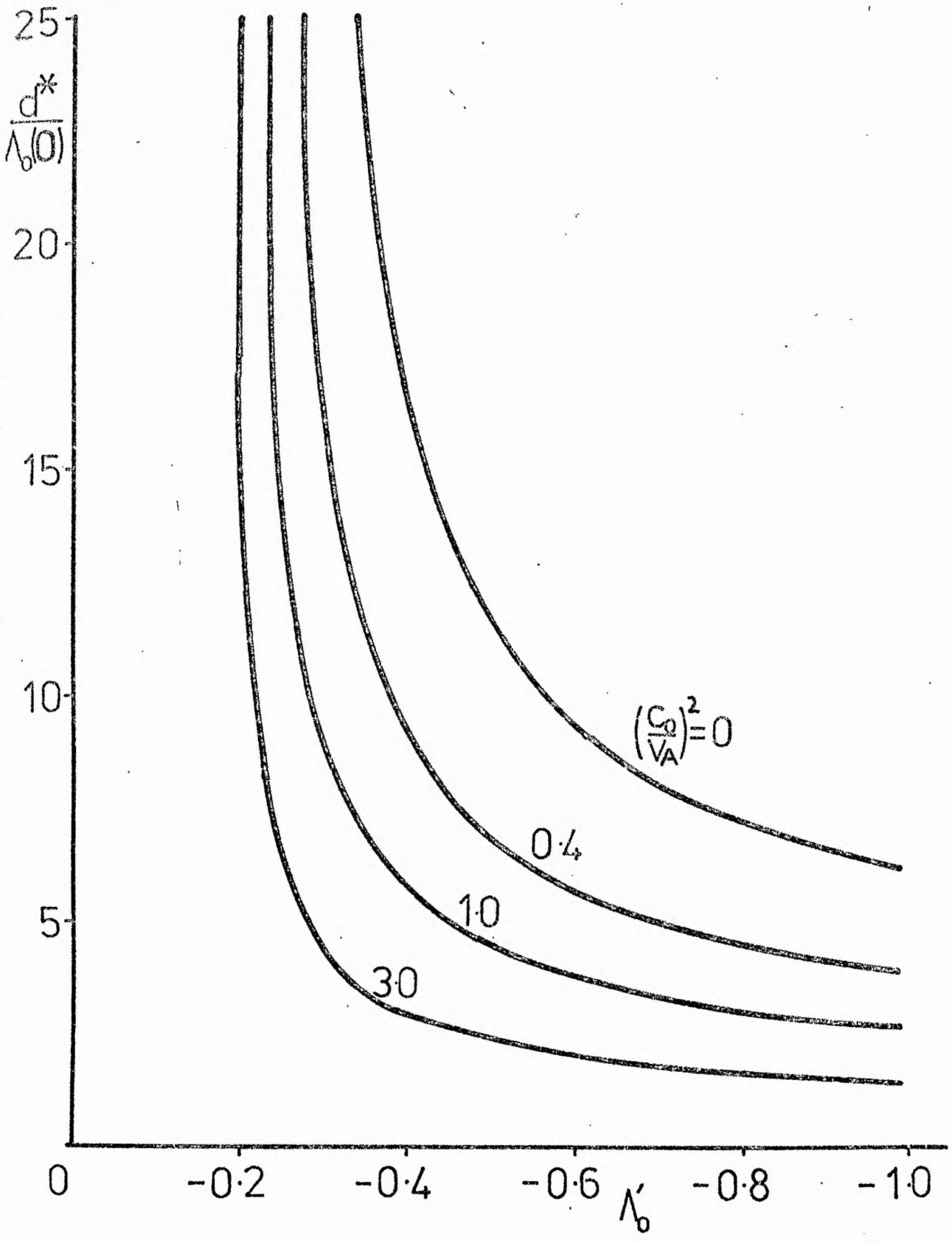

Figure 4.8 - The critical depth for stability as a function of Λ_b' for vario
c_0^2/v_A^2.

The application of these results to the solar atmosphere is considered in the following section.

4.7 Intense Flux Tubes in the Sun

Before considering the application of the above analysis to the Sun, it is perhaps convenient to summarise the main results we have so far obtained. The discussion falls into two parts: (a) conditions for stability in an arbitrary temperature gradient; and (b) instability in a uniform temperature gradient.

For an arbitrary temperature profile (case (a)), we have shown that a sufficient condition for stability to convection is

$$\left[\left(\frac{2-\gamma}{\gamma}\right)\left(1-\tau(z)\right)+\frac{\tau'(z)}{\tau(z)}\left(1+\frac{v_A^2(z)}{c_0^2(z)}\right)\Lambda_0(z)\right]\frac{\tau(z)c_0^2(z)}{(1-\tau(z))(c_0^2(z)+v_A^2(z))} > -\Lambda_0'(z)-\left(\frac{\gamma-1}{\gamma}\right),$$

to be satisfied throughout the depth of the tube (see Equation (4.4.6)). If the internal and external temperatures are equal, so that $\tau = 0$, then the above sufficiency condition is simply

$$N_0^2(z) > 0 , \qquad (4.4.8)$$

to be satisfied throughout the depth of the tube.

For a linear temperature profile (case (b)), with internal and external temperatures equal, condition (4.4.8), of course, guarantees stability to convection.

In a tube of infinite depth, with a linear temperature profile, a necessary and sufficient condition for convective stability is that $s^2 > 0$, i.e.

$$\frac{4}{\gamma\Lambda_0'^2}\left(\frac{\gamma-1}{\gamma}+\Lambda_0'\right)\left(\frac{\gamma}{2}+\frac{c_0^2}{v_A^2}\right)+\left(1+\frac{1}{2\Lambda_0'}\right)^2 > 0.$$

(see (4.6.12).) The stable ($\omega^2 > 0$) modes in a tube of infinite depth form a continuous spectrum; the unstable ($\omega^2 < 0$) modes, which occur if $s^2 < 0$, are discrete and infinite in number (with a point of accumulation at $\omega^2 = 0$).

In a tube of finite depth d, with a linear temperature profile, a necessary and sufficient condition for stability to convection is

$$e^{2\phi/\gamma} > \Lambda_0(-d)/\Lambda_0(0).$$

(See Equation (4.6.19).) Thus, there exists a minimum depth d^* below which (i.e. for a tube of depth d less than d^*) only stable modes exist. The critical depth d^* is given by Equation (4.6.20), and is sketched in Figure 4.8. The stable ($\omega^2 > 0$) modes, in a tube of finite depth, are discrete and infinite in number; there is no continuous spectrum. If $d > d^*$, then there exists at least one unstable ($\omega^2 < 0$) mode; again, there is no continuous spectrum of eigenvalues.

Consider now the application of these results to the solar atmosphere. In applying our analysis to the Sun, we are, of course, supposing that the basic (static) state of a flux tube is as that described in Section 4.2, and that any motions in the tube are adequately described by the linear analysis of Section 4.3. We shall also assume that the flux tube is in temperature balance with its surroundings. Further, we shall approximate the convection zone by a linear temperature profile (or, more precisely, a linear profile for the scale height $\Lambda_e(z)$), and take a mean value of the ratio of specific heats, γ. We use Spruit's model of the Solar convection zone (Spruit, 1974), and take z = 0 to correspond to optical depth $\tau_{5000} = 1$ (in the

surrounding photosphere). In fact, Spruit's model gives $-\Lambda_0'$ sharply peaked at about 40 km below $\tau_{5000} = 1$. Also γ varies rapidly over the first 100 km or so below $\tau_{5000} = 1$, (Spruit, 1977a). However, below a depth of about 100 km, and down to about 4000 km Λ_0' and γ are effectively constant. Thus, our assumption of a linear temperature profile is a reasonable one over this range.

The precise choice of values for Λ_0' and γ in our model is uncertain. However, if we take $\gamma = 1.15$ and Λ_0' in the range $-0.2 \gtrsim \Lambda_0' \gtrsim -0.3$, then the perturbation is unstable in a medium of infinite depth, for all values of c_0^2/v_A^2. Now the ratio of the sound speed to the Alfven speed is determined by its value at $z = 0$ (i.e. at observed levels), where it is roughly unity. Thus taking $c_0^2/v_A^2 = 1$, and the above values of Λ_0' and γ, we find that a tube of infinite depth is unstable. However, a tube of finite depth is stable provided its depth does not exceed about $1\text{-}2 \times 10^3$ km.

If, on the other hand, we choose to apply our boundary condition at a prescribed depth, say $z = -2000$ km (Roberts, 1976b), and take mean values of -0.25 for the scale-height gradient and 1.2 for the ratio of specific heats, over the range $z = 0$ to $z = -2000$ km, we find (using the upper boundary condition $\hat{v}' = 0$ at $z = 0$) that the perturbation is stable for $c_0^2/v_A^2 < 1.2$, i.e. the perturbation is stable for $B_0(0) > 1040$ gauss. Applying the lower boundary condition at a shallower depth would give a greater value of c_0^2/v_A^2; that is, a lower value of the field strength would be required for stability to convection.

In Table 4.I we give the critical value of c_0^2/v_A^2, where it exists, and the corresponding value of the field at $z = 0$, for various tube depths. The depths chosen correspond to the granular scale (10^3 km), the overstable cooling depth (2×10^3 km; Roberts, 1976a), the superadiabatic depth (3×10^3 km; Parker, 1978), the supergranular scale (1.5×10^4 km), and finally the depth scale of the convection zone ($\sim 10^5$ km).

TABLE 4.I: The critical field strength (in gauss) at $z = 0$ necessary for convective stability in a flux tube of given depth d and scale-height gradient Λ_0', for $\gamma = 1.2$ and $p_e(0) = 1.3 \times 10^5$ dynes cm^{-2}

	Depth d(km)				
Λ_0'	10^3	2×10^3	3×10^3	1.5×10^4	10^5
-0.15	stable	stable	stable	stable	stable
-0.2	490	670	770	1080	1280
-0.25	760	1040	1200	1750	unstable
-0.3	940	1290	1500	unstable	unstable

Table 4.II gives the growthrate of the instability, when present, for the above depths and $c_0^2/v_A^2 = 1$. For example, with $\Lambda_0' = -0.3$, a tube of depth 2000 km has a growthrate of $5.3 \times 10^{-3} s^{-1}$ (that is, the instability grows on an e-folding time of 190s); whereas, for a depth 1.5×10^4 km, the growthrate is $7.2 \times 10^{-3} s^{-1}$ (with an e-folding time of 140s). Taking a smaller value of γ, for example $\gamma = 1.1$, the growthrate increases to $9.7 \times 10^{-3} s^{-1}$ for a depth of 2000 km.

Given that convective instability occurs in the tube, what are its consequences? The instability may result in either a downflow or an upflow, which, unfortunately, linear analysis cannot discriminate between. Parker (1978) has shown that a steady downdraft (in the basic-state of a flux tube) leads to a temperature difference between the interior of the tube and the surrounding photosphere, and subsequently to field intensification.

In a flux tube that is in unstable equilibrium, either because its field strength is low or because it is deeply rooted, instability (as we have seen in this chapter) may manifest itself as a downflow, the consequence of which is to lead to an increase in field strength and thus eventually to a possibly stable (cooler) equilibrium. An upflow would presumably result in the magnetic field being dispersed at the surface by the diverging flow and enhanced temperature of the rising gas (Parker, 1978; Spruit and Zweibel, 1979).

Thus it is suggested that the downdraft observed in intense flux tubes (see Chapter 1) cannot be due to convective instability if the tubes are shallow. If the depths of the flux tubes are greater than about 2000 km, then the downflow, if resulting from convective instability, is likely to be a transient phenomenon (see also Galloway et al, 1977), taking place as the field strength intensifies and the flux tube moves to a state of hydrostatic equilibrium with an increased field strength. Of course, this does not exclude the possibility of other mechanisms giving rise to a downdraft in the tube. (The theoretical structure of a steady downdraft in a flux tube is considered further in Chapter 6).

TABLE 4.II: The growthrate (in s^{-1}), $i\omega_1$, of the most unstable mode for various depths d and scale-height gradients Λ_0', for $c_0 = v_A$, $\gamma = 1.2$ and $\Lambda_0(0) = 152$ km.

	Depth d(km				
Λ_0'	10^3	2×10^3	3×10^3	1.5×10^4	10^5
-0.15	stable	stable	stable	stable	stable
-0.2	stable	stable	stable	stable	1.2×10^{-3}
-0.25	stable	stable	3.2×10^{-3}	4.8×10^{-3}	4.8×10^{-3}
-0.3	stable	5.3×10^{-3}	6.7×10^{-3}	7.2×10^{-3}	7.2×10^{-3}

Consider, then, in summary, a possible scenario for the life of an intense flux tube. If the flux tube is a shallow phenomenon, then motions driven by convective forces are unlikely, and an equilibrium state presumably rules. If, however, the flux tube extends somewhat deeper (several thousand km, say) into the Sun, then a flux tube of moderate field strength (of several hundred gauss say) is convectively unstable. The result of this instability Spruit, 1979, is to lead either to the dissolution of the tube, with the field being dispersed; or to an increase in field, driven by a downdraft in the tube, until an equilibrium, with kilogauss field strengths, is once more possible. The tube would be cooler than its surroundings though, independently, overstable Alfven waves will also tend to cool the interior of the tube, and thus further intensify the field (Parker, 1976; Roberts. 1976a). There are, of course, uncertainties in this global description of field intensification: only a more detailed, presumably non-linear, analysis can further clarify such points.

It should be noted that we have neglected the effect of dissipation in our analysis. When dissipation is taken into account, overstability may arise, even when our conditions for stability are satisfied (Cowling, 1976). Dissipative processes may also relate to the possibility of cooling and field intensification (Parker, 1976; Roberts, 1976a). (The effect of dissipation on wave propagation will be discussed in the next chapter).

It is appropriate to end this chapter with a brief discussion of the recent work of others in this field. To begin with, the idea of field concentration occurring as a result of a downflow and cooling would appear to originate with Parker (1978), though Zwaan (1978) has proposed a model for field amplification in which radiative cooling and subsequent convective downflow reduces the temperature at the top of a flux tube, which then contracts to field strengths well above the local equipartition values. That the downdraft, observed in the solar network structure, is initiated in the form of an instability which develops into a finite amplitude flow, was suggested by Unno and Ando (1979; see also Unno et al, 1979), who based their analysis on the slender flux tube equations derived in Chapter 3 and which were derived independently of Roberts and Webb (1978). The presence of an instability has also been demonstrated by Spruit and Zweibel (1979; see also Spruit, 1979). (It is interesting to note that Galloway et al (1977) comment: "On the axis of a tube, (cool) gas is no longer supported by the pressure gradient and therefore falls. The density drops and the tube is squeezed by the external pressure until some equilibrium is reached.")

A somewhat different explanation of intense fields has been proposed by Galloway, Proctor and Weiss (1978), who describe the

concentration by three dimensional flow converging to an axis, and show that equipartition field strengths may be greatly exceeded, at least in a Boussinesq fluid. They derive expressions for the peak field reached in the ropes and apply their theory to the formation of intense magnetic fields (Galloway et al, 1977). The observed field strengths of 1600 G can be attained if the average field strength over a convection cell is about 16 G, i.e. for fluxes greater than about 10^9 Wb, which is consistent with estimates given in Chapter 1. Inside the flux ropes the field is locally strong enough to halt convection (Peckover and Weiss, 1978).

Chapter 5 : RADIATIVE RELAXATION

5.1 Introduction

The nature of wave motions in a magnetic flux tube was discussed in Chapter 3 (See also Cram and Wilson, 1975; Defouw, 1976; Wilson, 1979a; Wentzel, 1979; Roberts, 1980). Cram and Wilson considered the modes of vibration of a magnetic flux sheath embedded in a uniform non-magnetic region and showed that for symmetrical oscillations (pulsations) of the tube only the slow wave is a permissible mode of vibration. Roberts (1980) has pointed out that Cram and Wilson's observation is changed when temperature differences between the inside and outside of the tube are allowed. As we have seen in Chapter 2, if the tube is cooler than its surroundings a second mode (sound wave) is permitted.

In Chapter 3 we discussed the nature of longitudinal wave propagation in an intense magnetic flux tube embedded in a stratified, non-isothermal atmosphere. In a slender flux tube several simplifications in the analysis of wave propagation may be made. Such approximate treatments are especially desirable when the medium is stratified by gravity or when dissipative effects complicate the structure of wave propagation. We showed, in Chapter 3, that propagation occurs only for frequencies ω greater than a critical frequency ω_v, where ω_v depends upon the temperature scale height and its gradient, as well as the field strength of the tube. The expression for ω_v is particularly simple in an isothermal atmosphere for which

$$\omega_v^2 = \left(\frac{9}{16} - \frac{1}{2\gamma} + \frac{\gamma-1}{\gamma^2}\frac{c_0^2}{v_A^2}\right)\frac{c_0^2 v_A^2}{(c_0^2+v_A^2)\Lambda_0^2} \quad ,$$

where c_0 and v_A are the sound and Alfvén speeds, Λ_0 the scale-height, and γ the ratio of specific heats. Note that ω_v is not purely acoustic in nature; for, unlike the acoustic frequency $(\gamma g/4\Lambda_0)^{\frac{1}{2}}$, which arises for vertical propagation in a stratified non-magnetic atmosphere, ω_v tends to a finite value $(3v_A/4\Lambda_0)$ in the incompressible limit ($\gamma \to \infty$).

As an illustration of the tube cut-off frequency ω_v, we may set $v_A = c_0$ (typical of an intense flux tube) and $\gamma = 5/3$, and then ω_v^2 is simply

$$\omega_v^2 = \frac{67}{160}\left(\frac{g}{\Lambda_0}\right),$$

which is numerically very close to the acoustic cut-off frequency (squared) of $\frac{5}{12}\left(\frac{g}{\Lambda_0}\right)$. Taking an average $\Lambda_0 = 126$ km for the region from the photosphere (optical depth $\tau_{5000} = 1$) to the temperature minimum we find $\omega_v \approx 3 \times 10^{-2}$ s^{-1}. Thus, only those waves with frequency greater than 3×10^{-2} s^{-1} (period less than 210 s) propagate from the photosphere through to the temperature minimum. Waves with lower frequency (higher period) become evanescent (non-propagating) at some height between the photosphere and the temperature minimum. The amplitude of such waves, propagating adiabatically in an isothermal atmosphere, e-folds in about 4 scale-heights.

The existence of these tube waves clearly raises the question as to their contribution to the heating of the low chromosphere. As we have noted above, the tube waves are growing in amplitude and so may eventually reach shock strengths and thus dissipate their energy in this manner. However, the observations of Giovanelli, Livingston and Harvey (1978) indicate that while wave amplitudes do indeed grow with height they do not approach shock strength. Furthermore, it is well known (see Bray and

Loughhead, 1974) that radiative damping of waves is particularly important in the upper photosphere, where the radiative relaxation time may be short compared with the period of a wave.

Radiation enters the analysis of gas motion by way of a heating term in the energy equation, though, unlike conduction, radiative heating is not uniquely related to the thermal field and it is necessary to supplement the energy equation with the equation of radiative transfer (Vincenti and Traugott, 1971). The energy equation (1.4.31) may be written in the form (Unno and Spiegel, 1966)

$$\frac{\rho^{\gamma}}{\gamma-1}\frac{d}{dt}\left(\frac{P}{\rho^{\gamma}}\right) = Q + \phi + \nabla\left(\Lambda\nabla T\right) \qquad (5.1.1)$$

where ϕ is the mechanical dissipation per unit volume, Λ is the thermal conductivity and Q is the rate of heat addition per unit volume due to radiation. The local value of Q is given by $Q = -\nabla.\underline{Fr}$, with $\underline{Fr}$ the radiative heat flux vector. Defining the Bouguer number, Bu, by $Bu = KL$. where K is a mean absorption coefficient and L is the dimension of the region of interest, the two limits $Bu \ll 1$ and $Bu \gg 1$ are of interest. The first is optically thin ($Bu \ll 1$), with negligible radiation from outside the region of interest. Within the region the gas loses energy at the rate $Q = -4K\sigma T^4$ where σ is the Stefan-Boltzmann constant. This corresponds to emission under local thermodynamic equilibrium. The linearized form of Q, Q', will be given by $Q' = 16\sigma K T_0^3 T$, which is the approximation of Newton's law of Cooling which we adopt in this chapter. The opposite extreme is optically thick ($Bu \gg 1$), which occurs when the optical depth, τ, defined by

$$\tau = \int_z^{\infty} K\, dz ,$$

varies rapidly over a distance in which there is only a small change in the thermodynamic state (Vincenti and Traugott, 1971). Radiation transport then becomes diffusive and one finds $\underline{F}r = -k_r \nabla T$, with an effective radiative thermal conductivity $k_r = 16\sigma T^3/3\kappa$.

Since we are concerned with the effect of radiation on wave motions, an outline of the derivation of the linearized form of the energy equation, using the radiative transfer equation, is given in the appendix.

The effect of radiative damping is to heat the medium in which the wave propagates, and to limit the growth (due to the decrease in density) of wave amplitude with height, thus resulting in the appearance of shock waves at greater heights (Schatzman and Souffrin, 1967). Certain characteristics of the wave motion, such as the phase lag between the temperature fluctuations and the vertical velocity, depend critically on the actual energy balance (Schatzman and Souffrin, 1967). Accurate observations of such relationships may be important in identifying the wave modes actually present in the solar photosphere and chromosphere (Bray and Loughhead, 1974). Recent studies of phase delays using data from OSO 8 have been presented by Lites and Chipman (1979), Athay and White (1978, 1979a,b), White and Athay (1979), and Chipman (1978).

Since radiative relaxation has a pronounced effect on isotropic wave propagation in the upper photosphere it is of interest to examine the effect of radiative relaxation on the propagation of waves in an intense magnetic tube embedded in a stratified atmosphere. This is the object of the present chapter. We assume that Newton's law of cooling is appropriate so that radiative

relaxation of waves may be described in a relatively simple fashion. More sophisticated treatments, coupling the hydrodynamic and radiative transfer equations have been considered for a non-magnetic atmosphere (Schmieder, 1976, 1977, 1978), but we will have quite enough to do in taking account of the magnetic field without the additional burden of full radiative transfer.

By way of introduction we shall first discuss, in the following section, radiative relaxation in a uniform (non-gravitational) medium, leaving the complications introduced by gravity, to Section 5.3.

5.2 Radiative Relaxation in a Uniform Atmosphere

5.2.1 Introduction

The dynamical equations governing motions of a perfectly-conducting, inviscid, ideal gas (of pressure p, density ρ and temperature T) embedded in a magnetic field are

$$\frac{\partial \rho}{\partial t} + \nabla.(\rho \underline{v}) = 0 , \tag{5.2.1}$$

$$\rho\left(\frac{\partial \underline{v}}{\partial t} + (\underline{v}.\nabla)\underline{v}\right) = -\nabla p + \underline{j} \wedge \underline{B} , \tag{5.2.2}$$

$$\frac{\partial \underline{B}}{\partial t} = \nabla \wedge (\underline{v} \wedge \underline{B}) , \tag{5.2.3}$$

$$\frac{\partial p}{\partial t} + \underline{v}.\nabla p = \frac{\gamma p}{\rho}\left(\frac{\partial \rho}{\partial t} + \underline{v}.\nabla \rho\right) - \rho(\gamma - 1)\mathcal{L}(\rho, T), \tag{5.2.4}$$

$$p = \frac{R}{\mu}\rho T , \tag{5.2.5}$$

$$\mu_0 \underline{j} = \nabla \wedge \underline{B} , \quad \nabla.\underline{B} = 0. \tag{5.2.6}$$

In the above equations $\underline{v}$ is the velocity, $\underline{B}$ the magnetic (induction)

field, $\underline{j}$ the current density and μ_0 the permeability; γ is the ratio of specific heats (taken to be 5/3 in all of the numerical illustrations), R the gas constant and μ the mean molecular weight. In the energy equation (5.2.4) we have neglected the effects of viscosity and thermal conduction, and the function $\mathcal{L}$ represents the rate of heat loss per unit mass. We have assumed that the gas is sufficiently diffuse to be optically thin, so that $\mathcal{L}$ may be written as a function of the local values of ρ and T (Field, 1965). Equation (5.2.4) may be written in the alternative form

$$\rho c_v \left(\frac{\partial T}{\partial t} + \underline{v} . \nabla T \right) + p \nabla . \underline{v} = -\rho \mathcal{L} , \qquad (5.2.4)'$$

where c_v is the specific heat at constant volume. Equations (5.2.1) - (5.2.6), with thermal conduction included in the energy equation, have been discussed by Field (1965) in connection with the problem of thermal instability in a uniform atmosphere.

The basic state with which we are interested is given by

$$\rho = \rho_0, \; T = T_0, \; \underline{v} = \underline{0}, \; \underline{B} = B_0 \hat{\underline{z}}, \; \mathcal{L}(\rho_0, T_0) = 0 ,$$

representing an unbounded uniform gas in the presence of a uniform vertical magnetic field.

The behaviour of linear perturbations about the above basic state depends on the form of the radiative loss term $\mathcal{L}$. The linearized form of the energy equation (5.2.4) may be written

$$\frac{\partial P}{\partial t} = \frac{\gamma P_0}{\rho_0} \frac{\partial \rho}{\partial t} - \rho_0 (\gamma - 1) \left(\mathcal{L}_\rho \rho + \mathcal{L}_T T \right) , \qquad (5.2.7)$$

where p, ρ and T now refer to the perturbations and a subscript zero denotes equilibrium values. The coefficients $\mathcal{L}_\rho \equiv (\partial \mathcal{L} / \partial \rho)_T$ and $\mathcal{L}_T \equiv (\partial \mathcal{L} / \partial T)_\rho$ are evaluated in the equilibrium state.

Now the form of the radiative loss term, $\mathcal{L}$, has been considered by a number of authors. Spiegel (1957) has shown that for a homogeneous, grey atmosphere (i.e. one in which the absorption coefficient is independent of frequency), in local thermodynamic equilibrium, the smoothing of temperature fluctuations is governed by

$$\mathcal{L}_T = \frac{c_v}{\tau_R} \quad , \quad \mathcal{L}_\rho = 0 \, , \tag{5.2.8}$$

where τ_R is the radiative decay time. For an optically thin medium, τ_R is given by

$$\tau_R = \frac{\rho_0 c_v}{16 \sigma K T_0^3} \, , \tag{5.2.9}$$

where K is the mean linear absorption coefficient per unit length and σ is the Stefan-Boltzmann constant. (see also Delache and Froeschlé, 1972; Gille, 1968). We note that in terms of the time scale τ_R, and for perturbations having a time-dependence of the form $e^{i\omega t}$, the extreme $\omega\tau_R \gg 1$ corresponds to almost adiabatic perturbations, whilst $\omega\tau_R \ll 1$ relates to almost isothermal perturbations. Both of these extremes are likely to arise in the solar atmosphere, from the photosphere to low chromosphere, for typical frequencies ω of order 10^{-1} s^{-1}, since τ_R varies considerably over this height range. Another time-scale which arises naturally in the time τ_s for a sound wave to travel a distance L, namely $\tau_s = L/c_0$, where $c_0 = (\gamma P_0 / \rho_0)^{\frac{1}{2}}$ is the adiabatic speed of sound

5.2.2 Radiative Damping in an Unbounded Atmosphere

Before we consider, in the following sections, the effects of lateral boundaries we shall first discuss the nature of radiative damping in an unbounded medium. For particular cases of

the radiative loss term $\mathcal{L}(\rho,T)$ our analysis includes the results of Gille (1968) and Stein and Spiegel (1967), who have discussed the effect of radiative damping on sound waves in a field-free medium.

For linear perturbations about the basic state of the form

$$\underline{v} = \underline{v}(x)\exp i(\omega t + kz), \quad p = p(x)\exp i(\omega t + kz), \text{ etc.},$$

Equations (5.2.1) - (5.2.6) may be combined to give a single ordinary differential equations for v_x, namely

$$\frac{d^2 v_x}{dx^2} - \lambda^2 v_x = 0 , \tag{5.2.10}$$

where

$$\lambda^2 = \frac{(k^2 v_A^2 - \omega^2)(k^2 c_0^2 \Omega_0 - \omega^2)}{k^2 c_0^2 v_A^2 \Omega_0 - \omega^2 (v_A^2 + c_0^2 \Omega_0)} , \tag{5.2.11}$$

and

$$\Omega_0 = (i\omega - \tfrac{1}{\gamma} c_0 k_\rho + \tfrac{1}{\gamma} c_0 k_T)/(i\omega + c_0 k_T) .$$

Here $c_0 = (\gamma P_0/\rho_0)^{\frac{1}{2}}$ is the sound speed and $v_A = B_0/(\mu_0\rho_0)^{\frac{1}{2}}$ is the Alfvén speed. Following Field (1965), the wavenumbers k_ρ and k_T are defined by

$$k_\rho = \frac{\mu(\gamma-1)\rho_0 \mathcal{L}_\rho}{R\rho_0 T_0} , \qquad k_T = \frac{\mu(\gamma-1)\mathcal{L}_T}{R c_0} . \tag{5.2.12}$$

Note that with the form of $\mathcal{L}_T$ and $\mathcal{L}_\rho$ given by (5.2.8), k_ρ, k_T and Ω_0 reduce to

$$k_\rho = 0 , \quad k_T = \frac{1}{c_0 \tau_R} , \quad \Omega_0 = \frac{i\omega + \frac{1}{\gamma\tau_R}}{i\omega + \frac{1}{\tau_R}} . \tag{5.2.13}$$

The velocity component v_y is uncoupled from the other velocities and its frequency is that of a pure transverse Alfvén wave unaffected by the form of the energy equation.

For the unbounded medium under consideration here, Equation (5.2.10) admits plane-wave solutions with x-dependence of the form e^{ilx}, so that $l^2 + \lambda^2 = 0$, which may be rearranged to give the dispersion relation

$$\omega^5 - ic_0 k_T \omega^4 - m^2(c_0^2+v_A^2)\omega^3 + im^2\left(\frac{1}{\gamma}\, c_0^3(k_T-k_\rho)+c_0 v_A^2 k_T\right)\omega^2 +$$

$$+m^2k^2c_0^2v_A^2\omega - im^2k^2\,\frac{c_0^3}{\gamma}\,v_A^2(k_T-k_\rho) = 0\ , \qquad (5.2.14)$$

where $m = (l^2+k^2)^{\frac{1}{2}}$ is the magnitude of the propagation vector $\underline{m} = (l,0,k)$. Equation (5.2.14) is equivalent to that obtained by Field (1965 ; Equation (54)) for the case of no thermal conduction.

Using Equation (5.2.13), the dispersion relation (5.2.14) becomes

$$\omega^5 - \frac{i}{\tau_R}\,\omega^4 - m^2(c_0^2+v_A^2)\omega^3 + \frac{im^2}{\tau_R}\,(\frac{1}{\gamma}\, c_0^2+v_A^2)\omega^2 +$$

$$+ m^2k^2c_0^2v_A^2\omega - \frac{im^2k^2c_0^2v_A^2}{\gamma\tau_R} = 0\ . \qquad (5.2.15)$$

We may note that in the <u>adiabatic limit</u>($\tau_R \to \infty$) Equation (5.2.15) gives $\omega = 0$, or

$$\omega^4 - m^2(c_0^2+v_A^2)\omega^2 + m^2k^2c_0^2v_A^2 = 0\ , \qquad (5.2.16)$$

which is the usual magnetoacoustic dispersion relation for the fast and slow modes.

Returning to the non-adiabatic form of (5.2.15), we see that in the absence of a magnetic field, we have $\omega^2 = 0$, or

$$\omega^3 - \frac{i}{\tau_R}\omega^2 - m^2 c_0^2 \omega + \frac{i m^2 c_0^2}{\gamma \tau_R} = 0 , \qquad (5.2.17)$$

a special case of our treatment which has been discussed previously by a number of authors (Stein and Spiegel (1967), and references therein; Gille, 1968).

In order to draw comparison with the results that we shall obtain (in the following section) for a flux tube, it is worthwhile to consider Equation (5.2.17) further. For ease of exposition we shall restrict ourselves to the time-damped case (m assumed real).

We may note that (5.2.17) may be written in the dimensionless form

$$(\omega \tau_s)^3 \cos^2\theta - i\left(\frac{\tau_s}{\tau_R}\right)(\omega\tau_s)^2 \cos^2\theta - \omega\tau_s + \frac{i}{\gamma}\left(\frac{\tau_s}{\tau_R}\right) = 0 \qquad (5.2.17)'$$

where $\tau_s = (kc_0)^{-1}$ is the time taken by a sound wave to traverse a distance k^{-1}, and $\theta = \cos\left(\frac{k}{m}\right)$ is the angle between the wave propagation vector and the z axis. Equation (5.2.17)' shows that, for given γ, the dimensionless frequency $\omega\tau_s$ is determined purely in terms of the ratio τ_s/τ_R of the sound and radiative timescales, and the angle θ.

The solutions to Equation (5.2.17)', for $\tau_s \ll \tau_R$, are (to second order in τ_s/τ_R)

$$\omega_{1,2} \approx \pm m c_0 \left[1 - \frac{(\gamma-1)(\gamma+3)}{8\gamma^2}\cos^2\theta \left(\frac{\tau_s}{\tau_R}\right)^2\right] + \frac{1}{2} i \frac{\gamma-1}{\gamma} k c_0 \left(\frac{\tau_s}{\tau_R}\right), \qquad (5.2.18)$$

and

$$\omega_3 \approx \frac{i}{\gamma} k c_0 \frac{\tau_s}{\tau_R} . \qquad (5.2.19)$$

Thus, when the radiative decay time τ_R is much greater than the acoustic period τ_s, the modes (5.2.18) correspond to sound waves with speeds slightly reduced below the adiabatic sound velocity and modified by radiative effects to experience weak damping. The solution (5.2.19) corresponds to a purely damped mode (Gille, 1968).

In the opposite limit, $\tau_s >> \tau_R$, when the radiative decay time is much less than the acoustic period, Equation (5.2.17) yields

$$\omega_{1,2} \approx \pm \frac{mc_0}{\gamma^{1/2}}\left[1 + \frac{(\gamma-1)(\gamma-5)}{8\gamma\cos^2\theta}\left(\frac{\tau_s}{\tau_R}\right)^{-2}\right] + \frac{i}{2}\left(\frac{\gamma-1}{\gamma}\right)\left(\frac{\tau_s}{\tau_R}\right)^{-1}\frac{mc_0}{\cos\theta}, \qquad (5.2.20)$$

$$\omega_3 \approx ikc_0\left(\frac{\tau_s}{\tau_R}\right) \qquad (5.2.21)$$

The motion is nearly isothermal, with disturbances propagating at slightly above the isothermal sound speed $(c_0^2/\gamma)^{\frac{1}{2}}$, and again experiencing damping (in time).

It is convenient here to define $D_p = \left|\mathrm{Re}(i\omega)/\mathrm{Im}(i\omega)\right|$ as the damping per period (Stein and Spiegel, 1967). Equations (5.2.18) and (5.2.20) then show that Dp behaves, for $\tau_s << \tau_R$, as

$$D_p \sim \frac{1}{2}\left(\frac{\gamma-1}{\gamma}\right)\left(\frac{\tau_s}{\tau_R}\right)\cos\theta \to 0 \quad \text{as} \quad \tau_s/\tau_R \to 0;$$

and for $\tau_s >> \tau_R$, Dp behaves as

$$D_p \sim \frac{1}{2}\left(\frac{\gamma-1}{\gamma}\right)\left(\frac{\tau_s}{\tau_R}\right)^{-1}\frac{\gamma^{1/2}}{\cos\theta} \to 0 \quad \text{as} \quad \tau_s/\tau_R \to \infty.$$

These results indicate that there is a maximum in Dp as a function of τ_s/τ_R (Stein and Spiegel, 1967). Figure 5.1 gives Dp as a function of τ_s/τ_R for vertical propagation ($\cos\theta = 1$).

Now when a magnetic field is present the dispersion relation (Equation (5.2.15) is fifth order, and again it is convenient to consider the effect of a finite radiative decay time by looking for solutions of Equation (5.2.15) in the two extremes $\tau_s \ll \tau_R$ and $\tau_s \gg \tau_R$. In the former case, Equation (5.2.15) gives (for $\tau_s/\tau_R \ll 1$)

$$\omega_{1,2,3,4} \approx \omega^* + \frac{1}{2} i \left(\frac{\gamma-1}{\gamma}\right)\left[\frac{m^2 v_A^2 - \omega^{*2}}{m^2(c_0^2+v_A^2)-2\omega^{*2}}\right] kc_0\left(\frac{\tau_s}{\tau_R}\right), \qquad (5.2.22)$$

$$\omega_5 \approx \frac{i}{\gamma} kc_0\left(\frac{\tau_s}{\tau_R}\right)$$

where ω^* satisfies the dispersion relation for undamped magneto-acoustic waves, namely

$$\omega^{*2} = \frac{1}{2} m^2 \left[(c_0^2+v_A^2) \pm \left((c_0^2+v_A^2)^2 - 4\, c_0^2 v_A^2 \cos^2\theta\right)^{\frac{1}{2}}\right]. \qquad (5.2.23)$$

The positive sign characterizes the fast-mode and the negative sign to slow-mode. The introduction of a finite radiative decay time leads to the fast- and slow-modes being <u>damped</u> in time; in addition there is the thermal mode, $\exp(-\frac{t}{\gamma\tau_R} + ilx + ikz)$, which in this limit is unaffected by the presence of the magnetic field (see Equation (5.2.19)).

In the other extreme, when the radiative decay time is much smaller than the acoustic period (i.e. $\tau_s \gg \tau_R$), the solutions of (5.2.15) are

Figure 5.1 - The damping per period, $D_p = |\mathrm{Re}(i\omega)/\mathrm{Im}(i\omega)|$, for sound waves in a uniform field-free medium, as a function of the ratio τ_s/τ_R of the sound and radiative time-scales.

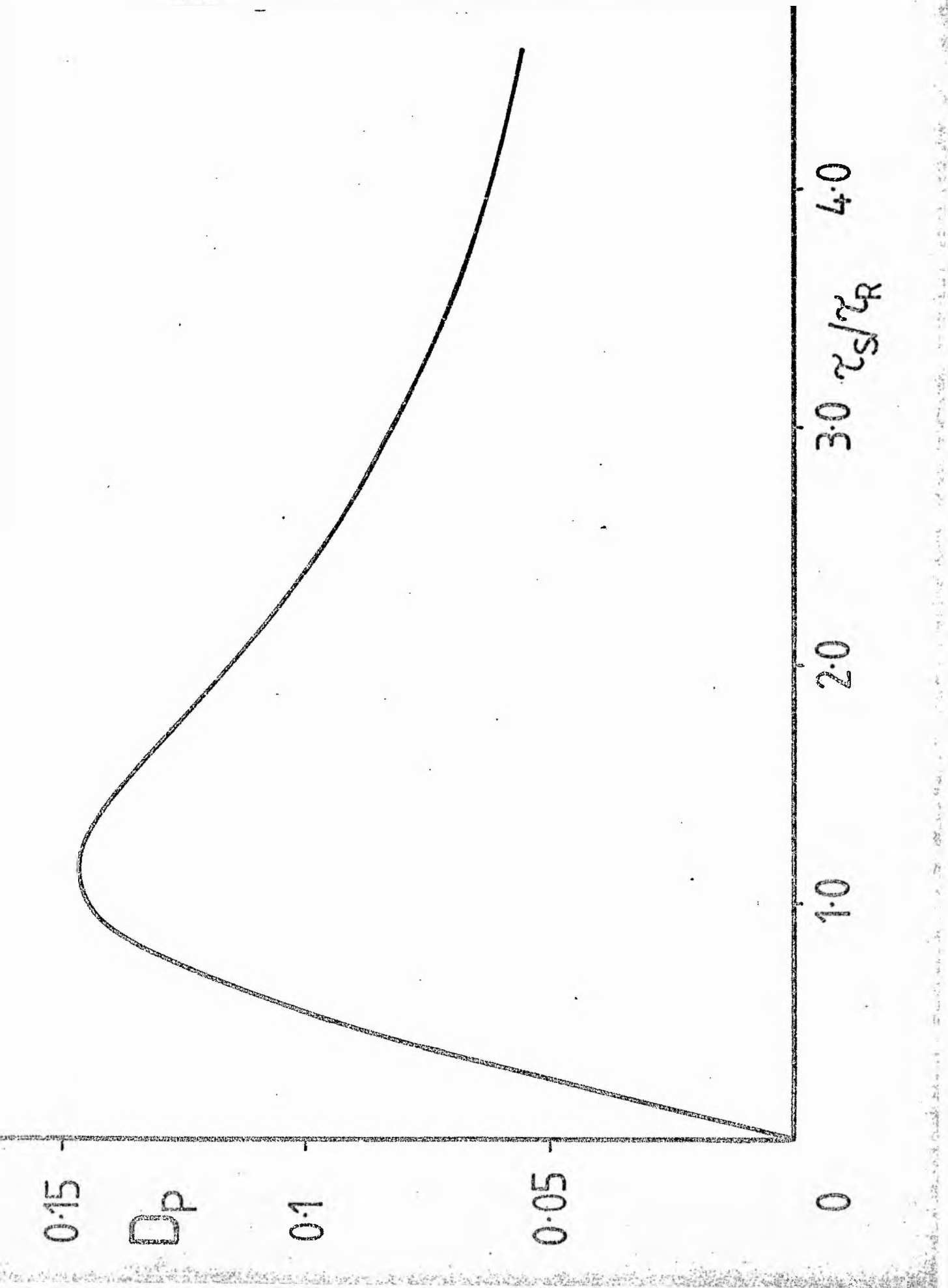

$$\omega_{1,2,3,4} \approx \omega^* + \frac{i(\gamma-1)\omega^{*2}\,(m^2v_A^2 - \omega^{*2})}{2m^2v_A^2\left[m^2\left(\frac{c_0^2}{\gamma} + v_A^2\right) - 2\omega^{*2}\right]} \frac{mc_0}{\cos\theta}\left(\frac{\tau_s}{\tau_R}\right)^{-1} ,$$

(5.2.24)

$$\omega_5 \approx ikc_0\left(\frac{\tau_s}{\tau_R}\right) ,$$

where now ω^* satisfies

$$\omega^{*2} = \frac{1}{2}m^2\left[\left(\frac{c_0^2}{\gamma} + v_A^2\right) \pm \left[\left(\frac{c_0^2}{\gamma} + v_A^2\right)^2 - \frac{4c_0^2v_A^2}{\gamma}\cos^2\theta\right]^{\frac{1}{2}}\right] . \quad (5.2.25)$$

Equation (5.2.25) is simply (5.2.23) with the sound speed, c_0, replaced by the isothermal sound speed $c_0/\gamma^{\frac{1}{2}}$. Again each mode is subject to damping in time. The damping per period, Dp, depends on the angle of propagation. For propagation along the magnetic field (k=m) Equation (5.2.15) factorizes to give $\omega^2 = m^2v_A^2$ (Alfvén waves, independent of τ_R), and

$$\omega^3 - \frac{i}{\tau_R}\omega^2 - m^2c_0^2\omega + \frac{im^2c_0^2}{\gamma\tau_R} = 0 ,$$

which is Equation (5.2.17) for sound waves, which experience damping (see Figure 5.1). For $k < m$, both modes are damped and Equations (5.2.22) and (5.2.24) show that there is a maximum in D_p as a function of τ_s/τ_R. D_p is sketched in Figure 5.2 for $\cos\theta = 0.9$ and $c_0 = v_A$. For adiabatic propagation ($\tau_s/\tau_R \to 0$) and for isothermal propagation ($\tau_s/\tau_R \to \infty$) the waves are not damped; but in the intermediate case heat generated in a compression is transferred by radiation to the cooler rarefactions and is dissipated, and the waves are damped (Stein and Spiegel, 1967).

In summary, then, we have shown in this section that the introduction of a finite radiative decay time in an unbounded atmosphere, with a uniform magnetic field present, leads to

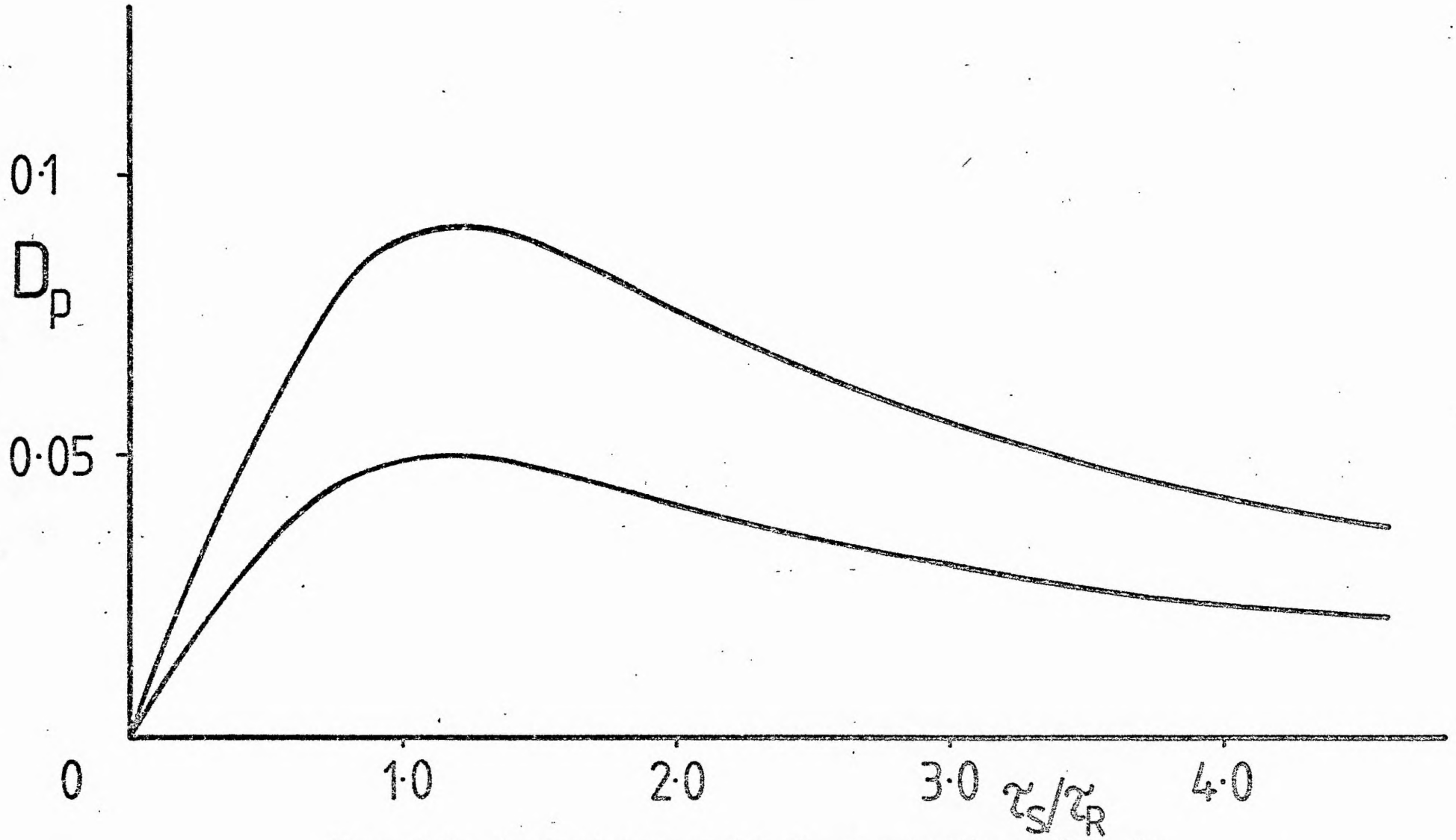

Figure 5.2 - The damping per period, D_p, as a function of τ_s/τ_R for magneto-acoustic waves. As an illustration we have taken cos θ = 0.9 and $c_0 = v_A$.

temporal-damping of the magneto-acoustic waves, and to a purely damped (thermal) mode. The damping depends on the angle of propagation; for waves propagating along the magnetic field, the Alfvén mode propagates undamped.

5.2.3 Radiative Damping in a Flux Tube

The dispersion relation

In the previous section we discussed the effect of radiative damping in an unbounded (uniform) medium. However, since we are primarily interested in the effect of radiative damping in a flux tube in the solar atmosphere, we shall now consider the important influences of lateral boundaries to the magnetic field.

Consider, then, a uniform vertical column of magnetic field, $B_0\hat{z}$, confined to $r < r_0$. It is convenient to use a cylindrical coordinate system (r,θ,z). The governing equations are (5.2.1) - (5.2.6) and the uniform equilibrium ($\underline{v} = 0$) is characterized by $\rho = \rho_0$, $T = T_0$, and $\mathcal{L}(\rho_0, T_0) = 0$ inside the tube, with similar relations holding in the exterior region (where $\underline{B} = 0$). The interior and exterior regions are related by the pressure balance condition:

$$p_0 + \frac{B_0^2}{2\mu_0} = p_e$$

(An index e will be used to denote exterior quantities.)

For axisymmetric ($\partial/\partial\theta \equiv 0$) linear perturbations in velocity and field of the form

$$\underline{v} = (v_r, v_\theta, v_z) , \quad \underline{b} = (b_r, b_\theta, b_z)$$

we find that v_θ decouples from v_r and v_z, and its frequency is that of an Alfvén wave. The amplitude $\hat{v}_r(r)$ of the radial component

of the velocity perturbation, $v_r = \hat{v}_r(r)\exp i(\omega t + kz)$ satisfies

$$\frac{d}{dr}\left(\frac{1}{r}\frac{d}{dr}(r\hat{v}_r)\right) - \lambda_o^2 v_r = 0 \ , \qquad (5.2.26)$$

where λ_o is as defined previously (Equation (5.2.11)):

$$\lambda_o^2 = \frac{(k^2v_A^2 - \omega^2)(k^2c_0^2\Omega_o - \omega^2)}{k^2c_0^2v_A^2\Omega_o - \omega^2(v_A^2 + c_0^2\Omega_o)} \ .$$

Equation (5.2.26) is a form of Bessel's equation, with solution for the radial component of velocity

$$v_r = A_0 I_1(\lambda_o r)e^{i\omega t + ikz} \ , \quad 0 \leq r < r_0 \ , \qquad (5.2.27)$$

where A_0 is an arbitrary constant, I_1 is the modified Bessel function of order one (Abramowitz and Stegun, 1967), and we have chosen the solution which is finite at the origin.

The corresponding solutions for p, v_z, b_r and b_z are

$$\left.\begin{aligned}
p &= \frac{-i\omega c_0^2\Omega_o}{(k^2c_0^2\Omega_o - \omega^2)}\rho_0\lambda_o A_0 I_0(\lambda_o r)e^{i(\omega t + kz)} \ , \\
v_z &= \frac{ikc_0^2\Omega_o\lambda_o A_0}{(k^2c_0^2\Omega_o - \omega^2)}I_0(\lambda_o r)e^{i(\omega t + kz)} \ , \\
b_r &= B_0\frac{k}{\omega}A_0 I_1(\lambda_o r)e^{i(\omega t + kz)} \ , \\
b_z &= iB_0\frac{\lambda_o}{\omega}A_0 I_0(\lambda_o r)e^{i(\omega t + kz)} \ ,
\end{aligned}\right\} \quad (0 \leq r < r_0) \qquad (5.2.28)$$

where I_0 is the modified Bessel function of zero order.

Similarly, in the exterior region, where the sound speed is c_e and $v_A = 0$, we find that

$$\left.\begin{aligned} p^e &= \frac{i\omega \rho_e c_e^2 \Omega_e \lambda_e}{(k^2 c_e^2 \Omega_e - \omega^2)} A_e K_0(\lambda_e r) e^{i(\omega t + kz)} , \\ v_r^e &= A_e K_1(\lambda_e r) e^{i(\omega t + kz)} , \\ v_z^e &= - \frac{ikc_e^2 \Omega_e \lambda_e}{(k^2 c_e^2 \Omega_e - \omega^2)} A_e K_0(\lambda_e r) e^{i(\omega t + kz)} , \end{aligned}\right\} \quad (r > r_0) \qquad (5.2.29)$$

where A_e is an arbitrary constant, K_0 and K_1 are modified Bessel functions of the second kind, and

$$\lambda_e^2 = k^2 - \frac{\omega^2}{c_e^2 \Omega_e} , \qquad (5.2.30)$$

with Ω_e being the corresponding expression to Ω_o for the exterior region. In (5.2.29) we have assumed that the real part of λ_e is positive so that perturbations are bounded as $r \to \infty$. (Note that in the adiabatic limit, when $\Omega_o = \Omega_e = 1$, the above solution reduces to that given in Chapter 3 for evanescent disturbances in the exterior region.)

Now, applying the appropriate boundary conditions, namely that across $r = r_0$, v_r and $p + \frac{B_0}{\mu_0} b_z$ are continuous, we arrive at the dispersion relation

$$(k^2 v_A^2 - \omega^2) \lambda_e \frac{I_0(\lambda_o r_0)}{I_1(\lambda_o r_0)} = \left(\frac{\rho_e}{\rho_0}\right) \omega^2 \lambda_o \frac{K_0(\lambda_e r_0)}{K_1(\lambda_e r_0)} . \qquad (5.2.31)$$

The adiabatic limit of Equation (5.2.31) has been discussed in detail in Chapter 3 for both the cases of $\lambda_e^2 > 0$ (evanescent disturbances in the exterior) and $\lambda_e^2 < 0$ (wave-like disturbances, when an appropriate combination of Y and J replaces K as the

solution in the exterior). Here λ_e^2 is complex and so the only solution which is bounded at infinity is the K solution (for $\mathrm{Re}(\lambda_e) > 0$). In the absence of demping, λ_e^2 is real and the cases of $\lambda_e^2 > 0$ and $\lambda_e^2 < 0$ must be treated separately since the assumption that the real part of λ_e is positive cannot be made. (See Chapter 3).

In order to investigate the dispersion relation (5.2.31) further, we shall suppose that the flux tube is slender and so restrict attention to circumstances for which $|kr_0|$ is small. For $|kr| \ll 1$ (for which we assume also that $|\lambda_0 r_0| \ll 1$; see Chapter 3)(5.2.31) reduces to

$$\omega^2(c_0^2\rho_0 + v_A^2) = k^2 c_0^2 v_A^2 \rho_0 , \qquad (5.2.32)$$

which (when written out) is seen to be a cubic in ω:

$$(c_0^2+v_A^2)\omega^3 - ic_0\left[\left(\frac{c_0^2}{\gamma}+v_A^2\right)k_T - \frac{c_0^2}{\gamma}k_\rho\right]\omega^2 - k^2c_0^2v_A^2\omega + ik^2\frac{c_0^3}{\gamma}v_A^2(k_T-k_\rho) = 0 . \qquad (5.2.33)$$

Recall that the corresponding Equation (5.2.15) for an unbounded medium is fifth order in ω. This is because the fast mode is not permitted for the axisymmetric vibration of a flux tube (Cram and Wilson, 1975; Defouw, 1976; Chapter 3). For Newton's law of cooling, for which k_ρ and k_T are given by (5.2.13), Equation (5.2.33) becomes

$$(c_0^2 + v_A^2)\omega^3 - \frac{i}{\tau_R}\left(\frac{c_0^2}{\gamma} + v_A^2\right)\omega^2 - k^2c_0^2v_A^2\omega + \frac{ik^2c_0^2v_A^2}{\gamma\tau_R} = 0 , \qquad (5.2.34)$$

where τ_R is the (constant) radiative decay time.

In the adiabatic limit ($\tau_R \to \infty$), (5.2.34) gives $\omega^2 = k^2c_T^2$, where $c_T = c_0v_A/(c_0^2 + v_A^2)^{\frac{1}{2}}$ is a characteristic speed of propagation for the tube (Defouw, 1976; Chapter 3), or $\omega = 0$.

Now, the damping of modes may be considered from two points of view, either as temporal damping, in an initial-value problem, or as spatial damping in a boundary-value problem. The temporal damping approach corresponds to supposing that the wavenumber m is real; the frequency ω , determined by the dispersion relation, is then complex. The spatial damping approach regards the frequency ω as prescribed real, with the wavenumber then complex.

Souffrin (1966, 1972) has considered the boundary-value problem as likely to be more representative of the solar photospheric situation, and has investigated the radiative relaxation of sound waves in an isothermal atmosphere. Zhugzhda (1972) has considered the problem of continuously-generated oscillations (and has therefore taken the frequency to be real). Spatial absorption applies to a progressive wave due to a constant source (Markham et al, 1951). The initial-value problem of radiative damping in time has been treated (in the solar context) by Stix (1970), who investigated a three-layer isothermal atmosphere. Stein and Spiegel (1967) also restrict their analysis to the time-damped case. Michalitsanos (1973a) points out that, although discrepancies exist in the conclusion reached by analyzing an initial-value and boundary-value problem, the boundary-value problem is probably more relevant to solar atmospheric conditions, where the long-lived oscillations are better represented by formulations which assume a steady series of excitations.

Temporally-damped disturbances

We shall now consider the dispersion relation (5.2.34), which holds for a slender ($kr_0 << 1$) flux tube in a uniform atmosphere for perturbations governed by Newton's Law of cooling and, firstly, we shall consider the temporal damping approach.

Equation (5.2.34) is similar to Equation (5.2.17), which holds in a uniform non-magnetic region, and we shall now discuss the forms of the solutions in the limiting cases of large and small radiative decay time. Note, however, that the incompressible limit of (5.2.34) gives $\omega^2 = k^2 v_A^2$ (i.e. Alfvén waves, unaffected by radiative relaxation) or $\omega = 0$.

For $\tau_s \ll \tau_R$, with $\tau_s = (kc_0)^{-1}$, the solutions of (5.2.34) are

$$\omega_{1,2} \approx \pm kc_T \left[1 - \frac{\gamma-1}{8\gamma^2}\left(3 + \frac{c_0^2+\gamma v_A^2}{c_0^2+v_A^2}\right)\left(\frac{\tau_s}{\tau_R}\right)^2 \right] + \tfrac{1}{2}i\left(\frac{\gamma-1}{\gamma}\right)\frac{c_T^2}{c_0^2 \tau_R} \quad , \qquad (5.2.35)$$

and

$$\omega_3 \approx \frac{i}{\gamma} kc_0 \left(\frac{\tau_s}{\tau_R}\right) . \qquad (5.2.36)$$

Clearly, then, for the radiative decay time much greater than the acoustic period, the solution (5.2.35) is the tube wave $\omega = kc_T$, with its propagation speed reduced slightly below the adiabatic value. The mode experiences damping in time, the decay rate being greater for a stronger magnetic field. In addition, a purely damped mode arises, with solution of the form $\exp\left[- \frac{t}{\gamma \tau_R} + ikz \right]$. This corresponds to the thermal wave (5.2.19) in an unbounded non-magnetic region.

In the opposite limit, $\tau_s \gg \tau_R$, we have the solutions

$$\omega_{1,2} \approx \pm kc_R \left[1 + \left(\frac{\gamma-1}{8\gamma}\right) \frac{v_A^2}{\left(\frac{c_0^2}{\gamma} + v_A^2\right)} \left(\frac{5(c_0^2 + v_A^2)}{\left(\frac{c_0^2}{\gamma} + v_A^2\right)} - \gamma \right) \left(\frac{\tau_R}{\tau_s}\right)^2 \right] +$$

$$+ i\tfrac{1}{2}\left(\frac{\gamma-1}{\gamma}\right) \frac{v_A^4}{\left(\frac{c_0^2}{\gamma} + v_A^2\right)^2 \tau_s} \left(\frac{\tau_R}{\tau_s}\right) , \qquad (5.2.37)$$

and

$$\omega_3 \approx -\left(\frac{\frac{c_0^2}{\gamma} + v_A^2}{c_0^2 + v_A^2}\right) kc_C\left(\frac{\tau_s}{\tau_R}\right) , \qquad (5.2.38)$$

where c_R, the characteristic tube speed for <u>isothermal</u> perturbations, is defined by

$$c_R^2 = \frac{\frac{c_0^2}{\gamma} v_A^2}{\frac{c_0^2}{\gamma} + v_A^2} < c_T^2 . \qquad (5.2.39)$$

Therefore, for a radiative decay time much less than the acoustic period, the propagation speed is increased from its isothermal value, c_R, and the mode again experiences damping.

The behaviour of the wavemodes in a slender flux tube in the two extremes $\tau_s >> \tau_R$ and $\tau_s << \tau_R$ is thus seen to parallel closely the behaviour of sound waves in an unbounded uniform atmosphere (as presented in Section 5.2.2).

We may note that D_p (the damping per period, introduced in Section 5.2.2 behaves, for $\tau_s << \tau_R$, as

$$D_p \sim \tfrac{1}{2}\left(\frac{\gamma-1}{\gamma}\right) \frac{c_T}{c_0} \left(\frac{\tau_s}{\tau_R}\right) \rightarrow 0 \quad \text{as} \quad \frac{\tau_s}{\tau_R} \rightarrow 0 ;$$

and, for $\tau_s >> \tau_R$, D_p behaves like

$$D_p \sim \tfrac{1}{2}\left(\frac{\gamma-1}{\gamma}\right) \frac{c_0}{c_R} \frac{v_A^4}{\left(\frac{c_0^2}{\gamma} + v_A^2\right)^2} \left(\frac{\tau_s}{\tau_R}\right)^{-1} \rightarrow 0 \quad \text{as} \quad \frac{\tau_s}{\tau_R} \rightarrow \infty .$$

More generally, we may solve (5.2.33) numerically for D_p as a function of τ_s/τ_R. The results are shown in Figure 5.3. We see that the damping is greater for a stronger magnetic field (smaller c_0^2/v_A^2; the limit $c_0^2/v_A^2 \to 0$ corresponds to $B_0 \to (2\mu_0 p_e)^{\frac{1}{2}}$, with ρ_0 and p_0 both tending to zero and the tube being evacuated by the magnetic field). There is a maximum in the damping which occurs, for the case $c_0^2 = v_A^2$, when $\tau_s \approx \tau_R$, i.e. when the acoustic period is approximately equal to radiative decay time. The phase-speed for isothermal propagation, c_R, is less than that for adiabatic propagation, c_T. The phase-speed is an increasing function of τ_R/τ_s, and is greater for a stronger magnetic field.

Spatially-damped disturbances

We shall now consider the problem of continuously-generated oscillations, and so take the frequency ω to be real. Thus, regarding the motions as having a sinusoidal time-dependence, but subject to spatial damping, Equation (5.2.34) may be written as a quadratic in k:

$$k^2 = a + ib \ , \qquad (5.2.40)$$

where

$$a = \frac{\omega^2}{c_T^2} + \frac{(\gamma-1)^2}{c_0^2(1+(\gamma\omega\tau_R)^2)} \ , \quad b = -\frac{(\gamma-1)\omega^2}{c_0^2(1+(\gamma\omega\tau_R)^2)}(\gamma\omega\tau_R). \qquad (5.2.41)$$

Writing $k = k_r + ik_i$, (5.2.40) gives

$$k_r^2 - k_i^2 = a \ , \quad 2k_r k_i = b \ . \qquad (5.2.42)$$

Now, the sign of the spatial absorption coefficient, k_i, is undetermined by (5.2.40), and so we must apply some constraint on the solution. For a mode, $\exp(i\omega t + ikz)$, to describe an

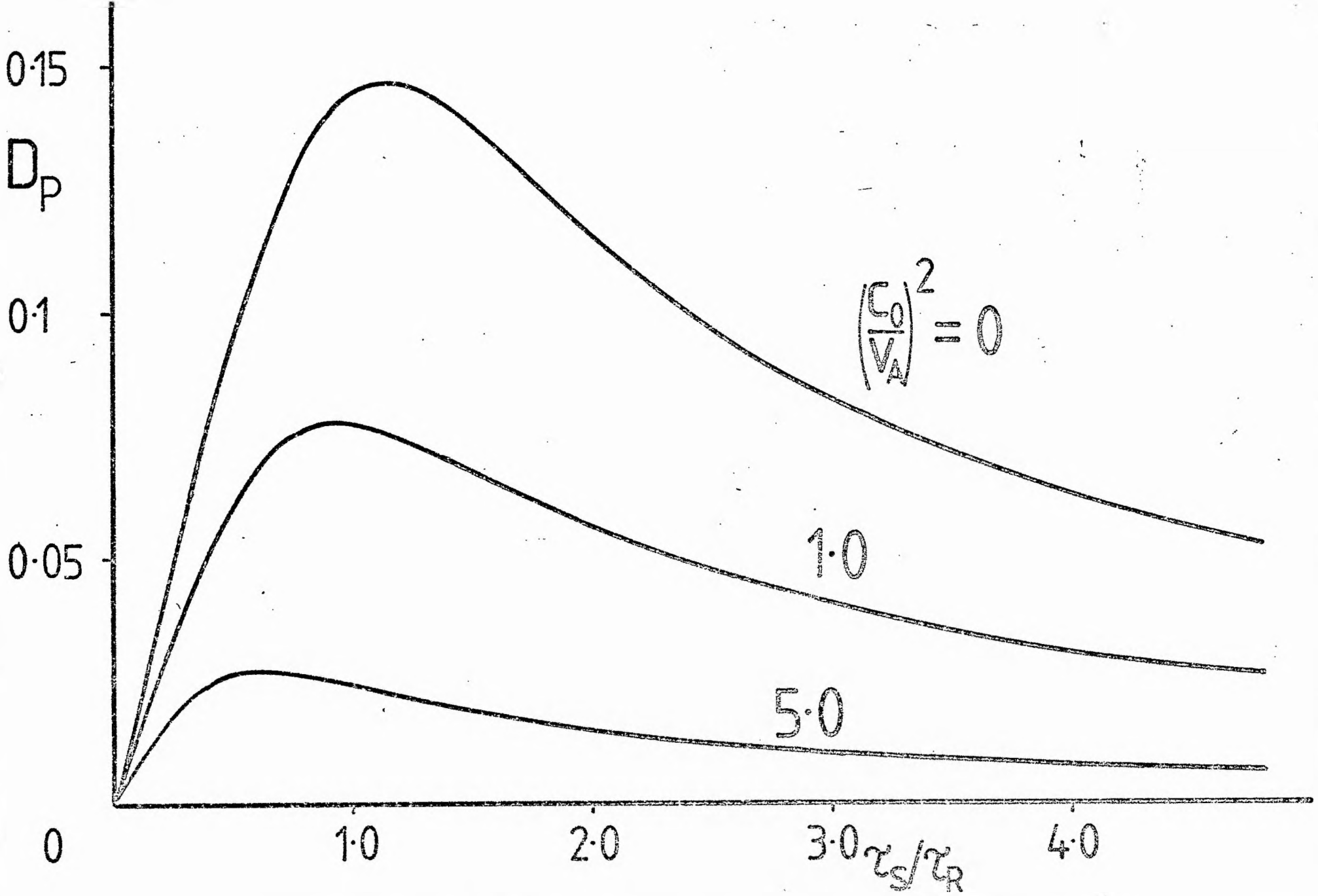

Figure 5.3 - The damping per period, D_p, as a function of τ_s/τ_R for the tube wave, illustrated for three values of c_0^2/v_A^2

upward propagating wave we require $\omega k_r < 0$, and hence (by (5.2.41) and (5.2.42)) we must have $k_i > 0$, so that the vertically propagating waves are damped.

In order to compare this approach with the time-damping analysis, we shall introduce $D_1 = \left|\frac{k_r}{k_i}\right|$ as the damping per wavelength, and consider (5.2.40) in the extremes $\omega\tau_R >> 1$ and $\omega\tau_R << 1$.

With $\omega\tau_R >> 1$, (5.2.40) gives

$$k = k_0\left[1 + \tfrac{1}{2}(\gamma-1)\frac{c_T^2}{c_0^2}\left(1 + \tfrac{1}{4}(\gamma-1)\frac{c_T^2}{c_0^2}\right)\frac{1}{(\gamma\omega\tau_R)^2} - \tfrac{1}{2}i\,\frac{\gamma-1}{\gamma}\,\frac{c_T^2}{c_0^2}\,\frac{1}{(\gamma\omega\tau_R)}\right], \quad (5.2.43)$$

where $k_0^2 = \omega^2/c_T^2$. Thus, for $\omega k_0 < 0$ (an upward-propagating wave), the speed of propagation is decreased and the wave decays vertically. As in the time-damping case, the damping increases for a stronger field. Note that the temporal decay rate in the corresponding limit is given by (5.2.35) as $-\frac{1}{2}\left(\frac{\gamma-1}{\gamma}\right)\frac{c_0^2}{c_T^2}\left(\frac{1}{\tau_R}\right)$, whilst the spatial decay rate (given above) is

$$k_i = -\tfrac{1}{2}\left(\frac{\gamma-1}{\gamma}\right)\frac{c_0^2}{c_T^2}\left(\frac{1}{\tau_R}\right)\frac{k_0}{\omega}\ .$$

In the other extreme, $\omega\tau_R << 1$, when the radiative decay time is very much less than the period, the solution of (5.2.40) is

$$k = k_0\left[1 - \frac{(\gamma-1)v_A^2}{8\left(\frac{c_0^2}{\gamma}+v_A^2\right)}\left(\frac{c_0^2+v_A^2}{\frac{c_0^2}{\gamma}+v_A^2} + 3\gamma\right)(\omega\tau_R)^2 - \tfrac{1}{2}i(\gamma-1)\frac{v_A^2}{\frac{c_0^2}{\gamma}+v_A^2}(\omega\tau_R)\right], \quad (5.2.44$$

where now $k_0^2 = \omega^2/c_R^2$, with c_R^2 given by (5.2.39). The waves propagate at slightly above the isothermal speed due to radiative effects and experience damping (for $\omega k_0 < 0$).

In these two limiting cases, we thus find that the damping per wavelength, D_ℓ, is given by

$$D_1 \sim \begin{cases} \frac{1}{2}\left(\frac{\gamma-1}{\gamma}\right)\frac{c_T^2}{c_0^2}(\omega\tau_R)^{-1}, & \omega\tau_R \gg 1, \\ \frac{1}{2}(\gamma-1)\dfrac{v_A^2}{\frac{c_0^2}{\gamma}+v_A^2}(\omega\tau_R), & \omega\tau_R \ll 1. \end{cases} \qquad (5.2.45)$$

The form of D_1 for general $\omega\tau_R$ is sketched in Figure 5.4. Again there is a maximum in the damping, which is greater the stronger the magnetic field.

5.2.4 Concluding Remarks

Radiative dissipation has a significant affect upon the nature of wave propagation in a flux tube. As a preliminary to investigating these effects, we derived (in Section 5.2) the dispersion relation for wave propagation in an unbounded medium. The presence of dissipation leads to temporal-damping of modes generated with a fixed wavenumber, and spatial-damping for modes generated at a fixed frequency. Concentrating on those modes with fixed wavenumber, we showed how the fast and slow mageto-acoustic waves are temporally-damped in an open atmosphere. Using the 'damping per period' D_p (Stein and Spiegel, 1967) as a measure of this damping, we showed that D_p has a maximum and that this maximum occurs when the sound and radiative timescales are comparable. Thus, those waves of wavelength the order of the distance traversed by a sound wave in a time 2π times the radiative timescale are the most severely damped.

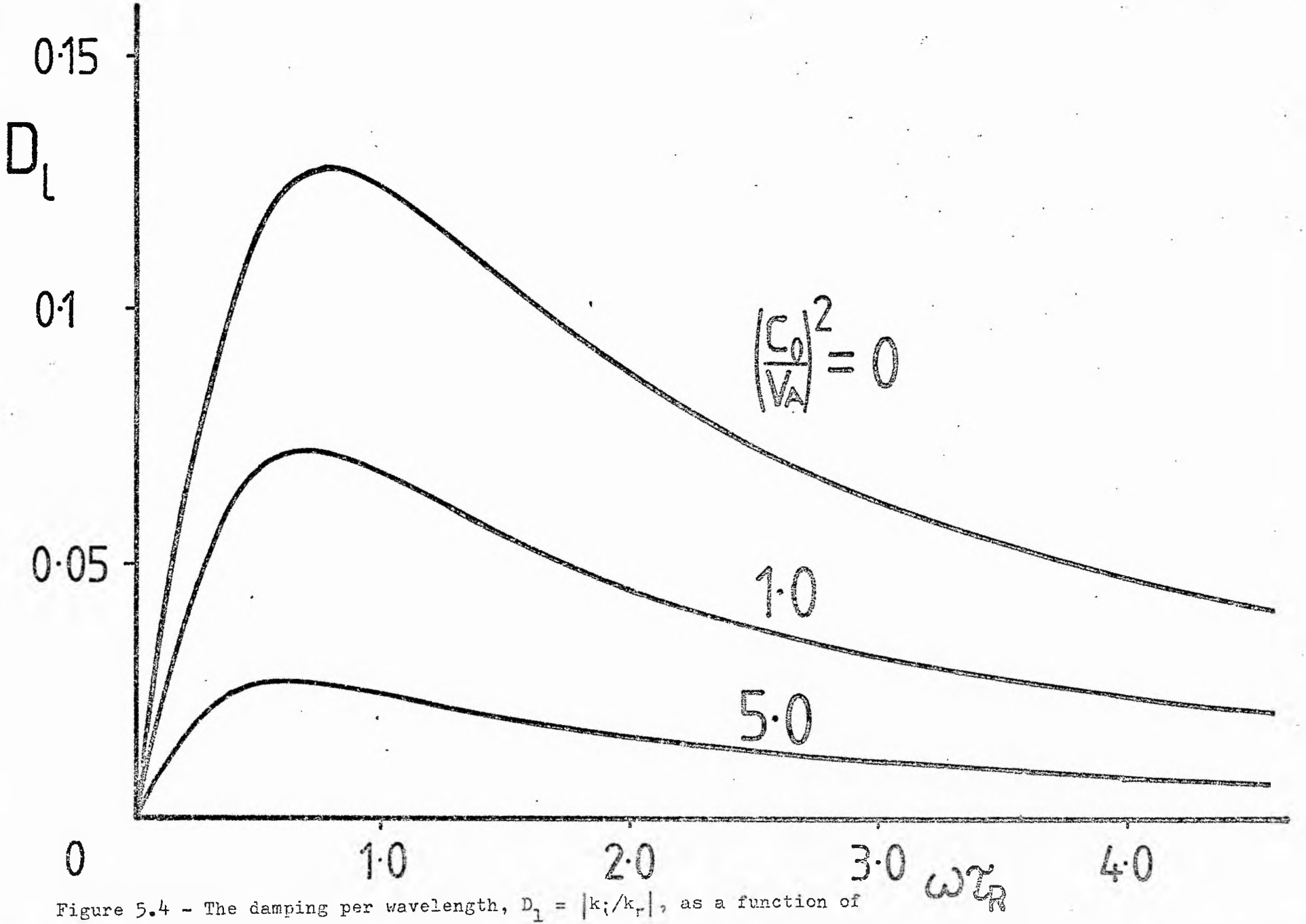

Figure 5.4 - The damping per wavelength, $D_l = |k_i/k_r|$, as a function of $\omega\tau_R$, the ratio of the radiative relaxation time to the period, for the

Turning to a flux tube we showed how the slow wave in a slender tube is damped by dissipation. The temporal-damping coefficient D_p again possesses a maximum when the sound and radiative timescales are comparable, and this damping is greater the stronger the magnetic field. The spatial-damping coefficient D_1 has much the same behaviour as D_p. In general terms, the qualitative behaviour of D_p and D_1 is comparable with the damping of sound waves in a uniform, unbounded, non-magnetic medium, with the tube speed c_T playing the role of the sound speed and c_R that of the isothermal sound speed $c_0/\gamma^{\frac{1}{2}}$.

As an illustration of the above results, we may consider how much a wave is attenuated, due to radiative effects, on propagating from the photosphere to the temperature minimum. Regarding τ_R and c_0 as given, it is a simple matter to show that $k_i c_0 \tau_R$ is an increasing function of $\omega\tau_R$, with the limits

$$k_i c_0 \tau_R \to \begin{cases} 0, & \text{as } \omega\tau_R \to 0, \\ \frac{1}{2}\left(\frac{\gamma-1}{\gamma}\right)\frac{c_T}{c_0}, & \text{as } \omega\tau_R \to \infty. \end{cases}$$

Thus, there is greater damping at the higher frequencies. For example, with $c_0 = v_A = 7.25$ km and $\tau_R = 80$s, as mean values for the sound and Alfvén speeds and radiative relaxation time inside the tube over the distance 0-500 km above $\tau_{5000} = 1$, the ratio of the amplitude of a wave at z = 500 km, to that at z = 0, namely $\exp(-500\, k_i)$, is 0.90 for a wave of frequency $\omega = 0.02\ s^{-1}$. The value of $k_i c_0 \tau_R$ increases for increasing magnetic field, but it is always less than than the value for vertically propagating sound waves in an open atmosphere (where $k_i c_0 \tau_R \to \frac{1}{2}(\gamma-1)$ as $\omega\tau_R \to \infty$). Thus, in this special case, for a given τ_R, the attenuation in a thin tube due to radiative effects is not so great as that

for sound waves in an open atmosphere.

However, care must be taken in applying the results obtained for a uniform atmosphere-such as in the above - to the highly-stratified atmosphere of the Sun. Indeed, as Souffrin (1972) has pointed out, an analysis such as the above would, if applied too literally, lead one to the erroneous conclusion that high frequencies are not damped (since $D_1 \to 0$ as $\omega\tau_R \to \infty$). It is important, then, to consider the nature of radiative dissipation in a stratified atmosphere. With the necessary preliminaries of a uniform medium dispensed with, we turn in the following section to an investigation of the more realistic stratified atmosphere.

5.3 Propagation in a Stratified Atmosphere

5.3.1 Introduction

Following the method presented in Chapter 3, we shall consider the effect of dissipation on the wavemodes in a slender flux tube in a stratified medium, paying particular attention to an isothermal atmosphere. The equations governing the motions are (5.2.1) - (5.2.6) with the gravitational term ρg added to the right-hand side of (5.2.2). In a cylindrical coordinate system (r,θ,z), in which there is no azimuthal dependence, each of the physical variables is expanded in its Maclaurin series about $r = 0$, retaining the zeroth order terms ($r \to 0$) and resulting in a set of non-linear equations describing vertical motions.

The equilibrium of such a flux tube, which has been described in detail in Chapter 3, is given by

$$p_0' = -\rho_0 g, \quad \mathcal{L}(\rho_0, T_0) = 0, \quad p_0 = \frac{R}{\mu}\rho_0 T_0, \qquad (5.3.1)$$

where a dash denotes differentiation with respect to the (vertical) z-axis. In addition, the interior of the flux tube is related to its environment by the pressure balance condition

$$p_0(z) + \frac{B_0^2(z)}{2\mu_0} = p_e(z) \ , \qquad (5.3.2)$$

where p_e is the gas pressure in the external field-free medium.

Linearizing the equations of motion about the basic state described above gives

$$\rho_0 \frac{\partial v}{\partial t} = - \frac{\partial p}{\partial z} - \rho g \ , \qquad (5.3.3)$$

$$\frac{\partial p}{\partial t} + p_0' v = \frac{\gamma p_0}{\rho_0} \left(\frac{\partial \rho}{\partial t} + \rho_0' v \right) + (\gamma - 1) \rho_0 \left(\ell_\rho \rho + \ell_T T \right) \ , \qquad (5.3.4)$$

$$B_0 \frac{\partial \rho}{\partial t} - \rho_0 \frac{\partial b_z}{\partial t} + (B_0 \rho_0' - B_0' \rho_0) v + \rho_0 B_0 \frac{\partial v}{\partial z} = 0 \ , \qquad (5.3.5)$$

$$\frac{p}{p_0} = \rho/\rho_0 + T/T_0 \ , \qquad (5.3.6)$$

where v, p, ρ, b_z and T refer to the perturbations, and the subscript zero denotes equilibrium quantities.

Assuming that the pressure perturbation in the exterior is negligible, the radial component of the momentum equation gives

$$p + \frac{B_0(z)}{\mu_0} b_z = 0 \ . \qquad (5.3.7)$$

The validity of such an approximation has been discussed in some detail in Chapter 3 (see also Wilson, 1979b; Roberts, 1980b).

Now, for perturbations obeying Newton's law of cooling (Equations (5.2.8) and (5.2.9)) the energy equation may be written in the form

$$\frac{\partial p}{\partial t} + p_0' v = c_0^2\left(\frac{\partial \rho}{\partial t} + \rho_0' v\right) - \frac{p_0}{\tau_R}\left(\frac{p}{p_0} - \frac{\rho}{\rho_0}\right). \qquad (5.3.8)$$

The assumption of optically-thin perturbations is justified for all layers of the solar photosphere and chromosphere having an optical depth $\tau < 1$ at the wavelengths concerned (Bray and Loughhead, 1974). However, the use of Equation (5.2.8) in the case of a stratified atmosphere is strictly justified only if the vertical scale of the perturbation is small compared to the local scale-height of the atmosphere (Thomas et al, 1971). Nevertheless, estimates of the effect of radiative transfer on motions using Newton's law of cooling have been made by a number of authors (Noyes and Leighton, 1963; Souffrin, 1966, 1972; Stix, 1970; Ulmschneider, 1971; Schmidt and Stix, 1973; Clark and Clark, 1973), and we shall use the approximation to investigate the damping of modes in a flux tube.

With time-dependence of the form $e^{i\omega t}$, Equations (5.3.3), (5.3.5), (5.3.7) and (5.3.8) may be combined to give a second-order differential equation for the velocity amplitude $\hat{v}(z)$, defined by $v = \hat{v}(z)e^{i\omega t}$, namely

$$\left[\frac{d}{dz} + \left(\frac{i\omega\gamma\tau_R + \gamma}{i\omega\gamma\tau_R + 1}\right)\frac{g}{c_0^2}\right]\left[\frac{\frac{d\hat{v}}{dz} - \left(\frac{B_0'}{B_0} - \frac{\rho_0'}{\rho_0} - \frac{i\omega\gamma\tau_R}{1+i\omega\gamma\tau_R}\left(\frac{N_0^2}{g}\right)\right)\hat{v}}{\frac{i\omega}{\rho_0 c_0^2}\left(\frac{i\omega\gamma\tau_R+\gamma}{1+i\omega\gamma\tau_R} + \frac{c_0^2}{v_A^2}\right)}\right] +$$

$$+ \frac{\rho_0}{i\omega}\left(\omega^2 - \frac{i\omega\gamma\tau_R N_0^2}{1+i\omega\gamma\tau_R}\right)\hat{v} = 0, \qquad (5.3.9)$$

where N_0 is the Brunt-Väisälä (buoyancy) frequency defined by

$$N_0^2 = -g\frac{\rho_0'}{\rho_0} - \frac{g^2}{c_0^2} .$$

It is convenient to consider Equation (5.3.9) under a number of simplifications. Firstly, we shall suppose that in the absence of any disturbances the flux tube is in temperature balance with its surroundings. The equilibrium is then completely characterized by the scale-height $\Lambda_0 \equiv RT_0(z)/\mu g$ (see Chapter 3). Secondly, we shall suppose that both the adiabatic exponent γ and the radiative coefficient τ_R are independent of z. The latter assumption deserves some comment. In fact, τ_R is not constant in the solar atmosphere but varies rapidly with height (primarily due to the rapid decrease of the opacity). We are thus neglecting the effect of a gradient in τ_R; we may, however, allow for the variation of τ_R with height in an approximate fashion by treating that variation in a 'local approximation' (see, for example, Souffrin (1972)).

With the above assumptions, Equation (5.3.9) may be written in the form

$$\frac{d^2\hat{v}}{dz^2} + \left(\alpha_1 + \left(\frac{1-i\Omega}{1+\Omega^2}\right)\alpha_2\right)\frac{d\hat{v}}{dz} + \left(\beta_1 + \left(\frac{1-i\Omega}{1+\Omega^2}\right)\beta_2\right)\hat{v} = 0 , \qquad (5.3.10)$$

where $\Omega = \gamma\omega\tau_R$, and

$$\left.\begin{aligned} \alpha_1 &= -\frac{1}{2\Lambda_0} , \quad \alpha_2 = -\frac{\Lambda_0'}{\Lambda_0} , \quad \beta_1 = \frac{\omega^2 - N_0^2}{c_T^2} + (1-\tfrac{1}{2}\gamma)\frac{N_0^2}{c_0^2} , \\ \beta_2 &= \left(\frac{\gamma-1}{\gamma}\right)\left[\frac{\omega^2}{g\Lambda_0} + \frac{1}{\Lambda_0^2}\left(\frac{c_0^2}{\gamma v_A^2} + \frac{1}{2}\right)\right] + \frac{\Lambda_0'}{\Lambda_0^2}\left(\frac{c_0^2}{\gamma v_A^2} + 1\right) - \left(\frac{\Lambda_0'}{\Lambda_0}\right)' . \end{aligned}\right\} \qquad (5.3.11)$$

In the adiabatic limit ($\omega\tau_R \to \infty$) Equation (5.3.10) reduces to

$$\frac{d^2\hat{v}}{dz^2} - \frac{1}{2\Lambda_0}\frac{d\hat{v}}{dz} + \left[\frac{\omega^2 - N_0^2}{c_T^2} + (1 - \tfrac{1}{2}\gamma)\frac{N_0^2}{c_0^2}\right]\hat{v} = 0 ,$$

which is Equation (3.3.57) of Chapter 3.

In the stratified atmosphere of the Sun, the radiative decay time, τ_R, is not constant and, in fact, varies rapidly with height (Stix, 1970; Bray and Loughhead, 1974). However, it is worthwhile to investigate Equation (5.3.10), in which τ_R is constant, in order to gain some qualitative insight into the effect of radiative damping in a slender flux tube. Further, we shall consider an isothermal atmosphere, which is a reasonable approximation for the region with which we are concerned (from about $\tau_{5000} = 1$ to $\tau_{5000} = 5 \times 10^{-4}$).

5.3.2 Isothermal Atmosphere

For an isothermal atmosphere ($\Lambda_0' \equiv 0$) the governing equation is

$$\frac{d^2\hat{v}}{dz^2} - \frac{1}{2\Lambda_0}\frac{d\hat{v}}{dz} + \left[\frac{\omega^2 - N_0^2}{c_T^2} + (1-\tfrac{1}{2}\gamma)\frac{N_0^2}{c_0^2} + \frac{1-i\Omega}{1+\Omega^2}\left[\frac{\gamma-1}{\gamma\Lambda_0}\left(\frac{\omega^2}{g} + \frac{1}{\Lambda_0}\left(\frac{c_0^2}{\gamma v_A^2} + \tfrac{1}{2}\right)\right)\right]\right]\hat{v} = 0, \qquad (5.3.12)$$

In the absence of gravity, (5.3.12) reduces to

$$\frac{d^2\hat{v}}{dz^2} + \left[\frac{\omega^2}{c_T^2} + \left(\frac{1-i\Omega}{1+\Omega^2}\right)(\gamma-1)\frac{\omega^2}{c_0^2}\right]\hat{v} = 0 , \qquad (5.3.13)$$

with solutions $\exp^{\pm}ikz$, where k satisfies

$$(c_0^2 + v_A^2)\omega^3 - \frac{i}{\tau_R}\left(\frac{c_0^2}{\gamma} + v_A^2\right)\omega^2 - k^2c_0^2v_A^2\omega + \frac{i}{\gamma\tau_R}k^2c_0^2v_A^2 = 0 . \qquad (5.3.14)$$

This is simply the dispersion relation (5.2.34). Thus, the zero gravity limit of the slender flux tube approximation gives the same dispersion relation as the one obtained for the thin flux tube limit of the zero gravity case.

Returning to Equation (5.3.12), and noting that c_0^2/v_A^2 is a constant for $\Lambda_0 = \Lambda_e$ (see Chapter 3), we see that Q, defined by $Q = \hat{v}\exp(-\frac{z}{4\Lambda_0})$, satisfies

$$Q'' + (a + ib)Q = 0 , \tag{5.3.15}$$

where

$$\left.\begin{aligned} a &= \frac{\omega^2}{c_T^2} - \frac{1}{\Lambda_0^2}\left((\tfrac{\gamma-1}{\gamma})\frac{c_0^2}{v_A^2} - \tfrac{1}{2}\right) - \frac{9}{16\Lambda_0^2} - \frac{b}{\Omega} , \\ b &= -\frac{1}{\Lambda_0^2}(\tfrac{\gamma-1}{\gamma})\frac{\Omega}{1+\Omega^2}\left(\omega^2\frac{\Lambda_0}{g} + \frac{c_0^2}{\gamma v_A^2} + \tfrac{1}{2}\right) . \end{aligned}\right\} \tag{5.3.16}$$

Equation (5.3.15) has solutions $\exp^{\pm}ikz$, where

$$k^2 = a + ib . \tag{5.3.17}$$

For ω^2 real, k^2 is in general complex, but in the <u>adiabatic</u> limit it is real and given by

$$k^2 = \frac{\omega^2}{c_T^2} - \left(\frac{9}{16} - \frac{1}{2\gamma} + (\tfrac{\gamma-1}{\gamma^2})\frac{c_0^2}{v_A^2}\right)\frac{1}{\Lambda_0^2} . \tag{5.3.18}$$

Thus, adiabatic propagation ($k^2 > 0$) in an isothermal atmosphere occurs for $\omega^2 > \omega_v^2$, with ω_v defined in Section 5.1:

$$\omega_v^2 = \frac{c_T^2}{\Lambda_0^2}\left(\frac{9}{16} - \frac{1}{2\gamma} + (\tfrac{\gamma-1}{\gamma^2})\frac{c_0^2}{v_A^2}\right). \tag{5.3.19}$$

(The tube cut-off frequency ω_v, and its generalization to a non-isothermal atmosphere, has been discussed in detail in Chapter 3.)

Spatial Damping

We shall now consider the case of real ω^2 and finite τ_R. In the presence of damping k is complex and the modes are no longer purely stationary or progressive. The modes which were formerly progressive now show spatial damping, due to the conversion of mechanical energy into heat, and the modes which were non-progressive are modified in such a way that they can carry enough energy to balance the dissipation (Schatzman and Souffrin, 1967). This may be illustrated by considering the form of (5.3.17) for large and small radiative decay times.

It is convenient to introduce the time-scale $\tau_s \equiv \Lambda_0/c_0$, as the time for a sound wave to travel a scale-height Λ_0. (In an intense flux tube τ_s is about 14s.) Then Equation (5.3.17), for $\tau_R \gg \tau_s$ (more strictly, $\left|\omega^2 - \omega_v^2\right| \frac{\Lambda_0}{g}\tau_R \gg \tau_s$), yields

$$k \approx k_0 \left[1 - \frac{i\left(\frac{\gamma-1}{\gamma}\right)\left[\omega^2 \frac{\Lambda_0}{g} + \left(\frac{c_0^2}{\gamma v_A^2} + \frac{1}{2}\right)\right]}{\frac{2\omega\Lambda_0^2}{g c_0}\left(1 + \frac{c_0^2}{v_A^2}\right)(\omega^2 - \omega_v^2)} \left(\frac{\tau_s}{\tau_R}\right) \right], \qquad (5.3.20)$$

where

$$k_0^2 = (\omega^2 - \omega_v^2)/c_T^2 \ .$$

The modes which were progressive in the absence of dissipation ($\omega > \omega_v$, k_0 real) are now attenuated, whilst those which were formerly evanescent ($\omega < \omega_v$, k_0 imaginary) now propagate. Similarly, for $\tau_R \ll \tau_s$, ($\omega^2 \neq \omega_v^{*2}$), (5.3.17) gives

$$k \approx k_0^* \left\{ 1 - \frac{i(\gamma-1)\,\frac{\omega\Lambda_0}{c_0}\left[\frac{\omega^2\Lambda_0}{g} + \frac{c_0^2}{\gamma v_A^2} + \frac{1}{2}\right]\left(\frac{\tau_R}{\tau_s}\right)}{\frac{2\Lambda_0}{g}\left(1 + \frac{c_0^2}{\gamma v_A^2}\right)(\omega^2 - \omega_v^{*2})} \right\} , \qquad (5.3.21)$$

where

$$\omega_v^{*2} = \frac{g}{16\Lambda_0\left(1 + \frac{c_0^2}{\gamma v_A^2}\right)} , \quad k_0^{*2} = \frac{1}{g\Lambda_0}\left(1 + \frac{c_0^2}{\gamma v_A^2}\right)(\omega^2 - \omega_v^{*2}) .$$

That is, in the isothermal limit ($\tau_R/\tau_s \to 0$), where there is propagation for frequencies greater than a critical value, ω_v^* ($\omega_v^* < \omega_v$), the effect of a non-zero value of the radiative decay time is to introduce a small amount of damping to those modes that were propagating ($\omega > \omega_v^*$) and those that were evanescent in the isothermal limit now propagate.

Returning to the general relation (5.3.17), we have the problem of choosing the correct sign for $k = k_r + ik_i$. We shall consider vertically propagating waves so that $\omega k_r < 0$, which implies that $k_i > 0$ and the waves are damped. The imaginary part of the wave number, k_i, may be shown (from (5.3.17) to satisfy

$$2k_i^2 = -a + (a^2 + b^2)^{\frac{1}{2}} , \qquad (5.3.22)$$

with a and b given by Equation (5.3.16). The quantity $\Lambda_0 k_i$ is a measure of the damping per scale-height. In the high-frequency limit ($\omega\tau_s \gg 1$), (5.3.22) gives

$$\Lambda_0 k_i \sim \frac{1}{2}\left(\frac{\gamma-1}{\gamma}\right)\frac{c_T}{c_0}\left(\frac{\tau_s}{\tau_R}\right) , \qquad (5.3.23)$$

showing heavy damping at high frequencies for small radiative decay times, with the damping being greater for a stronger field. The corresponding solution for the disturbance Q is

$$Q \sim \exp\left(-\tfrac{1}{2}\left(\frac{\gamma-1}{\gamma}\right)\frac{c_T}{c_0}\frac{\tau_s}{\tau_R}\frac{z}{\Lambda_0}\right)\exp i\omega\left(t-\frac{z}{c_T}\right),$$

which represents wave-propagation at a phase-speed $c_T = c_0 v_A/(c_0^2+v_A^2)^{\frac{1}{2}}$, but subject to spatial damping.

The behaviour of $\Lambda_0 k_i$ as a function of $\omega\tau_s$ is given in Figure 5.5. For $\tau_R \ll \tau_s$, the damping per scale-height decreases from $\frac{1}{4}$ at $\omega\tau_s = 0$ to a minimum value and then increases monotonically to its value at infinity, the high frequency limit being greater for smaller τ_R/τ_s. There is an intermediate range of frequencies for which the damping remains small for $\tau_R \ll \tau_s$. For $\tau_R \gg \tau_s$, $\Lambda_0 k_i$ increases to a maximum and then decreases to its high frequency limit, with the damping being small for frequencies greater than about ω_v.

In the non-dissipative case, the normal modes fall into two categories: progressive modes ($k_i = 0$, $k_r \neq 0$) and evanescent modes ($k_r = 0$, $k_i \neq 0$). In the presence of dissipation it is not possible to divide the modes into these categories, since $k_r k_i \neq 0$. However, by Equation (5.3.17), $k_r^2 - k_i^2 = a(k,\omega)$, the equation $a = 0$ gives a convenient division between the two modes, with $a < 0$ characterizing modified decaying modes ($k_i^2 > k_r^2$) and $a > 0$ characterizing damped progressive modes ($k_r^2 > k_i^2$).

The condition $a = 0$ may be written as a quadratic in ω^2:

$$\omega^2(\omega^2 - \omega_v^2) + \frac{1}{\gamma^2\tau_R^2}\left(\omega^2 + (\gamma-1)\omega^2\frac{c_T^2}{c_0^2} - \frac{c_T^2}{16\Lambda_0^2}\right) = 0, \quad (5.3.24)$$

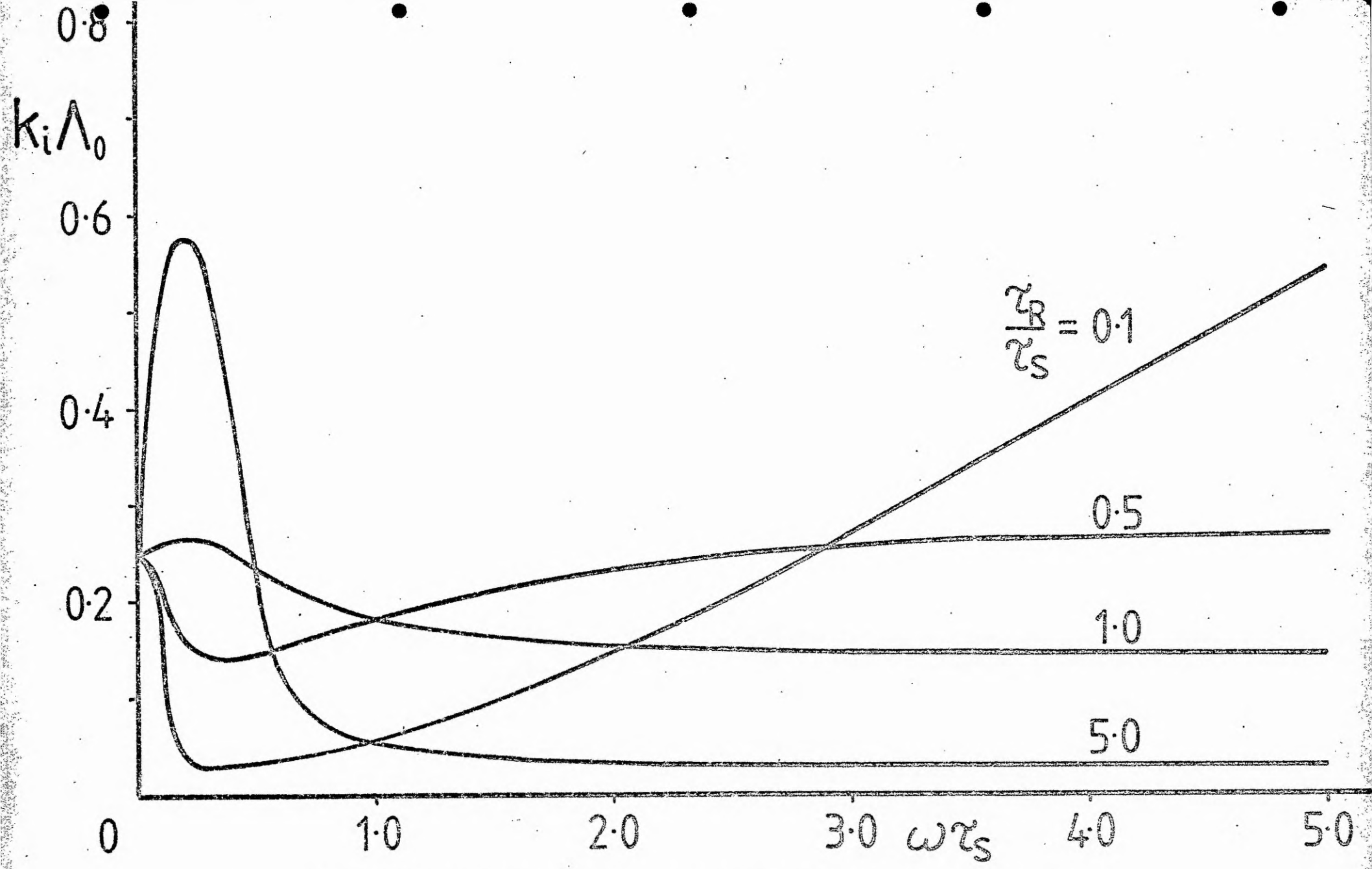

Figure 5.5 - The damping per scale-height, $k_i\Lambda_0$, as a function of $\omega\tau_s$ ($=\omega\Lambda_0 c_0$). Each solution is characterized by its value of τ_R/τ_s and

where the tube cut-off frequency ω_v is defined in (5.3.19). Equation (5.3.24) has one positive real root, ω^2_{vc}, for ω^2. Thus we have obtained a generalization of Defouw's result (5.3.19) to the case of finite radiative decay time. For $\omega^2 > \omega^2_{vc}$, the waves are mainly progressive, whereas for $\omega^2 < \omega^2_{vc}$, the waves are mainly damped. The curve $\omega^2 = \omega^2_{vc}$ is plotted in Figure 5.6a using local values of τ_R and Λ_0, calculated from the HSRA (Gingerich et al, 1971). It should be compared with the adiabatic case, sketched from (5.3.19) using local values of Λ_0. As may be readily seen, the difference between the adiabatic and dissipative curves occurs principally in the first few scale heights above $\tau_{5000} = 1$.

We should note that in applying our results to the solar atmosphere, it was necessary to assume a form for the density dependence of the mean opacity $\chi = \kappa/\rho$. Writing $\chi = \chi_0 \rho^\lambda T^\nu$, we have

$$\tau_R = \left(\frac{\rho_e}{\rho_0}\right)^\lambda \tau_{Re}$$

where τ_{Re} refers to the radiative decay time of the external atmosphere, that is

$$\tau_R = \left(1 + \tfrac{1}{2}\gamma \frac{v_A^2}{c_0^2}\right)^\lambda \tau_{Re} \quad .$$

The values of λ and ν depend upon the ranges of density and temperature. Although we are assuming temperature equality, the densities inside and outside the tube will be different. However, we shall assume that the same approximate law holds in the interior in order that we may see how the magnetic field

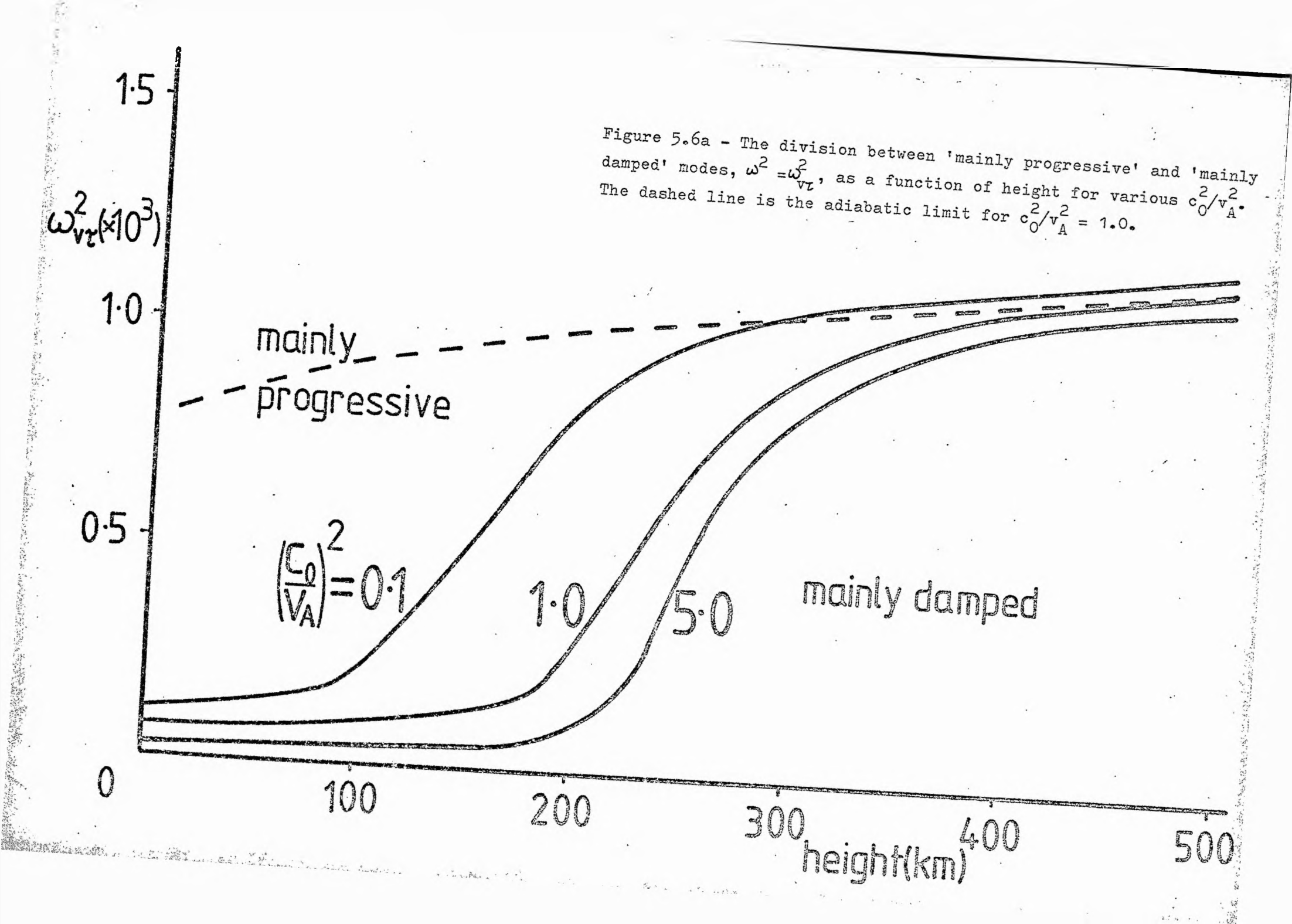

Figure 5.6a - The division between 'mainly progressive' and 'mainly damped' modes, $\omega^2 = \omega^2_{vt}$, as a function of height for various c_0^2/v_A^2. The dashed line is the adiabatic limit for $c_0^2/v_A^2 = 1.0$.

modifies the motions. In this end subsequent sections we shall take $\lambda = 0.5$ (Tayler, 1970), so that a stronger field leads to an increase in τ_R.

Figure 5.6a shows that the effect of radiative damping is very important in the upper photosphere, but by a height of 500 km above $\tau_{5000} = 1$ its effect on wave propagation is negligible. Modes which were previously evanescent in the upper photosphere now propagate. The boundary a = 0 should be considered as the middle of a broad band of frequencies separating the two types of mode. Figure 5.6b illustrates the variation with height of the amplitude of a wave (normalized so that $|v| = 1$ at $z = 0$) in the adiabatic and dissipative cases, for $\omega = 0.10 s^{-1}$ and $\omega = 0.02 s^{-1}$. In the adiabatic case, for a wave with frequency $\omega > \omega_v$ ($\approx 0.03 s^{-1}$) the amplitude grows with height as $\exp(z/4\Lambda_0)$, so that at $z = 500$ km, $|v| \approx 3.5\,|v(0)|$. The amplitude of an evanescent wave ($\omega < \omega_v$) will not increase so quickly with height, and may possibly decrease for ω sufficiently small (for example, with $\omega = 0.02 s^{-1}$ $|v| \approx 0.19\,|v(0)|$ at $z = 500$ km). With a finite radiative relaxation time the amplitude of a (formerly) propagating wave is <u>decreased</u> (for $\omega = 0.1 s^{-1}$, $|v| \approx 2.3\,|v(0)|$ at $z = 500$ km). However the amplitude ratio of the evanescent mode is <u>greater</u> than in the adiabatic limit (with $\omega = 0.02 s^{-1}$. $|v| \approx 0.47\,|v(0)|$ at $z = 500$ km). This results from the fact that in the low photosphere the wave is propagating and so initially grows as $\exp(z/4\Lambda_0)$. Thus, <u>the effect of radiative relaxation on propagating modes</u> ($\omega > \omega_v$) <u>is to decrease the amplitude, whilst the amplitude of evanescent</u> ($\omega < \omega_v$) <u>modes is increased</u>.

Figure 5.6b - The variation with height of the amplitude (normalized to unity at z = 0) for waves with frequency $\omega = 0.10s^{-1}$ and $\omega = 0.025s$. The dashed lines indicate the adiabatic limits and we have taken $c_0 = v_A$.

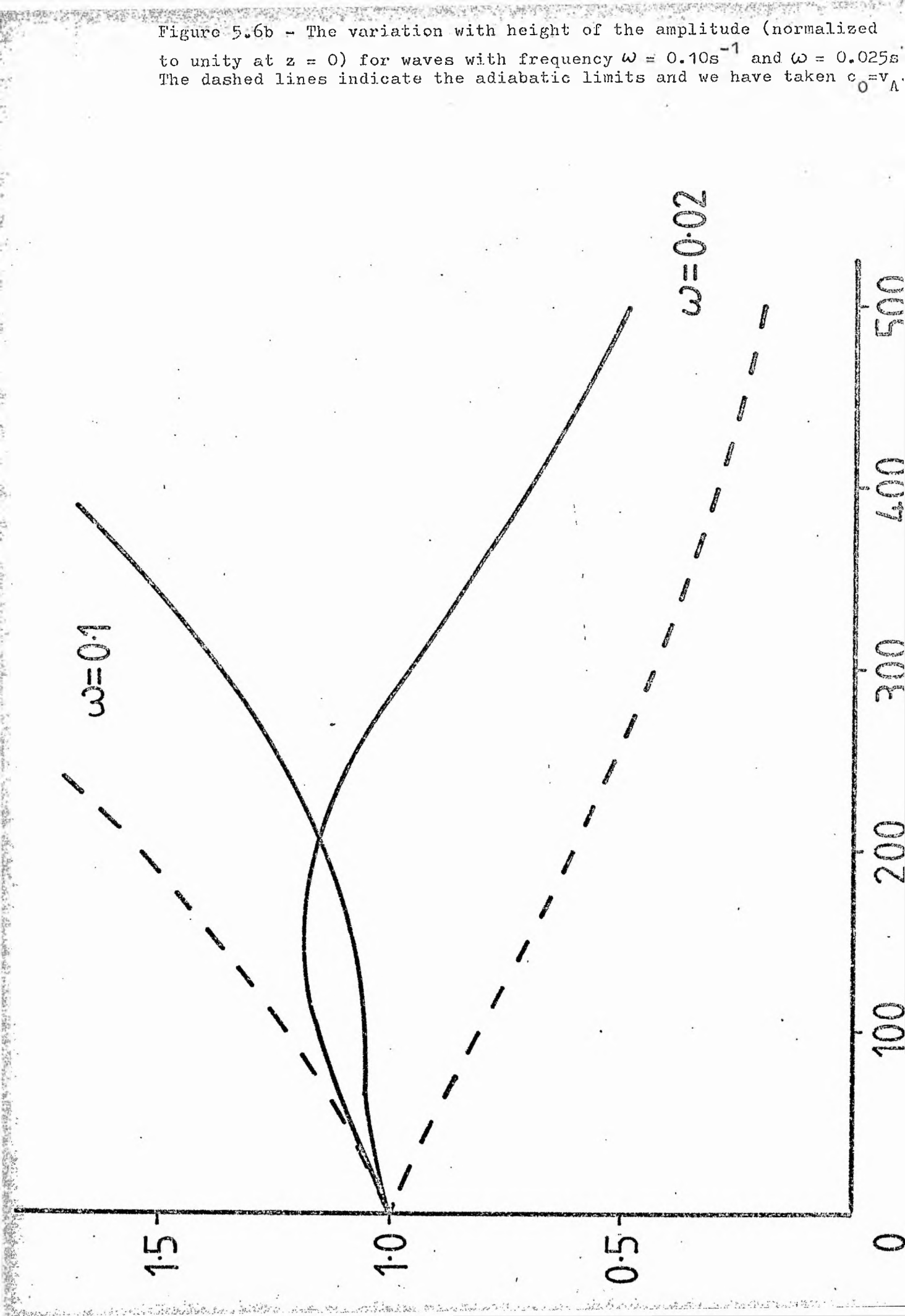

Phase and Amplitude relations

In this section we shall present results concerning the phase shift between velocity oscillations at two different levels, and the phase and amplitude relations between temperature and velocity at one height. The results are related to the observations in Section 5.3.3.

(a) Velocity-Velocity Phase Shifts

The amplitude ratio, $\hat{v}_2/\hat{v}_1$, of the velocity at two different levels z_1 and z_2, is given by

$$\frac{\hat{v}_2}{\hat{v}_1} = \exp\left[\left(\frac{1}{4\Lambda_0} - k_i\right)(z_2 - z_1)\right] \exp\left[ik_r(z_2 - z_1)\right] ,$$

and hence the phase-shift ϕ is

$$\phi(z_1, z_2; \omega) = (z_2 - z_1)k_r .$$

Taking mean values of Λ_0 and τ_R for the flux tube over the interval $z_1 \leq z \leq z_2$, we may calculate ϕ as a function of frequency. The phase-shift between velocities one scale-height apart (i.e. $z_2 - z_1 = \Lambda_0$) is sketched in Figure 5.7 for various τ_R.

(b) Temperature-Velocity Relations

The temperature and velocity perturbations may be shown, by Equations (5.3.3) - (5.3.7), to be related by

$$-\frac{1}{(\gamma-1)}\left(i\delta\omega + \frac{1}{\tau_R} + \frac{\gamma v_A^2}{c_0^2}\left(i\omega + \frac{1}{\tau_R}\right)\right)\frac{\Lambda_0}{c_0}\left(\frac{T}{T_0}\right) = \left(1+\frac{\gamma}{2}\frac{v_A^2}{c_0^2}\right)\frac{\hat{v}}{c_0} + \frac{\gamma\Lambda_0 v_A^2}{c_0^3}\frac{d\hat{v}}{dz} \quad (5.3.$$

Assuming solutions of the form $\frac{T}{T_0} \sim \exp(ikz + \frac{z}{4\Lambda_0})$ and $\frac{\hat{v}}{c_0} \sim \exp(ikz + \frac{z}{4\Lambda_0})$, Equation (5.3.25) may be written in the

Figure 5.7 - The phase-shift, $\Lambda_0 k_r$, between velocities at one scale-he
apart as a function of $\omega\tau_s (= \omega\Lambda_0/c_0)$ for various τ_R/τ_s, and $c_0 = v_A$.
straight line corresponds to the tube wave $\omega = kc_T$ and the dashed line
the adiabatic limit ($\tau_R/\tau_s \to \infty$).

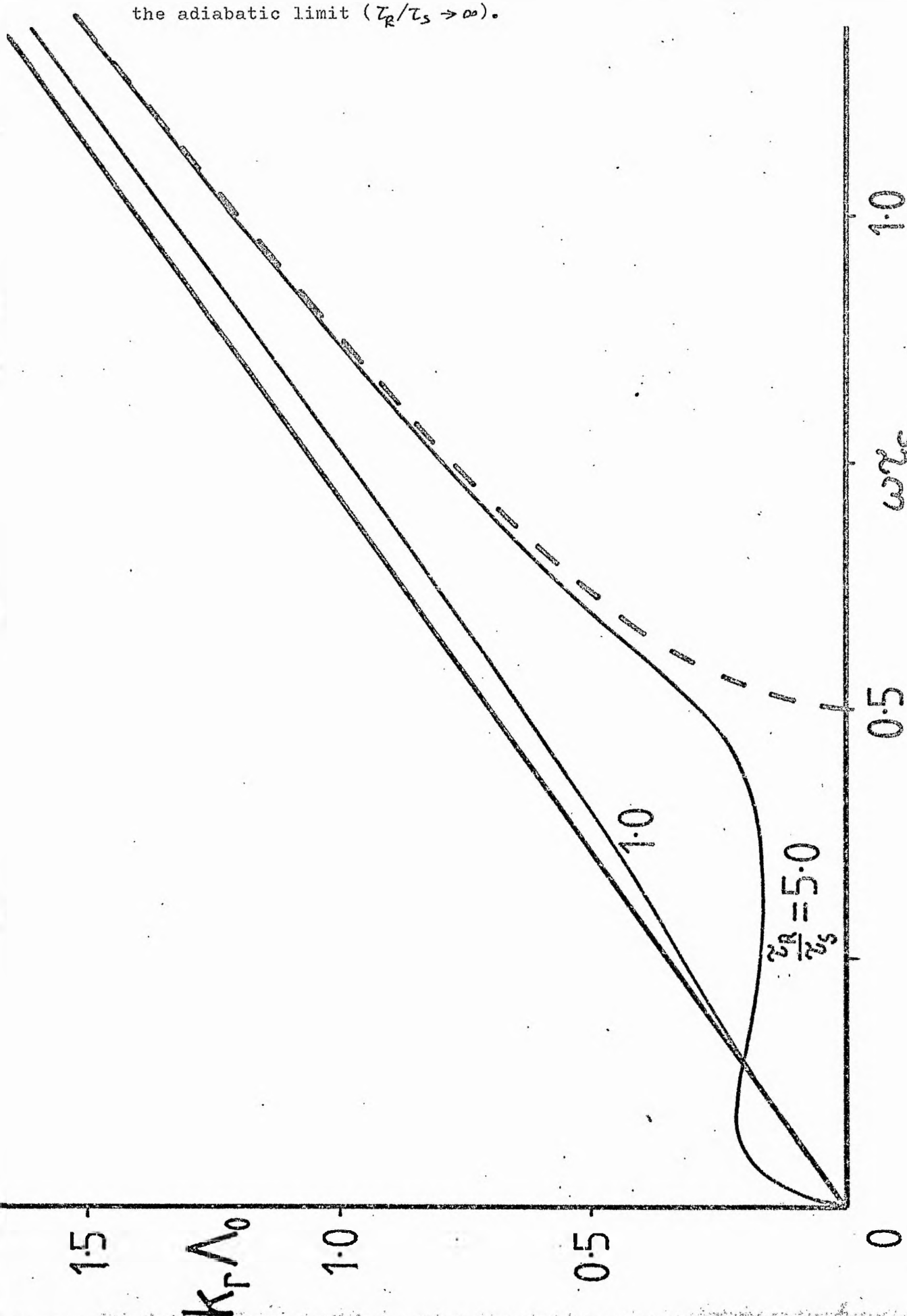

convenient form

$$\frac{T}{T_0} = re^{i\phi}\left(\frac{\hat{v}}{c_0}\right) , \tag{5.3.26}$$

where

$$re^{i\phi} = - \frac{(\gamma - 1)\left(\frac{3}{4} + \frac{c_0^2}{\gamma v_A^2} + ik\Lambda_0\right)\frac{c_0}{\Lambda_0}}{\frac{c_0^2}{v_A^2}\left(i\omega + \frac{1}{\gamma\tau_R}\right) + i\omega + \frac{1}{\tau_R}} , \tag{5.3.27}$$

with k given by Equation (5.3.17)

We shall consider only the case of real frequencies, with the modes being damped in space, so that $k_i > 0$ and $\omega k_r < 0$.

For adiabatic propagation, the phase ϕ and amplitude r are given by

$$\omega < \omega_v \ : \ \phi = \pi/2 , \quad r = \frac{(\gamma-1)c_0}{\omega\left(1+\frac{c_0^2}{v_A^2}\right)\Lambda_0}\left(\frac{c_0^2}{\gamma v_A^2} + \frac{3}{4} - \Lambda_0|k_0|\right) , \tag{5.3.28}$$

$$\omega > \omega_v \ : \ re^{i\phi} = \frac{(\gamma-1)c_0}{\omega\left(1+\frac{c_0^2}{v_A^2}\right)\Lambda_0}\left(\Lambda_0|k_0| + i\left(\frac{3}{4} + \frac{c_0^2}{v_A^2}\right)\right), \tag{5.3.29}$$

where k_0 is given by Equation (5.3.20), and in (5.3.29) we have chosen the negative root of k_0^2 corresponding to an upward propagating wave (for ω assumed positive).

Returning to the general expression (5.3.27), we find that for low frequencies ($\omega\tau_s \ll 1$)

$$\phi \sim \pi, \quad r \sim \frac{(\gamma - 1)}{\left(1 + \frac{c_0^2}{\gamma v_A^2}\right)} \left(\frac{1}{2} + \frac{c_0^2}{\gamma v_A^2} \right) \frac{\tau_R}{\tau_s} .$$

That is, at low frequencies, the amplitude of the temperature perturbation relative to the velocity perturbation is very large for $\tau_R \gg \tau_s$. For high frequencies ($\omega\tau_s \gg 1$)

$$\phi \sim 0, \quad r \sim \frac{(\gamma - 1)}{\left(1 + \frac{c_0^2}{v_A^2}\right)^{\frac{1}{2}}} ,$$

showing that the amplitude tends to a constant value, independent of τ_R.

The phase difference ϕ and amplitude r are plotted in Figures 5.8 and 5.9 as functions of height in the solar atmosphere, using local values of the scale-height and radiative relaxation time. Figure 5.8 shows that the higher frequencies have a lower phase difference, with the difference tending to zero as the frequency tends to infinity. The phase difference is greater than the adiabatic value, but is reduced for a stronger magnetic field. The amplitude (see Figure 5.9) is decreased from its adiabatic value by radiative effects, and is greater at lower frequencies for large τ_R/τ_s. This is in contrast to the results for purely vertical motion in a non-magnetic region (see Noyes and Leighton, 1963), where the amplitude is small for low frequencies. The difference is due to the fact that the motion in the magnetic flux tube is not purely vertical.

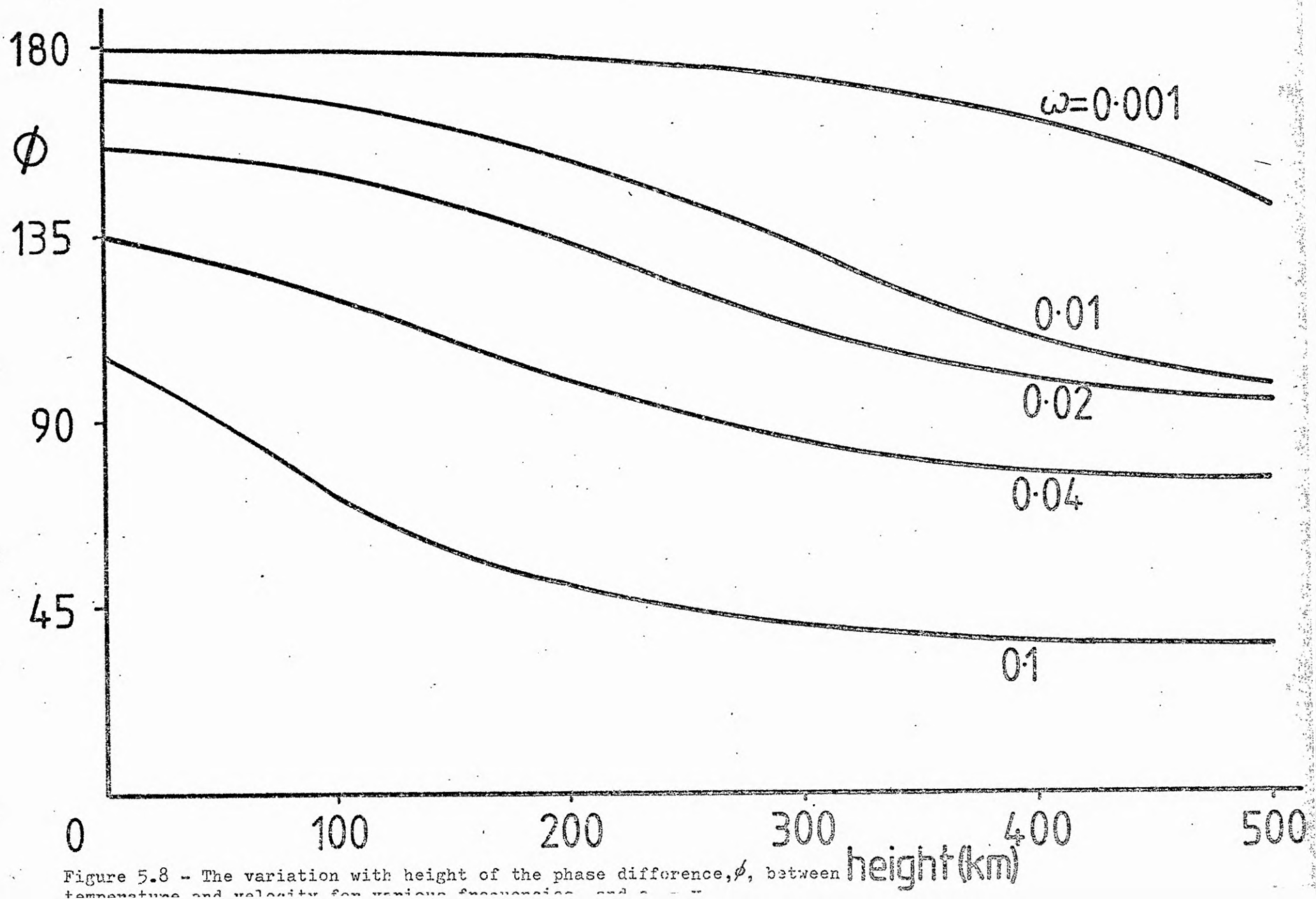

Figure 5.8 - The variation with height of the phase difference, ϕ, between

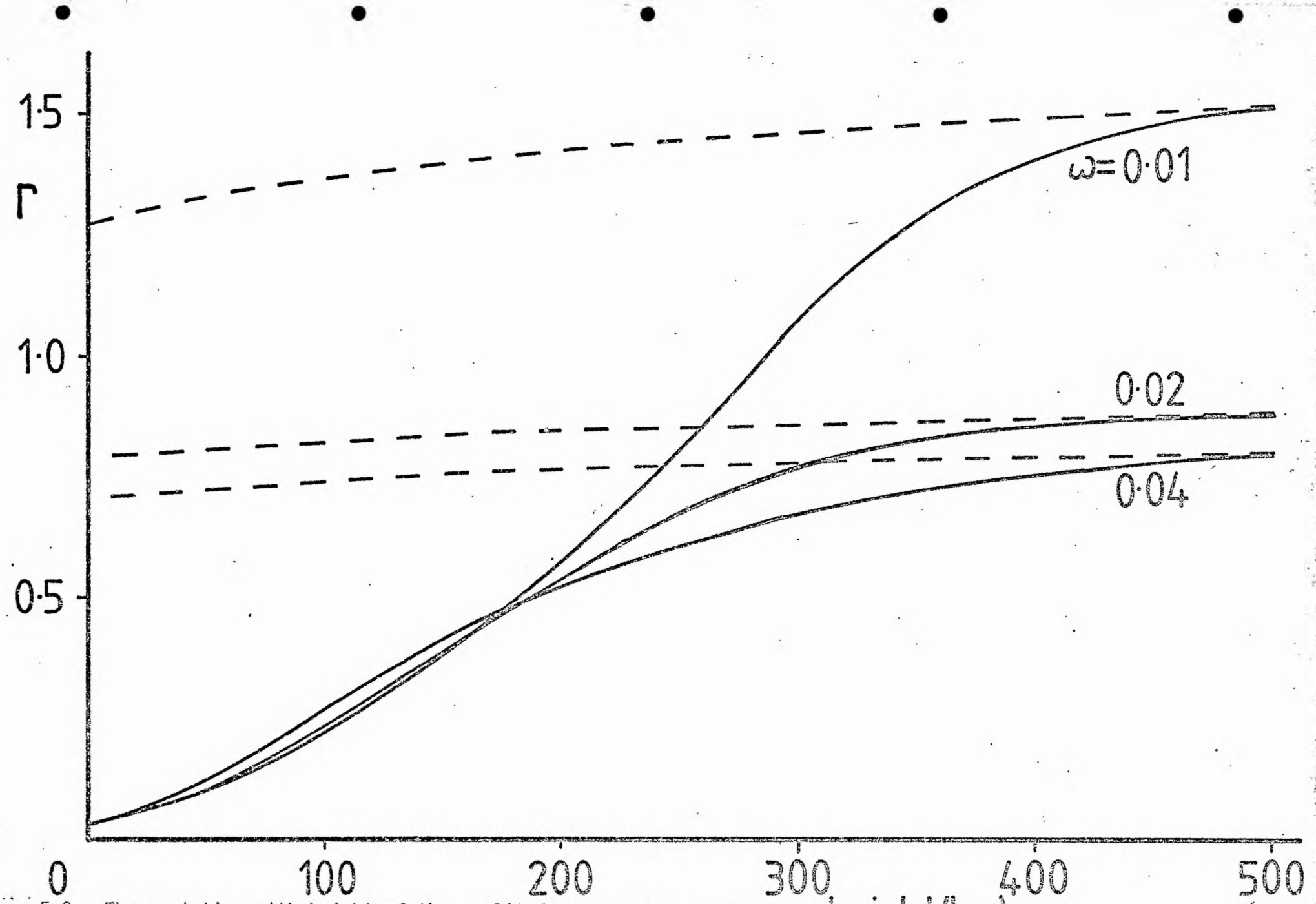

Figure 5.9 - The variation with height of the amplitude, r, of the temperature perturbation relative to the velocity perturbation for various frequencies.

Finally, in Figure 5.10 we give the dependence of the phase difference on frequency, for various values of τ_R, which correspond to different heights in the atmosphere.

5.3.3 Discussion

In this section we have considered the effect of radiative damping on the propagation of waves along an intense flux tube embedded in a stratified (but isothermal) atmosphere. The scale-height of the atmosphere provides a natural unit of length in which to measure the effect of damping, and so we have focussed attention on the 'damping per scale-height' (rather than the damping per wavelength, as in the uniform case). We find that for small radiative decay times τ_R high frequencies suffer a large amount of damping per scale-height (see also Souffrin, 1972), which is increased for a stronger magnetic field. Also for small τ_R the tube cut-off frequency for propagation is reduced (see Section 5.3.2), and there is an intermediate range of frequencies which experience little damping (Figure 5.5). Therefore we generalize Defouw's (1976) result by dividing the modes into mainly damped or mainly progressive (Schatzman and Souffrin, 1967). At the level $\tau_{5000} = 1$ radiation has a significant effect. The cut-off frequency is reduced by a factor of three from about $3.2 \times 10^{-2} s^{-1}$ (corresponding to a period of 196s) in the adiabatic limit to about $10^{-2} s^{-1}$ (with corresponding period 628s). However, this effect becomes negligible at a height of about 400 km (Figure 5.6).

In section 5.3.2 we determined the phase-shift between velocity oscillations at two different levels as a function of frequency (Figure 5.7) and phase and amplitude relations between

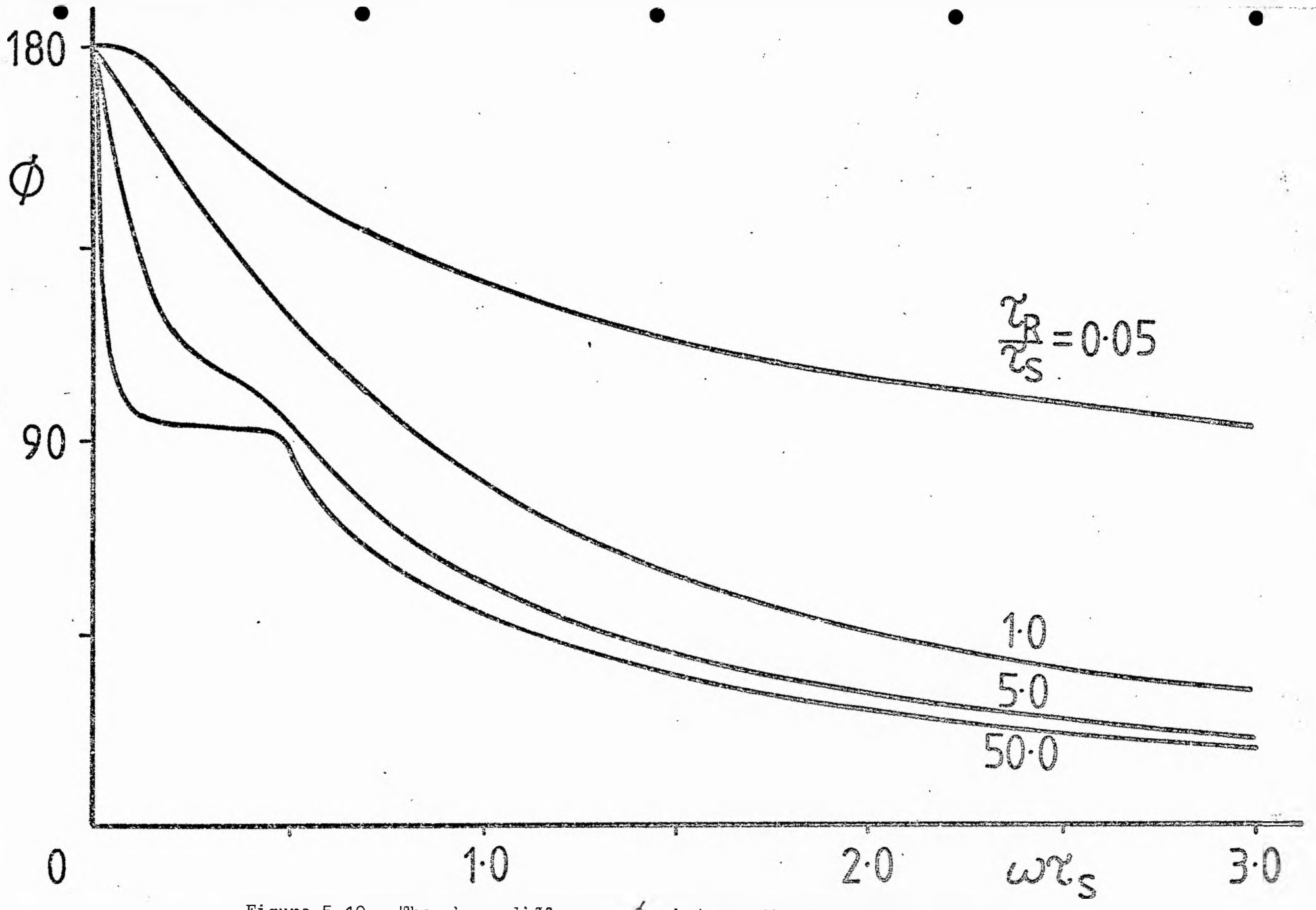

Figure 5.10 - The phase difference, ϕ, between the temperature and the velocity perturbations as a function of $\omega\tau_s (= \omega/\Lambda_0 c_0)$ for various values

temperature and velocity at one height (Figures 5.9 - 5.10). Observations of wave propagation in the mid-chromosphere and transition zone have recently been presented using results from OSO 8 (Athay and White, 1978, 1979a,b; Bruner, 1978; Chipman, 1978; White and Athay, 1979). This region is somewhat higher in the atmosphere than that with which we are concerned, though Lites and Chipman (1979) have measured velocities in spectral lines formed at heights from the low photosphere to the chromosphere. However, these observations do not apply specifically to intense magnetic fields but to a mean solar atmosphere.

The phase-shift between velocities at two different levels of separation one scale-height apart is sketched in Figure 5.7. The straight line corresponds to the tube wave $\omega = kc_T$. For large τ_R there is a maximum in the phase-shift at low frequencies, and as the frequency increases the phase decreases to a minimum value, corresponding to phase-speeds greatly in excess of the tube speed c_T. The tube cut-off frequency is approximately $\omega_v = 0.032 s^{-1}$ (for $c_0 = v_A = 7.25$ kms^{-1}). As a numerical illustration, consider the phase difference between velocities measured in the lines Fe I 5576 and Mg I 5173 as a function of frequency (as given by Lites and Chipman, 1979). Taking $\Lambda_0 = 115$ km and $\tau_R = 120s$, as mean values of the scale-height and radiative relaxation time in the tube between the two levels, and a separation of 333 km, we find that the phase increases from zero to a maximum of 35° at $\omega \approx 0.003 s^{-1}$, and then decreases to a minimum of 18° at $\omega \approx 0.02 s^{-1}$, before increasing rapidly at $\omega \approx 0.03 s^{-1}$. These values for the phases are larger by about a factor of three than those obtained by Lites and Chipman, who find a phase delay of approximately 5° for $\omega = 0.02 s^{-1}$.

The effect of radiative relaxation on the relative phase and amplitude of the velocity and temperature perturbations is illustrated in Figures 5.8 - 5.10. Supposing that these quantities depended only on the local values of the radiative decay time and temperature, we plotted such relationships in Figures 5.8 and 5.9 as functions of height in the solar atmosphere, above $\tau_{5000} = 1$ in the exterior, using data from the HSRA (Gingerich et al, 1971) and Ulmschneider's (1971) values for τ_R (also given in Bray and Loughhead, 1974, p. 326). The relative amplitude of the temperature perturbation to the velocity perturbation is decreased from its adiabatic value by radiative effects. In contrast to purely vertical motions, we find that the relative amplitude is greatest for lower frequencies (when τ_R is large).

Concerning the phase, we find that in the adiabatic limit the non-propagating modes ($\omega < \omega_v$; see (5.3.19)) have a phase difference of 90°, while the propagating modes ($\omega > \omega_v$), have a lower phase difference. For finite τ_R, we find that the phase difference is increased from its adiabatic value and is a decreasing function of height in the atmosphere. As an example, consider the frequencies of $0.02s^{-1}$ and $0.04s^{-1}$, corresponding to periods of 314s and 157s respectively. For $c_0 = v_A$ (i.e. a field of 1220 G at z = 0 for an external gas pressure of 1.3×10^5 dynes cm^{-2}), the phase difference between the velocity and temperature oscillation of frequency $0.02s^{-1}$ decreases from 157° at $\tau_{5000} = 1$ to 93° at 500 km. In this upper region propagation is almost adiabatic, and so the phase difference is close to its adiabatic value of 90°. The phase difference for a wave of frequency $0.04s^{-1}$ decreases from 136° at $\tau_{5000} = 1$ to 74°

at a height of 500 km, compared to its adiabatic value which increases from 61° to 72° over the range 0-500 km.

The phase difference between temperature and velocity fluctuations as a function of frequency is given in Figure 5.10. The phase is a decreasing function of frequency and tends to zero as the frequency tends to infinity. Comparing this with the observations of Lites and Chipman, for example, for the line Fe I 5576 (and assuming that increased intensity in the spectral line is proportional to an increase in temperature at the altitude of observation) we find good agreement for $\omega > \omega_v$, but for low frequencies the theory does not agree with the observations which give negligible phase-shift.

Altogether, then, there are a number of features of the present calculations that are in agreement with the available observations. That there are also areas of disagreement between theory and observation is perhaps not surprising in that there are several effects not accounted for in our calculations. For example, the discrepancy between Figure 6 and observations at low frequencies may be due to the presence of granular motions (see discussion in Lites and Chipman; Schmieder, 1980). Also, higher in the atmosphere observations in MgI 5173 indicate that the phase increases with frequency over the range $0.015 s^{-1} \lesssim \omega \lesssim 0.05 s^{-1}$, which is in contrast to both the results presented here and those of Schmieder (1977, 1978, 1979) for a <u>non-magnetic</u> atmosphere. Density fluctuations may be important in this region (Lites and Chipman, 1979). It must also be borne in mind that the available observations have not resolved the detailed wave propagation structure in an intense flux tube, but have instead assumed a <u>mean</u> atmosphere. We must therefore await future developments, both in theory and observation, before a comparison of the two is entirely sensible.

Appendix

The radiative transfer equation may be written in the form (Chandrasekhar, 1960)

$$-\frac{1}{K}\hat{\underline{s}}\cdot\frac{\partial}{\partial \underline{r}} I(\underline{r},\hat{\underline{s}}) = I - S \qquad (A.1)$$

where $I(\underline{r},\underline{s},t)$ is the integrated intensity (intensity integrated over all frequencies) at $\underline{r}$ of a beam in the direction of the unit vector $\hat{\underline{s}}$; K is the mean absorption coefficient per cm; is the density and S is the integrated source function.

Integrating Equation (A.1) over all solid angles we find that the flux of radiation, Fr, defined by

$$\pi F_{r_i} = \int I(\underline{r},\hat{\underline{s}}) s_i \, d\omega$$

is given by (Spiegel, 1957; Unno and Spiegel, 1966; Delache and Froeschlé, 1972)

$$\nabla.\underline{Fr} = -4\pi K (J-S) \qquad (A.2)$$

where J is the average intensity $= \frac{1}{4\pi}\int I d\omega$, and the integral is over all solid angles. Therefore, combining Equations (A.1) and (A.2) with the energy equation (5.1.1)(neglecting thermal conduction and mechanical dissipation), we have

$$\frac{\rho^{\gamma}}{\gamma-1}\frac{d}{dt}\left(\frac{p}{\rho^{\gamma}}\right) = +4\pi K(J-S) \qquad (A.3)$$

For an atmosphere is local thermodynamic equilibrium, the source function takes the form of the integrated Planck intensity, B(T),

$$S = B(T) = \frac{\sigma}{\pi} T^4 , \qquad (A.4)$$

where σ is the Stefan-Boltzmann constant. The mean intensity J may be shown to take the form (Delache and Froeschlé, 1971; Stein and Spiegel, 1967; Spiegel, 1957)

$$J(\underline{r},t) = \int_V K(\underline{\xi},t) S(\underline{\xi},t) \frac{\exp -\tau(\underline{r},\underline{\xi},t)}{4\pi r^2} \, d\underline{\xi} , \qquad (A.5)$$

where $d\underline{\xi}$ is the volume element and the integral is over all space;

The quantity $\tau(\underline{r},\underline{\xi},t)$ is the optical thickness at point $\underline{\xi}$ with respect to point $\underline{r}$ defined by

$$\tau(\underline{r},\underline{\xi},t) = \int_c \kappa(\underline{\xi}',t)d\underline{r}' \ ,$$

where the path c is along $\underline{r} - \underline{\xi}$ from $\underline{r}$ to $\underline{\xi}$; $\underline{\xi}'$ is an integration variable and $\underline{r}' = \underline{\xi}' - \underline{r}$.

The expressions for J and S are substituted into the energy equation and the resulting equation is linearized. Details may be found in Spiegel (1957) and Delache and Froeschlé (1972). The resulting linear equation, derived for a homogenous basic state is

$$\rho_0 c_v \frac{\partial T}{\partial t} + p_0 \nabla\cdot\underline{v} = -\frac{\rho_0 c_v}{t_R}\left[-\int \kappa_0 T \frac{e^{-\kappa_0 r}}{4\pi r^2} d\underline{\xi} + T \right] , \qquad (A.6)$$

where

$$t_R = \frac{\rho_0 c_v}{16\sigma k T_0^3} \qquad (A.7)$$

has the dimensions of time and characterizes the effectiveness of radiative damping. A subscript zero denotes the equilibrium state.

For perturbations of the form

$$T = \hat{T}\, e^{i\omega t}\, e^{i\underline{k}\cdot\underline{r}} \ ,$$

the term is the brackets on the left-hand side of (A.6) may be evaluated, thus:

$$\hat{T}\left(1 - \frac{\kappa}{k} \tan^{-1}\frac{k}{\kappa} \right) \ , \qquad (A.8)$$

and the radiative relaxation time, τ, is defined as

$$\tau = t_R / \left(1 - \frac{\kappa}{k} \tan^{-1}\frac{k}{\kappa}\right) . \qquad (A.9)$$

In the limit of small optical thickness ($k/K \to \infty$) $\tau \to t_R$ which is the approximation of Newton's law of cooling. At the other extreme, large optical thickness, $k/K \to 0$ and $\tau \to 3K^2 t_R / k^2$

In this chapter we have used the optically thin limit of (A.9), since we are concerned with waves in the photosphere where K is low and also, we found that the horizontal wavenumber is large for the tube wave in a slender flux tube. However the above analysis has been derived only for a homogeneous atmosphere. We shall give a further discussion of the limitations of our approach in Chapter 7.

Chapter 6 : STEADY FLOW IN MAGNETIC FLUX TUBES

6.1 Introduction

Observations of the solar transition region overlying the chromospheric network have indicated the presence of steady downflows of the order of a few kilometres per second (Lites et al, 1976; Doschek et al, 1976; Brueckner, 1977). At the photospheric level, where the magnetic flux outside sunspots occurs mainly in the form of highly-concentrated flux elements at the edges of supergranules, downdrafts have been observed within the magnetic field of 2.5 km s^{-1} (Spruit, 1976, deduced from Frazier, 1974; Harvey and Hall, 1975) and 0.5 km s^{-1} (Giovanelli and Brown, 1977; Stenflo, 1973). Simon and Leighton (1964) reported that the boundaries of supergranular cells are in strong correspondence with the descending matter (1 - 2 km s^{-1}) observed in H_α and H_β, and the magnetic field pattern (see also Tanenbaum et al, 1969). In fact, flux concentrations always appear to be correlated with downflow of matter, regardless of whether they occur in the quiet region network or in active region plages (Stenflo, 1976a).

The discovery that small-scale magnetic fields are found at supergranule boundaries has prompted a number of theoretical investigations concerning the kinematical concentration of magnetic flux by persistent velocity fields (Leighton et al, 1962; Noyes and Leighton, 1963; Simon and Leighton, 1964; Parker, 1963, 1974a,b; Weiss, 1964, 1966; Clark, 1966, 1968), the nature of motions (including both wave propagation and steady flows) within the flux tubes (Chapter 3; Defouw, 1976; Cram and Wilson, 1975; Wilson, 1978a, 1979a; Parker, 1978; Unno and Ribes, 1979;

Unno and Ando, 1979) and the statics of such structures (Spruit, 1976; Chapman, 1977, 1979).

A variety of mechanisms proposed for magnetic field concentration has been reviewed by Parker (1976), who suggests (Parker, 1978) that the concentration of the general magnetic field into isolated flux tubes at supergranule boundaries is a consequence of the strong superadiabatic temperature gradient, in the first few thousand kilometres beneath the photosphere. This 'superadiabatic effect' results from the general downdraft in the boundary. The downdraft is enhanced by the reduced temperature, and the upper portion of the field is strongly concentrated (Parker, 1978). Convective instability as a mechanism responsible for the high field strength observed for the small-scale field network, has also been proposed in Chapter 4 and also by Unno and Ando (1979) and Spruit and Zweibel (1979; see also Spruit, 1979). This takes place when the value of the field strength at the photospheric level is below a critical value, which divides stability and instability. The concentration of magnetic field by convection has been considered by Galloway et al (1977)(See also Galloway et al, 1978; Peckover and Weiss, 1978), whilst Zwaan (1978) suggests that magnetic flux emerging in active regions is already in concentrated form before penetrating the photosphere (see also Stenflo, 1976a).

In this chapter we turn to a consideration of the effect of a steady flow in a magnetic flux tube. The topic is of intrinsic interest but gains added interest in view of the observation correlation of field concentrations and flows (see Chapter 1). Steady flow along a magnetic flux tube has been considered by a number of authors. Parker (1977) has argued that the

observed concentration of field may be attributable, in part, to the dynamical flow of gas along the field. Ribes and Unno (1976) have investigated the hydromagnetic structure of the chromosphere near the supergranule boundary and have included the thermodynamic effect of compression (Unno and Ribes, 1979). Their model gives a temperature excess similar to that observed from facula observations (Chapman, 1970; Mehltretter, 1974; Stenflo, 1975; Muller, 1975), but the predicted high speed (6km s^{-1}) of the downdraft is somewhat larger than that observed. Spruit (1979) has proposed that the observed downdraft may be the result of an overstable oscillation, driven by lateral heat exchange just below the solar surface, but damped in higher layers.

Observations of the steady velocity component <u>as a function of height</u> in magnetic flux tubes in the photosphere have been presented recently by Giovanelli and Slaughter (1978), who find somewhat perplexingly that the mean <u>downward velocity increases rapidly with depth</u> (see Section 6.2, Figure 6.1). The magnitude varies from zero ($\pm$ 0.1 km s^{-1}) in the line Mg I 5183Å (formed in the <u>non</u>-magnetic atmosphere at approximately 840 km above $\tau_{5000} = 1$) to 0.6 km s^{-1} in the line CI 9111 Å (~ 160 km). Giovanelli and Slaughter also give a corrected value of 1.6 km s^{-1}, from Harvey's (1976) observations, for the 15648 Å line (~ 0 km). Spruit (1976) has derived from Frazier's (1974) data an upper limit of 2.5 km s^{-1} if the flow were confined within the magnetic structure. However, Stenflo (1976a), whose data indicates that the average downdraft velocity in magnetic elements is less than 1 km s^{-1} (Stenflo, 1973) argues that the velocity field does not have as pronounced a fine structure as the magnetic field. The velocity profile is broader than the

corresponding magnetic field profile, with a substantial fraction of the downward mass flux occurring immediately outside the magnetic structures.

In the chromosphere and chromosphere-corona transition zone above the supergranulation network, Lites et al (1975) have recorded systematic and persistent downward flows in both quiet and active regions. The mean velocities roughly double from the mid-chromosphere to the transition zone, generally being about 2 km s^{-1} for the chromospheric line of Si II and increasing to about 5 km s^{-1} for the transition zone line Si IV ($T_{ion} \sim 60{,}000$ K). These flows are an extension of the supergranular flows observed in photospheric lines, with the supergranular circulation extending upwards along the known magnetic field structure. Brueckner's results (see White, 1977) clearly demonstrate the existence of downflows of at least 10 km s^{-1} in the quiet chromosphere ($T_{ion} \sim 100{,}000$ K) and the excess of downflows over upflows. In the active regions of the Sun, downflows of 5 - 20 km s^{-1} have also been observed in a plage by Brueckner(White, 1977) in the C IV 1550 Å line, while Bruner et al (1976) also report 30 km s^{-1} in C IV emitted by a bright sunspot plume. In the lower-lying Si II line, Lites et al (1975) report downward motions of 4 - 6 km s^{-1} in a sunspot. Flows with velocities of 25 - 50 km s^{-1} into sunspots have also been observed (Haughen, 1967; Loughhead, 1968; Bray, 1974; Maltby, 1975).

Upward-flowing material has been recorded in the quiet chromosphere by Brueckner (White, 1977) in a quiet unipolar region, with a velocity of 5 - 10 km s^{-1}, and there is now evidence of upward flow in the supergranulation cells with a

very inhomogeneous downflow at the cell boundaries for the 15,000 K to 100,000 K range in the transition zone (White, 1977).

The complex pattern of flows that are an important part of the structure of the solar atmosphere has only begun to be investigated theoretically (see the recent review by Priest, 1980). The observed dominance of downflow over upflow poses the question as to the source of the material. Pneuman and Kopp (1977, 1978) point out that spicules supply material to the corona at a rate far in excess to that which is removed by the solar wind, and suggest that the observed downflow in the transition region network overlying the supergranulation boundaries may represent spicular material returning to the chromosphere after being heated to coronal temperatures. They also show that the enthalpy flux associated with the downflow of coronal material exceeds the inward flow due to thermal conduction by a considerable amount and may thus constitute an important if not dominant energy source for the transition region.

Further studies on steady flows in the chromosphere and corona include: the chromospheric counterpart of the Evershed effect, which is characterized by an inflow of material from the chromosphere into a sunspot (Maltby, 1975; Meyer and Schmidt, 1968); flows in the corona giving rise to quiescent prominences (Pikel'ner, 1971); and siphon flows in coronal loops (Cargill and Priest, 1980; Yeh, 1977). Stationary two-dimensional isothermal flow, parallel to magnetic lines of force, have also been considered in connection with the hydrodynamic support of a spicule, (Unno et al, 1974; see also Ribes and Unno, 1976).

Having presented a brief review of the observations and theory of steady flows in the solar atmosphere, we shall now proceed, in the following section, to consider the theoretical implications of the observations of Giovanelli and Slaughter (1978) of the decrease with height of the downflow in magnetic flux tubes in the photosphere.

6.2 Downflows in Magnetic Flux Tubes

Magnetic regions and in particular intense flux tubes at supergranule boundaries are almost always associated with downward velocities (Beckers and Schröter, 1968; Stenflo , 1976a). The recent results of Giovanelli and Slaughter (1978) indicate that, in solar magnetic tubes, the flow is steady and, over the height range observed (from Ca I 9111 up to Ca II 8542), the mean downward velocity increases rapidly with depth (see Figure 6.1).

If the flow is not confined within the magnetic structure, as suggested by-Stenflo (1976a), then the increase with depth of the vertical velocity component may simply be due to the increase in the vertical component of the supergranular motion outside the flux tube. However, Giovanelli and Slaughter (1978) propose that the increase may be a consequence of inflow of neutral matter in the neighbourhood of the temperature minimum (Giovanelli, 1977). In this section we shall investigate the dynamical equations governing the steady flow of an inviscid ideal gas along a magnetic flux tube and attempt to relate the results to observations.

Consider a flux tube of cross-sectional area A(z) embedded vertically in a non-magnetic region. The basic equations governing the steady longitudinal flow v(z) of a gas along the tube are (Parker, 1977; Unno and Ribes, 1979)

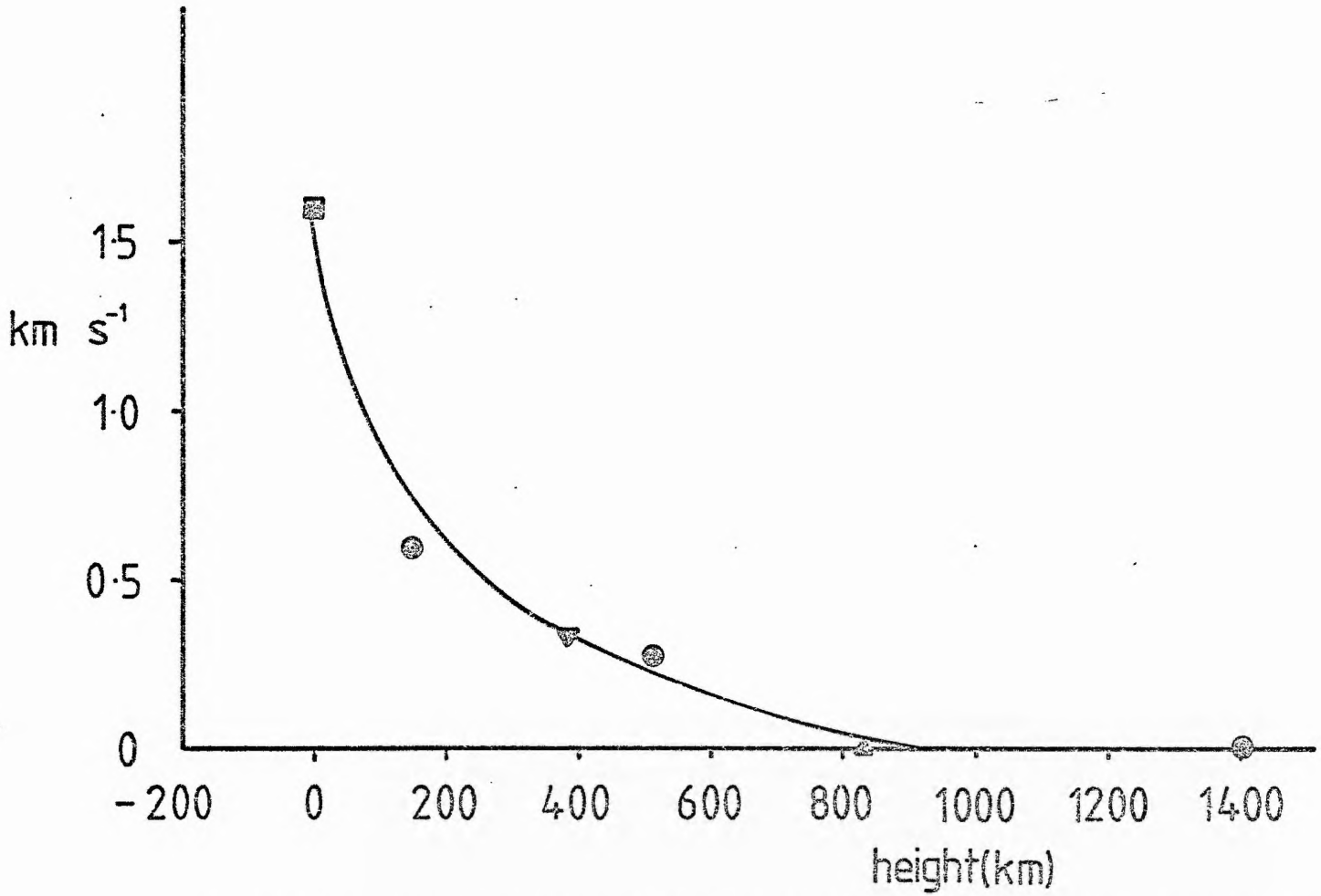

Figure 6.1 - Velocity of the steady component of gas flow in magnetic elements as measured in various lines, plotted against approximate height of formation in the non-magnetic atmosphere (Giovanelli and Slaughter, 1978).
Key: △ Plage ◉ isolated element (Giovanelli and Slaughter, 1978).
▩ Harvey (1976) ▽ Giovanelli and Ramsay (1971)
Giovanelli and Brown (1977)

$$vA = \phi \,, \tag{6.2.1}$$

$$BA = \Psi \,, \tag{6.2.2}$$

and

$$v \frac{dv}{dz} = - \frac{dp}{dz} - \rho g, \tag{6.2.3}$$

where p, ρ and B are the pressure, density and magnetic field intensity; ϕ is the mass flux and Ψ the magnetic flux (both constant) and g is the acceleration due to gravity. We have assumed that the physical quantities within the tube vary with height z only.

The pressure and density are related by the gas law, which we may write in the form

$$p(z) = \rho(z) g \Lambda_i(z) \,, \tag{6.2.4}$$

where the temperature scale-height inside the tube is $\Lambda_i(z) = RT_i(z)/\mu g$, with μ being the mean molecular weight and R the gas constant.

Combining Equations (6.2.1) to (6.2.4) gives

$$\left(1 - \frac{v^2}{g\Lambda_i}\right) \frac{v'}{v} = \frac{\Lambda_i'}{\Lambda_i} + \frac{1}{\Lambda_i} + \frac{B'}{B} \,, \tag{6.2.5}$$

where a dash refers to differentiation with respect to the vertical coordinate z.

We may note that by introducing the function

$$\Phi(z) = B(z)\Lambda_i(z) \exp\left(\int^{z} \frac{dz'}{\Lambda_i(z')} \right) \,, \tag{6.2.6}$$

Equation (6.2.5) may be re-written in the convenient form

$$\left(1 - \frac{v^2}{c_N^2}\right) \frac{v'}{v} = \frac{\Phi'}{\Phi} \,, \tag{6.2.5}'$$

where $c_N = (g\Lambda_i)^{\frac{1}{2}}$ in the 'Newtonian' (or isothermal) sound speed of gas inside the flux tube.

It is apparent from the above that for a <u>given</u> $\mathcal{F}$, i.e. for a given B(z) and $\Lambda_i(z)$, Equation (6.2.5)' is quadratic in v and so is incapable of distinguishing between ascending and descending motions. Such a distinction arises only when (6.2.5)' is supplemented by an energy equation, relating the flow v and scale-height $\Lambda_i(z)$. (For a more extensive discussion of the thermodynamics we refer the reader to the recent paper by Unno and Ribes (1979)).

Consider the implications of (6.2.5)', regarded as determining v(z) for given temperature and magnetic field profiles. We see that for a flow that is subsonic (with respect to the 'Newtonian' sound speed c_N, so $v^2 < c_N^2$), the velocity v(z) cannot decrease with height unless the magnetic field decreases sufficiently rapidly. For example, with an isothermal interior, the magnetic field would need to decrease faster than $\exp(-z/\Lambda_i)$ for the velocity to decrease with height. Observations do indeed imply that the magnetic fieldlines fan out rapidly with height (Frazier and Stenflo, 1972), but very little is known about the exact height variation of the field (Stenflo, 1976a). Both Spruit (1979) and Giovanelli and Slaughter (1978) state that the decrease of density above the surface is always faster than the increase in cross-section of the tube. Spruit concludes that the flow cannot be stationary and Giovanelli and Slaughter conclude (from Equation (6.2.1)) that there must be an inflow of matter from the exterior. Gabriel (1976) has calculated the expansion of the network field in the chromosphere and finds that, at a height

of 1500 km, the field has become almost horizontal and overlies the entire supergranule. Much above this height, photospheric flux tubes lose their individuality (Spruit, 1977).

Returning to Equation (6.2.5)', we see that if the magnetic field does not decrease sufficiently rapidly, so that the right-hand side of (6.2.6)' remains positive, then a steady subsonic stream, at $z = 0$ say, would <u>increase</u> with height $z > 0$, the limiting velocity being $v_c \equiv (g\Lambda_i(z_{max}))^{\frac{1}{2}}$, occurring at a limiting height z_{max}. This result shows that for such a magnetic flux tube it is impossible to have a stationary, one-dimensional flow of a gas in a gravitational field (Stanyukovich, 1960); <u>a dynamical solution does not exist throughout the atmosphere</u>.

The above result may be conveniently illustrated by again considering an isothermal atmosphere, when (6.2.5) has the first integral

$$\log\left(\frac{v(z)}{v(0)}\,\frac{B(0)}{B(z)}\right) - \frac{1}{2g\Lambda_i}\left(v^2(z) - v^2(0)\right) = \frac{z}{\Lambda_i} \quad . \qquad (6.2.7)$$

The solutions of (6.2.7) for a uniform magnetic field ($B(z) = B(0)$) are sketched in Figure 6.2, for several speeds $v(0)$ at $z = 0$.

In contrast to the above discussion, where the specification of the magnetic field provides a constraint upon the flow, we may allow the tube to respond to changes in the flow, and thus to changes in the internal gas pressure, by assuming that the gas pressure external to the tube is kept fixed.

To isolate the effects of flow inside the tube, we shall suppose that the gas outside the tube is in hydrostatic equilibrium, so that its pressure $p_e(z)$ and density $\rho_e(z)$ are

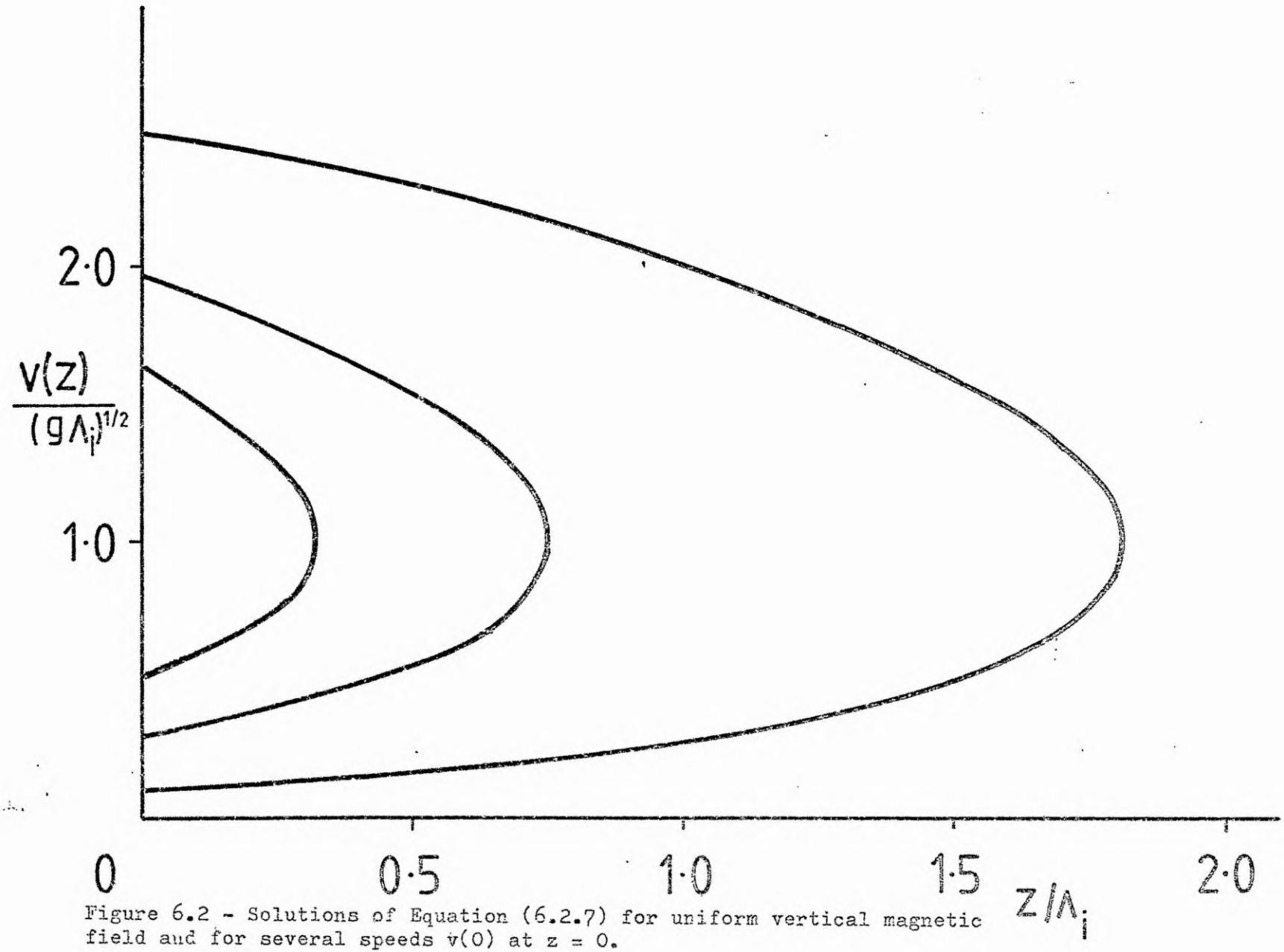

Figure 6.2 - Solutions of Equation (6.2.7) for uniform vertical magnetic field and for several speeds v(0) at z = 0.

related by

$$p_e'(z) = -\rho_e(z)g. \qquad (6.2.8)$$

In addition, we shall assume that the tube maintains lateral pressure balance, so that

$$p_e(z) = p(z) + \frac{B^2(z)}{2\mu_o}, \qquad (6.2.9)$$

where μ_o is the magnetic permeability. This is valid provided the tube is slender so that the effects of magnetic tension and centrifugal force are negligible. Then (6.2.5), (6.2.8) and (6.7.9) yield

$$(1 - \frac{v^2}{c_R^2})\frac{v'}{v} = \frac{\Lambda_i'}{\Lambda_i} + g\left(\frac{1}{c_0^2} - \frac{1}{2c_e^2}\right) + \frac{g}{v_A^2}\left(\frac{c_e^2 - c_0^2}{c_e^2}\right), \qquad (6.2.10)$$

where $c_0 = (\gamma p/\rho)^{\frac{1}{2}}$ is the adiabatic speed of sound inside the tube, $c_e = (\gamma p_e/\rho_e)^{\frac{1}{2}}$ is the corresponding speed in the tube's exterior, $v_A = B/(\mu_o\rho)^{\frac{1}{2}}$ is the Alfvén speed, and c_R is the Newtonian tube speed defined by

$$c_R^2 = \frac{c_N^2 v_A^2}{c_N^2 + v_A^2} = \frac{c_0^2 v_A^2}{c_0^2 + \gamma v_A^2}.$$

Equation (6.2.10) possesses a singular point at $v^2 = c_R^2$, and so has a solution extending throughout the atmosphere only if

$$\frac{\Lambda_i'}{\Lambda_i} + \gamma g\left(\frac{1}{c_0^2} - \frac{1}{2c_e^2}\right) + \frac{g}{v_A^2}\left(\frac{c_e^2 - c_0^2}{c_e^2}\right) = 0 \quad \text{at } v^2 = c_R^2. \qquad (6.2.11)$$

In particular, in an isothermal atmosphere with temperatures equal inside and outside the tube (so that the external scale-height Λ_e equals Λ_i), the condition (6.2.11) cannot be satisfied,

and so there is no steady solution throughout the atmosphere (Parker, 1977). However, if $\Lambda_i \neq \Lambda_e$ then there is a solution throughout the atmosphere provided

$$\frac{1}{2} < \frac{\Lambda_e}{\Lambda_i} < 1$$

(Unno et al, 1974).

In general, for $\Lambda_i \leq \Lambda_e$, and provided $v^2 < c_R^2$, the solution for the velocity will increase with height (unless Λ_i' is sufficiently negative), and break down at a height z_c, where $v^2 = c_R^2$. Therefore, we must conclude that the interior of the flux tube is hotter than the exterior for the flow to decrease with height. The question that arises is: what internal temperature distribution would give rise to a flow decreasing with height, and is this temperature excess supported by the observations?

The observations show that the small-scale magnetic fields of 1 - 2 kG are associated with strong atmospheric heating (Stenflo , 1976a). In the photosphere there seems to be a one-to-one correlation between magnetic field concentrations and the hotter regions in the network (Stenflo, 1973). Facula models, giving a temperature excess in the magnetic field above the photosphere, have been proposed. A facula model should be identical with a model of a magnetic element or a model of the quiet region network (Stenflo, 1976a; Mehltretter, 1974), but these may be two distinct but superimposed features (Muller, 1975). Models have been constructed describing faculae as structures having a temperature excess at higher photospheric layers (Rogerson, 1961; Chapman, 1970; Milkey, 1970; Stellmacher and Wiehr, 1971, 1973; Mehltretter, 1974; Muller, 1975; Stenflo, 1975).

Stenflo (1975) constructs a model of a basic element, with field strength 2 kG and with a temperature enhancement beginning at about 180 km above $\tau_{5000} = 1$ in the Harvard-Smithsonian Reference Atmosphere (HSRA)(Gingerich et al, 1971) and increasing rapidly with height. Milkey (1970) considers the problem of the heating of the chromosphere in the regions of intensified magnetic field, which occur above the boundaries of supergranulation cells, and he concludes that there should be a temperature enhancement in the regions of the chromospheric network, beginning at a height of 750 km and becoming more pronounced with height. Chapman (1970) constructs models of solar faculae, cospatial with strong photospheric magnetic fields, from continuum observations and the temperature of his adopted model begins to rise at about a height of 150 km and is approximately 1500 K above that of the undisturbed chromosphere at a height of 400 km. The source of the heating may be fast-mode hydromagnetic shock waves (Milkey, 1970; Stellmacher and Wiehr, 1973; Stenflo, 1976a; Osterbrock, 1961), though Unno and Ribes (1979) argue that this is insufficient to account for the large temperature excess and that a more natural explanation is the entropy transport from above.

In order to see whether the observed temperature excess is consistent with a downflow decreasing with height, we shall suppose that we have a (prescribed) steady downflow, decreasing with increasing height in the atmosphere in a region of intense magnetic field, and consider the consequences of Equation (6.2.10). If we specify the velocity profile, then there remain three parameters which govern the solution and must be specified in order to determine the magnetic field and temperature. These are

$$M = \frac{v^2(0)}{2g\Lambda_e(0)} \quad , \quad n = \frac{B^2(0)}{2\mu_0 p_e(0)} \quad , \quad \lambda = \frac{\Lambda_i(0)}{\Lambda_e(0)} \quad ,$$

but are not independent since we must have the solution for the velocity which passes through the critical point of (6.2.10). Therefore, we prescribe M and n and calculate the critical value of λ.

Introducing, following Parker (1977), the non-dimensional variables

$$\psi = \frac{B}{B(0)} \quad , \quad f = \frac{p_e}{p_e(0)} \quad , \quad \eta = \frac{v}{v(0)} \quad , \quad \zeta = \frac{z}{e(0)} \quad , \quad \hat{\Lambda}_i = \frac{\Lambda_i}{\Lambda_e(0)} \quad ,$$

Equations (6.2.1) - (6.2.4) combine to give

$$\psi \frac{d\psi}{d\zeta} = \frac{1}{2n}\left[\frac{(1-n)}{\lambda}\psi\frac{1}{\eta}\left(1 + 2M\eta\frac{d\eta}{d\zeta}\right) + \frac{df}{d\zeta}\right] \quad , \qquad (6.2.12)$$

for magnetic field in terms of the flow η. The internal temperature is given by

$$\hat{\Lambda}_i = \frac{\lambda}{\psi}\frac{f - n\psi^2}{1-n}\eta \, . \qquad (6.2.13)$$

Prescribing the velocity profile and the parameters M and n, we may solve Equation (2.6.12) for the magnetic field and use (2.6.13) to calculate the internal temperature. For example, taking n = 0.4 and M = 0.012, corresponding to a magnetic field of 1200G and a velocity of 1 km s^{-1} at z = 0, and taking the external pressure profile to be that given by the HSRA, we find that λ = 1.4 for a prescribed velocity profile of $\eta \equiv v/v(0) = \exp(-0.4\zeta)$, chosen to model the results of Giovanelli and Slaughter (1978). Figure 6.3 shows the external temperature profile (HSRA) and the corresponding internal temperature. The magnetic field profile is sketched in Figure 6.4.

Figure 6.3 shows that the temperature in the interior is greater than that in the exterior at z = 0, but the difference decreases with height until it is negligible at around the temperature

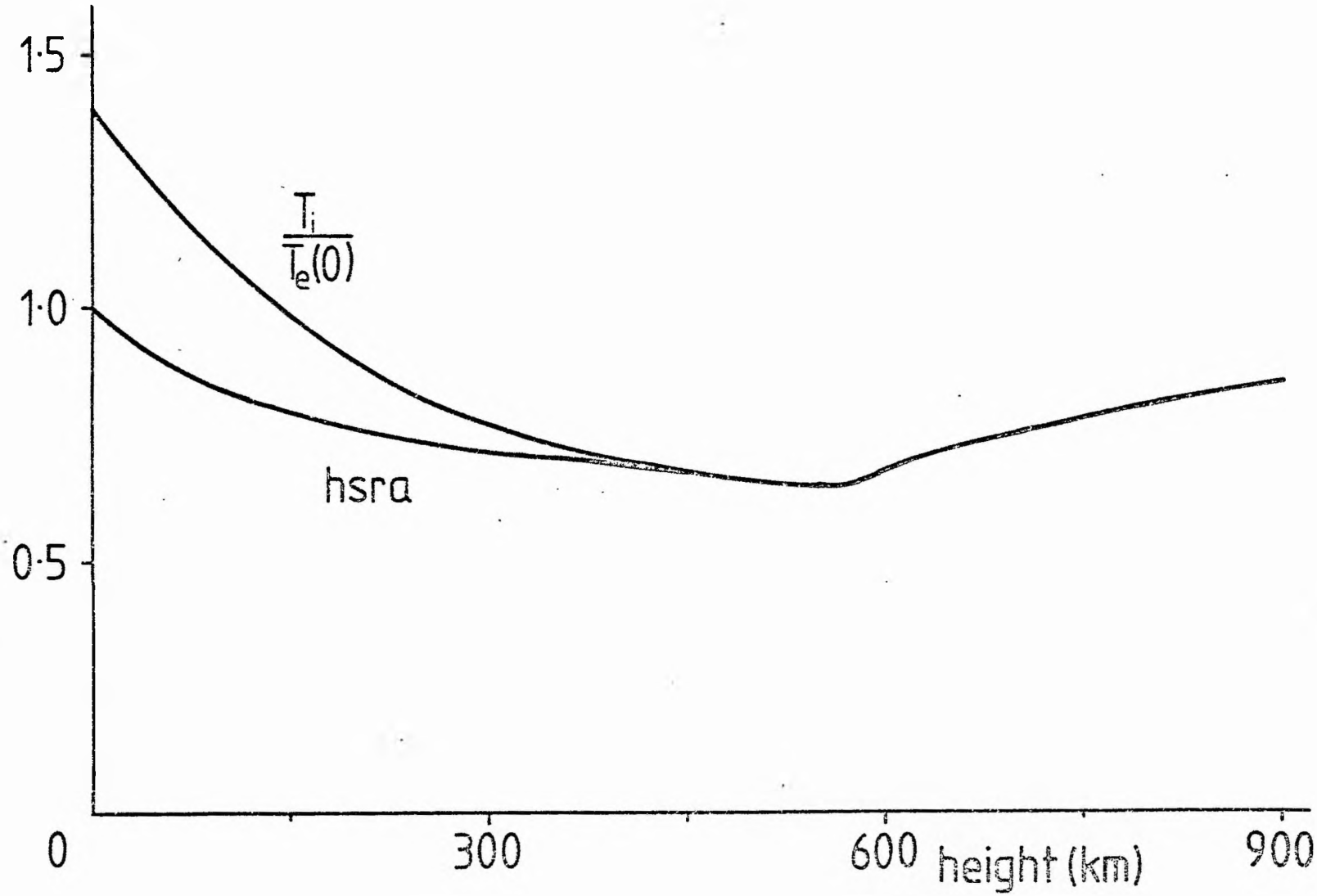

Figure 6.3 - The internal temperature profile (compared to the HSRA) required to give a decreasing velocity profile $v = v(0)\exp(-0.4z/\Lambda_e(0))$, matching the results of Giovanelli and Slaughter. We have taken n = 0.4 and M = 0.012.

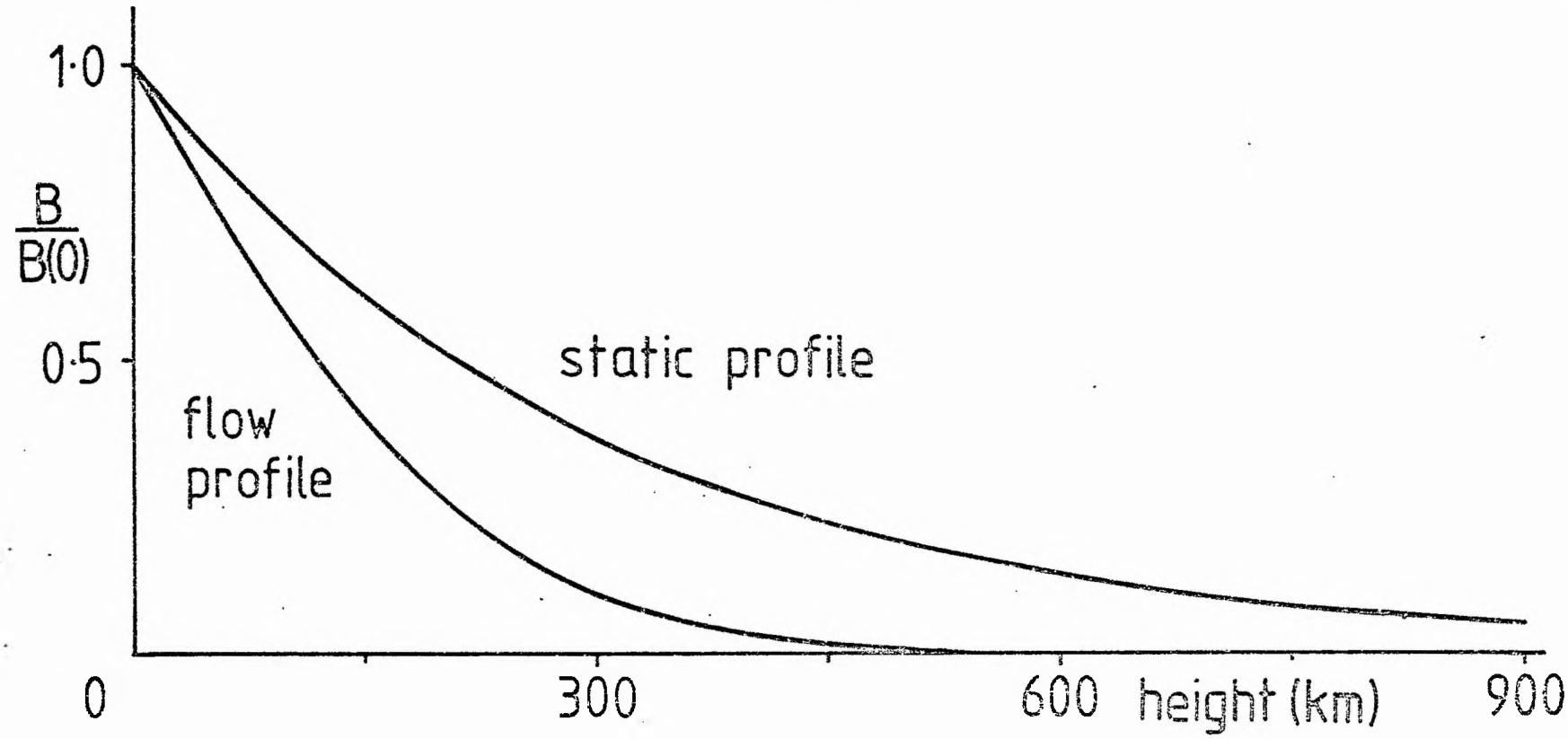

Figure 6.4 - The magnetic field profile for a flow $v = v(0)\exp(-0.4z/\Lambda_e(0))$, compared to the static profile. $n = 0.4$ and $M = 0.012$.

minimum. The temperature excess at the origin (2400K) is larger than that observed, though Chapman's model does give an excess of up to 1500K. Also, the temperature excess occurs over a lower range in the atmosphere than observations of photospheric faculae suggest. This is because we have assumed that the velocity decrease from 1 km s^{-1} takes place principally over the range 0-500 km above $\tau_{5000} = 1$. This may not be so, since Giovanelli and Slaughter's (1978) results, for the velocity of gas flow in magnetic elements as measured in various lines, are plotted against the approximate height of formation of the line in the non-magnetic atmosphere.

There are general uncertainties in the heights of formation of the lines (Schmieder, 1980), which may be very different inside the tube (Durrant, 1980; Giovanelli and Ramsay, 1971) and so Giovanelli and Slaughter's results could be misleading.

Figure 6.4 shows a very rapid decrease in magnetic field is required for a decreasing flow. A consequence of this is that there is a very rapid decrease in the Alfvén speed since $v_A^2 \sim B^2/\rho \sim v\,B$ by Equations (6.2.1) and (6.2.2) and both B and v are decreasing with height. This is in contrast to Stenflo's (1975) model, where the Alfvén speed increases with height.

We may conclude from the above calculations that in order to have a steady velocity decreasing with height in a magnetic flux tube in pressure balance with its surroundings, there must be a significant temperature excess giving rise to a rapid decrease in magnetic field. Improved observations are needed of the height variation of the magnetic field and the nature of the steady flow.

Finally it is worthwhile to comment upon some of the assumptions we have made. We have assumed that the flow is described by Equations (6.2.1) - (6.2.4) and that the total pressure (on the axis) is equal to the external gas pressure at the same height. This is a reasonable approximation where the tube is slender, but may become invalid when the tube begins to fan out rapidly. Also, we have assumed continuity of mass flux (Equation (6.2.1)), which, Giovanelli suggests (Giovanelli, 1977; Giovanelli and Slaughter, 1978) may be inappropriate, especially in the vicinity of the temperature minimum. Since the velocity increases with depth, A must decrease with depth and Giovanelli and Slaughter argue that ρ decreases faster with depth than A decreases, from which it follows that the flux of matter is unlikely to be constant but that it increases with depth due to inflow across the magnetic field.

Considering further the suggestion of Giovanelli and Slaughter, we sketch in Figure 6.5, a flux tube between the levels z_0 and z, (taken to be 160 km and 840 km above $\tau_{5000} = 1$) with downward mass flux ϕ_0 and ϕ_1 at each level. Giovanelli and Slaughter estimate $\rho_1 \sim \rho_0/500$ and $A_1 \sim 10A_0$, where ρ and A are the density and area of the flux tube and the subscripts refer to the levels z_0 and z_1. Therefore, for a downward velocity increasing with depth ($v_1 < v_0$), we have $\rho_1 A_1 v_1 \lesssim \rho_0 A_0 v_0/50$; and so the mass flow out of the flux tube at level z_0 must result from an inflow in the region between the heights z_0 and z_1. For $v_0 \sim 1$ km s^{-1} and a tube of radius 150 km at z_0, the mass flux, ϕ_0, is given by

$$\phi_0 \simeq 2.25\pi \rho_0 10^{19} \qquad (6.2.14)$$

where ρ_0 is in g cm^{-3}.

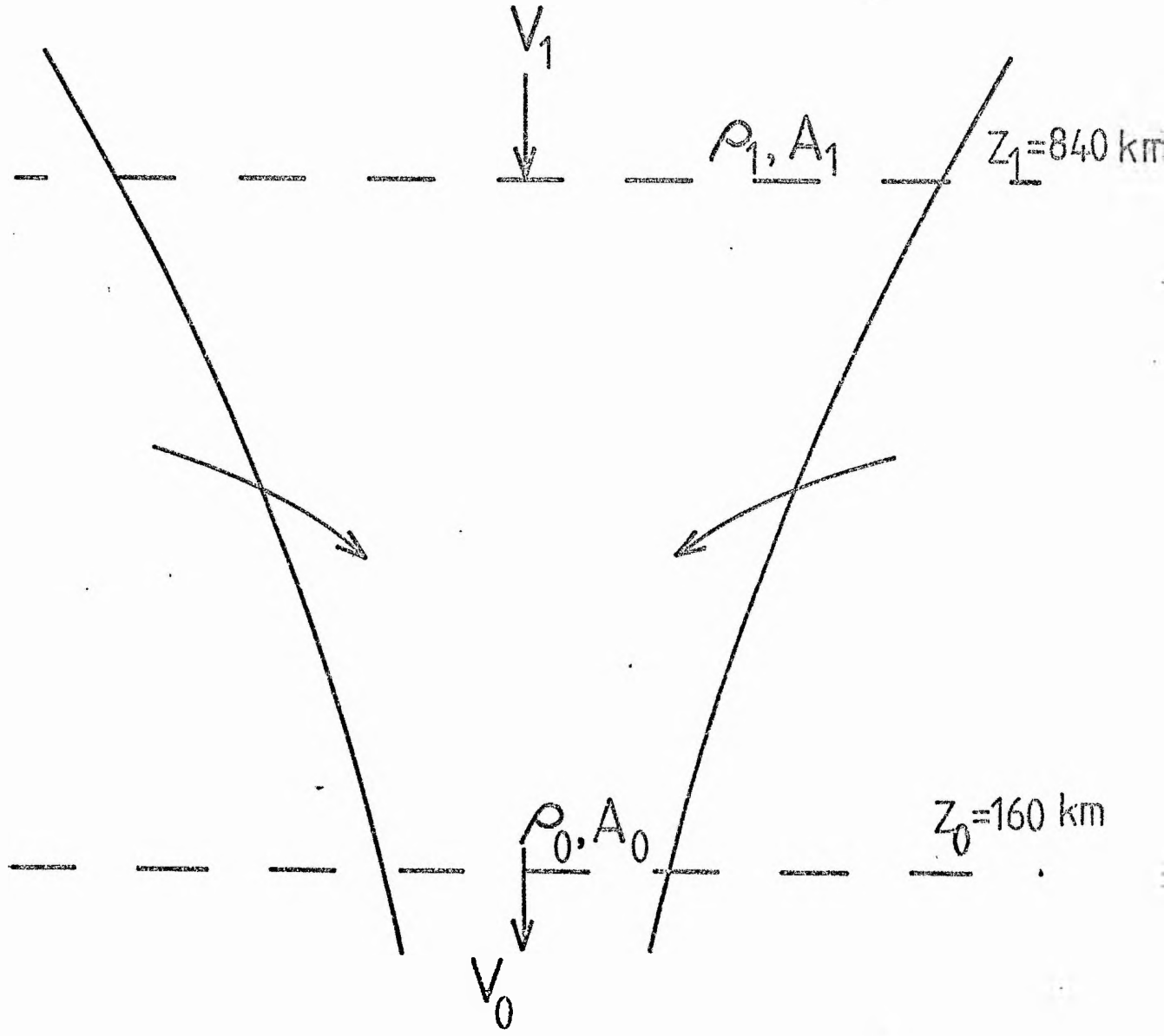

Figure 6.5 - Schematic representation of Giovanelli's inflow argument.

Now the mass, M, of the chromosphere, between the levels z_0 and z_1, above a supergranule cell of radius D is

$$M = \pi D^2 \int_{z_0}^{z_1} \bar{\rho}(z)dz, \qquad (6.2.15)$$

where $\bar{\rho}(z)$ is the density at height z averaged over a horizontal plane. Equation (6.2.15) may be approximated by

$$M \sim \pi D^2 \bar{\rho}(z_0)\Lambda_0 \qquad (6.2.16)$$

for a density profile $\bar{\rho} = \bar{\rho}(z_0)e^{-(z-z_0)/\Lambda_0}$, and $e^{-(z_1-z_0)/\Lambda_0} \ll 1$; Λ_0 is the scale height. For $\Lambda_0 \sim 150$ km and D ~ 15000 km, (6.2.16) gives

$$M \sim 3.37\,\pi\,10^{25}\,\bar{\rho}(z_0)\ . \qquad (6.2.17)$$

Since a flux tube has a lifetime of about 8 minutes* (see Chapter 1), then by Equations (6.2.14) and (6.2.17), the mass drained out of the chromosphere in that time (assuming $\bar{\rho}(z_0) \sim \rho_o$) is approximately

$$3.2 \times 10^{-4} M\ . \qquad (6.2.18)$$

This is not a significant fraction of the mass above the supergranular cell though it must be remembered that at any one time there are approximately 100 flux tubes per supergranular cell (see Chapter 1). If each one drains the amount given by (6.2.18) in its lifetime, then over a period of approximately 30 lifetimes (4 hours) the total mass would be drained.

* The lifetime of 8 minutes should be taken cautiously; it is very difficult to track a single flux tube for long, so it may just be that the tube is shunted around supergranular boundaries, preserving its identity, and 'disappears' from view in about this time; but it is still there, of course, only in a different position.

Thus, in a fairly short time-scale, flux tubes drain a significant amount of matter from the chromosphere. Presumably this is being replaced constantly by spicules. An alternative to the above argument would be to have $A_1 >> A_0$: i.e. for the field to decrease rapidly with height as we have suggested earlier in this chapter on different grounds.

It is unlikely that any appreciable flow across the magnetic field can occur except, perhaps, around about two scale heights of the temperature minimum (Durrant, 1980). If this is so, the inflow idea of Giovanelli would seem improbable, especially as he finds the major velocity changes near the photosphere, where inflow cannot occur to any appreciable extent.

6.3 Discussion

Observations do indeed show that intense fields are associated with strong atmospheric heating (Stenflo, 1976a). Further it is interesting to note that the recent calculations by Spruit (1979) of the collapsed state of a magnetic flux tube give an interior atmosphere significantly hotter, in the layers immediately above $\tau_{5000} = 1$, than the external atmosphere of the tube. With regard to the decrease in magnetic field strength, observations indicate a rapid fanning of the flux tube (Frazier and Stenflo, 1972) but very little is known about the exact height variation of the field (Stenflo, 1976a).

Thus, in summary, it would appear that the observed temperature excess over the first few hundred kilometres above $\tau_{5000} = 1$ contributes to the increase with depth of the observed steady velocity profile (Figure 6.1) in intense magnetic tubes. The calculation presented in Section 6.2 supports this and shows

that when a flow is present the magnetic field strength must decrease more rapidly with height than it does in the static situation. This must be so for the mass flux to remain constant with height. However, this may not be the whole story and there may be other effects which contribute to the observed structure in velocity. Possible alternatives that have been suggested are: an inflow of neutral gas through the sides of the flux tube in the neighbourhood of the temperature minimum (Giovanelli, 1977), as discussed earlier; a finite amplitude effect of convective instability (Unno and Ando, 1979); a non-steady flow resulting from overstability (Spruit, 1979). Also, the supergranular flow pattern, mentioned in Section 6.2 may influence the observations considerably. Unfortunately, none of these possibilities has been adequately explored, and further investigations (both observational and theoretical) are necessary before a clear explanation is likely to emerge. It may be that all of these effects (and so single effect) combine to give the observed velocity structure.

Chapter 7 : SUMMARY AND CONCLUDING REMARKS

This thesis has been concerned with the nature of motions in magnetic fields, with most emphasis being placed on the study of the small-scale intense magnetic fields located at the super-granular boundaries. The properties of these small-scale fields were summarized in Chapter 1 and, as a preliminary to our discussion of motions in such structures, we reviewed, in the first part of the second chapter, wave propagation in an unbounded atmosphere. In the second part of that chapter, we considered wave propagation in a stratified atmosphere permeated by a uniform, vertical magnetic field and we derived equations governing the velocity perturbations. Though the general forms of these equations were not discussed in detail, it was pointed out that both equations have regular singularities, where the solutions are well-behaved. Further investigation of the nature of these equations, in order to determine, for example, whether the 'value' effect (Acheson, 1972) occurs in the neighbourhood of the critical level, is considered worthwhile. Exact solutions for the velocity perturbations were obtained for the special cases of an isothermal atmosphere and a strong magnetic field; the latter was investigated in some detail to see if the resonance, suggested by Hollweg (1979), were present. There was found to be no maximum response in the region of the acoustic cut-off frequency for the vertical velocity driven by the horizontal velocity component. However, the results may be different for the vertical velocity driven by the pressure, as is found in the non-magnetic atmosphere, where there is a peak in the response for frequencies close to the acoustic cut-off frequency (Moore, 1974).

In Chapter 3 we considered the nature of waves in an isolated magnetic flux tube. The full complexity of wave propagation in a magnetic flux tube in a uniform atmosphere has only recently been treated in detail (Roberts, 1980) and, in the first part of Chapter 3, we presented results for axisymmetric perturbations only, deriving the governing dispersion relation and solving it for the case of a slender flux tube. The study of wave propagation in structured magnetic fields has wide application in the solar atmosphere, and should be an important area for future research. The propagation of waves in a flux tube in a stratified atmosphere, discussed in the second part of Chapter 3, was based on an approximate basic state and an expansion procedure for the perturbations. The expansion procedure was given in detail, since Chapters 4 and 5 rely heavily on its results. The equation derived for the vertical velocity perturbation was for the 'slow mode' wave only. Thus, perturbations in the exterior were considered negligible. The exterior sound wave solution may be important in determining the actual motions present in the tube.

The nature of convective instability, as a means of achieving the observed kilogauss fields, was explored in Chapter 4. A necessary and sufficient condition for convective stability to occur inside the tube was derived for a tube of infinite depth, with a uniform temperature gradient. We suggested that the observed downdrafts inside intense tubes, if a manifestation of convective instability, are thus likely to be a transient phenomenon in which the field inside the tube is intensified.

In Chapter 5 the effect of radiation on waves propagating in a magnetic field was discussed. Assuming Newton's law of

cooling we considered the propagation of magneto-acoustic waves in a (uniform) radiating atmosphere and then included the important effect of lateral boundaries, deriving the dispersion relation and solving for the circumstances of a slender tube. A flux tube in a stratified atmosphere was investigated using the approximation developed in Chapter 3. Difficulties arose in applying the results to the solar atmosphere, since observations of phase differences and phase lags refer to a mean atmosphere and not specifically to intense flux tubes. The results of the chapter may be indicative of the effect of damping of waves in magnetic tubes, but Newton's law of cooling is only an approximate form for a non-magnetic atmosphere, and until an adequate theory exists for wave propagation in a radiating atmosphere with a magnetic field present and more observations of tubes are made, it is not considered worthwhile to pursue this line of investigation.

In fact one of the main difficulties in applying the results of this thesis is the lack of detailed observations of motions in tubes and the structure of the field. This applies also to the final chapter on flows in magnetic fields. Whether or not the results of Giovanelli and Slaughter (1978) can be considered as truly representative of the flow in a magnetic flux tube is far from established yet. Theory indicates that the observed flow would require a very rapid decrease of the magnetic field with height, together with a significant temperature excess, or an excessive inflow of neutral matter in the neighbourhood of the temperature minimum. Perhaps a combination of the two mechanisms may be responsible for the observed flow profile.

The subject of intense magnetic fields is a varied and interesting one. In this thesis we have considered some of

the problems associated with these small-scale structures, yet there are many areas for further investigation. What is the connection between spicules and the flux tubes? Do the waves propagating along the tubes provide a significant source of energy for heating the chromosphere? Further studies, both theoretical and observational, are needed before such questions can be adequately answered.

REFERENCES

Abramowitz, M. and Stegun, I.A.: 1967, Handbook of Mathematical Functions, Nat. Bur. of Standards.

Abraham, Z. and Iben, I.: 1971, Astrophys.J. 170,157.

Acheson, D.J.: 1972, J. Fluid Mech. 53,401.

Acheson, D.J. and Hide, R.: 1973, Rep. Prog. Phys. 36,159.

Adam, J.A.: 1977a, Solar Phys. 52,293.

Adam, J.A.: 1977b, Astron. Astrophys. 60,171.

Athay, R.G.: 1976, The Solar Chromosphere and Corona : Quiet Sun, D. Reidel.

Athay, R.G. and White, O.R.: 1978, Astrophys. J. 226,1135.

Athay, R.G. and White, O.R.: 1979a, Astrophys. J. suppl.ser. 39,333.

Athay, R.G. and White, O.R.: 1979b, Astrophys. J. 229,1147.

Badalyan, O.G. and Prudkovskii, A.G.: 1973, Sov. Astron. 17,356.

Bahng, J. and Schwarzschild, M.: 1963, Astrophys. J. 137,901.

Beckers, J.M.: 1972, Ann. Rev. Astron. Astrophys. 10,73.

Beckers, J.M.: 1975, Bull. Am. Astron. Soc. 7,346.

Beckers, J.M.: 1977, in A. Bruzek, C.J. Durrant (eds) Illustrated Glossary for Solar and Solar-Terrestrial Physics, D. Reidel, p 71.

Beckers, J.M. and Schröter, E.H.: 1968, Solar Phys. 4,142.

Beggs, D.W. and Von Klüber, H.: 1956, Nature 178,1412.

Bel, N. and Leroy, B.: 1977, Astron. Astrophys. 55,239.

Bel , N. and Mein, P.: 1971, Astron. Astrophys. 11,234.

Bernstein, I.B., Frieman, E.A., Kruskal, M.D. and Kulsrud, R.M.: 1958, Proc. Roy. Soc. A244,17.

Boyd, T.J.M. and Sanderson, J.J. : 1969, Plasma Dynamics, Nelson.

Bray, R.J.: 1974, Solar Phys. 38,377.

Bray, R.J. and Loughhead, R.E.: 1974, The Solar Chromosphere, Chapman and Hall.

Brueckner, G.E.: 1977, see White, 1977.

Bruner, E.C., Chipman, E.G., Lites, B.W., Rottman, G.J. and Shine, R.A.: 1976, Astrophys. J. 210,L97.

Bruzek, A.: 1977, in A. Bruzek, C.J. Durrant (eds) Illustrated Glossary for Solar and Solar-Terrestrial Physics, D. Reidel, p 77.

Cargill, P.J. and Priest, E.R.: 1980, Solar Phys. in press.

Case, K.M.: 1960, Phys. Fluids 3,149.

Chandrasekhar, S.: 1960, Radiative Transfer, Dover.

Chapman, G.A.: 1970, Solar Phys. 14,315.

Chapman, G.A.: 1974, Astrophys. J. 191,255.

Chapman, G.A.: 1977, Astrophys. J. Supp. 33,35.

Chapman, G.A.: 1979, Astrophys. J. 232,923.

Chapman, G.A. and Sheeley, N.R.: 1968, Solar Phys. 5,442.

Chen, C.J. and Lykoudis, P.S.: 1972, Solar Phys. 25,380.

Chipman, E.G.: 1978, Astrophys. J. 224,671.

Clark, A.: 1965, Phys. Fluids 8,644.

Clark, A.: 1966, Phys. Fluids 9,485.

Clark, A. and Johnson, H.K.: 1967, Solar Phys. 2,433.

Clark, P.A. and Clark, A.: 1973, Solar Phys. 30,319.

Cowling, T.G.: 1976, Magnetohydrodynamics, Adam Hilger.

Cram, L.E. and Wilson, P.R.: 1975, Solar Phys. 41,313.

Defouw, R.J.: 1976, Astrophys. J. 209,266.

Delache, P. and Froeschlé, C.: 1972, Astron. Astrophys. 16,348.

Deubner, F-L.: 1967, Solar Phys. 2,133.

Doschek, G.A., Feldman, U. and Bohlin, J.D.: 1976, Astrophys. J. 205,L177.

Dragos, L.: 1975, Magnetofluid Dynamics, Abacus Press.

Dunn, R.B. and Zirker, J.B.: 1973, Solar Phys. 33,281.

Dunn, R.B., Zirker, J.B. and Beckers, J.M.: 1974, in R.G. Athay (ed.) Chromospheric Fine Structure, I.A.U. Symp. 56,45.

Durrant, C.J.: 1980, Private Communication.

Dyson, F.J.: 1960, Phys. Fluids 3, 155.

Erdélyi, A., Magnus, W., Oberhettinger, F. and Tricomi, F.G.: 1954, Tables of Integral Transforms, Vol II, McGraw-Hill.

Ferraro, V.C.A. and Plumpton, C.: 1966, An Introduction to Magneto-Fluid Mechanics, Clarendon Press.

Field, G.B.: 1965, Astrophys. J. 142,531.

Frazier, E.N.: 1970, Solar Phys. 14,89.

Frazier, E.N.: 1971, Solar Phys. 21,42.

Frazier, E.N.: 1974, Solar Phys. 38,69.

Frazier, E.N. and Stenflo, J.O.: 1972, Solar Phys. 27,330.

Frazier, E.N. and Stenflo, J.O.: 1978, Astron. Astrophys. 70,789.

Gabriel, G.A.: 1976, Phil. Trans. Roy. Soc. London A 781,339.

Galloway, D.J., Proctor, M.R.E. and Weiss, N.O.: 1977, Nature 266,686.

Galloway, D.J., Proctor, M.R.E. and Weiss, N.O.: 1978, J. Fluid Mech. 87,243.

Gille, J.C.: 1968, J. Atmospheric Sci. 25,808.

Gingerich, O. and De Jager, C.: 1968, Solar Phys. 3,5.

Gingerich, O., Noyes, R.W., Kalkofen, W. and Cuny, Y.: 1971, Solar Phys. 18,347.

Giovanelli, R.G.: 1977, Solar Phys. 52,315.

Giovanelli, R.G. and Brown, N.: 1977, Solar Phys. 52,27.

Giovanelli, R.G., Livingston, W.C. and Harvey, J.W.: 1978, Solar Phys. 59,49.

Giovanelli, R.G. and Ramsay, J.V.: 1971, in R. Howard (ed.) Solar Magnetic Fields, I.A.U. Symp. 43,293.

Giovanelli, R.G. and Slaughter, C.: 1978, Solar Phys. 57,255.

Gough, D.O. and Tayler, R.J.: 1966, Monthly Notices Roy. Astron. Soc. 133,85.

Gradshteyn, I.S. and Ryzhik, I.M.: 1965, Tables of Integrals, Series and Products, Academic Press.

Hale, G.E.: 1922, Publ. Astron. Soc. Pacific 34,59.

Harvey, J.: 1971, Publ. Astron. Soc. Pacific 83,539.

Harvey, J.: 1977a, in E.A. Muller (ed.) Highlights of Astronomy 4, part II,223.

Harvey, J.: 1977b, in A. Bruzek, C.J. Durrant (eds.) Illustrated Glossary for Solar and Solar-Terrestrial Physics, D. Reidel, p 13.

Harvey, J. and Hall, D.: 1975, Bull. Am. Astron. Soc. 7,459.

Haughen, E.: 1967, Solar Phys. 2,227.

Hollweg, J.V.: 1979, Solar Phys. 62,227.

Howard, R.: 1959, Astrophys. J. 130,193.

Howard, R.: 1972, Solar Phys. 24,123.

Howard, R. and Stenflo, J.O.: 1972, Solar Phys. 22, 402.

Ince, E.L.: 1956, Ordinary Differential Equations, Dover.

Jackson, J.D.: 1975, Classical Electrodynamics, Wiley.

Jeffrey, A.: 1966, Magnetohydrodynamics, Oliver and Boyd.

Jones, W.L.: 1976, Handbuch der Physik, XLIX/5, p 177.

Kuz'minykh, V.D.: 1965, Sov. Astron. 8,551.

Lamb, H.: 1945, Hydrodynamics, Dover.

Leighton, R.B.: 1959, Astrophys. J. 130,366.

Leighton, R.B.: 1963, Ann. Rev. Astron. Astrophys. 1,19.

Leighton, R.B.: 1965, in R. Lust (ed.) Stellar and Solar Magnetic Fields, I.A.U. Symp. 22,158.

Leighton, R.B., Noyes, R.W., Simon, G.W.: 1962, Astrophys. J. 135,474.

Lighthill, M.J.: 1960, Phil. Trans. Roy. Soc. A252,397.

Lighthill, M.J.: 1978, Waves in Fluids, Cambridge University Press.

Lites, B.W., Bruner, E.C., Chipman, E.G., Shine, R.A., Rottman, G.J., White, O.R. and Athay, R.G.: 1976, Astrophys. J. 210,L111

Lites, B.W. and Chipman, E.G.: 1979, Astrophys. J. 231,570.

Livingston, W.C.: 1968, Astrophys. J. 153,929.

Livingston, W.C. and Harvey, J.: 1969, Solar Phys. 10,294.

Loughhead, R.E.: 1968, Solar Phys. 5,489.

Magnus, W. and Oberhettinger, F.: 1949, Formulas and Theorems for the Functions of Mathematical Physics, Chelsea.

Maltby, P.: 1975, Solar Phys. 43,91.

Markham, J.J., Beyer, R.T. and Lindsay, R.B.: 1951, Rev. Mod. Phys. 23,353.

McLellan, A. and Winterberg, F.: 1968, Solar Phys. 4,401.

Mehltretter, J.P.: 1974, Solar Phys. 38,43.

Meyer, F. and Schmidt, H.U.: 1968, Z. Angew. Math. Mech. 48,218.

Meyer, F., Schmidt, H.U. and Weiss, N.O.: 1977, Monthly Notices Roy. Astron. Soc. 179,741.

Michalitsanos, A.G.: 1973a, Solar Phys. 30,47.

Michalitsanos, A.G.: 1973b, Earth Extraterrest. Sci. 2,125.

Milkey, R.W.: 1970, Solar Phys. 14,62.

Moore, D.W. and Spiegel, E.A.: 1964, Astrophys. J. 139,48.

Moore, R.L.: 1974, Solar Phys. 36,321.

Muller, R.: 1975, Solar Phys. 45,105.

Mullèr, R.: 1977, Solar Phys. 52,249.

Nakagawa, Y., Priest, E.R. and Wellck, R.E.: 1973, Astrophys. J. 184,931

Noyes, R.W. and Leighton, R.B.: 1963, Astrophys. J. 138,631.

Nye, A.H. and Thomas, J.H.: 1976, Astrophys. J. 204,573.

Osterbrock, D.E.: 1961, Astrophys. J. 134,347.

Parker, E.N.: 1955, Astrophys. J. 121,491.

Parker, E.N.: 1963, Astrophys. J. 138,552.

Parker, E.N.: 1974a, Astrophys. J. 189,563.

Parker, E.N.: 1974b, Astrophys. J. 190,429.

Parker, E.N.: 1976, Astrophys. J. 204,259.

Parker, E.N.: 1977, Astrophys. J. 210,816.

Parker, E.N.: 1978, Astrophys. J. 221,368.

Parker, E.N.: 1979a, Astrophys. J. 230,905.

Parker, E.N.: 1979b, Astrophys. J. 230,914.

Peckover, R.S. and Weiss, N.O.: 1978, Monthly Notices Roy. Astron. Soc. 182,189.

Pikel'ner, S.B.: 1971, Solar Phys. 17,44.

Pneuman, G.W. and Kopp, R.A.: 1977, Astron. Astrophys. 55,305.

Pneuman, G.W. and Kopp, R.A.: 1978, Solar Phys. 57,49.

Priest, E.R.: 1980, in Skylab Workshop on Active Regions (Ed. Orrall), Boulder, 1978-1979.

Provost, J.: 1975, Solar Phys. 40,257.

Reeves, E.M., Foukal, P.V., Huber, M.C.E., Noyes, R.W., Schmahl, E.J., Timothy, J.G., Vernazza, J.E. and Withbroe, G.L.: 1974, Astrophys. J. 188,L27.

Ribes, E. and Unno, W.: 1976, Astron. Astrophys. 53,197.

Roberts, B.: 1976a, Astrophys. J. 204,268.

Roberts, B.: 1976b, Solar Phys. 50,329.

Roberts, B.: 1979, Solar Phys. 61,23.

Roberts, B.: 1980, Solar Phys. submitted.

Roberts, B. and Webb, A.R.: 1978, Solar Phys. 56,5.

Roberts, B. and Webb, A.R.: 1979, Solar Phys. 64,77.

Roberts, P.H.: 1967, An Introduction to Magnetohydrodynamics, Longmans.

Rogerson, J.B.: 1961, Astrophys. J. 134,331.

Schatzman, E. and Souffrin, P.: 1967, Ann. Rev. Astron. Astrophys.5,67.

Schmidt, H.U. and Stix, M.: 1973, Mitt. Astron. Ges. 32,182.

Schmieder, B.: 1976, Solar Phys. 47,435.

Schmieder, B.: 1977, Solar Phys. 54,269.

Schmieder, B.: 1978, Solar Phys. 57,245.

Schmieder, B.: 1979, Astron. Astrophys. 74,273.

Schmieder, B.: 1980, private communication.

Schwarzschild, K.: 1906, Nachr. K. Ges. Wiss. Got. p 41 (see also Schwarzschild, M. 1958)

Schwarzschild, M.: 1958, Structure and Evolution of the Stars, Dover.

Sheeley, N.R.: 1966, Astrophys. J. 144,723.

Sheeley, N.R.: 1967, Solar Phys. 1.171.

Sheeley, N.R.: 1969, Solar Phys. 9,347.

Sheeley, N.R.: 1971, in R. Howard (ed.) Solar Magnetic Fields, I.A.U. Symp. 43,310.

Sheeley, N.R. and Engvold, O.: 1970, Solar Phys. 12,69.

Simon, G.W. and Leighton, R.B.: 1963, Astron. J. 68,291.

Simon, G.W. and Leighton, R.B.: 1964, Astrophys. J. 140,1120.

Simon, G.W. and Noyes, R.W.: 1971, in R. Howard (ed.) Solar Magnetic Fields, I.A.U. Symp. 43,633.

Simon, G.W. and Zirker, J.B.: 1974, Solar Phys. 35,331.

Slater, L.J.: 1966, Generalized Hypergeometric Functions, Cambridge.

Souffrin, P.: 1966, Ann. Astrophys. 29,55.

Souffrin, P.: 1972, Astron. Astrophys. 17,458.

Spiegel, E.A.: 1957, Astrophys. J. 126,202.

Spitzer, L.: 1962, Physics of Fully Ionized Gases, 2nd Edition, Interscience.

Spruit, H.C.: 1974, Solar Phys. 34,277.

Spruit, H.C.: 1976, Solar Phys. 50,269.

Spruit, H.C.: 1977a, Ph.D. Thesis, Utrecht.

Spruit, H.C.: 1977b, Proc. of OSO-8 Workshop, Boulder, Colorado.

Spruit, H.C.: 1979, Solar Phys. 61,363.

Spruit, H.C. and Zweibel, E.G.: 1979, Solar Phys. 62,15.

Stanyukovich, K.P.: 1960, Unsteady Motion of Continuous Media, Pergamon, chapter XIII.

Stein, R.F. and Leibacher, J.: 1974, Ann. Rev. Astron. Astrophys. 12,407.

Stein, R.F. and Spiegel, E.A.: 1967, J. Acoust. Soc. Am. 42,866.

Stellmacher, G. and Wiehr, E.: 1971, Solar Phys. 18,220.

Stellmacher, G. and Wiehr, E.: 1973, Astron. Astrophys. 29,13.

Stellmacher, G. and Wiehr, E.: 1979, Astron. Astrophys.

Stenflo, J.O.: 1973, Solar Phys. 32,41.

Stenflo, J.O.: 1975, Solar Phys. 42,79.

Stenflo, J.O.: 1976a, in Basic Mechanisms of Solar Activity, I.A.U. Symp. 71,69.

Stenflo, J.O.: 1976b, in The Energy Balance and Hydrodynamics of the Solar Chromosphere and Corona, I.A.U. Coll. 36,143.

Stix, M.: 1970, Astron. Astrophys. 4,189.

Syrovat-skii, S.I. and Zhugzhda, Y.D.: 1968, Sov. Phys. Astron. 11,945.

Tanenbaum, A.S., Wilcox, J.M., Frazier, E.N. and Howard, R.: 1969, Solar Phys. 9,328.

Tarbell, T.D. and Title, A.M.: 1975, Bull. Am. Astron. Soc. 7,459.

Tarbell, T.D. and Title, A.M.: 1977, Solar Phys. 52,13.

Tayler, R.J.: 1970, Structure and Evolution of the Stars, Wykeman.

Tolstoy, I.: 1973, Wave Propagation, McGraw Hill.

Uchida, Y.: 1965, Astrophys. J. 142,335.

Ulmschneider, P.: 1971, Astron. Astrophys. 14,275.

Unno, W. and Ando, H.: 1979, Geophys. and Astrophys. Fluid Dynamics, 12,107.

Unno, W., Osaki, Y., Ando, H. and Shibahashi, H.: 1979, Non-radial Oscillations of Stars, Univ. of Tokyo Press.

Unno, W. and Ribes, E.: 1979, Astron. Astrophys. 73,314.

Unno, W., Ribes, E. and Appenzeller, I.: 1974, Solar Phys. 35,287.

Unno, W. and Spiegel, E.A.: 1966, Publ. Astron. Soc. Japan 18,85.

Vernazza, J.E., Avrett, E.H. and Loeser, R.: 1976, Astrophys. J. Supp. 30,1.

Vincenti, W.G. and Traugott, S.C.: 1971, Ann. Rev. Fluid Mech. 3,89.

Vrabec, D.: 1971, in R. Howard (ed.), Solar Magnetic Fields, I.A.U. Symp. 43,329.

Weiss, N.O.: 1964, Phil. Trans. Roy. Soc. A256,99.

Weiss, N.O.: 1966, Proc. Roy. Soc. A293,310.

Weiss, N.O.: 1977, in E.A. Muller (ed.), Highlights of Astronomy 4, part II,241.

Wentzel, D.G.: 1979, Astrophys. J. 227,319.

White, O.R.: 1977, I.A.U. Coll. 36,75.

White, O.R. and Athay, R.G.: 1979, Astrophys. J. Supp. Ser. 39,347.

Wilson, P.R.: 1978a, Astrophys. J. 221,672.

Wilson, P.R.: 1978b, Astrophys. J. 225,1058.

Wilson, P.R.: 1979a, Astron. Astrophys. 71,9.

Wilson, P.R.: 1979b, Astron. Astrophys.

Worrall, G.: 1972, Astrophys. J. 172,749.

Yeh, T.: 1977, Solar Phys. 55,241.

Yih, C.-S.: 1965, Dynamics of Nonhomogeneous Fluids, MacMillan.

Yu, C.P.: 1965, Phys. Fluids 8,650.

Zhugzhda, Y.D.: 1979, Solar Phys. 25,329.

Zirker, J.B.: 1965, in R. Lust (ed.) Stellar and Solar Magnetic Fields, I.A.U. Symp. 22,208.

Zwaan, C.: 1967, Solar Phys. 1,478.

Zwaan, C.: 1978, Solar Phys. 60,213.